Structural and haemodynamic differences between emmetropic and highly myopic eyes

An exploratory study aiming to identify possible haemodynamic risk factors for glaucoma susceptibility in high myopes

KATRIN HIRSCH

Doctor of Philosophy

ASTON UNIVERSITY

March 2019

Contents

I General introduction into the subject 16

II Anatomy, Physiology and Definitions 19

1 Definitions 19

1.1 Myopia . . . 19

1.2 Glaucoma . . . 20

1.2.1 The site of the injury in glaucoma . . . 21

1.2.2 The role of IOP in glaucomatous damage . . . 22

1.2.3 The role of blood circulation in glaucomatous damage . . . 23

1.2.4 The role of biochemical factors in glaucoma . . . 24

1.2.5 Treatment in glaucoma . . . 25

1.2.6 Summary of risk factors for developing myopia and glaucoma . . . 26

2 Anatomy and Physiology 27

2.1 Retinal and the choroidal blood circulation and the measurement of blood circulation markers . . . 27

2.1.1 Retinal Circulation . . . 27

2.1.2 Choroidal Circulation . . . 28

2.1.3 Retinal haemodynamics and oxygen transport in vessels . . . 29

2.2 Optic nerve head and its blood supply . . . 30

2.3 Neuroretinal tissue - ganglion cell layer and retinal nerve fibre layer . . . 31

III Previous research findings - literature review 34

3 Visual function 34

4 Retinal structure 36

4.1 Ocular magnification - influence of ocular biometric data on retinal structure measurements . . . 39

4.1.1 Biometric measurement - AL . . . 40

5 Retinal haemodynamic measurements and calculations 41

5.1 Retinal vessel oximetry . . . 41

5.1.1 Retinal vessel oximetry - a systematic review and meta-analysis . 43

5.2 Static vessel analysis . . . 61

5.3 Retinal vessel complexity - spatial distribution of the retinal vessel network 62

5.4 Dynamic vessel analysis . . . 64

5.5 Ocular Perfusion Pressure and Vascular dysregulation . . . 65

6 Summary of previous research of structural and haemodynamic parameters in highly myopic and glaucomatous eyes leading to the objectives of this study 67

6.1 Structural measurements - Neuroretinal tissue thickness . . . 68

6.2 Retinal haemodynamic measurements - Vessel architecture . . . 68

6.3 Retinal haemodynamic measurements - Vessel function . . . 69

6.4 Retinal haemodynamic measurements - Oxygen content in retinal vessels and ocular perfusion pressure . . . 69

6.5 Study objective and research questions . . . 70

IV Material and Methods of this Research 73

7 Eligibility study cohorts - Inclusion/exclusion 73

7.1 Measurement procedure on the appointment . . . 75

8 Visual function and retinal structure measurements 76

8.1 Visual function . . . 77

8.1.1 HFA 750i perimeter - measurement principle . . . 77

8.1.2 Protocol and quality control . . . 77

8.2 Retinal structure measurements - GCL thickness and RNFL thickness measurements . . . 78

8.2.1 Spectral domain OCT - measurement principle . . . 78

8.2.2 Peripapillary retinal nerve fibre layer thickness measurement . . . 79

8.2.3 Ganglion cell inner plexiform layer measurement . . . 80

8.2.4 Axial length measurement and principle . . . 81

8.2.5 Compensation "OM" for ocular magnification . . . 82

8.2.6 Protocol and quality control . . . 83

9 Retinal haemodynamic measurements and calculations **83**

9.1 The RVA - instrumental set up . . . 84

9.2 Retinal vessel oximetry . . . 86

9.2.1 Protocol and quality control . . . 88

9.2.2 Compensation for retinal pigmentation . . . 88

9.3 Static vessel analysis . . . 92

9.3.1 Protocol and quality control . . . 92

9.4 Retinal vessel complexity . . . 96

9.4.1 Compensation for the shape of the retina . . . 97

9.4.2 Protocol and quality control . . . 98

9.5 Dynamic vessel analysis . . . 100

9.5.1 Protocol and quality control . . . 101

9.6 Ocular perfusion pressure calculation . . . 103

9.6.1 Blood pressure measurement . . . 103

9.6.2 Intraocular pressure measurement . . . 104

10 Statistical analyses **105**

10.1 Statistically, the study approached the research question as follows . . . 106

V Results of this study **109**

11 Demographic data - Sample statistics **110**

12 Observational features of the retinae **114**

13 Group comparisons **116**

13.1 Function - Visual field testing . . . 116

13.1.1 Mean deviation and pattern standard deviation . . . 116

13.1.2 Glaucoma hemifield test analysis . . . 117

13.2 Structural measurements . . . 120
13.2.1 Retinal nerve fibre layer thickness . . . 120
13.2.2 Ganglion cell layer thickness . . . 123
13.2.3 Summary structural measurements . . . 125
13.3 Retinal haemodynamic measurements and calculations . . . 127
13.3.1 Retinal vessel oximetry - oxygen saturation measurement . . . 127
13.3.2 Static vessel analysis . . . 129
13.3.3 Retinal vessel complexity - fractal analysis . . . 131
13.3.4 Dynamic vessel analysis - sequential and diameter response analysis (SDRA) . . . 134
13.3.5 Ocular perfusion pressure analysis . . . 135
13.3.6 Summary comparison of haemodynamic measurements . . . 137
13.4 Summary of all group comparisons . . . 138

14 Relationships in emmetropic, highly myopic and eyes with glaucoma 140

14.1 Haemodynamic intra-relationships - haemodynamic patterns . . . 140
14.2 Haemodynamic variables to predict neuroretinal thicknesses changes . . . 144
14.2.1 Haemodynamic vs RNFL thickness relationships . . . 144
14.2.2 Haemodynamic vs GCL thickness relationships . . . 146
14.2.3 Summary structural - haemodynamic relationships and hierarchical linear regression analysis . . . 147

VI Discussion of the findings 149

15 Sample statistics 150

16 Visual function measurements 151

17 Locations prone to the loss of neuroretinal tissue in healthy eyes 154

18 Retinal haemodynamic measurements **157**

18.1 Similarities and differences in between study cohorts 157

18.1.1 Oximetry 157

18.1.2 Retinal vessel architecture - Static vessel analysis and vessel complexity 160

18.1.3 Retinal vessel function - Retinal vessel reactivity 163

18.1.4 Perfusion pressure calculations 163

18.2 Haemodynamic intra-relationships in emmetropic vs in highly myopic and in a sample of glaucomatous eyes 165

18.3 Implications of all haemodynamic findings 167

19 Structural vs haemodynamic relationships and regression analyses **169**

19.1 Predicting RNFL thickness from haemodynamic measurements 169

20 Summary of findings of this study **170**

20.1 Visual function parameters 170

20.2 Structural parameters 171

20.3 Heamodynamic parameters and patterns 171

20.4 Predictability of neuroretinal tissue changes from haemodynamic parameters 172

VII A proposed hypothesis from findings of this research **173**

VIII Limitations of this research and future studies **175**

IX Bibliography **180**

X Appendices **205**

Appendix A Authors permission to use graphic **205**

Appendix B **206**

Protocol of Study 1 206

Approval Aston University Ethics Committee Study 1 211

Protocol of Study 2 212

Approval Aston University Ethics Committee Study 2 219

Appendix C **220**

Patient Invitation and Patient Consent Form Study 1 220

Patient Invitation and Patient Consent Form Study 2 222

Appendix D Distribution Analysis of Data **224**

Appendix E Correlation Matrices and Correlation Data Plots **229**

Appendix F Model Summaries of Regression Analysis **235**

Index

A

AL = axial length, length of the eye, distance between corneal apex and retinal pigment epithelium along the optical axis of the eye, 17

apoptosis = regulated dead of cells, 17

aSO2 = arterial oxygen saturation, 42

atrophy = tissue death, 27

autoregulation = the ability of tissue to adapt perfusion to individual metabolic needs, 65

A-V SO2 difference = arterial-venous difference in oxygen saturation, 42

AVR = arteriovenous ratio, 61

B

BDES = The Beaver Dam Eye Study (start: 1988, up to 20 years follow up, patient recruitment: in the city and town ship of Wisconsin/US, purpose: prevalence and incidence of age-related cataract, macular degeneration and diabetic retinopathy), 16

BDF = baseline diameter fluctuation, 100

BF = blood flow, 29

BP = plood pressure, 24

C

CRA = central retinal artery, 27

CRAE = central retinal artery equivalent, 29

CRV = central retinal vein, 27

CRVE = central retinal vein equivalent, 29

D

DA = dilation amplitude with $DA_A$for arteries and DA_V for veins, 100

dBP = diastolic blood pressure, 24

deltaD = percentage of vasodilation between flicker initiation and point of maximum diameter with $deltaD_A$for arteries and $deltaD_V$ for veins, 100

Df = retinal vessel complexity, fractal dimension of the retinal vessel network (box-counting method), 29

Dm = Fractal dimension calculated according to mass-radius-relation, 62

dPP= diastolic perfusion pressure, 24

DVA = dynamic vessel analysis, changes in retinal vessel diameter due to flicker light inervation, 29

E

Emmetropia = refractive error between +0.5 D and -0.5 D, 19

ET-1 = endothelin-1, molecule released from blood vessel walls to initiate vasoconstriction, 25

F

FDR = false discovery rate, statistical method controlling for committing type I error in multiple correlation testing, 106

G

GC = ganglion cells, 31

GCL = ganglion cell complex, represents the ganglion cell layer and the inner plexiform layer, 16

GHT = Glaucoma Hemifield Test, 34

GON = glaucomatous optic neuropathy, 20

H

HFA = Humphreys Visual Field Analyser, 76

hypoxia = deprived oxygen supply at the tissue level, 27

I

ICC = intra correlation coefficient, measure of reliability given by a dimensionless quantity, 36

interneurons = amacrine and bipolar cells, 31

IOP = intraocular pressure, 20

IPL = inner plexiform layer: connection between ganglion cells and amacrine + bipolar cells, 31

IQR = interquartile range, 115

isosbestic = not sensitive to the oxygen content of hemoglobin, 86

L

Lac = lacunaricity, spacing in between vessels, 95

LALES = The Los Angeles Latino Eye Study (start: 2004, patient recruitment:

around the city of La Puente in Los Angeles County, purpose: Prevalence of visual impairment, blindness, cataract, glaucoma, diabetic retinopathy, and age-related macular degeneration in a Latino population, 16

LCR = lamina cribrosa region, 30

M

MC = maximum percentage of constriction with $MC_A$for arteries and MC_V for veins, 100

MD = maximum percentage of vasodilation with $MD_A$for arteries and MD_V for veins, 100

MD_H = mean deviation in visual field results according to Heijl A., 17

MPP = mean ocular perfusion pressure, 102

N

neuroretinal rim = annulus framing the optic disc defined from the cup margin to the level of the Bruch's membrane opening, 30

NO = nitric oxide, molecule released from blood vessel walls to initiate vasodilation, 25

non-telecentric = entrance or exit pupil is not in infinity, 36

NOS = nitric oxide synthase, exists in three isoforms: nNOS responsible for neurotransmission, iNOS responsible for destructive activity during inflammation, eNOS responsible for vascular processes, 25

NTG = normal tension glaucoma, 21

O

OA = ophthalmic artery, 27

OCT = optical coherence tomography; interferometric measurement principle, 77

OCTA = optical coherence tomography angiography, 161

OD = optical density, 41

ODR = optical density ratio, 41

OM = ocular magnification, the magnification or minification of an image due to the change in distance to the devices focal length, 80

ONH = optic nerve head, 20

OPP = ocular perfusion pressure; defines the pressure difference between arterial tension and vein tension; can be estimated from blood pressure and intraocular pressure, 23

OPP =ocular perfusion pressure, 29

P

PACG = primary angle closure glaucoma, 21

PCA = posterior ciliary arteries, supplying choroid, ONH and ciliary body and iris, 28

PLR = prelaminar region, 30

POAG = primary open angle glaucoma, 16, 21

PSD = pattern standard deviation, 76

PVD = primary vascular dysfunction, 23

R

Retinal vessel oximetry = measurement of the oxygen content bound to hemoglobin in retinal vessels, 84

RNFL = retinal nerve fibre layer, 16, 32

RP = retinal pigmentation, 87

S

sBP = systolic blood pressure, 24

SDRA = sequential and diameter response analysis, 100

SE = spherical equivalent, calculated as spherical power+0.5x cylindrical power, 16

SiMES = The Singapore Malay eye Study (start/end: 2004/2006,purpose: collect and document frequency, causes and risk factors of blindness and visual impairment in the Malay community, 16

SITA = Swedish Interactive Threshold Algorithm, 34

SLD = super-luminescent light emitting diode, 77

SNFL = surface nerve fibre layer, adjacent to the vitreous, 30

SO2 = oxygen saturation, the measurement refers to retinal vessel oximetry, 29

sPP = systolic perfusion pressure, 102

T

Tukey HSD test = Tukey honestly signifi-

cant difference (HSD), 105

V

vascular dysregulation = regulation of blood flow is not adapted to the tissues oxygen needs, 27
vasoconstriction = decrease of vessel diameter, 64
vasodilation = increase of vessel diameter, 64
vSO2 = venous oxygen saturation, 42

List of Tables

1 Previous findings in myopia and glaucoma . . . 18

2 Risk factors myopia and glaucoma . . . 26

3 Demographic influences on neuroretinal tissue thickness . . . 39

4 Summary of studies on reliability of the method . . . 47

5 Studies included for pooled normative estimates of SO2 measurements . . . 49

6 Studies included for disease related changes in SO2 . . . 50

8 Summary normative SO2 values . . . 51

9 Synthesis of findings in diabetes and diabetic retinopathy . . . 53

10 Synthesis of findings in Retinal vein occlusions (RVO) stratified into central vein occlusion (CRVO) and branch retinal vein occlusion (BRVO) . . . 54

11 Synthesis of findings in glaucoma . . . 55

12 Synthesis of findings in retinitis pigmentosa . . . 56

13 Summary of findings in myopic vs glaucomatous eyes . . . 70

14 Measurements of the study . . . 76

15 Sequential and Diameter Response Analysis (SDRA) . . . 102

16 Weighting factors based on previous research . . . 108

17 Sample size for statistical analysis . . . 111

18 Sample statistics of the study . . . 113

19 Visual field test analysis: group averages . . . 118

20 Visual field test analysis group comparisons . . . 118

21 RNFL thickness group means . . . 121

22 Group comparisons of RNFL thicknesses . . . 122

23 GCL thickness group means . . . 123

24 Group comparisons of GCL thicknesses . . . 124

25 SO2 group means . . . 128

26 Group comparisons of SO2 measurements . . . 128

27 Vessel architecture measurement group means . . . 132

28 Group comparisons of architectural measurements of retinal vessels . . . 132

29 Sequential and diameter response analysis (SDRA) group means of the main variables . . . 134

30 Sequential and diameter response analysis (SDRA) - comparison group means of the main variables . . . 135

31 Summary of group comparisons . . . 139

32 RNFL thickness intra- relationships analysed using Pearson correlation . . . 142

33 Summary of statistically significant correlations between RNFL thickness and haemodynamic measurements . . . 146

34 Summary of hierarchical regression analysis in emmetropes - RNFL thickness . . . 148

List of Figures

1 Classification scheme glaucoma 21

2 Ocular blood supply 28

3 The blood supply of the ONH 31

4 Layers of the retina 33

5 Origin of the retinal nerve fibres 33

6 Glaucoma hemifield test (GHT) measurement zones and associated neuroretinal rim quadrants 35

7 Redistribution of RNFL in myopic eyes 38

8 Eligibility meta-analysis 45

9 Funnel plots to test for publication bias 48

10 Influence of retinal pigmentation on SO2 results 52

11 Influence of age on SO2 results 52

12 Measurement principle Cirrus HD-OCT 79

13 RNFL thickness measurements 80

14 GCL measurements 81

15 Measurement principle of the IOL Master 82

16 Retinal haemodynamic measurements using the RVA 84

17 The RVA setup and the flicker provocation protocol 86

18 SO2 measurement (oximetry) 87

19 Transformation of SO2 data to compensate for retinal pigmentation (1/2) 90

20 Transformation of SO2 data to compensate for retinal pigmentation (2/2) 91

21 Principle of static vessel analysis using the iFlexis software 94

22 Influence of image type on CRAE results 95

23 Influence of image type on CRVE results 96

24 Retinal vessel complexity using the iFlexis software 99

25 Influence of image type on Df results 100

26 Manual data cleaning process prior to SDRA. 102

27 Tukey HSD post-hoc testing for sBP and dBP . . . 114
28 Graphical representation of observational findings. . . . 115
29 Group comparisons for MD_H ,PSD and GHT analysis. . . . 119
30 Graphical representation of RNFL and GCL thickness for the study cohorts. . . . 126
31 Graphical representation of transformedSO2 results for the three study cohorts. . . . 129
32 Post-hoc test for CRAE and CRVE . . . 130
33 Graphical representation of SVA and vessel complexity results for the three study cohorts . . . 133
34 Graphical representation of SDRA results for the three study cohorts . . . 135
35 Graphical representation of group means sPP and dPP . . . 137
36 Haemodynamic intra-relationships analyzed using Pearson correlation in E 142
37 Haemodynamic intra-relationships analyzed using Pearson correlation in hM . . . 143
38 Haemodynamic intra-relationships analyzed using Pearson correlation in G 143
39 RNFL thickness - Haemodynamic relationships . . . 145
40 GCL thickness- Haemodynamic relationships . . . 147
41 Distribution of the residuals of the Multiple linear regression model in E 149
42 Proposed link between retinal haemodynamics and glaucoma . . . 174
D.43 Sample statistic - distribution data . . . 224
D.44 Distribution Visual field measurements . . . 225
D.45 Distribution structural measurements . . . 226
D.46 Distribution SO2 measurements . . . 226
D.47 Distribution SVA measurements . . . 227
D.48 Distribution DVA measurements . . . 227
D.49 Distribution perfusion pressure measurements . . . 228
E.50 Haemodynamic relationships analysed using Pearson correlation in E . . . 229
E.51 Haemodynamic relationships analysed using Pearson correlation in hM . . . 230
E.52 Haemodynamic relationships analysed using Pearson correlation in G . . . 231
E.53 Structure - haemodynamic relationships data-point representation in E . 232
E.54 Structure - haemodynamic relationships data-point representation in hM 233
E.55 Structure - haemodynamic relationships data-point representation in G . 234
F.56 Hierarchical regression model summary (RNFL) in E . . . 235

Aston University - Thesis Summary

Structural and haemodynamic differences between emmetropic and highly myopic eyes - An exploratory study aiming to identify possible haemodynamic risk factors for glaucoma susceptibility in high myopes

Katrin Hirsch - Doctor of Philosophy - 2019

It is well recognized that myopic eyes are more prone to develop glaucoma later on in life. The exact processes leading to the onset and progression of glaucoma however, is still not fully understood. Characteristic in glaucoma is the loss of neuroretinal tissue (ganglion cells and their axons). It is hypothesised that glaucoma develops due to an imbalance between intraocular pressure and impaired blood flow in the eye (vascular theory). This cross-sectional, explorative study carried out a wide range of retinal blood circulation measurements (vessel calibres, vessel network complexity as well as vessel function and oxygen content in retinal vessels) and related these with neuroretinal tissue thickness measurements in emmetropic and highly myopic eyes. A glaucoma sample was qualitatively compared with the healthy groups. The main objective was to determine haemodynamic parameters which may explain glaucoma susceptibility in myopic eyes.
Emmetropic eyes were not significantly different from highly myopic eyes regarding visual field indices, retinal nerve fibre layer thicknesses, retinal vessel complexity, vessel function and the retinal vessel oxygen content. Vessel calibres were significantly narrower in highly myopic eyes as well as the relationship between systolic and diastolic perfusion pressure. As expected, the glaucoma sample exhibited thinner neuroretinal tissue, narrower vessel calibres, a sparser retinal vessel network and a increased oxygen content in veins. Multiple correlation analysis between structural and haemodynamic parameters could not identify haemodynamic predictors for neuroretinal tissue loss in high myopes and glaucoma subjects.
The results of this study suggest that the impact of retinal haemodynamic parameters (CRAE and deficiency in perfusion) may partly contribute to the increased glaucoma risk in myopia.

Keywords: Retinal nerve fibre layer, ganglion cell layer, retinal vessel architecture, retinal vessel complexity, retinal vessel function

Part I

General introduction into the subject

According to a survey on behalf of The Vision Loss expert group on causes of vision impairment and blindness worldwide, uncorrected distance refractive error was one of the leading causes of blindness in 2010, constituting 20.9 % of all cases [24]. A recent study conducted by Holden et al. (2016) predicted the global prevalence of myopia to rise from 28.3 % in 2010 to 49.8 % in 2050 [125], representing an estimated 6056 million myopic people worldwide for 2050. Well known contributors to the prevalence of myopia such as urbanization, intensive schooling and computer-based activities are on the rise. Health care issues might arise because myopic eyes are prone to concomitant co-morbidities such as cataract, glaucoma and retinopathy [264], which require further need for treatment, more frequent consultations and even medication. Hence, myopia is approaching epidemic dimensions, causing enormous costs for the health care system.

Evidence for an increased risk to develop glaucoma in people with a high myopic refractive error showed a study of Marcus et al. (2011) [185]. This meta-analysis revealed a 1.88 fold higher risk to develop primary open angle glaucoma (POAG) in eyes with a spherical equivalent (SE) above -3.00 DS.

In addition, the increase in the ageing population (demographic change) might further contribute to rising cost for the health care system due to age being a risk factor in developing pathologies such as glaucoma [199], AMD [276] and diabetic retinopathy [146].

Although there is evidence for an existing association between high myopia and open-angle glaucoma (The Blue Mountains Eye Study (BME) [197],The Beaver Dam Eye Study (BDES) [316],The Singapore Malay Eye Study (SiMES) [241], The Los Angeles Latino Eye Study (LALES) [157]), the exact mechanism underlying this relationship remains unclear.

Since the invention of interferometric technology in the 1990s, structural analysis of the eyes in vivo became available and investigations on retinal anatomic features, such as

retinal nerve fibres (RNFL) and ganglion cell layers (GCL) became feasible [127, 60, 186, 145, 164, 163, 267]. Myopic eyes as well as eyes with glaucoma exhibit alterations in the thickness of the neuroretinal tissue (peripapillary RNFL thickness and Ganglion cell complex thickness) which might link myopia and glaucoma in terms of structural features. In myopic eyes the findings yielded a redistribution of peripapillary RNFL thickness that correlates with increasing axial length (AL) [170, 257, 140]. In glaucomatous eyes, peripapillary RNFL thinning has been found to be most pronounced at the inferior quadrant [212]. While in glaucoma the decrease in RNFL thickness might occur due to ganglion cell loss [250], in myopic eyes the alterations might be caused by mechanical stretch.

The loss of neuroretinal tissue (ganglion cells and their axons) in glaucoma happens gradually [232] and can be detected functionally through visual field testing. When the ganglion cell loss exceeds 20 % it reflects in mean deviation (MD_H) reduction of 5dB [249]. Similarly to glaucoma, in myopic subjects with a negative refractive error higher than -3.75 D (0.2 dB decrease per 1.00 D decrease in refractive error [7]) a reduction in sensitivity was detected. This reduction in MD_H is only marginal in myopic eyes up to -4.00 D, but it may lead to a misinterpretation of visual field results in a diagnostic procedure.

Although the exact mechanism causing the death of the ganglion cells and their axons is still uncertain in glaucoma, it is hypothesized that malfunction of the blood circulation (referred to as ocular haemodynamics) in the optic nerve head leads to hypoxia in the neuroretinal tissue. This in turn causes apoptosis of the ganglion cells and their axons [231, 67, 66]. Previous research revealed a reduced oxygen consumption in both myopia and glaucoma [330, 254]. Thus, the aspect of blood circulation might pose a possible link between glaucoma and myopia. Comprehensive investigations relating structural and functional aspects with haemodynamic factors are rare. In comparing retinal haemodynamic parameters between healthy emmetropic and healthy highly myopic eyes and a consecutive investigation on the predictive ability of these markers on neuroretinal tissue changes, this study aims to detect haemodynamic markers capable of explaining the increased risk of myopic eyes to develop glaucoma. Data of a sample of glaucoma subjects

was used to evaluate the importance of the findings.

Table 1 provides an overview on previous findings that might link myopia with glaucoma.

Type of feature	**Glaucoma**	**Myopia**	**similar ✔, different ✗, related ☆**
Structural	RNFL thinning due to ganglion cell loss [212, 250]	RNFL redistribution due to mechanical stretch of the retina (temporal thickening, but superior and inferior thinning) [170, 257, 140]	✔
Functional	Reduction in visual field sensitivity MD_H	Marginal general reduction in visual field sensitivity MD_H [7]	✔
Haemodynamics	Reduced blood flow at the ONH [67]	Reduced blood flow velocity in the Ophthalmic artery [72]	☆
Haemodynamics	Significant increased venous oxygen saturation while arterial saturation remains relatively unchanged, leading to decrease in arterio-venous difference and might reflect reduced oxygen consumption [254, 301]	Significant reduced arterial oxygen saturation and reduced arterio-venous difference [330] (reflecting a reduced oxygen consumption)	✔
Haemodynamics	Arterial narrowing [142] Reduced vessel reactivity (refers to impaired metabolism) [254, 87]	reduced vessel diameter [318] but vessel reactivity is not impaired [158]	☆
Haemodynamics	Vessel geometry: reduced retinal vessel complexity (Df) [319]	Vessel geometry: reduced retinal vessel complexity (Df) [38]	✔

Table 1: **Previous findings with respect to functional, structural and haemodynamic features of the retina in myopia and glaucoma**

Part II

Anatomy, Physiology and Definitions

1. Definitions

1.1. Myopia

Emmetropia is a balance between the refractive power of the eye and its length. Myopia, also known as short-sightedness, occurs when distant objects are focused anteriorly to the retinal plane. Most commonly it occurs either as a result of increased positive refractive power of the cornea-lens system (refractive myopia) or axial elongation (axial myopia) or as a combination of both of these factors. Myopia usually results from an eye that has become too long, particularly through elongation of the vitreal chamber [206].

The prevalence of myopia was found to be highest in Asian populations. In 2010 the highest prevalence was found in an Asia-Pacific high-income population (48.8 %), which is a urban population and hence, more exposed to near-work such as reading, writing and computer work. This prevalence was predicted to increase to 66.4 % in 2050 [125].

Besides the classification according to length and power of the eye , various other criteria can be applied to classify myopia: It can be categorized by the presence or absence of myopic retinopathy into physiological and pathological myopia (according to a grading scheme) or by the time of onset of myopia (youth onset, early-adult onset and late-adult onset). One commonly used grading scheme for myopic retinopathy is the AVILA grading scheme published by Avila et al. (1984) [8]. Furthermore, myopia can be stratified according to the refractive error, which varies among authors[206, 274, 125]. For example, Shen et al. (2016) grouped myopia according to the refractive error into low (-1.00 to -2.99 DS), moderate (-3.00 to -5.99 DS) and high ($\leq$-6.00 DS), whereas Holden et al. (2016) stratified into myopia (-0.50 to -4.99 DS) and high myopia ($\leq$ -5.00 DS) after finding this to be the most common method. The refractive status of an eye is determined by the refractive powers of cornea and crystalline lens, and the axial length. Despite AL being biologically important, the clinically meaningful variable is the refractive

power of an eye (referred to as refractive error). It determines spectacle or contact-lens correction independent of AL[206]. Hence, this study stratified the refractive status of its study cohorts according to the refractive error.

1.2. Glaucoma

A systematic review and Bayesian meta-analysis published in 2014 estimated the number of people suffering from primary open angle glaucoma in 2013 to be 64.3 million and by 2040 to be increased to 111.3 million [288]. The findings of this study reflect the significant present and future burden of glaucoma globally.

The term "Glaucoma" describes a range of ocular disorders which vary in their causes, risk factors, symptoms and prognosis. Thus, defining glaucoma is not straightforward and might at least partly explain as to why the pathophysiology of glaucoma is still not fully understood [34, 133]. Casson et al. (2012) proposed a definition, stating that glaucoma is as a group of ocular disorders of multifactorial aetiology. The clinical characteristic of glaucoma is the optic neuropathy (GON) with potentially progressive, clinically visible changes at the optic nerve head (ONH). These changes comprise focal or generalized thinning of the neuroretinal rim with excavation and enlargement of the optic cup, which is represented as neurodegeneration of retinal ganglion cell axons and deformation of the lamina cribrosa. The corresponding diffuse and localized nerve-fibre-bundle pattern visual field loss may not be detectable in early stages of the disease [86]. While the visual acuity is initially spared, disease progression can lead to complete loss of vision. The morphological changes (ONH changes) in glaucoma as well as the observed functional changes (visual field loss) define the term glaucomatous damage.

In normal eyes, this neuroretinal rim area is thickest inferiorly and thinnest temporally (referred to as the ISNT-rule). In eyes with GON the ISNT-rule is more likely to be violated [102]. Previous research has shown that the first signs of neuroretinal rim thinning may be found in the inferior quadrant [268, 238].

Figure 1 shows the classification of glaucoma. Acute angle closure glaucoma is a symptomatic form of glaucoma (i.e. headache and nausea) and occurs when the anterior chamber is blocked, which results in a sudden rise of intraocular pressure (IOP). A shal-

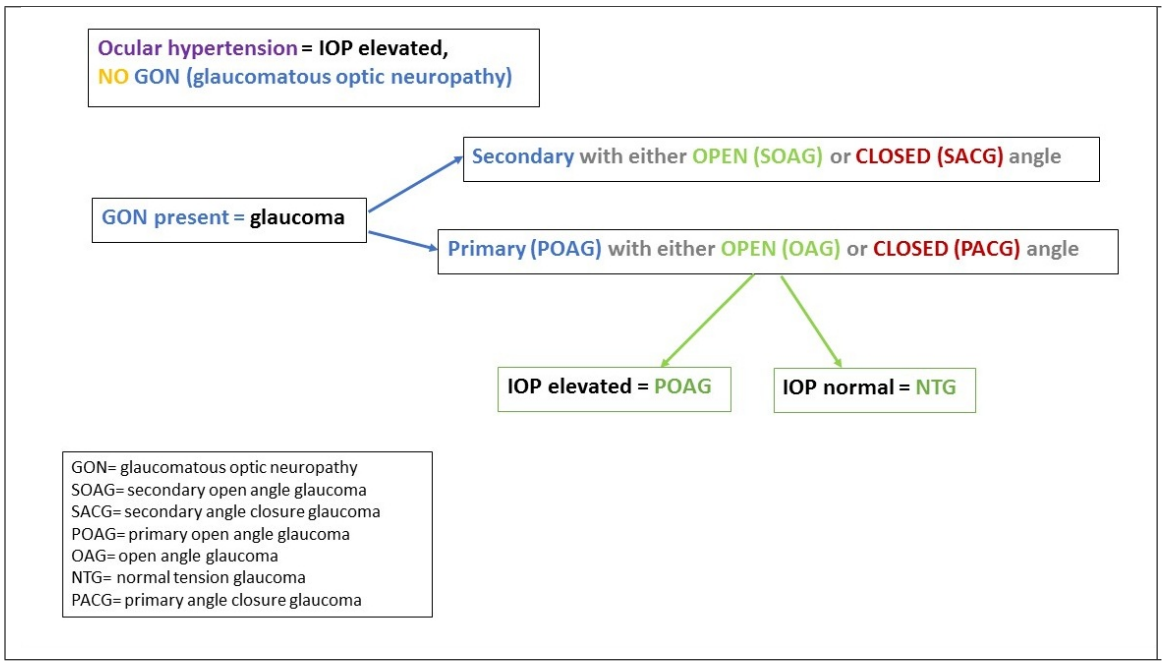

Figure 1: **Classification of glaucoma and associated conditions**

low anterior chamber and hyperopia (due to a thick crystalline lens) are risk factors for developing PACG [274].

Primary open angle glaucoma (POAG) can be sub-classified according to the status of IOP at diagnosis; normal tension (NTG) or high tension glaucoma. Some patients present with high IOP but no glaucomatous damage. These patients are termed ocular hypertensives and are considered to be at high risk of conversion to glaucoma. Previous research has identified various risk factors such as elevated IOP, vascular risk factors (i.e. "Flammer Syndrome") and family history of glaucoma. A detailed list can be found in table 2. This study investigated POAG and the risk factor myopia in an exploratory, cross-sectional method.

1.2.1. The site of the injury in glaucoma

Knowing the site of the injury enables to target the damaging processes. For glaucoma, the end point is well recognized as the loss of retinal ganglion cells (GCL) and their axons (RNFL). The exact mechanism causing ganglion cell death is still not known. Most of the working hypotheses identify the ONH (the immediate peripapillary retina, disk, or anterior lamina cribrosa) as the primary site of injury, most likely as the consequence of

the axons specific vulnerability as they make the turn through this zone [247, 306], while some of more recently proposed mechanisms are the injury to axonal bundles, ischaemia, the loss of trophic support by astrocytes and the activation of phagocytic astrocytes due to impaired blood circulation (review by Flammer et al. (2007) [65]).

1.2.2. The role of IOP in glaucomatous damage

Intraocular pressure was attributed to glaucoma since the 17th century (Bannister in 1622). The invention of the ophthalmoscope by Helmholz in 1850 enabled the observation of retinal changes associated with glaucoma. These observations led to the mechanical theory of glaucomatous damage. It explains that ganglion cell degeneration in glaucoma occurs as a result of elevated IOP, causing mechanical force on the optic nerve head (ONH). Consequently, a disturbed axoplasmic transport (retrograde system: from cell body to axon) triggers the death of the retinal ganglion cells and their axons[246]. A generally elevated IOP is a well recognized as an important modifiable risk factor in incidence and progression of glaucoma. The aspect of fluctuations in IOP came into focus in recent years. It is hypothesized that IOP fluctuations influence at least disease progression. A positive association has been observed between duration as well as magnitude of IOP elevation and retinal ganglion cell death in rats [207, 36, 173]. Liu et al. (2003) monitored IOP during a 24-hour period (short-term fluctuation) in 24 glaucoma subjects and compared the results with an age-matched group of healthy volunteers. The authors reported a significant smaller diurnal-to-nocturnal increase in IOP in the glaucoma group, despite showing a generally higher IOP than the control group during the daytime [181]. In healthy individuals, nocturnal values were higher than daytime values [180]. While short-term IOP fluctuations are becoming of increasing interest in the clinical management of glaucoma, the role of long-term fluctuation in the disease process remains controversial. Long-term IOP fluctuation was a strong and independent predictor of visual field damage progression in the Advanced Glaucoma Intervention Study (AGIS) [33]. By contrast, the EMGT identified elevated IOP as a strong factor for glaucoma progression, while long-term IOP fluctuation was not correlated with disease

progression [15]. The authors of the latter study explained this controversial finding by the difference in study population characteristics and intervention strategies during the study period compared to previous studies. While the EMGT included newly diagnosed patients with no intervention in treatment procedure during the study period, the AGIS study population consisted of subjects with uncontrolled IOP and maximally tolerated medical treatment which could have been altered during the 8 year follow up period.

Elevated IOP is often a consequence of impaired aqueous humour outflow due to physiological changes in the trabecular meshwork. The trabecular meshwork has been shown to exhibit cytoskeletal changes in cells (increased CLAN expression in TM cell lines) [41], alterations in cellularity [3] and changes in the extracellular matrix (ECM) [70]. Stringent regulation of IOP often helps to slow down disease progression. Unfortunately, glaucomatous damage occurs in approximately a third of glaucoma patients without elevated IOP [291, 91, 34]. Thus, elevated IOP is recognized as an important, but not the only risk factor responsible for optic nerve damage. Epidemiological research suggests that vascular risk factors such as diabetes or systemic hypertension and hypotension also play a role in the onset and progression of glaucoma (Los Angeles Latino Eye Study [192]; Baltimore Eye Survey [290]; Blue Mountains Eye Study [198]; Egna-Neumarkt Glaucoma Study [20]).

1.2.3. The role of blood circulation in glaucomatous damage

The earliest reference to a vascular aetiology in the pathogenesis of glaucoma was made by von Jaeger in 1858 [129]. The vascular theory of glaucoma suggests that glaucomatous damage occurs as a consequence of reduced perfusion pressure (OPP) in the ocular vasculature due to elevated IOP and/or other risk factors such as Primary vascular dysfunction (PVD) leading to a reduction of the ocular blood flow and consequently, ischaemia [290, 67, 63, 107]. Fluctuations in perfusion pressure which are found in PVD are thought to contribute to reperfusion damage in the ONH [85]. A growing body of evidence from epidemiological studies suggests that impaired blood flow regulation is involved in the incidence and progression of glaucoma. Normal tension glaucoma is

associated with low blood pressure (BP) in the Barbados Eye Study, the Egna-Neumarkt Study and the VER Study [167, 20, 251]. The Los Angeles Latino Eye Study reported that both, low diastolic blood pressure (dBP) and high systolic blood pressure (sBP) are associated with increased prevalence of POAG [192]. Interestingly, both systemic hypertensives and systemic hypotensives show higher glaucoma susceptibility. This might suggest a dual influence of IOP and blood pressure in the development of glaucoma [64]. Despite clear evidence of vascular aspects playing a role in POAG pathogenesis, it cannot be regarded as causative for ganglion cell apoptosis in glaucoma. Patients with systemic blood circulatory disorders such as PVD or systemic hypertension do not necessarily develop glaucoma. Nevertheless, reduced diastolic perfusion pressure (dPP) is regarded an important risk factor for POAG [20].

1.2.4. The role of biochemical factors in glaucoma

Investigations into biochemical factors have tried to address the pathophysiological processes involved in glaucoma and the molecular processes which accompany the regulation of the vascular tone. This complex area is not fully understood and further studies are required to better understand the biochemical mechanisms. Cellular apoptosis, as seen in glaucoma, is the programmed cell death in the absence of inflammation, characterized by DNA fragmentation, chromosome clumping, cell shrinkage and membrane blebbing [58]. Apoptotic processes in cells are thought to be the primary mechanism in ganglion cell death and can subsequently lead to cell-toxic effects [1, 173]. Changes to the extracellular matrix (ECM) in response to elevated IOP seem to play a role in ganglion cell apoptosis [89]. IOP related ECM changes have been detected in the trabecular meshwork of glaucoma subjects and in the retina of rats [89, 286]. The major cell-matrix degrading enzymes involved in ECM remodelling are matrix metallo-proteines (MMP) [89]. An increase of the enzyme MMP-9 expression is thought to be associated with an upregulation of glutamate receptors in retinal cells, which has a toxic effect on ganglion cells [328, 305].

Interestingly, an upregulation of MMP-9 expression has also been associated with vas-

cular dysregulation in patients with vasospastic NTG [83].

Endothelin-1 (ET-1, vasoconstriction) and nitric oxide (NO, vasodilation) play an important role in maintaining the vascular tone (referred to as homeostasis). Both molecules are released from the endothelial cells of the blood vessel wall to facilitate the metabolic adaption to tissue needs. Elevated ET-1 levels are associated with oxidative stress and NO, a molecule produced by nitric oxide synthase (NOS) by oxidation of L-arginine, is known to have a neurotoxic effect when it exceeds the physiological demand [179, 287, 219]. High ET-1 levels reduce blood flow and are associated with changes in the cells of the trabecular meshwork and disease progression [230, 233]. Increased ET-1 is not specific to glaucoma, it can also be observed in other diseases (e.g. Susac Syndrome) which contradicts a possible unique role of ET-1 in the development and progression of glaucoma [67]. The molecule NO has important physiologic and pathological roles in the body: NO plays a vital role in neurotransmission (via nNOS / NOS1), in the control of inflammation processes (via iNOS / NOS2), in the regulation of the vascular tone in the blood vessel beds (via eNOS/ NOS3) and in the IOP regulation in the eye [26, 219].The neurotoxic effect of NO is due to causing an increased release of glutamate which reacts with superoxide anions to form peroxynitrite radicals, adding to oxidative stress-induced ganglion cell damage [179]. A genetic association has been observed between the isoform iNOS and POAG [208].

1.2.5. Treatment in glaucoma

Currently, the reduction of IOP by pharmacological or/and by surgical procedures is the main therapeutic intervention in glaucoma. Nevertheless, the preferential aim of glaucoma treatment is neuroprotection. The use of blood flow regulating agents such as Carbonic anhydrase inhibitors (e.g. acetazolamide) which are thought to improve the blood flow in the ONH is well established. Blood flow enhancing therapeutics (calcium channel blocker) was discarded due to its blood pressure lowering effect. The advanced understanding of the biochemical processes involved in glaucomatous optic neuropathy lead to a variety of attempts to target the molecular aspects involved in cell-apoptosis more specifically (neurotrophic factors BDNF, antioxidant, NOS-inhibitor). Despite promis-

ing results in experimental models, research has failed to prove the beneficial effect on humans for e.g. Memantine [311]. Further research into the pathogenesis of glaucoma is needed to better understand the processes leading to the onset and progression of glaucoma.

1.2.6. Summary of risk factors for developing myopia and glaucoma

A large number of epidemiological studies have identified risk factors for both conditions, myopia and glaucoma. Table 2 provides a list of known risk factors for myopia (right column) and glaucoma (left column).

Type of risk	**Glaucoma**	**Myopia**
Ethnicity	African race: 3 to 4 fold higher risk than White race [291]; Asian race: higher prevalence of NTG [274]	Asia-Pacific population: prevalence of 48.8 % in 2010 [125]
	Age (4 fold higher risk at the age of 75 than at the age range 43 to 54 years) [149]	Environmental risks (extensive near work, time spend outdoors) [205, 263]
Genetic/ hereditary	Family history of glaucoma [61]; gene, located on chromosome 1q [280]	mutation of myocilin-a [326]
Gender	Conflicting results: ▪ being **male** as risk factor: The Tema Eye Survey [29], The Rotterdam Study [48], The Barbados Eye Study [166] ▪ being **female** as risk factor: The Blue Mountain Eye Study [199], Epidemiology of Glaucoma in Japan study [275]	
Cardio-vascular issues	low diastolic blood pressure[167, 332, 243] high systolic blood pressure[192, 292]	
Refractive error and axial length	high Myopia - pooled OR (7 studies included) was 1.88 (95 % CI, 1.60 to 2.20) [185], higher risk for NTG if AL exceeds 25 mm [226]	
Corneal thickness (CCT)	1.4 (OR) higher risk for onset of OAG per per 40 μm thinner corneal thickness [167, 84]	

Table 2: **Risk factors for developing glaucoma (centre column) and myopia (right column).**

2. Anatomy and Physiology

2.1. Retinal and the choroidal blood circulation and the measurement of blood circulation markers

2.1.1. Retinal Circulation

The retina is a tissue with a high oxygen demand, but it is not able to store oxygen. Thus, maintaining a constant oxygen supply is crucial for the tissue's health. The blood supply to the retina originates from the ophthalmic artery (OA), a branch of the carotid artery. The central retinal artery (CRA) is a branch of the OA. The CRA enters the eye through the optic nerve head (ONH) and branches into smaller vessels. It distributes the blood to the capillaries via perfusion with the aim of supplying the inner layers (from the nerve fibre layer down to the outer plexiform layer) of the retinal tissue with oxygen and nutrients. This process is named metabolism and is an essential mechanism for maintenance of tissue function.

Whilst arteries and arterioles down-stream nutrients and oxygen towards the tissue, the deoxygenated blood is transported backwards within the venules and veins leaving the optic nerve head towards the pulmonary system within the central retinal vein (CRV). However, the responsible force in an artery which transfers oxygen towards the tissue is termed ocular perfusion (OP) and describes the efficiency of the blood supply. Ocular perfusion pressure can be calculated from arterial pressure (BP) and venous pressure (RVP). Venous pressure is roughly the same value as IOP due to the fact that veins would collapse if IOP exceeds RVP. Hence, OPP can be estimated from BP and IOP according to equation 11 (see section 9.6).

Any alteration in the metabolic cycle is called vascular dysregulation and can lead to disturbances within the tissue, referred to as hypoxia, which results in structural damage and functional impairment (i.e. loss of vision). The worst-case scenario is cell-death (apoptosis) which is followed by tissue death (atrophy). The major aspect in maintaining healthy retinal tissue is the balance between oxygen supply and drainage of metabolic waste products. The optic nerve is where the CRA enters and the CRV leaves the eye

and hence is a vulnerable location for any alterations in the blood circulation [314]. Figure 2 provides an overview of the ocular tissue and its supplying artery.

2.1.2. Choroidal Circulation

While the retinal circulation supplies the inner two thirds of the retina, the macular area and the anterior portion of the optic nerve is supplied by the choroidal circulation. The choroidal circulation receives the blood from the posterior ciliary arteries (PCA), which are also branches of the OA.

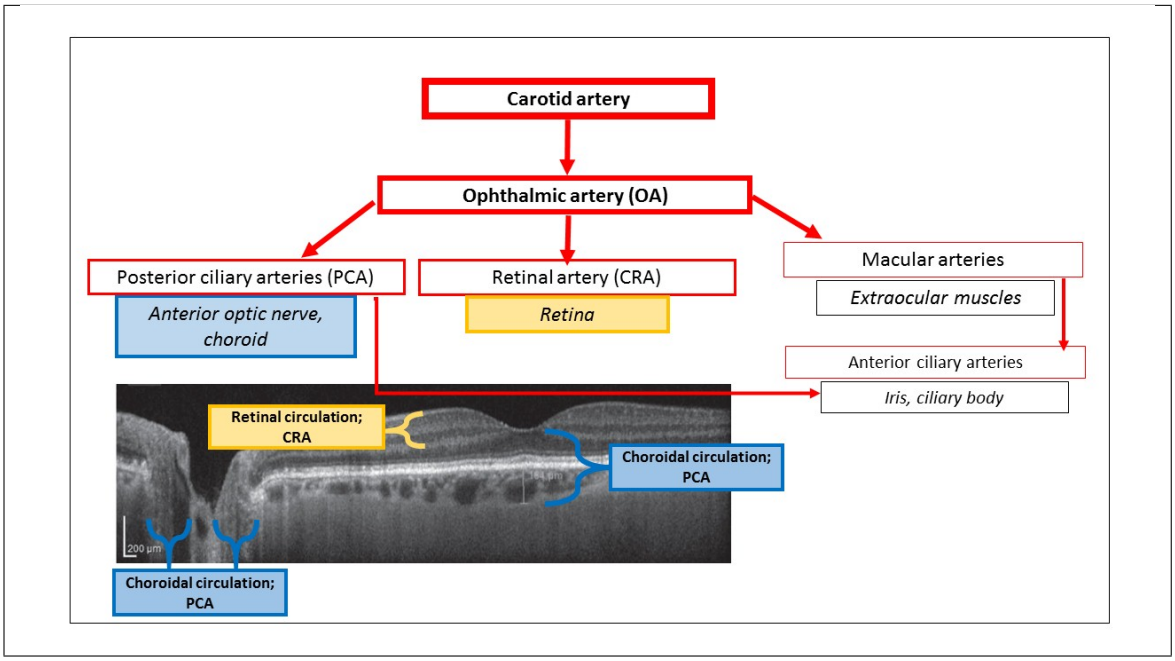

Figure 2: **Ocular blood supply.**

2.1.3. Retinal haemodynamics and oxygen transport in vessels

Considering a balanced blood circulation is essential for ocular health, valuable markers of oxygen metabolism are blood flow (BF), ocular perfusion pressure (OPP), oxygen saturation of the blood (SO2) and architectural (vessel calibres CRAE and CRVE, and the density of the vessel network Df) as well as functional (dynamic vessel analysis DVA retinal vessel markers. Haemodynamics is the sum of all forces keeping the heart pumping and circulating the blood through the body with the purpose of supplying the tissue with oxygen [278]. Retinal haemodynamics describes any measure of oxygen circulating in the retinal vasculature with the purpose of supplying the retina with oxygen and nutrients and draining it from waste products and exceeding oxygen (referred to as oxygen metabolism). Haemodynamic parameters allow the interpretation of oxygen delivery and drainage and autoregulation. Hereby, autoregulation is the adaptation of the vascular tone and of the vessel resistance of arteries to either metabolic tissue needs or to a change in OPP. The principle of autoregulation is based on flow physics in fluids, Poiseuille's law (see equation 1) and the physiological principle of minimum work [210]. The principle of minimum work implies that the size of the artery is proportional to the demand of the system (tissue) with the aim to avoid excessive energy or insufficient energy supply.

$$Q = \frac{diffP * R^4}{\frac{8}{Pi} * vis * L} \tag{1}$$

Hereby, *Q* refers to as volume-flow-rate and *diffP* refers to as pressure difference across a vessel section. Additionally, *L* is the length of the vessel section, *R* is the radius of the vessel and, *vis* refers to as viscosity of haemoglobin.

Autoregulation effectively happens due to vasoconstriction (decreasing arterial diameter to reduce flow rate) and vasodilation (increasing arterial diameter to increase flow rate). Poiseuille's law additionally implies that branching characteristics also alter the blood flow in arteries. Although it is a rather passive process, vasodilation and vasoconstriction for transportation of blood can also be found in veins. Evidence for this that a similar mechanism also exists for veins is the fact that the flicker stimulation also triggers a reaction for veins [215, 220, 234].

2.2. Optic nerve head and its blood supply

The optic nerve head (ONH) is 1 mm long and its diameter is approximately 1.5 mm, with the vertical diameter being slightly greater than the horizontal diameter [108, 195]. Its diameter depends on the diameter of the chorioscleral canal at the level of the Bruch´s membrane. The shape of the canal varies but the most common shape is a conical form with the posterior part being wider than the anterior. The ONH can be subdivided into three zones (axial direction):

- The surface nerve fibre layer (SNFL)
- The prelaminar region (PLR)
- The lamina cribrosa region (LCR)

Laterally the ONH is divided into the disc area which is defined by the Bruch's membrane opening, and the cup area which is the area where no nerve fibres are present. The width of the neuroretinal rim is normally at its thickest inferiorly, followed by the superior rim width. It is thinnest at temporal side of the disc. This relationship is understood as the ISNT-rule [102, 134]. The surface nerve fibre layer contains unmyelinated nerve fibres and is separated from the vitreous by the inner limiting membrane (of Elschnig). Furthermore, this zone contains a dense capillary network on its surface supplied by the CRA and drained by the CRV (figure 2). The prelaminar region is located posterior to the surface nerve fibre layer zone. This part is also known as the glial or choroidal part of the ONH, as it consists primarily of fine glial cells orientated perpendicularly to the nerve fibres and adjoins to the choroid peripherally. It also comprises a capillary network located in the glial septa which is supplied by branches of the short PCA and the choroidal circulation (figures 2 and 3). The CRA does not contribute to the blood supply in that region. The PLR and the LCR are connected via a transition zone, which consists of a mixture of glial and connective tissue leading to the lamina cribrosa region. This transition zone is attached to the scleral part of the chorioscleral canal and is

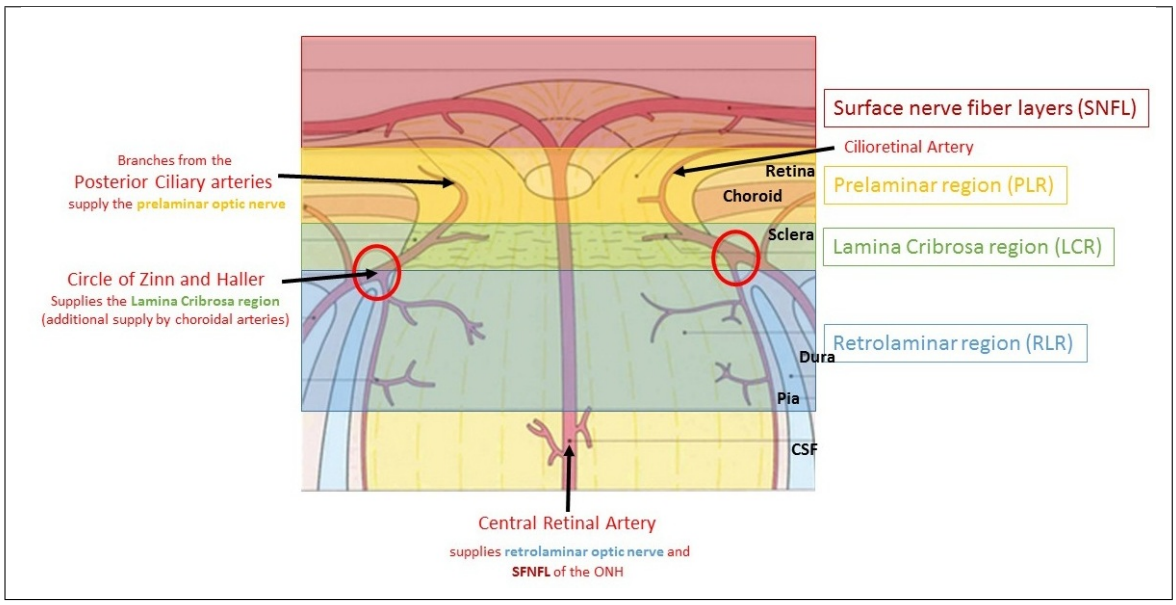

Figure 3: **The tree zones and blood supply of the optic nerve head (ONH)**

supplied by the short PCA. The lamina cribrosa is a region consisting of tightly packed connective tissue of a lamellar nature to allow nerve fibre bundles to leave the retina at the level of the sclera. Behind the LCR nerve fibres become myelinated, which affects the diameter of the chorioscleral canal to become approximately two times greater. The LCR is entirely supplied with blood by branches of the short PCA, either through the circle of Zinn and Haller or directly [106].

2.3. Neuroretinal tissue - ganglion cell layer and retinal nerve fibre layer

According to Quigley et al. (1982) there are at least one million ganglion cells (GC) in a human eye [247]. They are complex signal processing cells in the inner part of the retina [154], connected with the amacrine and bipolar cells, which in turn transfer the chemical signals from the photoreceptor cells to the ganglion cells (figure 4). When measuring the thickness of the ganglion cell layer, the inner plexiform layer (IPL) has to be taken into account, as it is an important area for the visual signal transfer. Ganglion cells are the final output neurons that transform chemical signals about the visual world arriving from the retinal interneurons into electrical signals. These signals then are transmitted to the retinal recipient areas in the brain by their axons (nerve fibres, RNF) in the form of transient train spikes. More than 20 different types of GC are known (named G4-G23) and these GC are selectively tuned to detect specific types of visual information (colour,

size, speed of motion, direction). Approximately fifty percent of the retinal ganglion cells are located within an annulus of 0.4 mm to 2 mm radius (16^o) of the fovea and take up 30 to 35 % of the total retinal thickness in that area [45]. The foveal area is free of ganglion cells and their axons as they are pushed away to the foveal slope [322]. The axons of the GC (RNF) run in an arcuate course towards the disc. Hereby, fibres arising from ganglion cells nearer to the disc (shorter fibres) lay more superficially than fibres originating from a greater distance from the disc (peripheral or long fibres). Consequently, when arriving at the disc the peripheral fibres lay more peripherally from the ONH centre, while fibres arising near to the disc leave the globe near the centre of the ONH (figure 5, [126]).

RNF run in bundles above the inner limiting membrane towards the optic nerve head where they leave the globe towards the brain (referred to as retinal nerve fibre layer: RNFL). One can differentiate five different types of RNF [51]: visual afferent fibres, pupillary afferent fibres, efferent retinal fibres, photostatic fibres, autonomic fibres.

To understand optic nerve neuropathies, functionally identified by distinct visual field defects and clinically presented by reduced RNFL thickness, it is important to know the arrangement of the nerve fibres in the optic nerve head and their corresponding topographic location on the retina. Figure 5 visualizes the retinal nerve fibre pattern (a) and the exit locations at the ONH associated with individual fibres (b).

The GCL and the RNFL are supplied with oxygen and nutrients by the retinal circulation (see section 2.1.1)

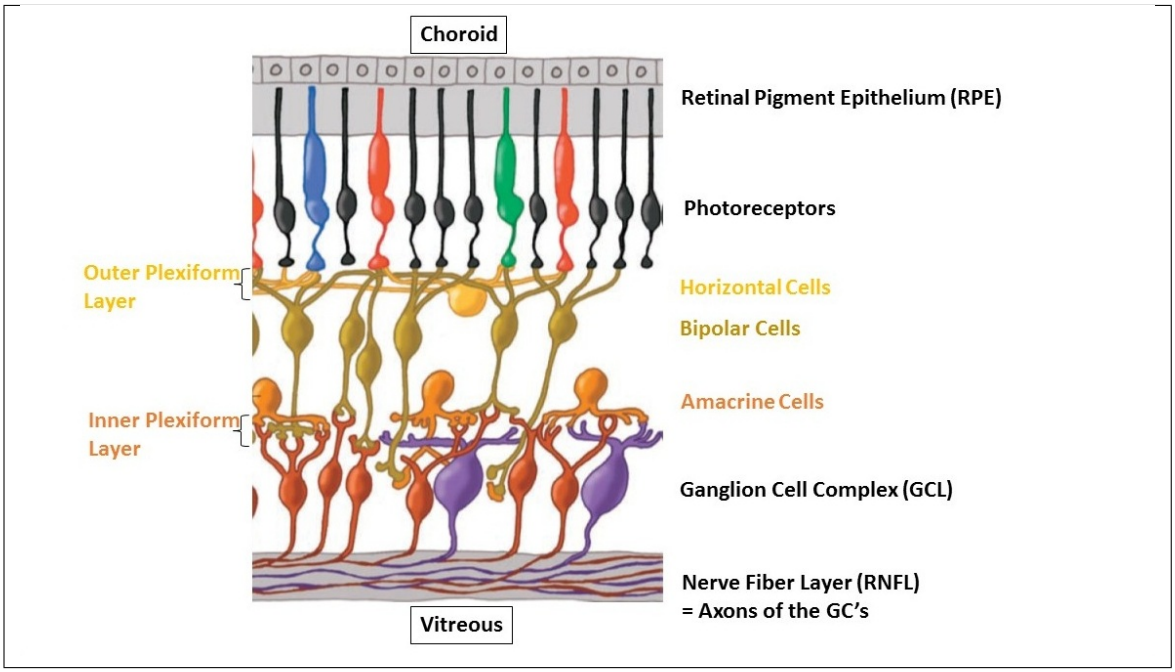

Figure 4: **Layers of the retina (adapted from http://webvision.med.utah.edu/)**

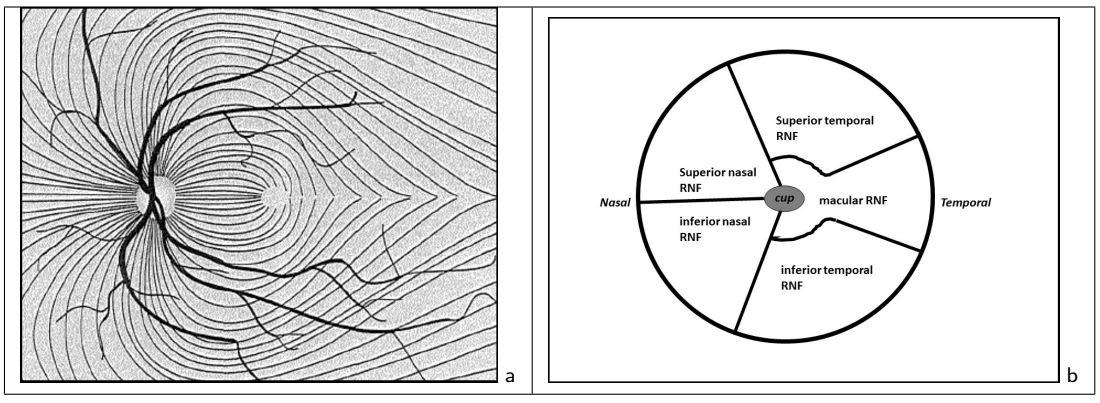

Figure 5: **Origin of the retinal nerve fibres: a) Retinal nerve fibre pattern at the retina (see [110, page 79, Fig 7-1]) b) Origin of the nerve fibres at the ONH**

Part III

Previous research findings - literature review

3. Visual function

In glaucoma the state-of-the-art visual function test in an optometric practice is perimetry (referred to as a visual field test). It is part of the clinical triad used to diagnose glaucoma (Clinical triad: Perimetry, IOP measurement and ONH assessment). In this study the Humphrey visual field analyser (HFA) was used to test visual function. It provides the SITA standard test strategy (Swedish Interactive Threshold Algorithm) which has been described in detail by Bengtsson et al. (1998) [14]. The SITA strategy is capable of reducing testing time by 66 % when compared to the Full threshold test and still showing high sensitivity and specificity ($>$96 %, [30]) in detecting glaucoma related losses [14]. To perform age-matched comparisons for MD_H, Pattern standard deviation, total deviation plot and standard pattern deviation plot the device utilizes the STATPAC II software which includes data of more than 275 otherwise healthy subjects aged between 10 and 80 years and refractive error $<\pm$5.00 D and astigmatism $<$ 3.00 D. Previous research has shown that MD_H is a useful marker to classify the extent of visual field (VF) loss in glaucoma, and thus was applied as variable in numerous previous studies to define study cohorts [31, 238, 144, 204, 228]. The mean deviation result (MD_H) refers to a generalised reduction (in dB) of visual field sensitivity of the subject when compared with an age-matched control group, as visual field sensitivity results reduce with older age. A percentage number after the MD_H-result exhibits the percentage of the control group participants revealing the same result and thus, refers to a probability measure. A more sophisticated method to classify sensitivity patterns (24-2 and 30-2 tests) based on focal losses commonly seen in glaucoma is given by the glaucoma hemifield test algorithm (GHT, see figure 6 a) [141, 5]. The GHT compares

five pattern deviation zones in the superior hemifield with the mirrored zones in the inferior hemifield. Results are stratified into "Within Normal Limits", "General reduction in sensitivity" or "Abnormally high sensitivity", "Borderline" and "Outside Normal Limits" based on probabilities of the normative database (STATPAC II, explained in section 8.1.1). It has been reported to have 84 % specificity in glaucoma diagnostic if borderline findings are considered "outside normal limits" [141].

Typical visual field loss in glaucoma is associated with pathology related structural changes (neuroretinal tissue loss and ONH atrophy, see figure 6 b) [313, 25, 222, 104, 238, 223]. Investigations of the relationship between RNFL thickness and VF results revealed a strong relationship between thinner RNFL regions and visual field losses at the associated hemifields [123].

Previous investigations reported a reduced sensitivity in visual field test results in myopic eyes [260, 7]. Aung et al. (2001) found a 0.2 dB reduction in MD_H per 1.00 D decrease in refractive error. Based on the previous findings it is possible that MD_H might be reduced in myopic eyes due to a reduced neuroretinal tissue thickness as result of a stretch to the retina.

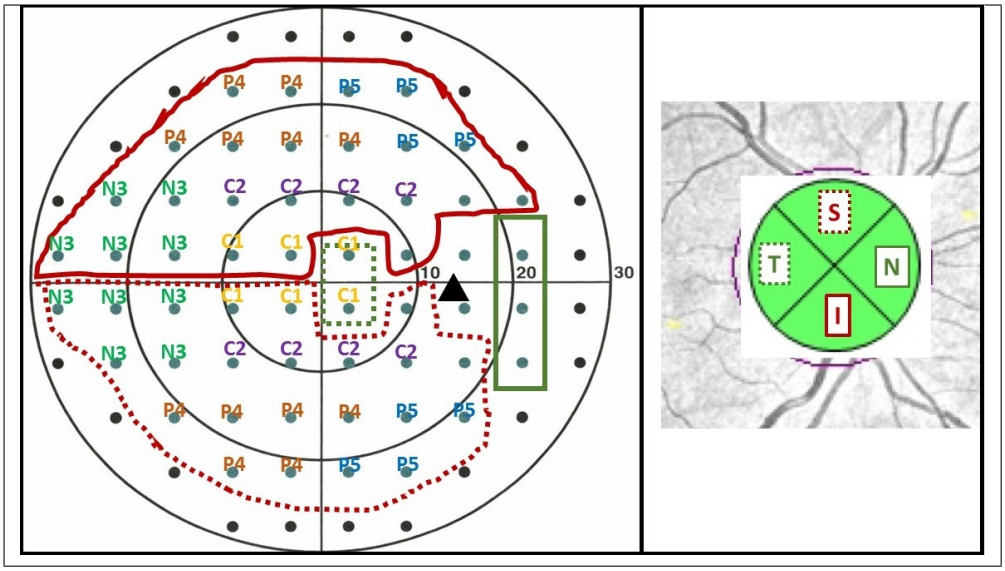

Figure 6: **The right image shows the glaucoma hemifield test points projected onto the 30-2 visual field test pattern. Furthermore, both images (left image: visual field test point pattern and right picture) show the association between neuroretinal rim quadrants and visual field test points in a 30-2 test pattern: The superior quadrant is represented by a red dotted line. The inferior quadrant is represented by a red line. The temporal quadrant is represented by a green dotted line. The nasal quadrant is represented by a green line.**

4. Retinal structure

Of particular interest in glaucoma diagnostic is the neuroretinal tissue (referred to as GCL and RNFL, see section 2.3) which dies gradually as the disease progresses [34, 133]. Quigley et al. (1987) reported a higher susceptibility of large fibres to be lost in glaucoma [250]. Nevertheless, the loss of neuroretinal tissue as observed in glaucoma is almost certainly represented by thinning of the RNF and GCL and precedes functional signs [249, 277].

The advent of optical coherence tomography technology (OCT) in the 1990s allowed the non-invasive measurement of thicknesses of single retinal layers. Thus, the measurement of RNFL and GCL thicknesses using OCT technology can be regarded as a indirect measurement of neuroretinal tissue loss. Previous studies on the reproducibility of RNFL measurements using OCT technology (described in detail in section 8.2.1) yielded intraclass correlation coefficients (ICC) of more than 0.89 [186, 74, 169, 214]. Furthermore, the reproducibility of RNFL thickness measurement expressed as inter-visit variation (SD) was found to range from 2.18 μm [329] to 7 μm [186] in healthy subjects. For GCL measurements, the inter-visit reproducibility yielded values between 1.16 μm [214] and 1.36 μm [329] for the average GCL thickness with a greater variability in inferior sectors. A study by Mwanza et al. (2011) found ICCs of 0.94 to 0.98 for inter-visit reproducibility in a cohort of fifty-one glaucoma subjects [214].

When interpreting the results of retinal thickness measurements it is crucial to be aware that the AL of the examined eye has a profound influence on the fixed measurement area size due to the effect of ocular magnification. This aspect accounts for all non-telecentric imaging systems (i.e. the Zeiss Cirrus HD-OCT which was used in this study) and is described in detail in section 4.1.

Previous studies revealed an independent influence of age and race on results of RNFL measurements. Regarding age dependency, studies reported a 1.9 μm [151] and 2 μm [28] reduction in RNFL thickness per decade of older age in cross-sectional studies, and 1.4 μm [329] up to 5.2 μm [171] reduction per decade in longitudinal studies. Whereas the average follow up time was 2.5 $\pm$ 1.2 years in the study of Zhang and colleagues, the average follow up time reported in the study by Leung and colleagues was 2.5 years

with a interval in between the measurements of 4 months. Leung et al. 2012 carried out a quadrant specific analysis and found a greater decrease of RNFL thickness in the inferior quadrant after adjusting for baseline thickness, refractive error, disc area and signal strength (-1.35 (95% CI, 2.05 to 0.65) μm/year). In the same study the nasal and temporal RNFL quadrants did not exhibit a significant reduction in thickness with age. Furthermore, RNFL thickness reduction proceeds more rapidly in subjects with thicker RNFL at baseline [171, 172]. Investigations on the influence of ethnicity revealed that subjects of Asian descent had the thickest (average) RNFL (M= 107.7 $\pm$ 9.9 μm) compared to other ethnic groups, and that Caucasians had the thinnest RNFL (M= 98.1 $\pm$ 10.9 μm) [28, 151, 211]. Gender was not found to influence the RNFL thickness results.

For the interpretation of the GCL thickness results there are two independent factors influencing the measurement; sex and age. Mwanza et al. (2011) studied the effect of age, ethnicity and sex for GCL results and revealed a stable GCL thickness between the age of 18 to 49 years. Above that age the GCL thickness decreases progressively. Furthermore, in men a significant thicker GCL thickness was found in the supero-temporal and infero-temporal sectors when compared with women. This relationship remained significant after accounting for AL. The same study did not find an effect of ethnicity on GCL thickness results [211]. An overview of the influences on RNFL and GCL thicknesses can be found in table 3.

Previous studies suggested that inferior RNFL as well as average (360^o) RNFL and GCL thickness have the greatest diagnostic value in glaucoma [25, 145, 238, 92]. The main feature in myopic eyes is the elongation of the eyeball, which can be determined by AL measurement (see section 8.2.4). Various investigations exploring the relationship between AL and/or spherical equivalent refractive error (SE) and the thickness of the RNFL found conflicting results. While some authors reported a significant decrease in RNFL thickness in superior and inferior peripapillary quadrants and a significant thickening in the temporal peripapillary quadrant [308, 140, 272, 144], other authors failed to find significant results [75, 124]. The conflicting findings can be explained by the influence of the elongation of the eye in myopes on the image size when thicknesses are

compared (ocular magnification). Many of these studies did not compensate for ocular magnification. Kang et al. (2010) found an inverse association between AL and average RNFL thickness when adjusting the (raw) measurement data for ocular magnification [140]. A consistent finding in the previous studies was a different distribution pattern of the RNFL thickness (referred to as redistribution of RNFL) in myopic eyes. In detail, the authors reported that the temporal RNFL thickness was increased whilst the other locations (nasal, superior and inferior) exhibited a decreased RNFL thickness. The different RNFL distribution pattern in myopic eyes can be explained by the shape of the elongated myopic eyeball (along the optical x-axis) and the anatomical position of the ONH (nasally to the optical axis) in the eye. In the direction of the y- axis tissue will be compressed (thickening) whilst in the direction of the x-axis the tissue will be stretched (thinner). Image 7 graphically shows this effect.

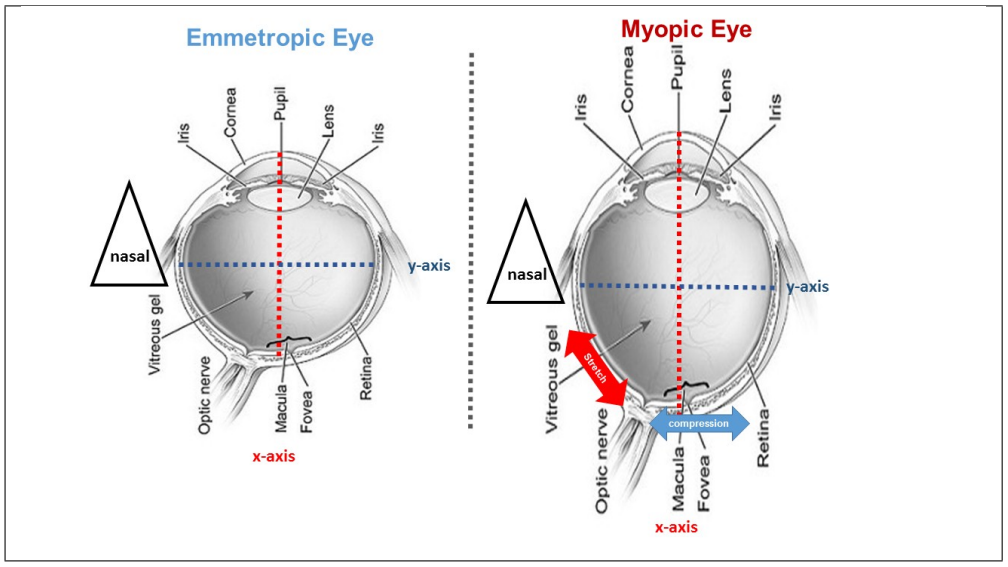

Figure 7: **The image represents an emmetropic eye (left side) and a myopic eye (right side). The rule of thumb for thicknesses in the peripapillary RNFL quadrants is: Inferior >Superior >Nasal >Temporal. In highly myopic eyes the eye is elongated. The stretching forces to the retina are stronger along the optical axis (x-axis) whilst less stretching force applies to the tissue in the direction of the y-axis. This results in a compression of tissue temporal to the ONH and a thinning of the tissue to the nasal side of the ONH in longer eyes.**

	RNFL measurement	GCL measurement	study-design
age	1.9 μm to 2 μm reduction per decade (Knight et al. 2012 [151], Budenz et al. 2007 [28])	1.7 $\pm$0.5 μm reduction per decade (Zhang et al. 2016 [329])	cross-sectional
	1.4 μm to 5.2 μm reduction per decade (Leung et al. 2012 [171])	2.5 $\pm$0.5 μm reduction per decade (Zhang et al. 2016 [329])	longitudinal
	greater decrease inferiorly (Leung et al. 2012 [171])		longitudinal
		stable between age 18 to 49 years (Mwanza et al. 2011 [211])	cross-sectional
		above 49 years progressive decrease (Mwanza et al. 2011 [211])	cross-sectional
ethnicity	Asians thickest global 360^o average (Mwanza et al. 2011, Knight et al. 2012 and Budenz et al. 2007 [211, 151, 28])		cross-sectional
	Caucasians thinnest global 360^o average (Mwanza et al. 2011, Knight et al. 2012 and Budenz et al. 2007 [211, 151, 28])		cross-sectional
		no influence (Mwanza et al. 2011 [211])	cross-sectional
gender	no influence (Mwanza et al. 2011 [211])	men thicker in temporal sectors than women (Mwanza et al. 2011 [211])	cross-sectional

Table 3: **Demographic influences on RNFL and GCL thicknesses according to previous research**

4.1. Ocular magnification - influence of ocular biometric data on retinal structure measurements

When interpreting the results of RNFL and GCL thickness measurement it is essential to be aware that refractive error and more importantly, axial length has an influence on the measurement area size of thickness measurements due to the effect of ocular magnification (OM). Ocular magnification occurs in non-telecentric imaging systems caused by the difference of the AL of the eye from the calibration AL of the device (24.46 mm for the Cirrus HD-OCT device used in this study). A previous investigation by Parthasarathy et al. in 2015 discussed the effect of OM on lateral measurements due to longer eyes in detail [239]. The lateral direction of the OCT image corresponds to the measurement area for the analysis of RNFL thickness (set at a 3.46 mm circular area)

and GCC thickness (elliptic annulus around the fovea, see also section 8.2.3). In other words, in eyes with shorter AL's than the calibration AL, the measurement area covers a smaller retinal area than in longer eyes resulting in incomparable analyses. A similar effect was found when different refractive errors were induced. Lee et al. (2010) reported an underestimation of thickness measurements for induced myopic refraction. Average RNFL thickness was underestimated by 0.50 μm (mean) per 1 D of induced myopic refractive error [162]. Unfortunately, the analysis software of the Cirrus HD-OCT does not compensate for varying axial lengths or refractive errors. Therefore, adjustments for OM were carried out for all RNFL and GCL thickness measurements before statistical analysis in this study. Section 8.2.5 describes the procedure of adjustment for ocular magnification.

4.1.1. Biometric measurement - AL

Axial length measurements determine the elongation of eyes and allow to calculate OM for non-telecentric devices with known calibration AL for unbiased comparisons. Previous studies using interferometric measurement principles revealed highly reliable AL and anterior chamber depth measurements (99 % and 97.8 %, respectively) [303, 44, 122, 50]. A high intra-observer reliability of ± 20 μm Hitzenberger et al. (1993)) up to ± 25.6 μm (Vogel et al. in 2001) was found for interferometric AL measurement principles [122, 303]. These values are standard deviations and were determined from eight to twelve consecutive measurements on 196 eyes of 100 cataract patients in the study published by Hitzenberger et al. (1993) and from 20 consecutive measurements of 10 emmetropic to mildly myopic, healthy subjects in the publication by Vogel et al. (2001). Hitzenberger reported that results carried out using an interferometric AL measurement principle were not influenced by the stage of cataract and thus, justify the use of it to determine intra-ocular lens dimensions [122].

Axial lengths between 22.6 mm and 24.09 mm are assigned "normal" and are associated with emmetropic eyes [105]. Thus, values above 24.09 mm might be considered as abnormal elongation of the eye and relate to myopia [46].

5. Retinal haemodynamic measurements and calculations

5.1. Retinal vessel oximetry

Besides OPP, the measurement of the oxygen content inside a retinal vessel (referred to as SO2 measurement) is likely to provide useful information on the supply and drainage of the retinal tissue. The first attempts of oxygen saturation measurement date back to 1959 and were made by John B. Hickam and colleagues [118, 117] and Francois C. Delori et al. (1988) [47]. A detailed historic review was published by James Beach (2014) [10]. In 1999 Beach et al. described in detail a method based on the Beer-Lambert-Law to measure the oxygen content in blood vessels using a two-wavelength imaging principle [11]. The research group determined experimentally an inverse linear relationship between the SO2 in % and the ratio of the logarithmic optical density value at the vessel plane and beside the vessel (surrounding retinal tissue). This density ratio is termed optical density ratio (ODR).

SO2 measurement is influenced by stray-light (referred to as light scattering, see [269]), back-scattering at the vessel wall (due to the index miss-match between the wall and the lumen of the vessel, see [161, 289]) and the pigmentation of the background-tissue (referred to as retinal pigmentation [11, 94]. Various constants (a,b,c,d in equation 2) and calibrations (measurements under oxygen breathing, wherein the arterial SO2 is known [11]) were introduced for determination of optical densities (OD) with the aim of compensating for influencing factors. Nevertheless, SO2 measurement is a relative measurement rather than an absolute one.

For gathering the SO2 data using the RVA system (RVA Imedos Systems UG, Jena), arteries and veins are. manually selected within a pre-defined measurement area and then computed by the software (figure 18). The measurement area is automatically chosen by the Vesselmap software to account for vessel diameter and fluctuation in fundus reflectance in accordance to findings of Schweitzer et al. (1999) [269] and Knudtson et al. (2003) [152].

$$SO2\% = 100\% - \left(\frac{ODR - ODR_{a,100}}{OS}\right) - (a - VD) \times b + \left(c - \frac{\log_{out}^{610}}{\log_{out}^{548}}\right) \times d \quad (2)$$

Hereby $ODR_{a,100}$ refers to as systemic SO2 obtained by fundus spectroscopy data for calibration purposes (see [11]). OS is the oxygen sensitivity derived from the knowledge that arteriovenous difference is 34% in the brain. The term $(a - VD) \times b$ refers to compensation for vessel diameter and was determined experimentally. $\left(c - \frac{\log_{out}^{610}}{\log_{out}^{548}}\right) \times d$ refers to compensation for the fundus pigmentation by melanin and is also determined experimentally.

SO2 reproducibility of the RVA instrument was found to be between 1.67 and 3.25 % (mean SD) for arteries and 2.52 and 5.6 % (mean SD) for veins [298, 160, 97, 294]. The measurement of arterial (aSO2) as well as venous SO2 (vSO2) and the calculation of the arterial-venous difference SO2 (A-V SO2 difference) from both measurements provides information about the distribution (aSO2), drainage (vSO2) and consumption (A-V SO2 difference) of oxygen in the retinal tissue. To gain quantitative information on "normative values" for aSO2 and vSO2 a meta-analysis was performed prior to the data-collection of this study. This quantitative synthesis of published literature until October 2016 included retinal vessel oximetry results carried out on the two commercially available devices: the Oxymap (Oxymap ehf., Iceland) and the RVA (RVA Imedos Systems UG, Jena). In summary, the meta-analysis revealed pooled retinal vessel oximetry results to be 93.70 % (95% CI, 92.92 % to 94.47 %) and 58.68 % (95% CI, 57.25 % to 60.10 %) for arterial and venous SO2, respectively. However, high heterogeneity which refers to the measure of the inter- and intra-study variation for pooled aSO2, vSO2 and A-V SO2 difference results (I^2 of 88 %, 94 % and 93 %, respectively) suggests the influence of co-variates (also known as moderator variables). Thus, subsequent meta-regression analyses investigated moderator variables such as "the device used", "ethnicity" and "age". While retinal vessel oximetry results of the two devices seem to be comparable (Mann-Whitney-U test, $p>0.05$ for aSO2, vSO2 and A-V SO2 difference, respectively), an influence of age and ethnicity (serves as surrogate for retinal pigmentation) on retinal vessel oximetry results was found (stratification reduced heterogeneity). The meta-analysis is described in section 5.1.1 below.

Meta-Analysis Introduction

The retina has one of the highest oxygen demands in the body. Constant supply is vital to ensure normal tissue function. Since the introduction of interferometric devices in the 1990s, such as Laser Doppler flowmetry and spectrophotometric imaging devices in the 2000s, it is possible to quantify not only blood flow (BF) and blood flow velocity (BFV) as well as oxygen saturation (i.e. oximetry) in vivo [11, 269, 13]. Changes in ocular BF are insufficient in describing the development of tissue hypoxia and/or neovascularization [12]. Thus, besides blood flow measurements, the assessment of oxygen saturation in retinal arteries (aSO2) and veins (vSO2) and its difference (A-V SO2 difference) can provide additional information on ocular haemodynamics in retinal pathologies. A considerable amount of literature on oxygen saturation measurements in retinal diseases has been published since its first introduction by Delori (1988) [47] and Beach et al. (1999) [11]. While some focussed on systemic diseases [296], others examined ocular pathology, normative data and measurement reliability (see table 5). For clinical decisions, the interpretation of changes in SO2 results rely not only on the precision of the instrument, but also on knowledge of the amount of change due to pathology and normative values. Thus, knowledge about alterations between consecutive measurements (i.e. repeatability and reliability) and normative values are crucial for clinical decision making. Normative data allows to interpret any difference observed to be "pathological" or "normal". Four previous investigations provide normative oximetry data of 329 healthy subjects [80, 184, 131, 202]. They explored associations with age and gender but yielded conflicting results. Whereas Man et al. (2014) [184] and Mohan et al. (2015) [202] found aSO2 and vSO2 to increase with age, Jani et al. (2014) revealed opposing results. Similarly to Jani et al., Geirsdottir et al. (2012) found the vSO2 and A-V SO2 difference to reduce with age, while aSO2 remained unchanged. Unfortunately, these findings do not reflect the true ageing-process due the cross-sectional study design. With respect to gender, Geiersdottir et al. (2012) [80] reported a decrease in venous saturation with increasing age in men, but not in women. The majority of current publications on retinal vessel oximetry used either the Oxymap oximeter (Oxymap ehf.,

Iceland) or the Oximetry module from Imedos (Vesselmap, Imedos Systems, Germany). Both devices use a dual wavelength technology to measure saturation parameters. For data comparisons, it is vital to establish whether the results of these two devices are in agreement or not. A recent review-article summarizing oximetry findings provided a qualitative analysis of ischemic retinal diseases [258]. The study included pathologies such as diabetic retinopathy and retinal vein occlusions. While this provides an overview of some findings, it lacks comparison to other common ocular diseases with a vascular component such as retinal vessel occlusions, glaucoma and AMD. The present meta-analysis expands the current evidence base by providing a quantitative comparison of SO2 parameters of healthy individuals and changes in SO2 due to vascular pathologies. Furthermore, combined knowledge of normative data and device reliability allows to distinguish between physiologic changes and measurement variation.

Meta-Analysis Methods

A meta-analysis approach was chosen in order to determine normative values and changes due to pathology in oxygen saturation parameters. There is evidence that combining results of "smaller" studies into one large data-set can provide the same significance as determined by one large study [21]. The pooled results for aSO2, vSO2 and A-V SO2 differences were analysed. A-V SO2 difference is not a direct measurement but provides important information as a surrogate measure of oxygen consumption [309, 178].

Inclusion and exclusion criteria: A description of the literature selection process can be found in Figure 8. Peer-reviewed English and German publications on dual wavelength retinal oximetry published until October 2016 were searched in PubMed and Web of Science. The search terms used were "oxygen + saturation" OR "oximetry" AND "retina* ". As the purpose of this study is to address the question of SO2 results in retinal vessels of human adults, animal- and "in vitro"-studies were excluded. Examinations determining oxygen saturation parameters using solely finger-pulse oximetry or measuring retinal tissue were also excluded as they determine oxygen saturation in the skin capillaries or the tissue, but not in the retinal circulation. To determine SO2 changes in retinal diseases, only case-control studies were included in the meta-analysis. Manually excluded

were review-papers and letters to the editor as they will not provide new data. In addition, in order to focus on retinal diseases only, reports on oximetry data of patients with pulmonary and cardio-vascular diseases were excluded.

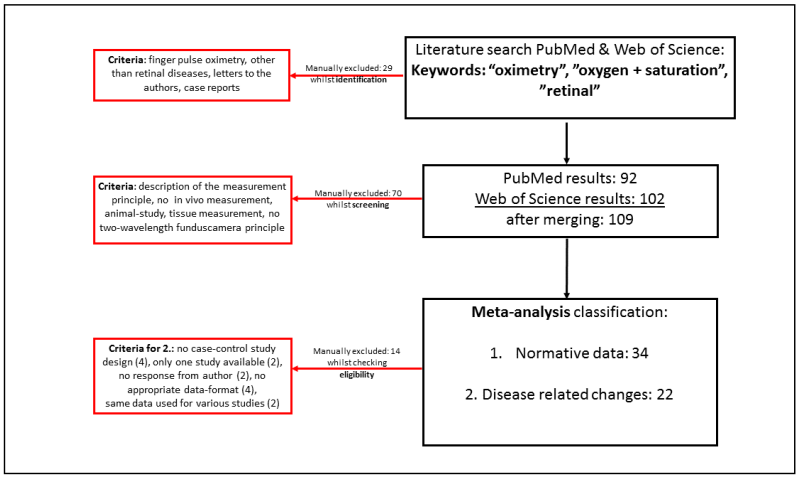

Figure 8: **Eligibility for meta-analysis**

Statistical analysis of the Meta-Analysis

To synthesize findings on oxygen saturation results a meta-analysis approach using the continuous random effects model (REM) applying the "DerSimonian-Laird" weighting method and a confidence level at 95% was carried out. The random effects model was chosen because it takes into account the variations across the studies ($SD\delta 2 \neq 0$) [266]. Factors known to influence retinal oxygen parameters such as device used, disease stage, age and ethnicity were employed as moderator variables (i.e. covariates) to explore their relationship. Effect sizes for the meta-analysis were defined as:

a) mean SO2 to determine normative data on SO2 parameters

b) SO2-differences (or change in SO2) were pathology related SO2 changes were analyzed.

To quantify the heterogeneity of the included studies the T^2 statistic was used. Herein the value for T^2 equals the true variability (variance) across the studies (referred to as dispersion of the effect) [22]. The I^2 statistic was used as a qualitative measure of the heterogeneity [120, 119]. The results of I^2 can vary between 0% and 100% with a value of I^2 =0% corresponding to an observed variance (T^2) solely due to study errors, whereas a value of 100% indicates that the observed variance is due to other factors. In cases of

high heterogeneity ($I^2 \geq 75\%$) further investigations, such as subgroup-analysis (referred to as meta-regression) was carried out. Heterogeneity was assigned according to Higgins et al. 2003 [120]:

$I^2 = 0\%$ no heterogeneity (▲)
$I^2 = 25\%$ low heterogeneity (△)
$I^2 = 50\%$ moderate heterogeneity (▽)
$I^2 = 75\%$ high heterogeneity (▼)

The critical point in carrying out a meta-analysis is the problem of not including all suitable studies, which is referred to as publication bias. Publication bias was tested graphically (funnel plots) according to Egger et al. (1997) [53]. Hereby the grade of asymmetry of the funnel plots indicates the grade of publication bias. In this approach an additional source of bias was the use of the same control subject data among several research publications resulting in duplicated data sets (data doubling bias). To avoid this type of bias, only the study with the largest number of healthy control subjects of a given research group was included to assess normative SO2 parameters unless there was more than 1.5 years between the publication dates or the research group in question confirmed that different subjects were included in their publications. The meta- and subgroup-analysis was performed using the open source software "OpenMetaAnalyst" Version 0.1503 (http://www.cebm.brown.edu/openmeta/). A p-value of less than 0.05 was regarded as significant for all analyses. Subsequent (logistic) regression analysis was carried out using Statistica 13.1 (Dell). After testing for a normal distribution the appropriate statistical test was chosen to investigate the relationships.

Results - qualitative analysis

Test-retest reliability

Twelve publications included data on test-retest reliability, inter- and intra-session reliability and short and long term reproducibility (see table 4). Results were given in various effect sizes, such as mean SD (%) in eight studies [98, 237, 182, 82, 194, 97, 160, 298], coefficient of variance (CoV,%) in three studies [97, 160, 298], limits of agreement (LoA,%) of Bland-Altman statistics in two studies [225, 147] and coefficients of repro-

ducibility (CoR, %) in one study [82]. Seven studies also provided intra-class correlation coefficients (ICC) [182, 325, 82, 147, 194, 160, 298]. While most data was collected from healthy participants only, three studies also examined eyes with pathology [98, 82, 298]. Due to aforementioned inconsistencies in effect size and methodology, a descriptive synthesis was conducted. All publications were in agreement with respect to vSO2 parameters showing larger variability than those obtained from retinal arteries. Table 4 provides a detailed overview of these studies and their findings. ICCs of arteries ranged from 0.82 [194] to 0.99 [325], whereas for retinal veins the lowest reported ICC was 0.59 [194] and the highest ICC was 0.99 [325]. Studies using SD measures as indicator for test reliability reported a group average SD for retinal arteries of 1.65 % [298] to 3.3 % [194] for the RVA device and 0.69 % [182] to 3.7 % [98] for the Oxymap instrument.

								Result artery			Result vein		
Author	Year of publication	Device	Subjects	Measurement protocol	Repetition of measurements	Reliability test protocol	mean SD [%]	CoV / LoA [%]	ICC	mean SD [%]	CoV / LoA [%]	ICC
Hardarson et al.	2006	Oxymap	10 diabetes +healthy)	1 major vessel segment,	5	5 consecutive images (automated analysis)	**3.70**	-	-	**5.30**	-	-
Palsson et al.	2012	Oxymap	26	1 vessel segment at st quadrant, (60 degree images)	2	two consecutive images of one session, one grader	**0.80**	±2 (LoA)	-	**1.3**	±2.5 (LoA)	-
Man et al.	2013	Oxymap	20	0.5 dd to 1 dd zone, 30 degree image	2	**intraobserver reliability** (two images 5 days apart, one observer), **interobserver reliability** (one image assessed by two graders) **Intrasubject reproducibility** (2 consecutive images 10 minutes apart, one grader)	0.56 1.22 **0.69**	-	0.99 0.94 **0.98**	0.55 1.01 **0.79**	-	0.99 0.98 **0.98**
Yip et al.	2013	Oxymap	50 20	1.0 dd to 1.5 dd zone, (50 degree image)	2	**Intragrader reliability** (one grader, two consecutive images taken 1 week apart), **Intergrader reliability** (one image assessed by two different graders), **Intravisit repeatability** (two consecutive images at one visit by one grader)	-	-	**0.93** (s-t) to **0.99** (i-t), 0.77 (s-n) to 0.94 (s-t and i-n), 0.88 (s-i) to 0.96 (i-t)	-	-	**0.89** (i-t) to **0.99** (s-t and s-n), 0.78 (s-t) to 0.94 (i-t), 0.85 (s-n) to 0.95 (i-n)
O'Connell	2014	Oxymap	18	all available vessels >120 micrometer, 50 degree image	10 taken - 2 used, 2 sessions	**Intrasession reliability** (2 consecutive images of one session, one grader), **Intersession reliability** (comparisson of means of 10 measurements of the two sessions, one grader)	-	±10.0 (LoA) ±4.0 (LoA)	-	-	±15.75 (LoA) ±8.75 (LoA)	-
Goharian et al.	2015	Oxymap	**22 healthy,** 29 glaucoma patients	4 main vessel pairs within 1.5 dd and 3 dd zone, 50 degree image	2	more than 2 high quality images, one grader	**0.86 (h)** 1.46 (gl)	**±0.96 (h)** ±1.6 (gl)	**0.97 (h)** 0.97 (gl)	**2.26 (h)** 2.36 (gl)	**±4.8 (h)** ±5.9 (gl)	**0.93 (h)** 0.96 (gl)
Kiefer et al.	2015	Oxymap	18	0.5 dd to 1 dd zone, 50 degree image	2	**Short-term** repeatability (two consecutive measurements, one grader) **Long-term** repeatability (1 to 102 days apart, one grader)	-	±1.9 (LoA) **±2.9 (LoA)**	0.98 **0.97**	-	±2.9 (LoA) **±4.7 (LoA)**	0.98 **0.93**
Michelson et al.	2006	RVA	12	1 distinct sites at the vessel, 1500x400 micrometer slit	10	10 consecutive measurements, one day	**3.30**	-	**0.82**	**8.00**	-	**0.69**
Hammer et al.	2008	RVA	10	10 vessel sections arteries and veins, 60 degree image	5	5 consecutive images	**2.62**	**±1.23**	-	**3.25**	**±1.78**	-
Lasta et al.	2012	RVA	20	3 branch vessel segments	3 to 6	**test-retest variability/** reproducibility (3 consecutive images assessed, one grader), **short-term** reproducibility (six images of one study day, one grader), **day-to-day** reproducibility (mean of day one versus mean of day two, one grader)	3.24 2.91 **3.97**	±3.18 ±2.42 **±2.67**	0.94 0.94 **0.91**	4.82 4.76 **6.18**	±3.57 ±3.14 **±3.36**	0.88 0.88 **0.84**
Heitmar et al.	2012	RVA	12	main branch, macular and peripheral zones, 30 degree image	3	**Short-term** variability (3 consecutive images, one grader)	Macular 1.8 Periphery 1.8	-	-	Macular 2.9 Periphery 4.7	-	-
Tuerksever et al.	2015	RVA	**22 healthy,** 18 glaucoma, 21 inherited retinal diseases	0.5 dd to 1 dd zone, 50 degree image	4	4 consecutive measures 10 seconds apart, one grader	**1.65 (h)** 1.83 (gl) 1.54 (IRD)	**±1.8 (h)** ±1.92 (gl) ±1.56 (IRD)	**0.92 (h)** 0.70 (gl) 0.93 (IRD)	**2.33 (h)** 2.85 (gl) 2.43 (IRD)	**±4.48 (h)** ±4.71 (gl) ±3.9 (IRD)	**0.76 (h)** 0.69 (gl) 0.82 (IRD)

Table 4: **Summary of studies on reliability of the method**

Retinal artery occlusion

In case of a retinal artery occlusion (RAO) Gehlert et al. (2010) explored the change in oxygen saturation in a pre and post treatment for RAO including 11 patients [78]. They showed that arterial and venous SO2 baseline measurements (aSO2 of 73 $\pm$ 16 %, vSO2 of 55 $\pm$ 14 %) increased after treatment (87 $\pm$ 11 % and 59 $\pm$ 8 %, respectively).

Age-related macular degeneration

Similar to data on RAO, till October 2016 little informationwas available on oximetry findings in AMD. The only study published to date by Geiersdottir et al. (2014) compares oxygen saturation measurements of 46 eyes of patients with exudative age-related macular degeneration (AMD) and 120 eyes of healthy controls [79]. The comparison showed no difference in aSO2. However, venous saturation was found to be higher in patients with exudative AMD than in controls for those of the age of 76 years and older. In addition, patients with exudative AMD showed a reduced A-V SO2 difference than the control group. This reduction was particularly pronounced in patients older than 70 years of age.

Results - meta-analysis

General data

Testing for publication bias for the meta-analyses revealed high symmetry for arterial, venous SO2 and the A-V SO2 difference (figure 9).

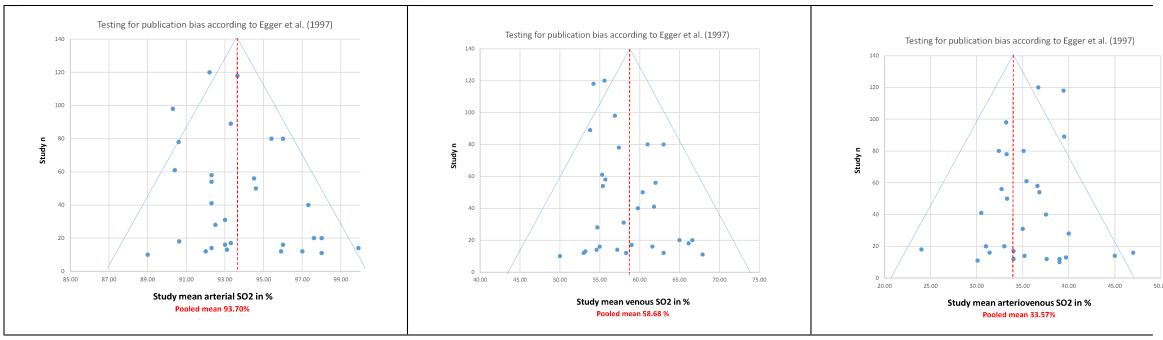

Figure 9: **Funnel plots to test for publication bias**

The meta-analyses for normative SO2 results included pooled oxygen saturation results of 28 investigations. In total the healthy cohort consisted of 1287 participants. Table 5

on the following page shows the characteristic of the studies to obtain normative data results. The disease related meta-analysis approach covers the following pathologies:

- Diabetes and diabetic retinopathy: 8 publications, 524 patients in total
- Glaucoma (OAG): four publications, 257 patients in total
- Retinal vein occlusion: five publications, 107 patients in total,
- Retinitis Pigmentosa: five publications, 178 patients in total

Category/ objective of publication	**Number of studies**	**Number of healthy subjects**	**References**
Reliability	5	184	[97, 115, 325, 225, 98]
Sensitivity / Influences	4	91	[270, 236] [113, 111]
Normative	4	329	[184, 131, 80]
Glaucoma	4	241	[194, 227, 253, 301]
Diabetes	6	184	[96, 101, 93, 143, 139, 148]
Retinitis Pigmentosa	4	241	[293, 300, 334, 9]
Other disease	1	17	[296]
Total	**28**	**1287**	

Table 5: **Studies included for pooled normative estimates of SO_2 measurements**

Pathology	Author (Year) [reference]	Number of patients [n]	Device
Diabetes/ DR	**Schweitzer et al. (2007) [270]**	56	RVA
	Hammer et al. (2009) [96]	41	RVA
	Hardarson & Stefansson (2012) [101]	20	Oxymap T1
	Hammer et al. (2012) [93]	18	RVA
	Khoobehi et al. (2013) [143]	93	Oxymap T1
	Joergensen et al. (2014) [139]	156 (-30)	Oxymap T1
	Joergensen and Bek (2014) [138]	149	Oxymap T1
	Klefter et al. (2015) [148]	21	Oxymap T1
Glaucoma	**Michelson and Scibor (2006) [194]**	94	RVA
	Ramm et al. (2014) [253]	41	RVA
	Olafsdottir et al. (2014) [228]	74	Oxymap T1
	van Keer et al (2015) [301]	48	Oxymap T1
RVO	**Hardarson et al. (2010) [99]**	8	Oxymap T1
	Hardarson et al. (2012) [100]	18	Oxymap T1
	Eliasdottir et al. (2015) [54]	14	Oxymap T1
	Traustason et al. (2014) [295]	17	Oxymap T1
	Lin et al. (2015) [177]	50	Oxymap T1
RP	**Eysteinsson et al. (2014) [56]**	10	Oxymap T1
	Battu et al. (2015) [9]	29	Oxymap T1
	Zong et al. (2015) [334]	68	Oxymap T1
	Ueda-Consolvo et al. (2015) [300]	28	Oxymap T1
	Todorova et al. (2015) [293]	43	RVA

Table 6: **Studies included for disease related changes in SO2. NOTE: Joergensen and Bek (2015) expanded the patient group of the previous study of Joergensen et al. (2014), which results in a reduction of the total number of included patients in the meta-analysis by 30. In studies investigating retinal vein occlusions the affected eyes were compared with the fellow eyes**.

The pooled SO2 result is given by the changes in oxygen saturation when the patient cohort was compared to a healthy cohort (difference between the mean result of the control group and the patient group). Twenty-two studies incorporating 1066 patients were included in this approach (table 6).

Normative data

In a healthy population the pooled arterial and venous SO2 are 93.7 % and 58.68 %, respectively. Furthermore, the pooled results for A-V SO2 difference was 35.57 %. Heterogeneity of these results was high for the three oxygen saturation aspects. Table 8 shows details of the analyses. The across study variation T^2 revealed 3.31% for aSO2 and 16.48 % for vSO2 measurements. Consecutive logistic regression analysis revealed comparable results for the two different devices used to obtain SO2 measurements: p= .121, p= .427 and p= .106 for arterial, venous and A-V difference SO2 results (Mann-Whitney U-test for independent variables).

While **ethnicity** was correlated with aSO2 (Kruskal-Wallis ANOVA, H(2,n=96)= 25.50886, p< .01) venous and A-V SO2 difference were not correlated with ethnicity (Kruskal-Wallis ANOVA, H(2,n=95)= 5.8529, p= .0523 and H(2,n=96)= 0.2416, p= .8862 for venous and A-V difference SO2, respectively). Figure 10 synthesizes the findings.

Furthermore, arterial and venous SO2 were correlated with **age** (Kruskal-Wallis ANOVA: p< .01 for both), while there was no significant relationship between A-V SO2 difference and age (Kruskal-Wallis ANOVA: p= .087). The subgroup analyses with age as moderator variable revealed a reduction in heterogeneity to moderate and low levels for young age groups (see figure 11). However, for aSO2 the heterogeneity of the subgroup analysis remained high in the age groups "40 to 50 years" and "50 to 60 years" (I^2= 89.72 % and I^2= 89.64 %, respectively) while for vSO2 the heterogeneity remained high in the age groups "50 to 60 years" and "60 to 70 years"(I^2= 97.63 % and I^2= 87.1 %, respectively).

	pooled result (95% CI)	**I2, p**	**T2 (across study variation)**
arterial SO2	93.7% (92.92% to 94.47%)	87.57%, p≺0.01	3.31%
venous SO2	58.68% (57.25% to 60.10%)	93.78%, p≺0.01	16.48%
A-V SO2	35.57% (34.33 to 36.80%)	93.09%, p≺0.01	NA

Table 8: **Summary normative SO2 values**

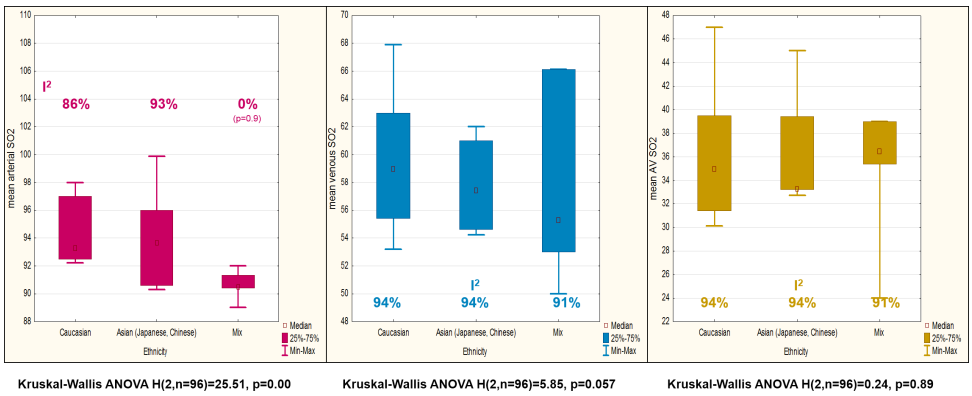

Figure 10: **Influence of retinal pigmentation (given by ethnicity of subjects) on SO2 results.**

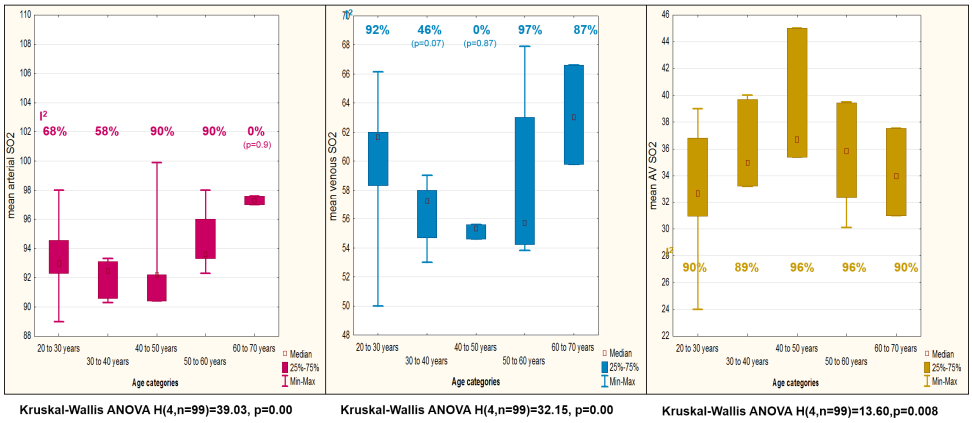

Figure 11: **Influence of age (from mean ages individual studies) on SO2 results**

Diabetis and diabetic retinopathy

Eight studies (524 included patients in total) were included for the diabetes related meta-analysis approach. In three studies aSO2 was found to be significantly increased in the patient group after adjustments for age were made [101, 143, 148]. For vSO2 measurements three studies exhibited a significant higher oxygen saturation in the diabetes group when compared with an age-matched control group [96, 101, 143]. Furthermore, two studies revealed a significant reduction in A-V SO2 difference in diabetes patients [96, 139]. Uniformly, all included studies found a relationship of SO2 measurements with the stage/severity of the disease. Table 9 synthesizes the meta-analysis results for diabetes.

Diabetes and DR	aSO_2[%]	vSO_2 [%]	AV-SO_2 [%]
	↑	↑↑	↓
Pooled difference in SO_2	-2.77	-5.47	2.14
95% CI	(-3.90 to -1.65)	(-6.86 to - 4.09)	(0.72 to 3.55)
overall Heterogeneity I^2	74.36%, p <0.01 ▼	69.51%, p <0.01 ▼	75.1%, p <0.01 ▼
Heterogeneity I^2 of subgroup "no DR"	74.95%, p=0.05 ▽	0%, p=0.84 ▲ (pooled difference -1.26)	69.74%, p=0.07 ▽ (pooled difference -0.31)
Heterogeneity I^2 of subgroup "moderate NPDR"	87.17%, p=0.00▼	0%, p=0.74 ▲ (pooled difference -11.21)	36.06%, p=0.21 △ (pooled difference 4.69)

Table 9: **Synthesis of findings in diabetes and diabetic retinopathy. Stratification into severity of diabetic retinopathy improved the results for vSO2 findings for the categories "no DR" and "moderate NPDR" and the arteriovenous SO2 findings for "moderate NPDR". For aSO2 the subgroup analysis could not improve heterogeneity level. ▼= high heterogeneity; ▽= moderate heterogeneity; △=low heterogeneity; ▲=no heterogeneity**

Retinal vein occlusion

Five studies (107 patients in total) exploring oximetry measurements in RVO were included. All investigations compared affected eyes with the fellow eyes. One study exploring oxygen saturation changes in branch retinal vein occlusion (BRVO) compared SO2 results of affected eyes versus eyes of a healthy control group [177]. Furthermore, the studies were grouped into central retinal vein occlusion (CRVO, two studies) and BRVO (three studies). All studies used the Oxymap device to carry out oximetry. A subgroup analysis with the co-variate "CRVO vs BRVO" revealed homogeneous findings for CRVO ($I^2 = 0$ %) although not significant (p= .44). Further exclusion of the ischemic cases in BRVO revealed homogeneity ($I^2 = 0$ %, p= .67) for aSO2 results although this effect is not significant. For the vSO2 results the exclusion of ischemic cases had no effect. A synthesis of the meta-analysis results (pooled differences in SO2 between healthy and diseased study groups) in oximetry for RVO can be found in table 10.

RVO	aSO_2[%]	vSO_2 [%]	AV-SO_2 [%]
CRVO	↑↑	↓↓	-
BRVO	↑	↓	-
Pooled difference in SO_2 (95% CI) **CRVO**	-0.56 (-3.63 to 2.51)	18.72 (12.43 to 25.00%)	-
Pooled difference in SO_2 (95% CI) **BRVO**	-6.16 (-10.5 to -1.80)	9.31 (-4.12 to 22.74)	-
Heterogeneity I^2CRVO	0%, p=0.75 ▲	0%, p=0.44 ▲	-
Heterogeneity I^2BRVO	39.98%, p=0.17 Δ	92.09%, p=0.00 ▼	-
Heterogeneity I^2 in BRVO, exclusion of ischemic type in study of Lin et al (2015)	0%, p=0.53 ▲ (pooled difference -2.0)	91.51%, p=0.00 ▼	-

Table 10: **Synthesis of findings in Retinal vein occlusions (RVO) stratified into central vein occlusion (CRVO) and branch retinal vein occlusion (BRVO). Heterogeneity for pooled aSO2 improved (0%) after exclusion of ischemic types of BRVO. ▼= high heterogeneity; ∇= moderate heterogeneity; Δ=low heterogeneity; ▲=no heterogeneity**

Glaucoma

Four studies (257 patients) were included for open angle **glaucoma** (referred to as OAG) related analyses. Michelson et al 2006 [194] additionally investigated retinal vessel oxygen saturation measurement in normal tension glaucoma (NTG). The study of Olafsdottir and colleagues in 2014 [228] investigated the relationship between the stage of the disease (defined by visual field mean defect) and SO2 results. The study revealed an increasing vSO2 and decreasing A-V SO2 difference as glaucoma progresses.

For aSO2 one out of four studies found a significant increase (Van Keer et al. 2015 [301]). A significantly increased vSO2 was found in three out of four studies. However, the study of Michelson and colleagues investigating SO2 in NTG, showed a tendency of increased vSO2 [194]. A significantly decreased A-V SO2 difference was found in 75% of the investigations [228, 253, 301]. Table 11 provides the synthesis of the meta-analysis results.

Glaucoma	aSO_2 [%]	vSO_2 [%]	AV-SO_2 [%]
	$\approx$	$\uparrow\uparrow$	$\downarrow\downarrow$
Pooled difference in SO_2	-0.31	-2.96	2.50
(95% CI)	(-1.82 to 1.19)	(-4.91 to -1)	(1.03 to 3.98)
Heterogeneity I^2	83.56%, p<0.01 ▼	64.25%, p=0.02 ▽	43.65%, p=0.11 △
Heterogeneity I^2, exclusion Michelson and Scibor (NTG) and Van Keer et al. (2015)	39.59%, p=0.19 △ (pooled difference -0.08)	NE	NE
Heterogeneity I^2, exclusion Van Keer et al. (2015)	NE	18.94%, p=0.30 ▲ (pooled difference -2.05)	NE

Table 11: **Synthesis of findings in glaucoma. NE = no effect; ▼= high heterogeneity; ▽= moderate heterogeneity; △=low heterogeneity; ▲=no heterogeneity**

Retinitis Pigmentosa

Five studies (178 eyes in total) were included for the meta-analyses regarding **retinitis pigmentosa** (RP). Todorova et al. (2015) [293] included primarily both (43) eyes of 22 patients, whereas Eysteinsson et al 2014 [56] included 7 eyes of 10 patients for aSO2 measurements and 10 eyes of 10 patients for vSO2. In 80 percent of the studies aSO2 is increased in patients with RP. All studies found a higher vSO2 when compared with a healthy control group. The study from Zong et al. (2015) categorized the RP patients in "young" patients (mean age ± SD: 28.5 years±4.6 years) and in "older" patients (mean age ± SD: 50.9 years±6.6 years) [334]. They found a significant difference in vSO2 only for the old patient group.

Regarding A-V SO2 difference the studies mirror the results from aSO2: Four out of five studies revealed a decreased A-V SO2 difference, whereas the study of Battu and colleagues (2015) revealed larger A-V SO2 difference results for the patient group [9]. Furthermore, this study found significant higher aSO2 in younger patients and a significant lower aSO2 in older patients. The results for the A-V SO2 difference were similar. For vSO2 results these relationships were not significant. A synthesis of the meta-analysis results for RP can be found in table 12.

Retinitis pigmentosa	aSO_2 [%]	vSO_2 [%]	AV-SO_2 [%]
	↑↑	↑↑	↓
Pooled difference in SO_2	-3.67	-5.05	1.12
(95% CI)	(-8.78 to 1.27)	(-8.91 to -1.20)	(-5.22 to 7.45)
Heterogeneity I^2	93.41%, p<0.01 ▼	89.85%, p<0.01 ▼	94.59%, p<0.01 ▼

Table 12: **Synthesis of findings in retinitis pigmentosa. ▼= high heterogeneity; ∇= moderate heterogeneity; Δ=low heterogeneity; ▲=no heterogeneity**

Discussion and Conclusion of the Meta-Analysis

This meta-analysis is a synthesis of retinal vessel oximetry results in healthy and diseased retinas. The findings indicate that retinal vessel oximetry might allow to monitor and classify retinal diseases in providing an additional haemodynamic measurement. With respect to reliability of measurement, a meta-analysis approach was not possible due to inconsistency in outcome variables and procedural differences. Furthermore, only one study existed for AMD and retinal artery occlusions resulting in a qualitative synthesis of the findings rather than a meta-analysis approach.

Reliability: Investigations on test-retest reliability consistently showed a greater variation for vSO2 than for aSO2 measurements (table 4 shows details). Furthermore, the results suggest a similar short-term repeatability for aSO2 for both devices, the Oxymap and the RVA when comparable measurement protocols were used (LoA for Oxymap derived data (healthy): 1.9% and LoA for RVA derived data (healthy): 1.8%, table 4). However, the same does not hold true for vSO2: The Oxymap device exhibited lower variance than the RVA for short-term repeatability (CoV Oxymap: 2.9 % vs CoV RVA: 4.48 %, healthy eyes). These differences may be mainly a result of different measurement algorithms.

Normative: For normative data across study variation (T^2) for arteries was within the range of reliability for both devices (T^2 arteries = 3.31%) and, for veins T^2 was within the reliability-range for the RVA device (T^2= 16.46 %). Thus, SO2 results can be considered "normative". Subsequently, subgroup analyses were carried out to detect moderator variables to explain high heterogeneity results (I^2= 87.57 % for arterial, I^2= 93.76 % for venous and I^2= 93.09 % for A-V SO2 difference).

Besides the device used for measurement, age and ethnicity (a surrogate for retinal pig-

mentation) could potentially influence SO2 results. The subgroup-analyses regarding age reduced heterogeneity to moderate or low levels for various age groups suggesting that age might have an influence on oximetry results. However, heterogeneity remained high for aSO2 in the age groups within the range 40 to 60 years and for vSO2 in the age groups within the range 50 to 70 years. For A-V SO2 difference heterogeneity remained high for all age groups. A possible explanation of the remaining (high) heterogeneity in "older" age groups may be the effect of measurement artefacts due to media opacity (e.g. cataract) or alterations in systemic blood circulation (e.g. systemic hypertension). In older participants (above age 50) it is very likely that the haemodynamic measurements are affected by cataract and systemic diseases [111]. However, previous investigations regarding the age vs SO2 relationship for oximetry data revealed conflicting findings [80, 131, 184, 202]. Whereas Man et al. (2014) [184] and Mohan et al. (2015) [202] found arterial and venous SO2 to increase with increasing age, a study of Jani et al. (2014) [131] revealed opposing results. Similarly to Jani et al., Geirsdottir et al. (2012) reported a decrease in vSO2 and an increase in A-V SO2 difference with increasing age whilst aSO2 remained stable[80]. Unfortunately, the cross-sectional study design of these studies does not sufficiently reflect ageing-processes. In this study a consecutive curve fit analyses for arterial and venous SO2 results (mean age as dependent variable) exhibited a third-degree polynomial for age whereas previously mentioned studies assumed a linear model. Nevertheless, this study added data of further 24 studies to explore the age vs SO2 relationship. The results suggest that other effects, such as retinal pigmentation, structural changes in vessel wall reflectance and image quality (cataract, i.e.) due to media opacity might likewise contribute to SO2 results [97, 111, 130].

With respect to the influence of retinal pigmentation on oximetry measurements, Hammer et al. (2008) [97] found a significant influence of iris colour (referring to as retinal pigmentation) on venous oximetry results. A compensation term was added to the SO2 calculation algorithm in the RVA system. Other authors found no significant association between retinal pigmentation represented by the ethnicity of the study cohort and SO2 results when the Oxymap device was used [131]. This study investigated the influence of retinal pigmentation given by the ethnicity of the study groups. Neither pooled vSO2

nor A-V SO2 difference results exhibited a significant association with ethnicity (Kruskal-Wallis ANOVA, p= .0536 for vSO2 and p= .8862 for A-V SO2 difference), while pooled aSO2 was significantly associated with ethnicity. Moreover, this study synthesized results measured by two different devices (Oxymap and RVA) using different algorithms. However, the result of the Mann-Whitney U-test confirms the comparability of both devices (Mann Whitney U test: U = 976; p= .1225 for arterial, U = 1088; p= .429 for venous and U = 986: p= .107 for A-V SO2 difference). Separate subgroup-analyses for ethnicity showed comparable heterogeneity results, whilst the standard error was larger in the mixed ethnicity cohort when compared to Caucasian or Asian cohorts. Possible reasons for our findings might be firstly, that ethnicity is not a sufficient marker for retinal pigmentation. A more detailed stratification such as e.g. a classification scheme regarding iris colour, may be a more appropriate marker to referring to retinal pigmentation [69]. Nonetheless, data for iris colour of the study subjects were not available for this study. In summary, our investigation suggests that variation in pigmentation is rather represented in standard errors than in heterogeneity results.

DR: Central characteristic features in diabetes and diabetic retinopathy (DR) are thought to be the alteration in blood glucose level leading to a disturbed blood circulation and consequently, retinal tissue impairment [285]. Therefore, investigations on oxygen supply and consumption of the retinal tissue (retinal vessel oximetry) might add additional information on retinal heamodynamic characteristic in diabetes. Meta-analysis results exhibited high heterogeneity for all pooled SO2 results (see table 9) which were reduced for vSO2 and A-V SO2 difference due to stratification into severity stages (moderate NPDR showed I^2= 0 % for pooled vSO2 results and I^2= 36.06 % for pooled A-V SO2 difference results). This finding suggests that the severity/stage of the disease influences the SO2 results. Unfortunately, not all authors classified DR stages equally which resulted in inconclusive subgroup-analyses for DR stages (no information on heterogeneity for some stages). Moreover, oxygen saturation measurements in retinal vessels do not reflect any micro-circulatory (capillaries) dysfunction occurring in diabetes and hence, do not provide the full picture of blood circulatory disturbances in DR [285].

RVO: Retinal vein occlusion is a retinal pathology which has a strong linkage with

vascular dysfunctions (vessel wall injury, hypercoagulability, stasis) of either systemic or ocular nature [153]. Thus, it has to be expected that retinal vessel oxygen saturation is affected in the disease. RVO is classified according to the affected location into central vein occlusion (CRVO), hemi-central retinal vein occlusion (HCVO) and branch retinal vein occlusion (BRVO) which might refer to as severity of RVO. The findings of this meta-analysis represent this hypothesis by revealing larger changes in pooled SO2 results in CRVO than in BRVO (see table 10). The meta-analysis for CRVO results showed homogeneous findings (see table 10). The exclusion of the ischaemic BRVO study group in the BRVO category resulted in 0% heterogeneity for pooled aSO2 results suggesting a strong effect of the disease stage (severity). Nonetheless, the exclusion of the ischaemic subgroup had no effect on heterogeneity for pooled vSO2 results. Measurement artefacts might explain the persisting high heterogeneity and large variation in venous results (vSO2 difference variation in between studies from - 4.12 % up to 22.74 %, table 10). Generally, authors reported difficulty in vessel depiction for determination of the SO2 in RVO patients suggesting that measurement artefacts contribute to SO2 results in RVO.

Glaucoma: Glaucoma is a chronic disease leading to damage of the optic nerve head and the neuroretinal tissue due to an imbalance between ocular perfusion and blood flow [62]. Thus, it is hypothesized that the retinal oxygen metabolism is altered in glaucoma. All included studies reported an increase in vSO2 results (table 11), although not statistically significant in one of them. Heterogeneity was moderate for pooled vSO2 (I^2= 64.25%, p= .02) and improved after exclusion of the study of van Keer et al. [301] to a low level (I^2 = 18.94%, p= .30). This study did not adjust for age in SO2 comparisons. For pooled A-V SO2 difference results the meta-analysis results exhibited moderate heterogeneity (I^2 = 43.65 %, p= .11). The arterial results showed a high heterogeneity (I^2 = 83.56%, p<0.01) which improved to a moderate level (I^2 = 39.59 %, p= .19) after exclusion of the normal tension glaucoma group of the studies of Michelson and Scibor [194] and Van Keer et al. [301]. The findings of this meta-analysis indicate that the oxygen consumption of the retina is reduced in glaucoma, which may reflect retinal tissue apoptosis in glaucoma. Further evidence for this hypothesis is the correlation between the extend of mean deviation (MD) in visual field results and increased vSO2 results in

the study of Olafsdottir et al. [228].

RP: Retinitis (RP) is a hereditary retinal dystrophy affecting the retinal photoreceptors. The retinal appearance in RP shows typical signs, such as retinal bone-spicule pigment, arterial attenuation and a waxy disc pallor (triad in RP). These changes in retinal morphology might affect any reflectivity measurement, such as retinal oximetry. In RP, the majority of investigations (80 %) found an increased aSO2. Additionally, all studies determined an increased vSO2 and a reduced A-V SO2 difference (see table 12). Larger vSO2 and lower A-V SO2 difference findings may be a consequence of a reduced oxygen consumption in diseased retinas. However, measurement artefacts due to narrower arteries resulting in an overestimation of SO2 results in RP may partly explain increased aSO2 results [269]. Nonetheless, heterogeneity findings were high for all effect sizes (arterial, venous and A-V SO2 difference, table 12) and could not be improved by any study exclusion or stratification. Moreover, it is noticeable that photoreceptors are supplied by the choroid. Thus, changes in retinal blood circulation as measured in retinal vessel oximetry might not conclusively explain atrophic changes occurring in RP [9].

In summary, besides a deeper insight into the field of oximetry, this study faced various limitations: Firstly, six studies were excluded due to authors not responding. Secondly, the effect sizes used for the analysis approach were the individual study means rather than their raw data, which might have biased the outcome of the meta-analysis. Finally, it is important to note, that SO2 measurement in retinal vessels reflects only the retinal blood circulation. Nevertheless, this study was able to synthesize quantitatively previous retinal vessel oximetry findings in various retinal diseases as well as in "normal" eyes. Oximetry shows adds to the knowledge of the oxygen metabolism in diseases and may be an additional tool to monitor retinal diseases and disease progression.

Since finishing the meta-analysis, a study of Told et al. (2018) showed a significant difference for aSO2 between the two devices while vSO2 did not show a significant difference [294]. With respect to the impact of age on oxygen saturation the results of previous research were conflicting. This study applied the findings of Man et al. (2014) and Mohan et al. (2015) to weight comparison analyses for age [184, 202]. The reasons for this choice were firstly, that the meta-analysis used mean ages (of individual studies)

instead of an exact age categorization to determine the age- SO2 relationship resulting in less robust findings. Secondly, both studies used the same device as this study (RVA) for data collection. Hence, the findings might be best applicable to determine weighting factors for SO2 data in the present study. Both studies found a significant increase of aSO2 and vSO2 with age ($\beta_{arteries}$=0.31 and β_{veins}=0.26 for the study of Man and colleagues and $\beta_{arteries}$=0.26 and β_{veins}=0.19 for the study of Mohan and colleagues). Furthermore, the meta-analysis synthesized data of four case-control studies comparing oxygen saturation results of glaucoma patients with healthy controls (see table 11) [301, 253, 228, 194]. Whereas the studies of Michelson et al., Ramm et al. and Olafsdottir et al. compared findings of the glaucoma cohorts with healthy subjects of similar age, the study of van Keer et al. compared mean SO2 of a young control group (mean age 21.6 $\pm$ 1.1 years) with those in a glaucoma group of a mean age 72.0 $\pm$ 9.1 years. All studies found conclusively higher vSO2 results accompanied with decreased A-V SO2 difference results indicating a reduced oxygen consumption in glaucoma. Moreover, the heterogeneity of the meta-analysis results for vSO2 improved from 64 % to 19 % when the findings of the publication by Van Keer was excluded (see table 11).

Similar to the findings for glaucoma, studies published by Man et al. (2013) and Zheng et al (2015) revealed a reduced oxygen consumption in myopic retinas [183, 330]. Both studies suggested that the oxygen consumption in myopic eyes is reduced due to a thinner retina requiring less oxygen.

5.2. Static vessel analysis

Static vessel analysis is the determination of retinal vessel diameter by computing the mean width of an equal number of manually selected arterial or venous vessel segments (referred to as CRAE and CRVE) and, calculated from both the arterio-venous ratio (AVR). It describes the width of the vessels and its branching characteristics. The method to determine CRAE and CRVE was introduced by Hubbard in 1999 [128] and refined to account better for branching characteristics of the vessels in 2003 [152]. Static vessel analysis is proven to depict vessel abnormalities that might be predictive markers for the risk of developing cerebrovascular and cardiovascular diseases [189, 128,

315, 281]. Additionally, the longitudinal study arm of the Blue Mountains Eye Study (BMES) revealed that narrower arterial calibres are associated with a 1.77-fold higher susceptibility to develop open angle glaucoma [142]. Thinner vessel calibres were also related to thinner RNFL in glaucoma [35, 331] as well as with myopia [240]. Wong et al. (2004) found a narrowing of 2.8 μm in arteries and 3.3 μm in veins per -1.00 D increase in refractive error (BDES, [317]). The same study (BDES) additionally reported the influence of age on the narrowing of retinal arteries. The authors reported a 0.22 μm decrease of arterial calibre per one year increase of age [317]. As this narrowing occurs in both, arteries and veins, the AVR is not affected in myopic eyes [240, 158]. Moreover, these findings in myopic eyes might be a result of the image minification (referred to as OM) due to the devices used in these studies.

5.3. Retinal vessel complexity - spatial distribution of the retinal vessel network

To obtain quantitative information about the oxygen supply and drainage of the retinal tissue by the retinal vessel network, it is important to determine the spatial distribution of the retinal vasculature (referred to as vessel complexity or vessel architecture). This approach will help to determine as to whether the retina has insufficient architectural properties. The retinal vessel tree exhibits a structure, where the pattern of a fraction of the retinal vessel tree resembles the whole vessel tree. This resemblance of a certain pattern can be quantified mathematically as a fractal, expressed as fractal dimension [187]. The determination of the spatial distribution of the vessel tree can be derived either by the box-counting method (Df) or by the mass-radius-relation (Dm). In case of a uniform distribution of the vasculature across the whole image (as it is in a healthy retina) it can be assumed that a rectangular section resembles the whole retina regarding its pattern and another rectangular section of the section show a similar behaviour. This method is called the box-counting method and is the appropriate method to determine the complexity of the retinal vessel network in cases of uniform vessel distribution (i.e. no neovascularisation). In cases of a less uniform distribution (referred to as dissimilar, resemblance of pattern does not hold true), which is present in cases of disease affecting the retinal microvasculature (i.e. DR), the mass-radius-relation might be the better

method as it allows to calculate the Dm for various regions. In this study the box-counting method (Df) was used to describe the spatial distribution of the retinal vessel tree. The principle for calculating Df by applying the box-counting method is plotting the log of the box size (x-axis) against the log of the number of boxes (y-axis). Df is then defined as the slope of this plot [159]. It is calculated according to equation 3.

$$D_f = \lim_{r \to 0} \left(\frac{logN}{log1/r} \right) \tag{3}$$

Hereby is N the number of boxes and r represents the box-size. Applying equation 3 the results in a two-dimensional space are between 0 and 2. The results can be interpreted as a larger value representing a denser network and a lower value of Df representing a sparser retinal vessel network. The "gaps" in between the pattern formation are named lacunarity (lac). Mathematically "lac" is a measure of the rotationally and translationally invariance of the complex pattern.

Previous investigations found the fractal dimension of the human vessel tree in healthy adults to be between 1.4 and 1.7 [187, 307, 176, 284, 159]. Df varies depending on tortuosity and branching patterns. In addition to depicting diseases of the microvasculature (i.e. new vessel growth) [327, 38, 37], it might also serve as a measure of the efficiency of oxygen distribution and drainage of retinal tissue. The primary factors influencing Df in an inverse proportional way are age (β= -0.42 ([176]) to -0.311 ([38]), $p<.001$ for both studies) and systemic hypertension [176]. Cheung et al. (2012) found a proportional relationship for Df with refractive error (β= 0.152, $p< .001$ ([38])). Furthermore, image quality, such as dark (i.e. due to insufficient flash intensity) and/or blurred (i.e. due to media opacities) images, influences the results of the analysis [307].

In glaucoma retinal vessel network Df was investigated on 2666 healthy and 123 glaucoma subjects in the SiMES [319]. Image analysis using the Singapore I Vessel Assessment (SIVA) software revealed a significant lower Df in the glaucoma group when compared with the healthy group (SiMES findings published by Wu et al. (2013): 1.37 $\pm$ 0.10 vs 1.41 $\pm$ 0.04, $p<.001$). Currently, investigations on retinal vessel complexity in glaucoma focus on the ONH region, rather than the wider retina [40, 255, 324, 256]. Ciancaglini at al. (2015) explored the fractal dimension of the lamina cribrosa vessel network in a

group of 36 glaucoma subjects and 18 control subjects using Scanning Laser Doppler Flowmetry (SLDF) and reported a decrease of 0.12 in glaucoma (1.68 $\pm$ 0.04 (healthy) vs 1.56 $\pm$ 0.07 (glaucoma)) [40]. Other authors applied an OCT angiography (OCTA) principle and reported similar results as for the SLDF method [255, 256, 324]. Vessel network complexity at the ONH is reduced in subjects with glaucoma when compared to subjects of similar age without glaucoma.

5.4. Dynamic vessel analysis

Dynamic vessel analysis is the assessment of the behaviour of vessels (vasodilation and vasoconstriction) larger than 60 μm at baseline when the retinal tissue metabolism is stimulated by flicker light. Flicker light is thought to stimulate retinal photoreceptor cells. In turn, these trigger the (parasympathetic) signal to release the molecule NO (mediates vasodilation) and ET-1 (mediates vasoconstriction) in vascular endothelial cells [49].The procedure of dynamic vessel analysis allows identification of vessel structure abnormalities (e.g. reduced functionality) such as in cardiovascular diseases [114]. Previous investigations on healthy participants revealed a physiologically normal mean change in vessel diameter (referred to as dilation amplitude) of 3.9 % for arteries and 5.4 % for veins [220]. This procedure is proven to be highly reproducible (ICC of 0.96 to 0.98 for arteries and ICC of 0.97 to 0.98 for veins) [234, 217]. Previous research found no significant influence of age on venous reactivity [150, 218]. Regarding arterial vessel reactivity findings are conflicting. While Nagel et al (2014) [218] reported no significant effect of age on arterial baseline-corrected fluctuation (bFR), Kneser et al. (2009) found a significant regression model for arterial bFR (Nagel: β_{bFR}= -0.048, p= .20 vs Kneser: β_{bFR}= -0.073, $p_M <$ .001). The authors of the later study argued that the significant result might be due to a larger sample size (twice as many as in the study of Nagel). Nevertheless, the publication of Kneser et al. (2009) does not provide information about significance and effect size (β and t) of the predictor variable. Thus, this information was not implemented for statistical analysis. In glaucoma the vessel reactivity was found to be reduced indicating that vascular dysregulation contributes to pathology onset and progression [77, 87, 88, 209]. Garhoefer et al. (2004) used a refined standard analysis

protocol (adjusted for bDF) and found a significantly reduced flicker response in veins but not in arteries [77]. In agreement with the findings of Garhoefer et al. (2004), Ramm et al (2014) also reported a significantly reduced venous response [253]. The studies of Mroczkowska et al. (2013) and Gugleta et al. (2012) exhibited an effect on both arterial and venous flicker responses in glaucoma (reduced bDF in the study by Mroczkowska et al. [209] and reduced flicker responses (FR) in the study by Gugleta et al. [87]). However, it is hardly possible to compare the studies due to the fact that different flicker protocols and different analysis methods (bDF vs FR) were used for analyses. Gugleta et al. (2012) and Mroczkowska et al. (2013) and Ramm et al. (2014) used the standard protocol of 50 seconds baseline, followed by three cycles of 20 seconds flicker light and 80 seconds recovery afterwards, whereas the study of Garhoefer et al. (2004) used an individual protocol with increasing flicker periods (16, 32 and 64 seconds). Despite the differences in methodology, the authors unanimously hypothesized the presence of vascular dysregulation in glaucoma. No change of vascular reactivity was reported in myopic eyes when compared to emmetropic eyes [158].

5.5. Ocular Perfusion Pressure and Vascular dysregulation

The driving force for the distribution of oxygen to the retinal tissue is OPP. Perfusion pressure is defined as the difference between the tension in arteries and veins. It can be estimated from blood pressure and IOP due to the fact that venous tension cannot be less than the IOP (the vein would otherwise collapse). The vascular bed has the ability to remain a stable blood flow by adapting its vascular resistance to a certain range of changes in perfusion pressure (referred to as autoregulation).The vascular bed of the ONH exhibited autoregulatory capacity of up to 45 to 55 mm/Hg IOP raise in a study by Pillunat et al. (1997) [242]. If autoregulation is disturbed, any change in perfusion pressure due to IOP or BP variations can translate into tissue perfusion [64]. The disturbance of the autoregulation is named vascular dysregulation. Reperfusion damage to the ONH , hypoxia and ischaemia are possible consequences of an disturbed autoregulation [85, 65].

A body of evidence from epidemiological and smaller studies suggest that low OPP

plays a role in the incidence and progression of glaucoma [168, 332, 175, 132]. The SiMES reported that participants with low diastolic and mean perfusion pressure (dPP and MOPP, respectively) as well as low diastolic blood pressure (dBP) have a higher risk of developing OAG than participants with higher dPP, MOPP and dBP [332]. The the Handan Eye Study reported similar results [175]. In the latter study, sPP, dPP and mean PP were consistently lower in eyes with POAG when compared with eyes of glaucoma suspects. Low sBP leading to low OPP was found to be a risk factor for the development of glaucoma in the Barbados Eye Studies [167]. The Early Manifest Glaucoma Trial (EMGT) reported an almost 50 % higher risk for disease progression in patients with low sPP [165]. The EMGT aimed to determine long-term progression factors in monitoring 255 glaucoma subjects over a period of 11 years.

The LALES reported that both, low dBP and high sBP are associated with increased prevalence of POAG [192]. Systemic hypertension seems to play a protective role against glaucoma in young subjects, whilst posing a risk to older subjects (Baltimore Eye Survey) [292]. The authors explained this finding by a reduced ocular blood flow due to vascular sclerosis in older patients.

More importantly, 24-hour fluctuations in OPP are thought to be responsible for glaucoma progression [181, 283, 175]. Blood pressure and IOP follow a diurnal vs nocturnal pattern. In healthy subjects, the BP decreases during the sleeping hours by 1 - 12 % and 14 - 17 % for sBP and dBP, respectively [265]. This physiological process is called dipping. Non-physiological nocturnal dipping (i.e. not at all or to an extreme extend) in sBP was associated with disease progression in a longitudinal study following 51 POAG patients and 19 NTG patients over a period of two years [43].

However, some research in this area did not find a significant relationship between OPP and glaucoma.The Beijing Eye study investigated the relationship between OPP and OAG in a population-based setting (3251 subjects). No significant correlation was found between OPP and prevalence of OAG [321]. The authors explained the discrepancy to previous research findings by different inclusion criteria of the studies. The majority of glaucoma subjects in the Beijing Eye study were without IOP lowering treatment. Similar findings were reported for the Central India Eye and Medical Study [136]. The

investigation on 4711 Asians revealed that OAG was significantly associated with higher IOP ($p<.001$; odds ratio 1.19; 95%CI 1.15,1.24) or with elevated translamina cribrosa pressure difference ($p< .001$; odds ratio 1.15; 95 %, CI 1.10,1.19), but no significant association with OPP ($p< .37$) in multivariate analysis. The same study reported a significant association for the prevalence of ACG and lower OPP ($p< .04$). Jonas et al. (2015) explained the discrepancy between the findings of the Central India Eye and Medical Study and previous investigations by differences in statistical analysis. The author emphasized that the translamina cribrosa pressure difference may be more important for the pathophysiology of glaucomatous optic nerve damage due to to the local association with the ONH [136, 137].

Nevertheless, OPP derived from a measurement at one point in time has to be interpreted carefully due to the facts that firstly, it is not measured directly and secondly, it follows a natural fluctuation over 24 hours. The Handan Eye Study further reported that the lowest OPP occurs between 10 am and 2 pm in 60 % of POAG patients[175]. Thus, in this study all measurements were carried out at between 10 am and 2 pm.

6. Summary of previous research of structural and haemodynamic parameters in highly myopic and glaucomatous eyes leading to the objectives of this study

Glaucoma is well recognized as the loss of neuroretinal tissue (RNFL and GCL), which causes vision impairment and potentially blindness [34, 133, 249, 248]. Myopic eyes, highly myopic eyes in particular, are known to have an up to 1.88-fold higher risk of developing glaucoma [185, 264]. To date the link between the condition "myopia" and the pathology "glaucoma" is not fully understood. Table 13 synthesizes previous research contributing to the question as to why myopic eyes are more susceptible to the incident of glaucoma. As can be seen from this table, these investigations explored aspects of glaucoma (visual field, neuroretinal tissue thickness and retinal haemodynamics) separately, but none has investigated a broad range of parameters in one study.

6.1. Structural measurements - Neuroretinal tissue thickness

Previous investigations have shown that RNFL and GCL thicknesses are decreased generally (360^o average) as well as for inferior locations in glaucoma [25, 145, 238]. Furthermore, the study of ganglion cell death due to experimentally induced glaucoma in ten monkeys revealed a more rapid atrophy of larger ganglion-cells [250]. For myopic eyes previous research applying OCT technology showed a redistribution of retinal nerve fibres in the retina, with thinner locations at the inferior and superior quadrants [308, 140, 144, 272].

6.2. Retinal haemodynamic measurements - Vessel architecture

The main identified risk factors for the development of glaucoma are elevated IOP and impaired blood flow regulation in the eye (see section 1.2, [246, 65]. The vascular theory of glaucoma suggests that an imbalance of IOP and retinal blood flow leads to decreased ocular perfusion pressure, which in turn may be responsible for the neuroretinal tissue damage [67, 65]. The oxygen metabolism in the retina relies on a complex mechanism. This system comprises the size of the vessels and their distribution across the retina (referred to as retinal vessel architecture), the vessel function (referred to as retinal vessel reactivity) and the amount of oxygen transported through the vessels (referred to as oxygen saturation: SO2) and the perfusion pressure releasing oxygen to the tissue.

The BMES found a significant association between decreased arterial vessel size (arterial calibres) and the ten-year incidence of POAG (OR=1.77, 95% CI: 1.12 to 2.79; [196, 142]. In the SiMES however, narrower arterial and venous calibres were associated with an increased prevalence of glaucoma (OR=1.29, 95% CI: 1.07 to 1.56 and OR=1.49, 95% CI: 1.24 to 1.79 for arteries and veins, respectively) [4]. The conflicting finding regarding the association of glaucoma and venous calibres might be explained by the different study designs. Whilst the BMES analysed baseline vessel diameters with the incidence of glaucoma after 5 or 10 years, the SiMES applied a cross-sectional study design to identify the relationship of vessel calibres and prevalence of glaucoma. Additionally, straighter retinal arteries and veins (tortuosity) were associated with glaucoma

in the SiMES [319]. In the same study, spatial distribution of the network (Df) was not associated with glaucoma but with ocular hypertension (OR=1.37, 95% CI: 1.04 to 1.82). In myopic eyes previous research has shown narrower vessel calibres for both, arteries and veins as well as reduced retinal network complexity [318, 240, 330, 38]. The authors explained these findings by the elongation of the myopic eye also effecting the embedded retinal vessels.

6.3. Retinal haemodynamic measurements - Vessel function

Whereas no significant difference in arterial and venous vessel reactivity was found between emmetropic and highly myopic eyes [158], retinal veins exhibited a reduced vessel reactivity in glaucomatous eyes [77, 253]. From the findings of their study, La Spina et al. (2016) concluded that retinal vessels of highly myopic eyes are functionally comparable to emmetropic counterparts despite smaller vessel calibres. Ramm et al. (2014) investigated retinal vessel reactivity (referred to as vessel diameter change induced by flicker light) as well as the oxygen content of retinal vessels (referred to as oxygen saturation: SO2) in 40 POAG subjects and compared the results with a control group of similar age [253]. Based on the findings of a reduced venous response as well as an increased vSO2, the authors suggested an impaired blood flow regulation in glaucomatous eyes.

6.4. Retinal haemodynamic measurements - Oxygen content in retinal vessels and ocular perfusion pressure

The difference between the arterial SO2 and venous SO2 measurements results in A-V SO2 difference, a surrogate for the consumption of oxygen in the retinal tissue. Previous research conclusively found a reduced oxygen consumption in glaucomatous eyes [194, 228, 253, 301]. Based on these findings, it cannot be concluded as to whether these findings represent the cause for ganglion cell loss (i.e. ischaemia) or the consequence of a reduced number of consuming cells. A reduced A-V SO2 difference was also observed in highly myopic eyes [183, 330]. Man et al. (2013) explained the protective role of myopic eyes in development of diabetic retinopathy (DR) by a reduced oxygen consumption in myopic retinas which in turn, reduces the likelihood of myopic retinas

to exhibit hypoxic retinal tissue as seen in DR. Quigley and Cohen (1999) suggested a decreased OPP due to an increased pressure attenuation in myopic retinal arteries (a consequence of reduced vessel diameters) might explain the protective role of myopia in the development of DR [252]. However, decreased OPP, particularly low dPP is also associated with an increased glaucoma incidence and progression [332, 167, 165, 175].

Measure	Myope	Glaucoma
Visual Field (VF)	generally reduced sensitivity (MD_H) [260, 7]	asymmetry along the horizontal line, reduced sensitivity (MD_H) [141, 5]
RNFL thickness	redistribution (temporal quadrant thicker) [308, 140, 144, 272]	reduced thickness in inferior quadrant and in 360^o average RNFL [25, 145, 238]
GCL thickness	NA	reduced inferior and in 360^o average GCL [25, 145, 238]
SO2	reduced oxygen consumption (A-V SO2 difference) [183, 330]	reduced oxygen consumption (A-V SO2 difference) [301, 253, 228, 194]
SVA	narrower vessel calibres for arteries and veins [318, 240, 330]	narrower arterial calibres [196, 142, 35] narrower arterial and venous calibres [4]
DVA	normal vessel reactivity [158]	reduced reactivity for veins [254, 77, 209, 87]
Vessel complexity	lower Df than emmetropic eyes [38]	reduced arterial and venous tortuosity [319]
OPP	NA	fluctuations associated with glaucoma progression [73, 175], low OPP [332, 165, 167]

Table 13: **Summary of findings in myopic vs glaucomatous eyes**

6.5. Study objective and research questions

The findings of numerous previous studies suggest that alterations in haemodynamic parameters or haemodynamic patterns (i.e. a combination of haemodynamic measures) might at least partly contribute to neuroretinal tissue loss in glaucoma. Moreover, links between myopia and glaucoma can be assumed from findings of a range of studies. Unfortunately, to date there is no study available exploring structural and haemodynamic aspects and their relationships in highly myopic eyes. Thus, the objective of this cross-sectional study was to explore structural, functional and a range of haemodynamic parameters of physiological high myopia in adults and compare these measures with those of an emmetropic study cohort. Data of a glaucoma sample were used for qualitative comparison. Identifying either individual variables or patterns within a measurement type

that are different in healthy highly myopes when compared with healthy emmetropes, but exhibit similarities with glaucoma subjects may indicate aspects that could potentially explain the greater glaucoma susceptibility in physiological myopia. In detail, GCL and RNFL thicknesses (structural measurement type), visual field indices such as MD_H and PSD as well as GHT patterns (functional measurement type), retinal vessel calibres for arteries and veins (haemodynamic measurement type), retinal vessel network complexity (haemodynamic measurement type), retinal vessel reactivity for arteries and for veins (haemodynamic measurement type) as well as ocular perfusion pressure calculations (haemodynamic measurement type) were compared between a healthy highly myopic and a healthy emmetropic group. The results of a group of POAG patients were used to qualitatively explore similarities and differences to the group of healthy high myopes.

Furthermore, this study aimed to explore differences in haemodynamic patterns between emmetropic and highly myopic eyes. To compare these patterns in between the study cohorts, correlation analyses were carried out for each study cohort separately. In highly myopic eyes, changes in the retinal blood circulatory mechanisms (architecturally and/or functionally) indicated by a haemodynamic pattern different from those of emmetropic eyes may suggest alterations in oxygen metabolism, contributing to tissue loss.

Additionally, this study investigated haemodynamic predictor variables which determine changes in structural parameters in the study cohorts. Predictor variables in healthy highly myopic eyes which cannot be found in healthy emmetropic eyes or have a different predictive ability may contribute to an increased glaucoma susceptibility in highly myopic eyes. In detail, the following questions were explored:

- How do otherwise healthy, highly myopic individuals differ from emmetropes with respect to structural and functional and haemodynamic parameters?
- How are retinal structure and haemodynamic parameters related in emmetropes vs high myopes?
- How are retinal haemodynamic parameters inter-related in emmetropes vs high myopes?

- Do any of the parameters and/or relationships of highly myopic eyes resemble in a sample of patients with POAG?

Part IV

Material and Methods of this Research

7. Eligibility study cohorts - Inclusion/exclusion

Participants were recruited from Aston University Optometry eye clinic, Optegra eye hospital, Aston University staff and students as well as others via posters, leaflets (see AppendixC.1 and AppendixC.2) and personal invites. Informed consent was obtained from each participant and the Universities Ethics Committee approved all methodology (see appendices AppendixB.2 and AppendixB.4). All methods adhered to the tenets of the Declaration of Helsinki for research involving human subjects.

The subjects for the study had to meet the following criteria:

1. The **emmetropic** cohort included healthy adults (age 18 years and older), who had a refractive error between -0.50 DS and +0.50 DS (SE). Additionally, these subjects had to be free of a history of ocular surgery and ocular disease. Furthermore, to be included in the study the subjects had to have a visual acuity better than 0.3 logMAR as well as no nystagmus or amblyopia. Self-reported family history of glaucoma was recorded but was not an exclusion criteria.

2. The **highly myopic** cohort included healthy adults (age 18 years and older), who had a refractive error of more than -5.75 DS (SE). Additionally, these subjects had to be free of a history of ocular surgery (except for refractive surgery) and ocular disease. In case of any previous refractive surgery, the eye had to be fully recovered (at least 3 months after refractive surgery). Furthermore, to be included in the study the subjects had to have a visual acuity better than 0.3 logMAR as well as no nystagmus or amblyopia and a myopia grading of M1 or M0 (AVILA

myopic retinopathy grading scheme [8]). Self-reported family history of glaucoma was recorded but was not an exclusion criteria.

3. The **glaucoma** cohort included adults (age 18 years and older), who were previously diagnosed with glaucoma by an ophthalmologist (confirmed diagnosis by an ophthalmologist) in at least one eye independent of the refractive error. Glaucomatous eyes were defined as those with RNFL thinning (inferior and/ or superior quadrant) and was confirmed by the OCT results. Glaucoma duration and glaucoma medication as well as medications for systemic diseases and previous cataract and/or glaucoma surgery were recorded. Subjects with controlled systemic hypertension (BP readings below 140 mmHg for sBP and below 90 mmHg for dBP) or diabetes type II were not excluded from the study due to the high prevalence of these conditions in this study group [131, 227, 228]. However, untreated systemic hypertension and any ocular pathology other than glaucoma was an exclusion criterion. Furthermore, this study did exclude glaucoma suspects.

4. For all cohorts; subjects were excluded if adverse reactions to the drug used to dilate the pupil (Tropicamide 1 %) were known.

5. For all cohorts; subjects were excluded if intraocular pressure exceeded 24 mmHg (controlled or uncontrolled) and/or the anterior chamber depth measurement resulted in values below 2.1 mm due to the risk of a sudden pressure rise.

6. For all cohorts; subjects exhibiting cataract were excluded if the stage of the cataract obscured the images (CII to CIV and PI to PIII according to the lens opacity classification system II (LOCS II[39])).

The classification for emmetropic and highly myopic eyes was chosen in accordance to the classification scheme of Shen et al. (2016) and Xu et al. (2016) [274, 320]. A highly myopic cohort was chosen instead of any myopia to enable for a larger effect size. Due to the fact that refractive surgery has no impact on the elongation of the eye and hence, the retinal measurements (haemodynamic and structural), subjects who previously had undergone refractive surgery were included. The ability to be able to focus on a fixation

target is crucial for the image- and analysis quality of any imaging technique. To reduce the effect of bias due to bad quality measurements a good visual performance (visual acuity and a good ability to fixate) was an inclusion criterion.

7.1. Measurement procedure on the appointment

The participants had to refrain from caffeinated products, cigarettes and alcohol for at least 4 hours prior to the appointment due to the known influence of these substances on haemodynamic measurements [103, 18]. After consenting to participate, the volunteer underwent a comprehensive optometric examination including best-corrected visual acuity testing, BP and IOP measurement and medical as well as family history. The full assessment took less than two hours in total and was predominantly carried out on one appointment. To capture the lowest PP in the study subjects, BP and IOP were measured between 10 am and 2 pm [175]. One eye was selected (randomly for emmetropic eyes and the eye with the larger refractive error for the highly myopic participants) as no differences between right and left eye is to be expected for haemodynamic and structural measures in healthy eyes. In glaucoma subjects, if both eyes had a confirmed diagnosis of glaucoma the eye with the better visual acuity was chosen with respect to image quality. Otherwise the glaucomatous eye was chosen for the measurements. IOP measurement and anterior chamber depth measurement determined the potential risk of developing a sudden rise in IOP prior to instillation of drops using Tropicamide 1% (Minim, Bausch & Lomb). Additional to pupil dilation, the patient was instructed to blink naturally during the assessments with the aim to achieve the best possible image quality due to good lubrication of the cornea.

The individual study measurements and assessments will be expanded on in the following sections. Additionally, table 14 lists the measurements according to its order in the study procedure and provides information about its purpose.

No	Device and derived variables for analysis	Purpose	Pupil dilation ✔/✗
1a	SRW-5000 (Shin-Nippon Tokyo): refractive error [D]	Determines Inclusion or exclusion, selection of study eye	✗
1b	Bailey Lovie chart5 (NVRI of Australia): Visual accuity [logMAR]	Quantification of visual function, exclusion of VA>0.3 because of poor fixation	✗
2	IOL-Master 500 (Zeiss): AL [mm] and ACD [mm]	Classification of the elongation of the study-eye	✗
3	HFA 750i (Zeiss): MD_H , PSD, differences between superior and inferior normalised total deviation results according to the glaucoma hemifield test pattern (C1, C2, N3, P4, P5) [dB]	Quantification of visual function	✗
4	iCare ic100 (Mainline Instruments Ltd): IOP [mmHg]	Exclusion of subjects with ocular hypertension (IOP $>$ 24 mmHG), calculation of ocular perfusion pressure (OPP) (NICE guidelines)	✗
5	Tropicamide 1% one drop	To allow image capturing	NA
6	UA-767 Plus 30 (A&D Medical): systolic and diastolic blood pressure (sBP, dBP), heart rate	Exclusion of subjects with high blood pressure (>140/90 mmHG, http://www.escardio.org/Guidelines), calculation of mean arterial pressure and ocular perfusion pressure	NA
7	RVA (Imedos, Jena) comprising of FF450+ (Zeiss) and flicker stimulus: 350 sec video sequence in 30^0 camera setting	Diameter change of vessels when light stimulates oxygen metabolism	✔
8	RVA (Imedos, Jena) comprising of FF450+ (Zeiss)+ Oximetry-filter: 30^0 **(*)** and 50^0 - fundus images: disc centred for SO2 [%], CRAE [au] and CRVE [au] and AVR	Oxygen saturation measurement Vessel calibre determination (CRAE and CRVE), Determination of vessel geometry (Df and Lac)	✔
9	Cirrus HD-OCT (Zeiss) a) disc 200x200 and b) macula 200x200 a) RNFL thickness and b) GCL thickness in [μm]	Measurement of structural properties of the retina (ganglion cells and their axons)	✔

Table 14: **Measurements taken during the visit; * data collected until March 2017**.

8. Visual function and retinal structure measurements

This section describes the setup used in this study to assess retinal function and structure of the study subjects and explains quality criteria for data to be included in statistical analyses.

8.1. Visual function

8.1.1. HFA 750i perimeter - measurement principle

The HFA 750i perimeter (Carl Zeiss Meditec Inc, Dublin, California, USA) tests the sensitivity to light by presenting light stimuli of different intensities and sizes at different positions of the retina. Light sensitivity is measured in decibels (dB), whereby 0 dB refers to maximum brightness and 40 dB refers to a less bright stimulus. A physiologically normal peripheral sensitivity range is between 19 and 38 dB [109]. White-on-white perimetry was performed (background illumination 31.5 asb) using the 30-2 SITA standard threshold algorithm (Swedish Interactive Threshold Algorithm), which tests 76 points in a grid with a spacing of six degrees between test points. Additionally, a foveal threshold was measured to provide central visual performance information. White-on-white static threshold perimetry has been the gold-standard test for glaucoma detection and monitoring since the 1970s.

8.1.2. Protocol and quality control

To gain reliable results when performing the test the refractive error in high myopic participants was corrected with trial lenses (referred to as optimal correction of the refractive error) [312, 259, 155]. Presbyopic participants performed the test with a near-correction. Furthermore, the participants received clear instructions regarding the test procedure. To improve reliability in participants who have not had a visual field performed before, a one-minute practice session was implemented. Only test results with false-positive and false-negative results below 15% were included for later analysis. In accordance with previous literature, VF tests exceeding a fixation losses of 20 % were excluded for analyses [203, 145].

For statistical analysis the mean deviation (MD_H), pattern standard deviation (PSD) results were used. Furthermore, the total deviation plot data was analysed using the glaucoma hemifield test pattern (GHT, see figure 6): The mean of the total deviation results from five zones (1 = central, 2 = para-central, 3 = nasal, 4 = nasal periphery and 5 = temporal periphery) of the inferior hemifield was subtracted from the mirroring

zone of the superior hemifield. The absolute value of these difference results was used for statistical analyses. The advantage of using total deviation plot values is that the data is already compared to an age-matched database. Hence, no age-adjustment is required for statistical analyses. Moreover, the absolute value was used in the GHT pattern related analysis to avoid bias in the group mean due to the fact that not all losses happen in the same hemifield.

8.2. Retinal structure measurements - GCL thickness and RNFL thickness measurements

8.2.1. Spectral domain OCT - measurement principle

Optical coherence tomography (OCT) was utilized to determine thicknesses of the neuroretinal layers. Under optimal conditions, the method allows measurement of the depth of a structure (referred to as axial measurements, A-scan) along adjacent positions (referred to as lateral measurements, B-scan) by using low-coherence interferometry [59]. The commercially available devices performing OCT are based on three different low-coherence interferometry principles: swept source, time domain and spectral domain OCT. For this study the spectral domain OCT Cirrus HD-OCT (Carl Zeiss Meditec, Germany; model 4000 up to the 11th December 2017 and model 5000 from 12th December 2017 till the end of data collection) was used for determination of the thickness of the Ganglion cell inner plexiform layer (referred to as GCL) and their axons (referred to as RNFL).

In low-coherence interferometry, light is sent along two optical paths, one being the sample path (into the eye) and the other the reference path of the interferometer. The light source is a superluminescent light emitting diode (SLD, 840 nm in the Cirrus HD-OCT) with its centred wavelength in the near infrared. Light returning from the sample and reference paths are combined (interfere) at a detector. Because of the short coherence length of the SLD, the strength of the interfering return signal is a measure of the reflectance of a small volume of tissue at each location of the scanning spot. The Cirrus HD-OCT uses a fixed reference path ("reference mirror" M) which analyses the interfering light beams as a function of the wavelength (referred to as Fourier-transformation)

using a spectrometer. The depth profile of the tissue (A-Scan) is a result of several steps of computation of this Fourier transformation. By repeating this process along several locations, a two-dimensional (2-D) depth-resolved image of the tissue is obtained [323]. Figure 12 shows the low-coherence interferometry principle graphically.

The instrument employs the spectral domain optical coherence tomography technique to provide depth-resolved structural information about the retinal nerve fibre tissue with an axial resolution of 5 μm and a scan-depth of 2 mm [191, page 1.1 (Introduction)]. The manufacturer states a reproducibility of 4.8 μm (given by the SD) for the 200×200 central sub-field measurements.

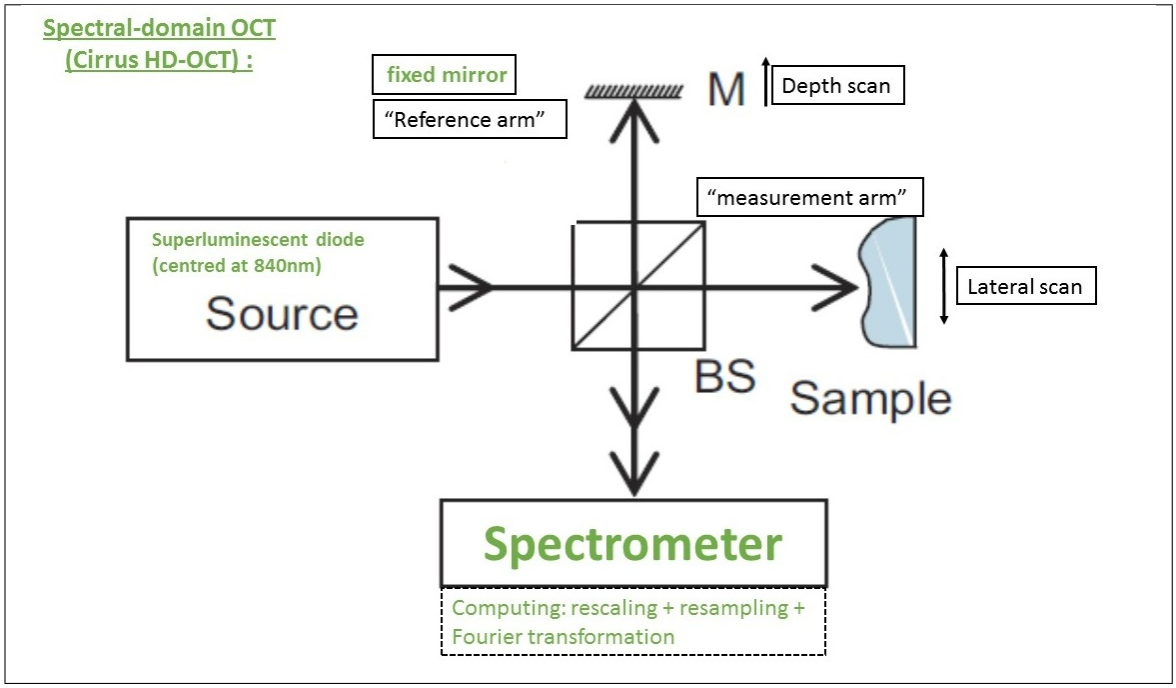

Figure 12: **Optical coherence tomography measurement principle Cirrus HD-OCT**

8.2.2. Peripapillary retinal nerve fibre layer thickness measurement

For the analysis of the peripapillary RNFL thickness the optic disc 200×200 data cube protocol was selected. This protocol is based on a three-dimensional scan of a 6 $\times$ 6 mm^2 area centred on the optic disc where information from a 1024 (depth) $\times$ 200 $\times$ 200-point parallelepiped is collected ($>$40 million data points with 30 μm spacing). The RNFL analyses uses depth data from a 3.46 mm-diameter circular scan area which is placed around the optic disc (corresponding to an angular size of 12.5^o in an eye with an axial length of 24.46 mm [224]). Thus, it obtains information about peripapillary

RNFL thickness (see figure 13). The borders of the neuroretinal rim are defined as the distance between the boundary of the optic disc (disc contour line on Cirrus) at the level of the inner termination of Bruch's membrane (i.e. Bruch's membrane opening) and a reference plane separating the neuroretinal rim from the cup. This plane is set 200 μm above the level of the plane of Bruch's membrane [200]. An integrated algorithm accounts for tilted discs and any disruptions of the tissue due to any kind of retinal pathology (see Zeiss brochure, [191, chapter 5-2 RNFL thickness analysis]).

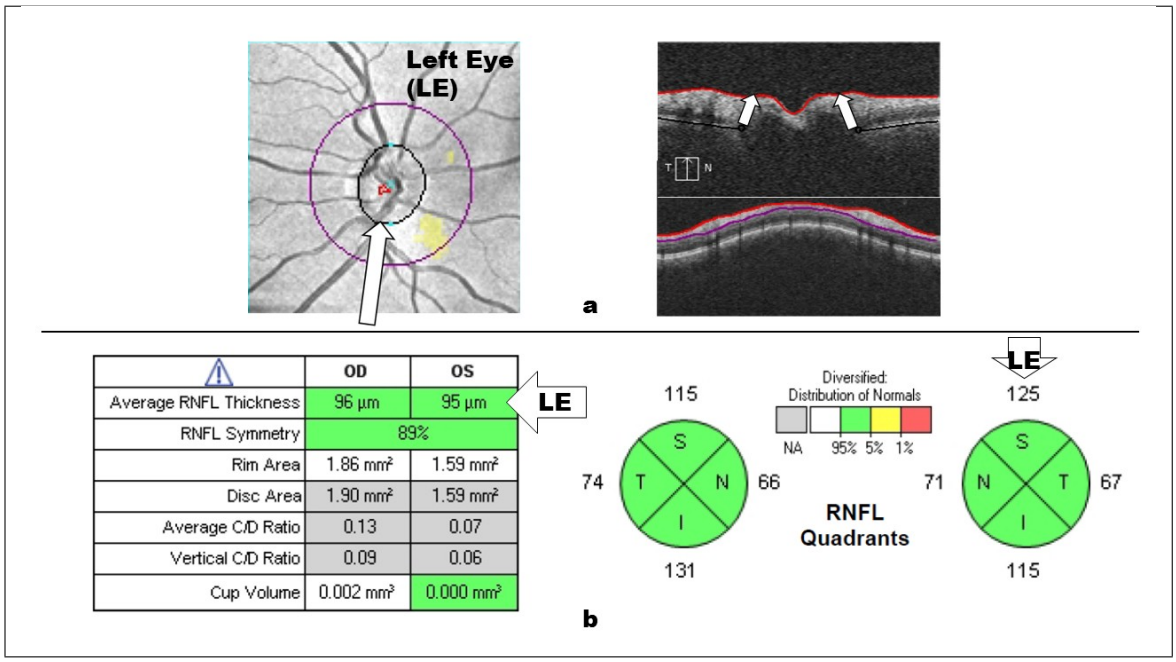

Figure 13: **RNFL thickness measurement at the peripapillary region in a left eye: (a) location of measurement, (b) measurement protocol "average thickness"(bottom left) and averaged in quadrants" (bottom right)**

8.2.3. Ganglion cell inner plexiform layer measurement

The thickness of the GCL is measured in an elliptic annulus with a horizontally 20% bigger radius than the vertical radius. This protocol analyses data of a $6 \times 6 \times 2$ mm cube within an elliptic annulus with following dimensions: vertical radii are from 0.5 to 2 mm and horizontal radii from 0.6 to 2.4 mm from the foveal centre. For GCL analysis the 200×200 macular cube protocol was chosen. Previous research has determined the size of the annulus experimentally (47 healthy subjects, [213]) to conform closely with the real anatomy [45]. The thickness profile of the ganglion cell inner plexiform layer is given by the difference in thickness between the RNFL outer boundary and the inner

plexiform layer outer boundary, because this comprises the ganglion cell bodies and its dendrites (represented by the inner plexiform layer).

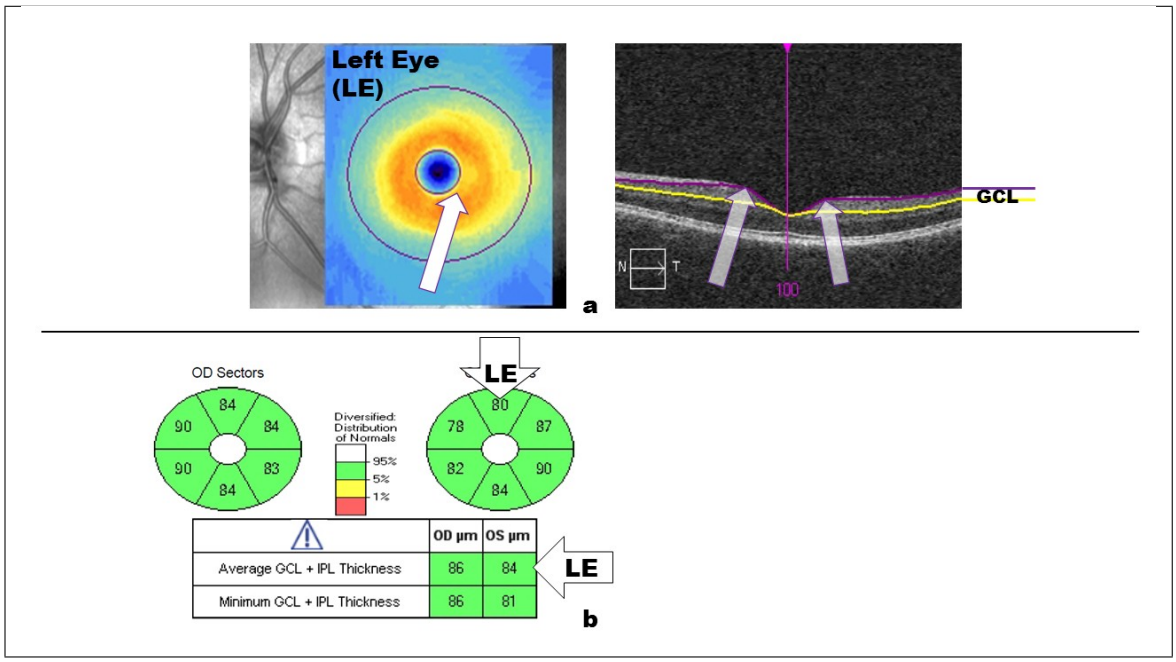

Figure 14: **GCL measurement at the macula region of a left eye: (a) shows the location of the measurement at the retina (inner radii: 0.6 mm horizontally and 0.5 vertically; outer radii: 2.4 mm horizontally and 2 mm vertically) and, (b) shows the analysis report output of the average 360^o GCL (bottom) and sector thicknesses (top)**

8.2.4. Axial length measurement and principle

To compare OCT data across the study cohorts, raw measurement values had to be adjusted for OM (see section 4.1). To do so, AL measurements of the study eye were carried out using the IOL Master 500 (Carl Zeiss Meditec, Germany). The instrument measures axial lengths within a range of 14 to 38 mm in 0.01 mm steps and anterior chamber depths within a range of 1.5 to 6.5 mm in 0.01 mm steps. Furthermore, the instrument allows the measurement of the corneal curvature within a range of 5 to 10 mm within 0.01 mm steps and the iris diameter (referred to as White-to-White) within a range of 8 to 16 mm in 0.1 mm steps. By using an interferometric principle, it provides contactless measurements of the biometric data. Hence there is no risk of injuring the cornea. The distance between the front surface of the cornea and the retinal pigment epithelium (RPE) determines AL which allows to adjust the measurement results of ocular magnification (see sections 4.1).

The apparatus works on the basis of a Michelson-Interferometer [121, 262] as shown in

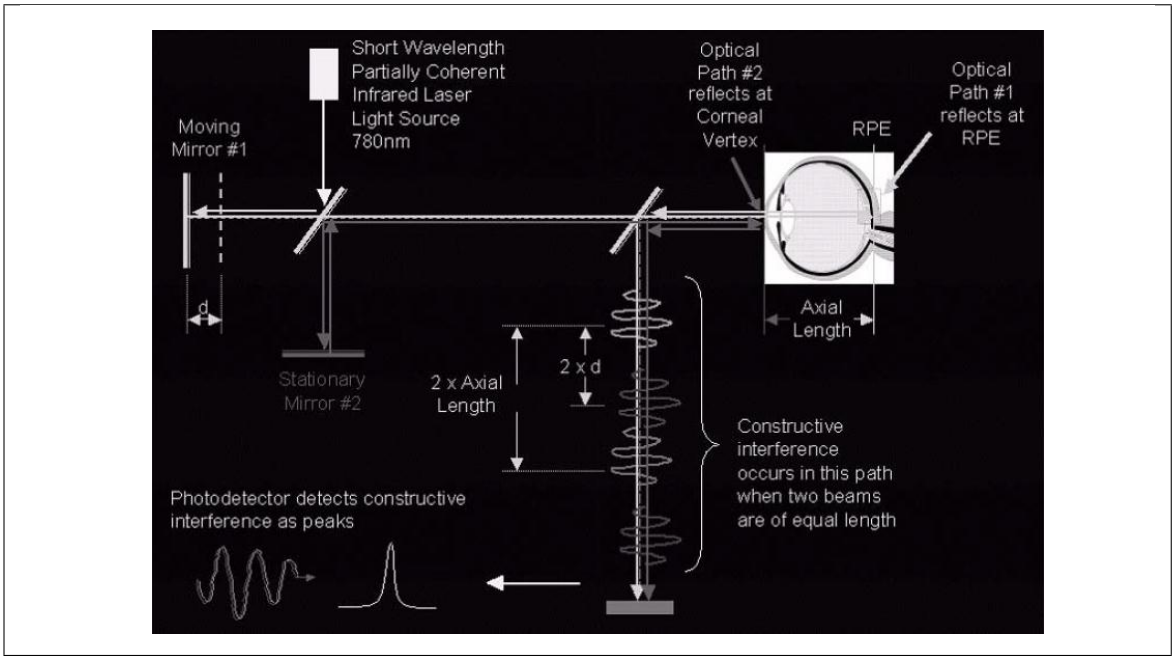

Figure 15: **Measurement principle of the IOL Master, reproduced with permission of Carl Zeiss Jena (see AppendixA)**

figure 15. For AL measurement the light of a short wavelength partially coherent infrared light source (780 nm; Laser Class 1) with long spatial depth and a short coherence length is split into two parallel coaxial beams using a beam-splitter. Both beams enter the eye and are reflected at the corneal vertex (see figure 15: path2) and at the RPE (see figure 15: path1) which results in a path-length difference of the beams when leaving the eye. The apparent path-length difference defines the AL by applying the principle of 100 % constructive interference: Constructive interference occurs if the path-length difference equals a multiple of the path-length of the beam ($n*\lambda$). During measurement one mirror (see figure 15: mirror1) is moved until the path-length difference between the two beams results in constructive interference, which is then detected by a photodetector. At the point of constructive interference, the quantity of AL equals two times the distance (d) that mirror 1 was moved.

8.2.5. Compensation "OM" for ocular magnification

To account for ocular magnification prior to statistical analyses, the raw data of the RNFL and GCL thickness measurements were multiplied by "$OM_{subject}$" which is the magnification factor for the individual. Generally, according to Bennett et al. (1994)

the true scan length "t" can be derived from the equation [17]:

$$t = p \times q \times s \tag{4}$$

Hereby "p" is the instruments magnification (3.382 for the Cirrus HD-OCT), "q" is the ocular magnification of the eye (calculated according to the equation $q = 0.01306 \times (AL - 1.82)$) and "s" is given by the default spacing between two A-scans (30 μm for the 200 $\times$200 scan area).

"$OM_{subject}$" was calculated as follows: Firstly, q_Z was computed for the calibration AL= 24.46 mm of the device and refers to OM_Z= 1 (zero magnification). $OM_{subject}$ of any individual was then calculated using the equation:

$$OM_{subject} = q_{subject} * OM_Z / q_Z \tag{5}$$

All RNFL and GCL thickness measurements were adjusted for $OM_{subject}$ prior to statistical analyses. Consequently, adjusted thickness measurements in longer eyes resulted in larger values than their raw data and shorter eyes exhibited smaller adjusted thicknesses than the raw data.

8.2.6. Protocol and quality control

The mean thickness of three consecutive measurements was adjusted for OM resulting in "adjusted" thickness values for each study subject. In order to be included, OCT scans were reviewed for centration of the scan area and had to have a signal strength $\geq$7 and no movement artefacts. Locations used for statistical analyses of the RNFL thicknesses were the means of four quadrants (superior, inferior, nasal and temporal quadrants, figure 13/b), as well as the global 360^o average result. For GCL thicknesses the results of six sectors and the global 360^o average value were used for statistical analyses (figure 14/b). For statistical analyses only "adjusted" thicknesses were used.

9. Retinal haemodynamic measurements and calculations

This section describes four retinal haemodynamic measurements carried out for this study. In detail, these are retinal vessel oximetry (SO2 measurement), static vessel

analysis (CRAE, CRVE and AVR), dynamic vessel analysis (according to the sequential and diameter response analysis method [112]) and fractal analysis of the retinal vessel network (Df, lac). All images were captured using the RVA system (Retinal Vessel Analyser, Imedos Systems GmbH, Jena) and further analysed as shown in figure 16. Furthermore, this section explains the quality criteria for data inclusion and the way raw data were processed prior to statistical analyses.

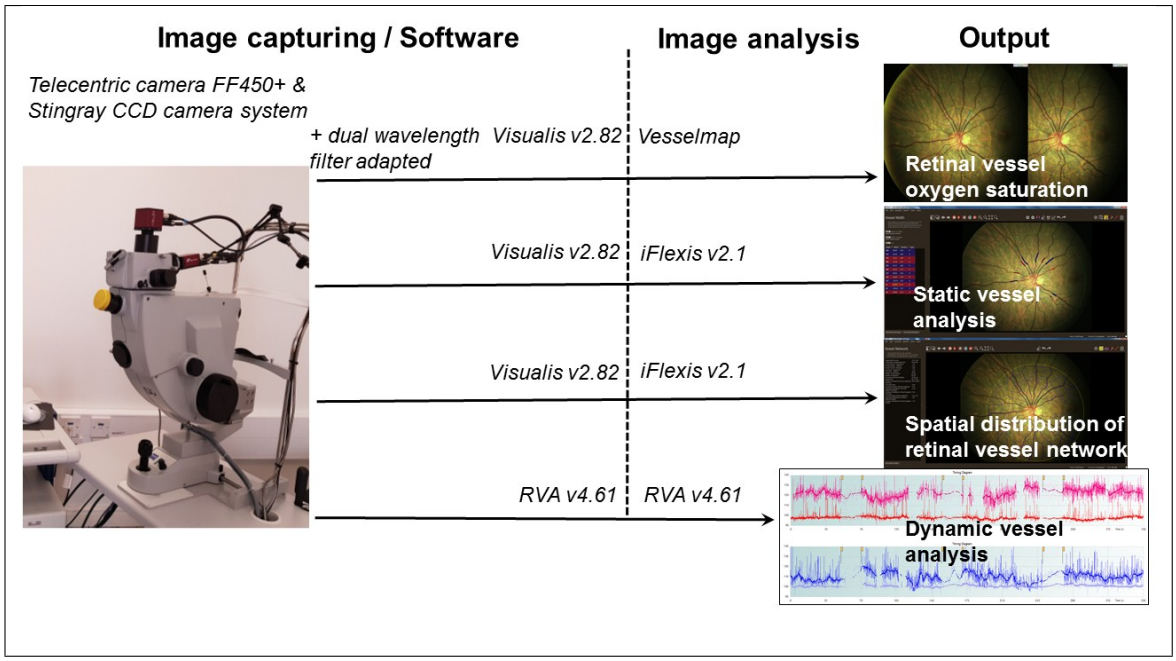

Figure 16: **Retinal blood circulation measurements carried out in this study using the RVA and its included software packages as well as additional iFlexis software**

9.1. The RVA - instrumental set up

To obtain static and dynamic retinal vessel analysis as well as retinal vessel oximetry data the RVA was used. The system is based on a telecentric fundus camera FF450^{Plus} (Carl Zeiss Meditec AG, Germany) with adapted CCD coupling devices (Stingray, Allied Vision Technologies) to digitalise fundus images (employing Visualis software) and fundus videos (employing RVA software).

For **dynamic vessel analysis** (see sections 5.4 and 9.5) the RVA system records a video sequence of pre-selected vessel-sections (30^o image size, selection of up to eight vessel sections) with a sampling rate of 25 Hz at baseline (50 seconds) and during three cycles consistent of 20 seconds flicker provocation followed by 80 seconds recovery (no

flicker light) each. The RVA system has a spatial resolution of 180 μm in the vessel direction and < 1 μm in the measurement direction [273]. Flicker is produced by an opto-electronic shutter in the illumination path producing alteration of bright and dark light stimuli with a frequency of 12.5 Hz according to previous investigations [234, 216]. Figure 17 shows the instrument setup (a) and the flicker protocol (b).

For **retinal vessel oximetry** (see sections 5.1 and 9.2), static vessel analysis and for fractal analysis of the retinal vessel network, 50^o disc-centred retinal images were captured using the Visualis software (version 2.82). Furthermore, for retinal vessel oximetry the RVA system employs a dual-bandpass filter which is inserted in the illumination path of the fundus camera (FF450^{Plus}) to simultaneously capture images at one isosbestic wavelength (548 µm) and an oxygen sensitive wavelength (610 µm). The VesselMap software (RVA in-build) analyses the images semi-manually.

Static vessel analysis results (see sections 5.2 and 9.3) and **fractal analysis** results (see sections 5.3 and 9.4) were computed using the iFlexis software version 2.1.1 (Vito Health, Belgium).

General requirements for optimal image quality and measurements are:

- dark room for measurement to eliminate stray-light and to obtain maximum effects for flicker provocation
- maximum dilation and minimum eye movements to achieve best possible fundus illumination with best contrast and definition
- minimal media opacities [111], only cataract classified as C1 according to the LOCS II grading scheme
- flash intensity according to the findings of Heitmar and Cubbidge (2013) [113] for optimal brightness and contrast to enable reliable oxygen saturation results

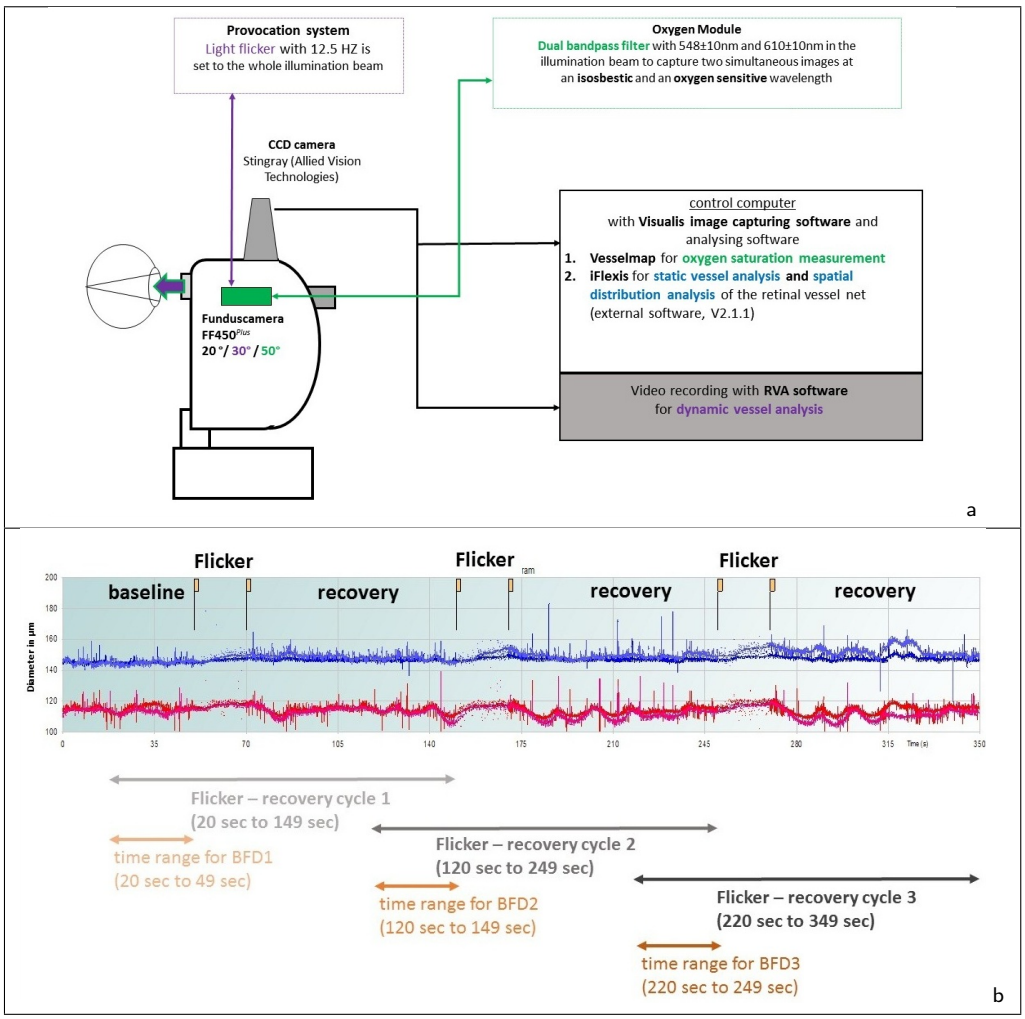

Figure 17: **a) The RVA device used for image capturing b) the flicker provocation protocol used in this study (measurement takes 350 seconds in total)**

9.2. Retinal vessel oximetry

Retinal vessel oximetry is the measurement of the oxygen content (in percent) in retinal vessels. It is based on spectral (absorbance) measurements of oxygenated and reduced (de-oxygenated) blood and obeys the Beer-Lambert Law (see Equation 6):

$$A = \log_{10} \frac{I_0}{I} = \varepsilon \times l \times c \tag{6}$$

Where A is referred to as the absorbance of light of a particular wavelength, I_0 is the intensity of light entering the solution, I is the intensity of the light emerging from the solution. The Greek letter epsilon ε is the extinction coefficient (determined by van Assendelft, 1970 [333]). Furthermore, "l " is the path length [cm] of the solution the light passes through, and c is the concentration of the solution [mol dm^{-3}]. The Beer-Lambert-Law relates the intensity of incident light of a specific wavelength (I_0) passing through a solution of a particular path-length to the transmitted light (I). Retinal vessel oximetry can therefore be considered an optical density measurement.

The ratio of the optical densities of an image captured at an oxygen insensitive (isosbestic) wavelength and an oxygen-sensitive wavelength is proportional to the oxygen content of haemoglobin [11, 47]. Thus, SO2 in percent can be calculated according to equation 2.The isosbestic wavelength transmits at 548 $\pm$10 nm full width and the oxygen sensitive wavelength transmits at 610$\pm$10 nm full width. The software automatically adjusts for specular reflections at the vessel wall by cutting off values that are 20% above the mean value at the vessel [95]. The measurement was carried out at a defined measurement annulus to obtain data of vessels of more than 50 μm in diameter (approximately 100 μm) and at a specific distance from the optic disc to reduce the variation in results [269]. It is defined as a peripapillary annulus with an inner radius of 1 disc diameter and an outer radius of 1.5 disc diameter. Results are optical densities (OD) according to equation 2 and SO2 in percent for arteries and veins. Results on arterio-venous differences (referred to as A-V SO2 difference) were calculated manually. The measurement for OD at the vessel (referred to as OD_{in}) will be taken along the selected vessel-segment. The accompanying measurement beside the vessel (referred to as OD_{out}) will be taken at 3 pixels beside the vessel borders at the neighbouring tissue. The Vesselmap software uses equation 2 to determine SO2 [in %] according to Hammer et al. (2008) [97].

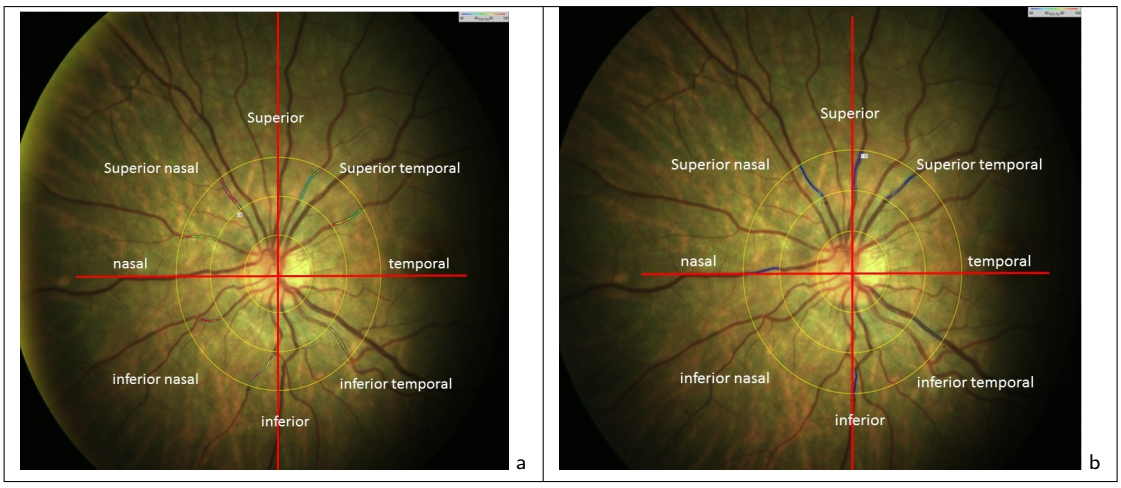

Figure 18: **SO2 measurement: every vessel section is selected manually and the SO2 percentage is calculated. Once all vessels in the measurement area (arteries and veins separately) are selected, the mean SO2 for arteries (a) and veins (b) can be calculated manually.**

9.2.1. Protocol and quality control

The mean of three consecutively captured images (thirty-degree images until March 2017, after March 2017 (software upgrade) fifty-degree disc centred images were used) were used for analysis in this study. Only vessel segments with a diameter between 50 μm and 150 μm were chosen for analyses. The mean SO2 of three images of the same vessel segment was calculated. The data was considered usable if firstly, the coefficient of variance for vessel diameter (CV) in the output data was below 10 and the measurement result was considered "valid" by the software (minimum ten measurements for the vessel section). In cases of "no valid" data, but at least 5 single values, the mean of these measurements was taken for vessel-segment analysis. The mean SO2 for individual vessel locations was computed (locations: superior temporal, temporal, inferior temporal, inferior, inferior nasal, nasal, superior nasal and superior) and the overall mean SO2 from all locations. The overall mean SO2 result was used for statistical analysis.

9.2.2. Compensation for retinal pigmentation

Although previous investigations found a weak influence of retinal pigmentation on SO2 measurements and this influence primarily accounts for the retinal veins [97], the equation to determine the percentage value of SO2 (relating the reflectivity of the vessel plane to the reflectivity of the surrounding tissue) suggests a dependency of arterial and venous SO2 results on the pigmentation of the retina (RP). The RVA instrument provides a pigmentation value ("RP") which is calculated as a log function (base 10) of the fraction of the optical density at 610 nm and the density value at 548 nm (isosbestic) measured at the tissue plane ($RP = \log 10(\frac{I_{out}610}{I_{out}548})$).

To validate the assumption of a pigmentation dependency on SO2 values, a graph of SO2 results was drawn to investigate a possible relationship (see figure 19/a and b). A significant correlation indicated a relationship between RP and SO2. Pearson correlation analysis was significant for both, aSO and vSO2 (arteries: r_P= 0.857, p<.001 and veins: r_P= 0.633, p<.001). A linear relationship between RP and SO2 values was found (see graph a in figure 19). Thus, a SO2 data transformation was conducted to compensate

for the influence of RP as follows:

1. Firstly, a graph was drawn with normalised RP values for the x-axis and SO2 results for the y-axis (see figure 20/c). For the normalization of RP, the AU-RP values were transformed into percent values with the difference between smallest and highest AU-RP value representing 100 %. This difference was 0.5262255. Only SO2 results of healthy subjects were chosen to determine the transformation factor to eliminate the impact of glaucoma on SO2 results. For both data sets the linear trend-lines were $y_{Artery} = 0.808 * x + 84.614, R^2 = 0.735$ and $y_{Vein} = 0.358 * x + 39.173, R^2 = 0.563$. The normalized RP value is represented by "x".

2. Subsequently, the data sets were rotated clockwise around the point $(0; intercept)$ applying a rotation matrix:

$$\begin{bmatrix} cos(Rt) & sin(Rt) \\ -sin(Rt) & cos(Rt) \end{bmatrix} \tag{7}$$

   with

$$tan(Rt) = \frac{slope * RP}{RP} \tag{8}$$

   The values for the rotation angle "Rt" were 0.6796 rad and 0.3437 rad for arteries and veins, respectively. The $intercept$ values (derived from the trend-line) were 84.62 for arteries and 39.17 for veins. The resulting transformation graphic is shown in figure 20/d.

3. After data rotation a Pearson correlation analysis was done to confirm that transformed SO2 values were independent of retinal pigmentation. The results were not statistically significant (r_P= 0.082, p=.552 for arteries and r_P= 0.158, p=.249 for veins) and hence, independence of RP on SO2 has been confirmed.

For subsequent statistical analysis the transformed SO2 results were used.

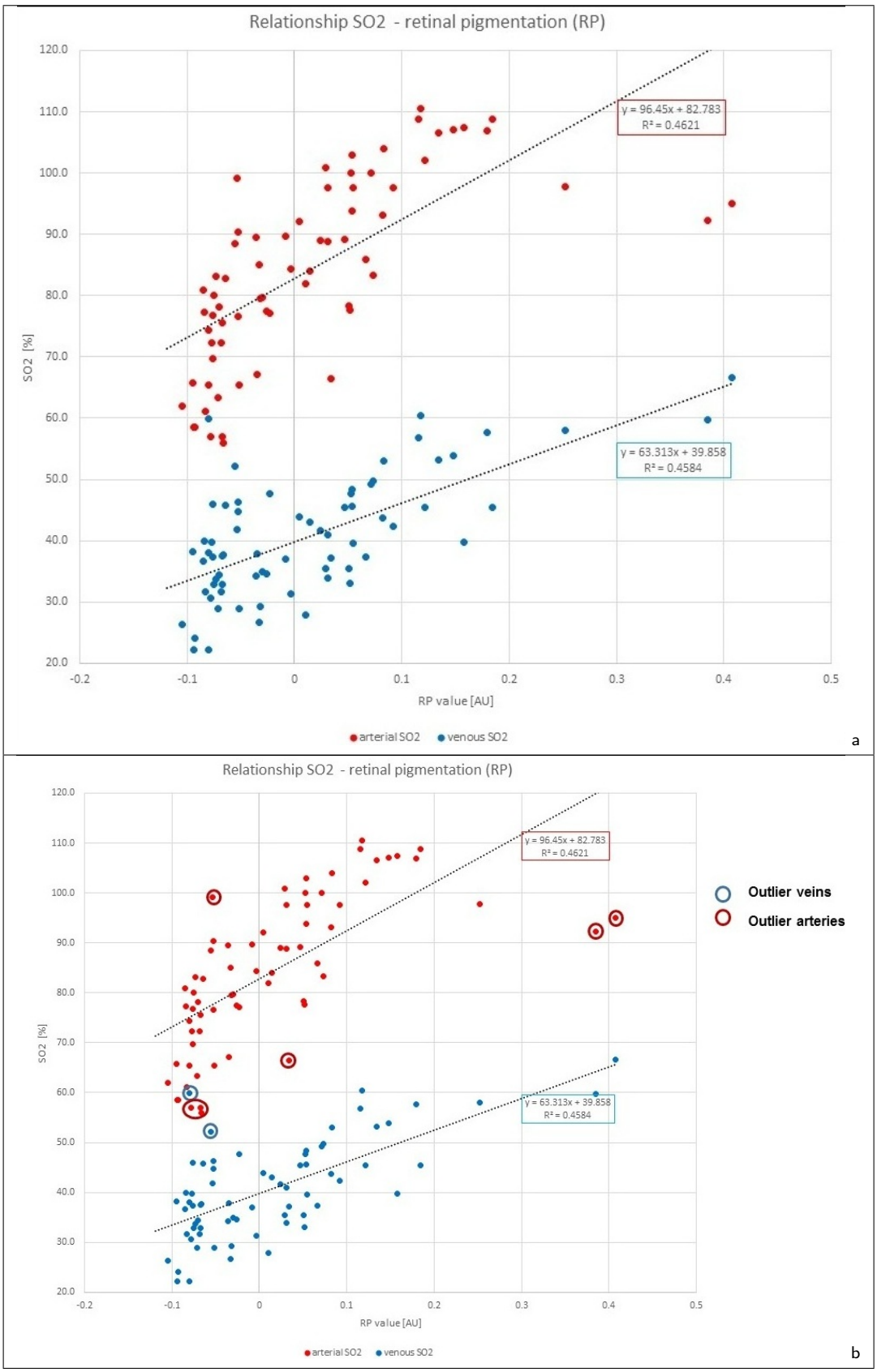

Figure 19: **Transformation of SO2 data to compensate for retinal pigmentation (1/2): Graph a represents the relationship of arterial SO2 (red data points) and venous SO2 (blue data points) and retinal pigmentation. After outlier were removed (graph b), both data axes were normalised (shown in picture figure 15 c) and via rotation matrix rotated around the intercept of the normalised value representation (shown in picture figure 15 d) to compensate for retinal pigmentation in SO2 measurement results.**

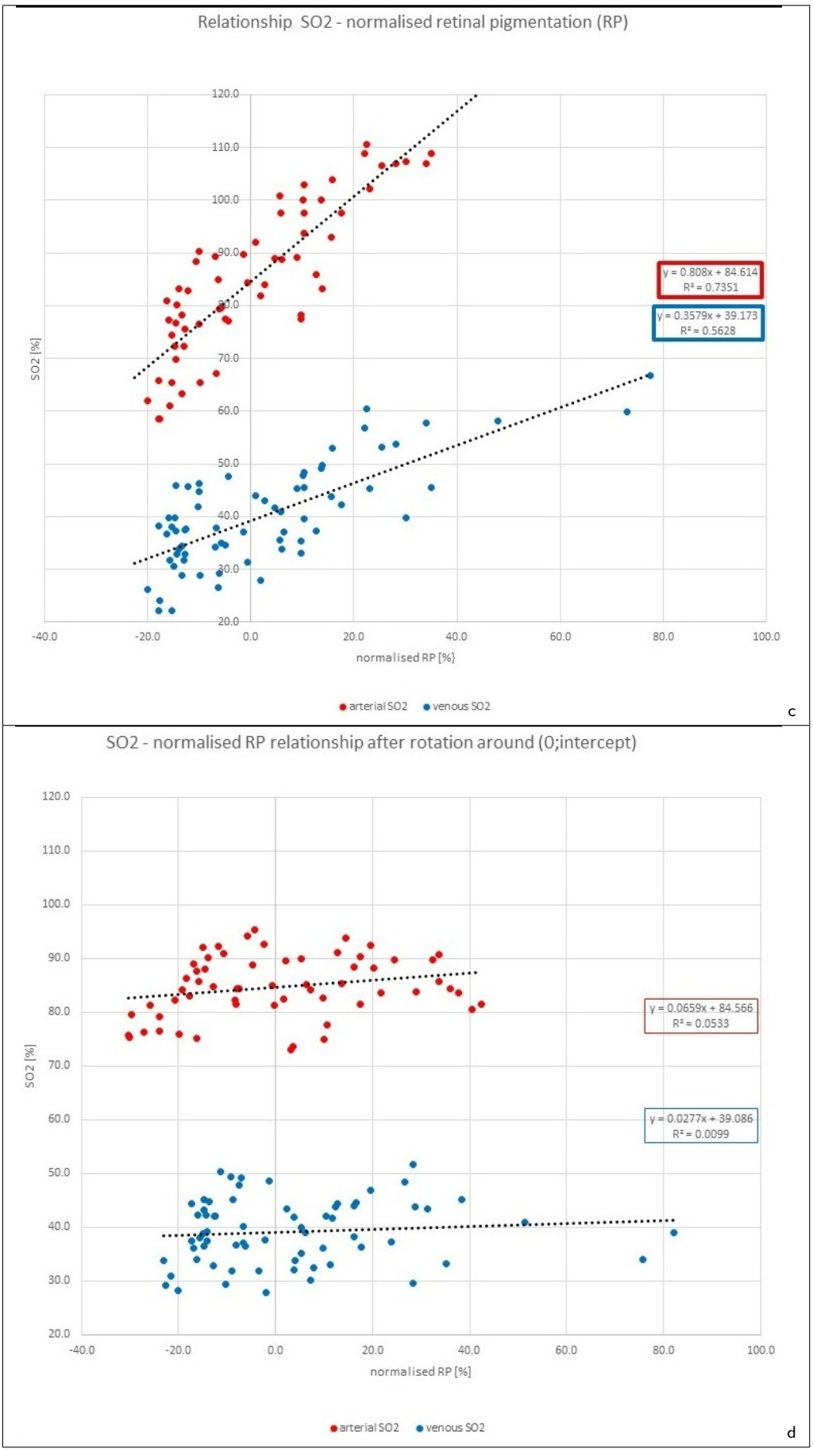

Figure 20: **Transformation of SO2 data to compensate for retinal pigmentation (2/2): Graph c shows the relationship between SO2 results and normalised pigmentation value. Graph d represents the rotated (rotated around the intercept of the graphs in picture c) SO2 data.**

9.3. Static vessel analysis

Static vessel analysis is the determination of retinal vessel narrowing by computing the mean width reduction of an equal number of manually selected arterial or venous vessel segments (referred to as CRAE and CRVE) and describes the width of the vessel and its branching characteristics. This semi-automated measurement is carried out according to the revised Parr-Hubbard formula [152, 128] in a predefined circumferential zone between 0.5 and 1 disc diameter from the optic disc margin. The ratio between arterial and venous calibres is referred to as AVR. The measured diameter refers to the diameter of the blood column rather than the complete vessel including the vessel wall [273]. For reliable results, vessels selected for analysis should be at least 25 μm in diameter, since its borders are hard to detect leading to measurement bias [128].

Fundus images acquired using the RVA funduscamera (see also section 9.1) were analysed with the semi-automated iFlexis software (Version 2.1.1). While the Vesselmap analysis algorithm to determine CRAE and CRVE uses the initial Parr-Hubbard formula, iFlexis employs the updated analysis algorithm published by Knudtson et al. (2003) [152]. For this study the Knudtson algorithm was used to determine CRAE, CRVE and AVR.

9.3.1. Protocol and quality control

The mean of three clear images (image types: oximetry image, colour image and red-free image) was used for analyses. A minimum of four vessel pairs (artery and vein) up to six pairs were used to compute CRAE, CRVE and AVR. Figure 21 shows one example of the analysis. To investigate as to whether the image type effects vessel calibre measurement a Bland-Altmann (B-A) analysis was carried out. SVA data of study subjects with one clear image of each image type were included (N= 68). Glaucoma was not an exclusion criterion due to the objective of this investigation. This investigation explored as to whether the mean vessel calibre calculated from three different images is biased by the image type. To qualify "in good agreement", 90 % of the data had to be within the 95 % LOA limits. For both, CRAE and CRVE the B-A analysis which is given as "mean difference (limit of agreement (LOA))" revealed that the mean results are not biased due to the usage of different image types. For CRAE the mean difference between different

image types was -0.5 µm (LOA 13.61 µm, -14.55 µm) for comparison of colour vs red-free, -0.70 µm (LOA 16.21 µm, -17.61 µm) for comparison of oximetry vs colour, and -1.10 µm (LOA 18.34 µm, -20.54 µm) for comparison of oximetry vs red-free images. For CRVE the B-A analysis of agreement exhibited -0.75 µm (LOA 15.64 µm, -17.13 µm) for comparison of oximetry vs colour, -0.90 µm (LOA 15.91 µm, -17.69 µm) for comparison of colour vs red-free, and -1.52 µm (LOA 21.88 µm, -24.93 µm) for comparison of oximetry vs red-free images. The plots are shown in figure 22.

a

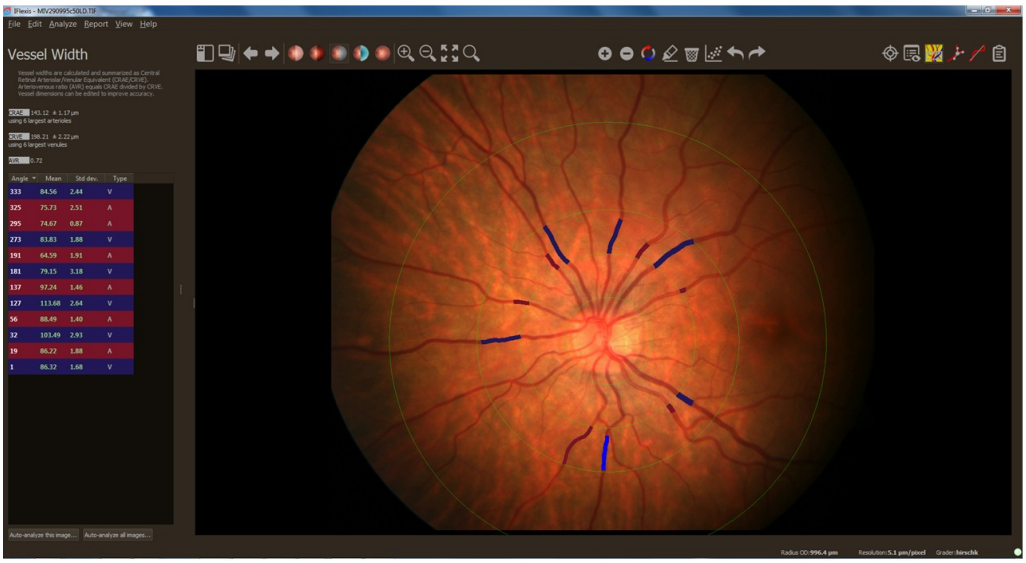

b

c

Figure 21: **Principle of static vessel analysis using the iFlexis software (v 2.1.1.): a) oximetry image, b) colour image, c) red-free image**

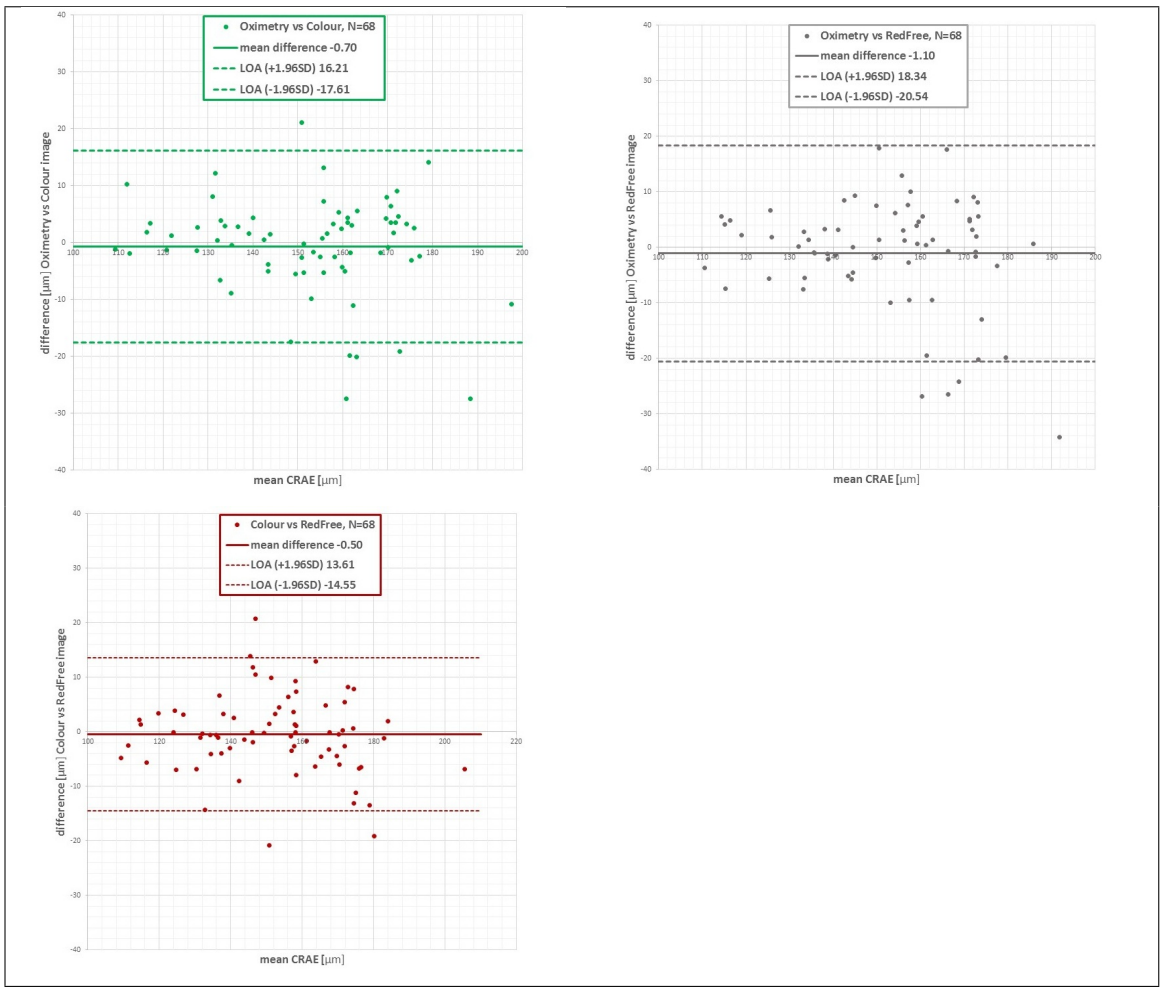

Figure 22: **Investigation on the question if the image type influences CRAE results and hence, confirmation that three images of different type can be used to compute the mean. The B-A analyses confirmed that three different image types can be used to compute mean CRAE and mean CRVE without causing any image type related bias. The sample size for B-A analysis was N=68. Between 3 (4 %) and 6 (9 %) data points were outside the LOA for the CRAE analysis.**

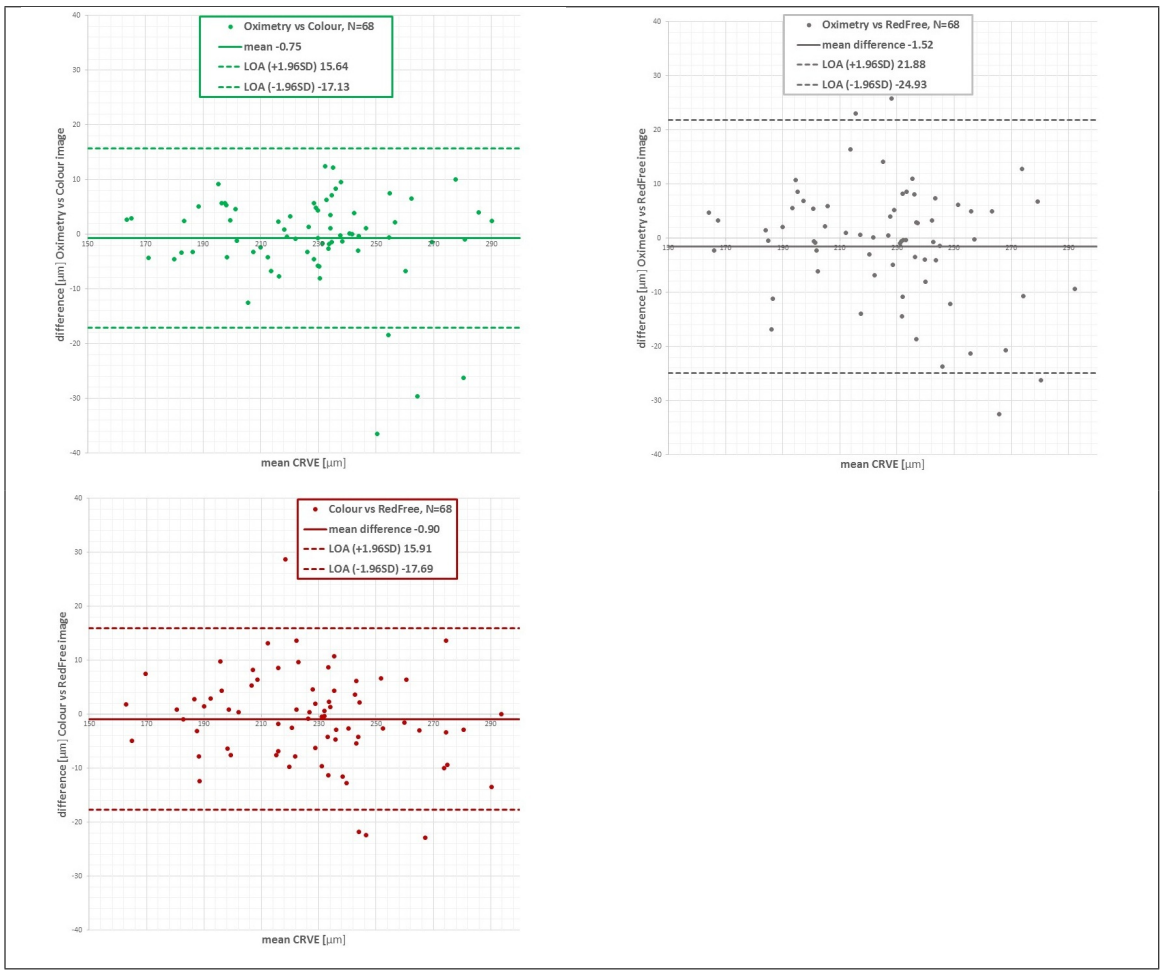

Figure 23: **Investigation on the question if the image type influences CRVE results and hence, confirmation that three images of different type can be used to compute the mean. The B-A analyses confirmed that three different image types can be used to compute mean CRAE and mean CRVE without causing any image type related bias. The sample size for B-A analysis was N=68. For veins 4 (6 %) data points were outside the LOA in all three B-A analyses.**

9.4. Retinal vessel complexity

The spatial distribution of the retinal vessel network was analysed using the Df (complexity of the network) and Lac (Lacunarity, spacing in between vessels) results of the box-plot method (termed in the software as "fractal analysis-segmented" and "lacunarity - segmented"). Images were saved in a high-quality Tiff - format as to provide the appropriate amount of image information such as resolution, colour-information and contrast information for analysis. Previous investigations have shown that clear images with an even brightness across the image achieve best reliability [307]. Three images (oximetry, colour and black-and-white) were analysed using iFlexis (Version 2.1.1, see figure 24). The retinal vessel complexity analysis was determined from a disc-centred image in a measurement area with an inner radius of 1.5 times the disc radius and an outer radius

of five times the disc radius. The software assumes the disc to have a diameter of 1.8 mm if not specified otherwise.

9.4.1. Compensation for the shape of the retina

The imaging software converts a spherical image into a plane image which in this study is used for the vessel complexity analysis. Conversion software assumes a modified Gullstrand eye [304] (AL_G=24 mm and Rxy= -13.50 mm) with a spherical shape (conicoid with asphericity Q=0). However, when assessing the density of a network, the observation angle may influence the measurement result. The vessel network complexity of an image from a more prolate ellipsoid appears peripherally denser than the one from a less prolate (maybe oblate) ellipsoid determined by the asphericity Q [6]. The asphericity value Q is determined according to the equation

$$Q = \frac{Rxy^2}{Rz^2} - 1 \tag{9}$$

Hereby R$_{xy}$ and R$_z$ are the radii of the ellipsoid in three-dimensional space. For a sphere Q yields zero and for a prolate ellipsoide (long eye length) $-1 < Q < 0$ is valid. An oblate ellipsoid shows $Q > 0$.

Although the effect of asphericity of the retina might not be large, Df and Lac results were also adjusted for this effect. Assumptions herein were that Rxy is a constant value for all eyes. Furthermore, R$_z$ is determined by the AL of the individual (AL_i) and the difference between AL and Rv of the Gullstrand schematic eye ($constant = AL_G - R_v = 10.50$ mm). Consequently, asphericity of an individual (Q_i) was calculated according to the following equation:

$$Q_i = \frac{(13.50mm)^2}{(AL_i - 10.50mm)^2} - 1 \tag{10}$$

Finally, the measured value was multiplied by the adjustment factor: $1 - \frac{Q_i}{100\%}$. The adjustment factor was < 1 for AL greater than 24 mm and > 1 for eyes shorter than the AL of 24 mm to adjust for any overestimation in eyes with AL$>$ 24 mm and underestimation in eyes with AL$<$ 24 mm.

9.4.2. Protocol and quality control

The mean result (Df or Lac) of three clear 50^0 disc-centred tiff-images with the best brightness distribution across the image was used for statistical analyses. To achieve the required quality, the circular alignment ring (from the fundus camera) had to be clear on the subjects cornea and the camera had to focus on the subjects retina. The ocular of the fundus camera allows the observer to check for exact focusing. Furthermore, the participant was instructed to blink before the image was captured which improved the image quality further. To investigate if the different image types used to compute the mean may bias the result of mean, a Bland-Altmann (B-A) analysis was carried out. To qualify "in good agreement", 90 % of the data had to be within the 95 % LOA limits. Vessel complexity data of study subjects with one clear image of each image type were included (N= 68). Glaucoma was not an exclusion criterion due to the objective of this investigation. B-A analyses confirmed that Df results of three different image types are comparable and thus, can be used to determine a mean value for each study subject to be used for consecutive statistical analysis (see figure 25). The B-A analyses revealed good agreement within the $\pm$1.96 SD limits of agreement for colour vs red-free, oximetry vs red-free and oximetry vs colour images: -0.0026 (LOA 0.028, -0.034) for colour vs red-free images, 0.0019 (LOA 0.034, -0.03) for oximetry vs red-free images, and 0.038 (LOA 0.038, -0.031) for oximetry vs colour images.

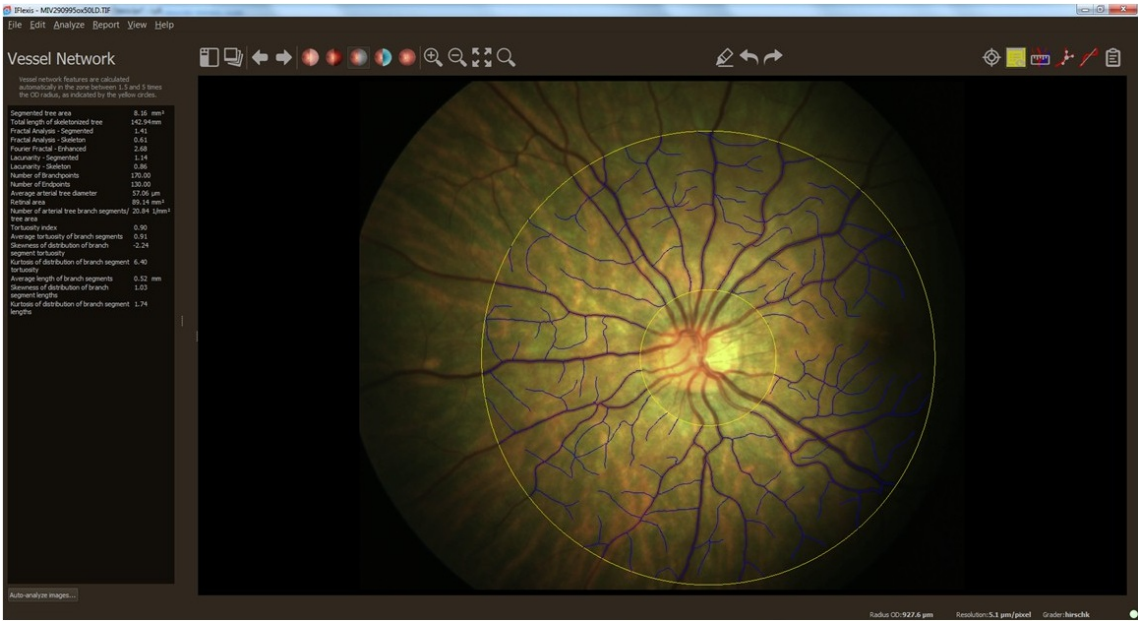

a

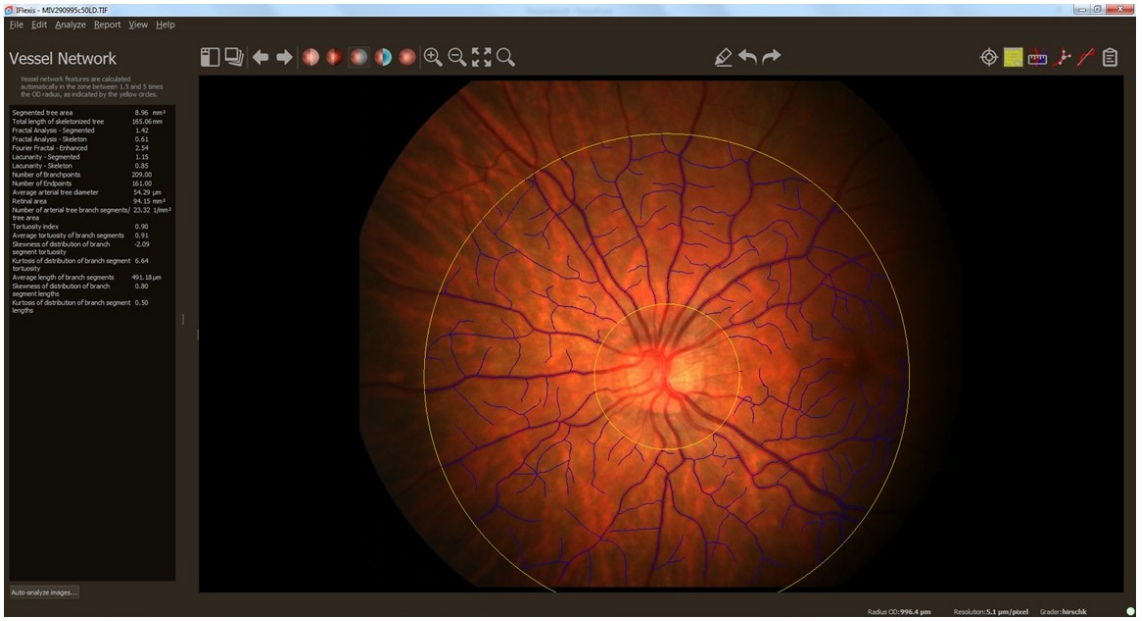

b

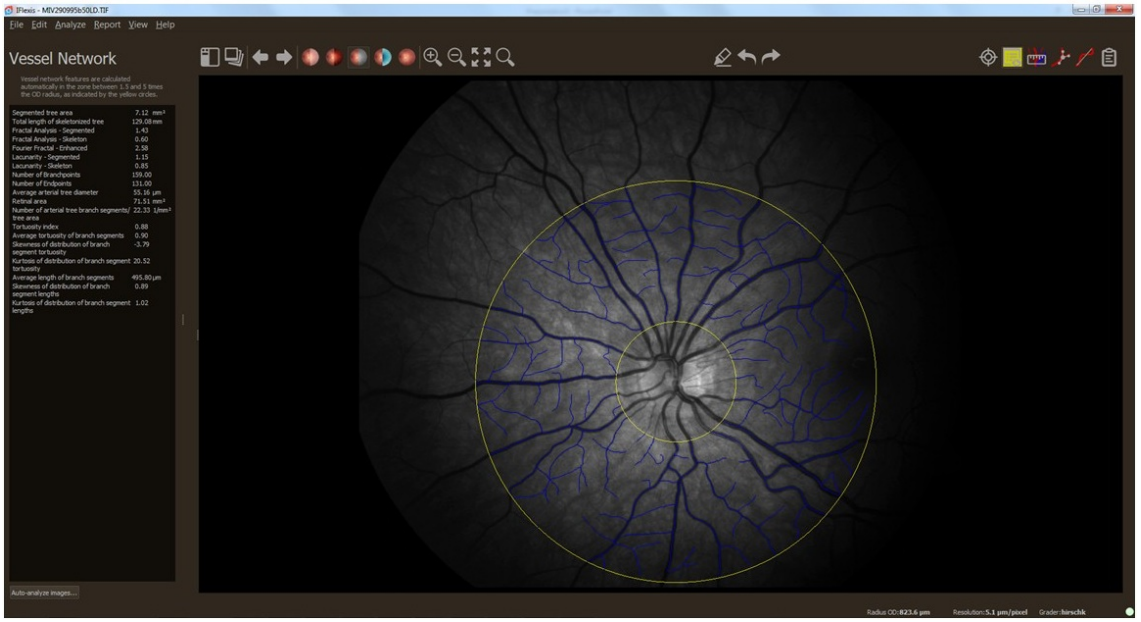

c

Figure 24: **Retinal vessel complexity analysis using the iFlexis software (v 2.1.1.): a) oximetry image, b) colour image, c) red-free image**

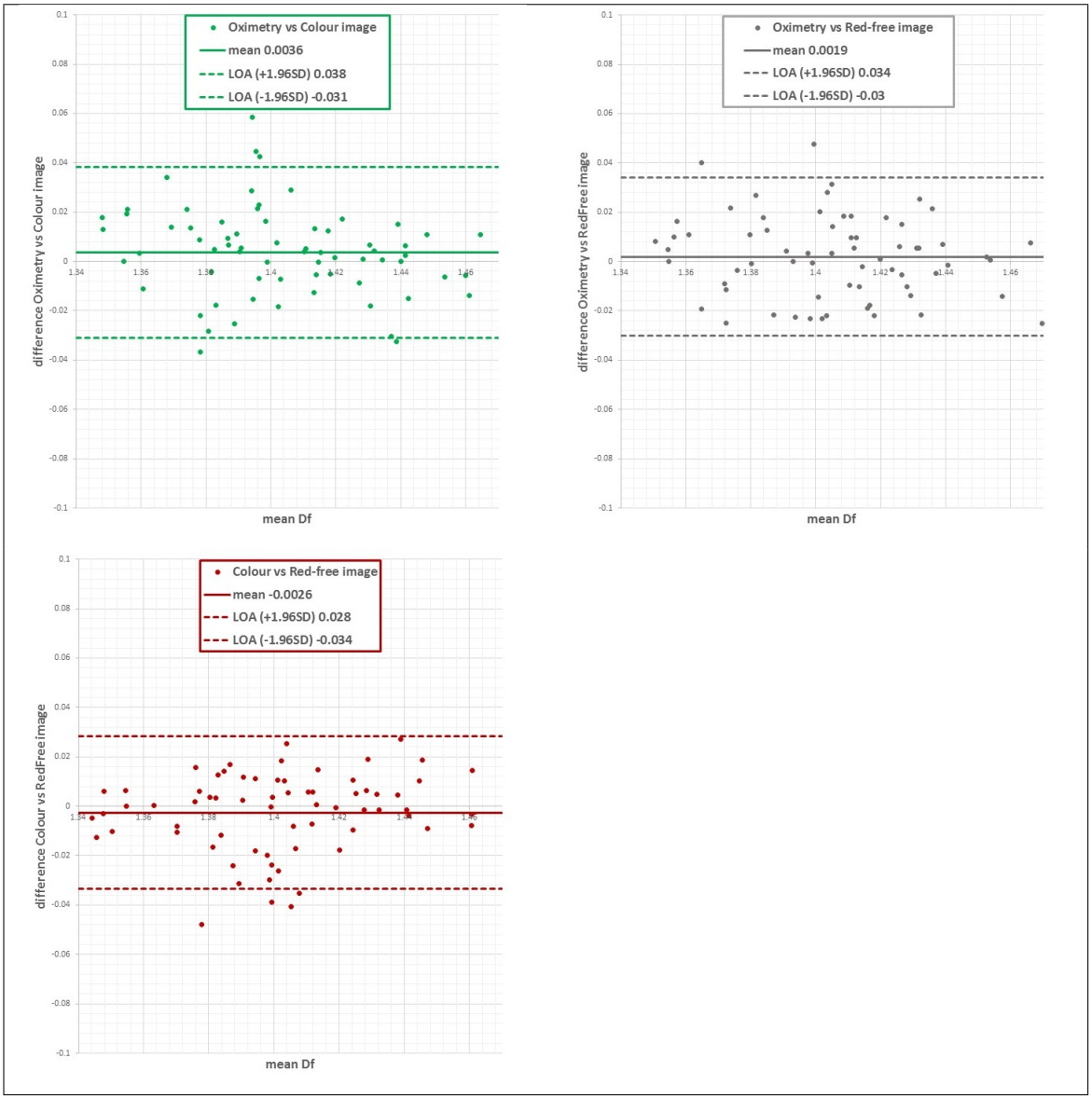

Figure 25: **Investigation on the question if the image type influences Df results and hence, confirmation that three images of different type can be used to compute the mean. The B-A analyses confirmed that three different image types can be used to compute mean Df without causing any image type related bias. The sample size for B-A analysis was N=68. Up to five ($< 7\%$) data points were outside the LOA, which confirms a very good agreement of results of different image types.**

9.5. Dynamic vessel analysis

The vessel diameter behaviour during three periods of flicker provocation (20 seconds) and consecutive recovery periods (80 seconds; 350 seconds in total) was video recorded using the RVA setup as shown in figure 17/b. For dynamic vessel analysis (DVA, referred to as vessel reactivity measurement or retinal vessel function) the RVA system records video images of pre-selected vessel-sections with a sampling rate of 25 Hz. The RVA system has a spatial resolution of 180 μm in the vessel direction and < 1 μm in the

measurement direction [273]. The instrument setup is shown in figure 17/a.

9.5.1. Protocol and quality control

For this study three consecutive flicker-recovery cycles (see figure 17/b) of at least one vessel section for each vessel type were analysed. The data was treated according to the sequential and diameter response analysis (SDRA) published by Heitmar et al. (2010) [112]. This approach was found to be sensitive to individual differences in response characteristics. Additionally, the authors found different vessel reactivity characteristic for arteries and veins which should be addressed when exploring retinal vessel reactivity. Hence, this approach might provide a more detailed information than the traditional analysis method provided by the RVA software. In detail, the baseline diameter fluctuation (BDF, [%]), dilation amplitude (DA, [%]), maximum constriction (MC, [%]), maximum dilation (MD, [%]) and degree of vasodilation between FL initiation and MD (deltaD, [%]) of each vessel section within each flicker-recovery cycle (129 sec per cycle) was calculated. The mean of three flicker cycles from up to two vessel sections (of the same type) was used for statistical analysis. The vessel segments were chosen from the superior vessel arches for all study subjects. Previous investigations have shown that superior and inferior vessel arches do not necessarily show identical behaviour [88]. A detailed explanation of the SDRA variables can be found in table 15. From the beginning of data collection in October 2016 to March 2017 the software allowed only for the selection of one artery and one vein. A software-upgrade (April 2017) allowed to select up to eight vessel sections. Thus, eight emmetropic and nine myopic subjects had only data of three flicker cycles from only one vessel section. The raw data of the mean vessel diameter per second for four vessel sections (two arteries and two veins) provided by the RVA were manually edited to remove noise before variables (BDF, DA, MD, MC and deltaD) were calculated. The editing process meant deleting spike values and replacing them with the previous value (see figure 26). No more than three consecutive data values were deleted at the same time.

Abbreviation	Unit	Explanation
DA DAA for arteries, DA$_V$ for veins	%	difference in diameter between minimum diameter and maximum diameter in flicker time + 5 sec $MD\% - MC\%$
BDF BDFA for arteries, BDF$_V$ for veins	%	difference in diameter between maximum and minimum diameter of baseline (20 to 49 sec for cycle 1, 120 to 149 sec for cycle 2 and 220 to 249 sec for cycle 3) $(maxBLdia - minBLdia) * 100/avBLdia$
MD MDA for arteries, MD$_V$ for veins	%	percentage change in vessel diameter during flicker time relative to average baseline diameter, $(maxFLdia - avBLdia) * 100/avBLdia$
MC MCA for arteries, MC$_V$ for veins	%	percentage change in vessel diameter after flicker time relative to average baseline diameter, $(minpostFLdia - avBLdia) * 100/avBLdia$
deltaD deltaDA for arteries deltaD$_V$ for veins	%	difference between maximum dilation diameter (flicker time+5sec) and diameter at 49 sec (cyle 1) or 149 sec (cycle 2) or 249 sec (cycle 3) $(diabeforeFL - maxFLdia) * 100/avBLdia$

Table 15: **Sequential and Diameter Response Analysis (SDRA) markers according to Heitmar et al. (2010)**

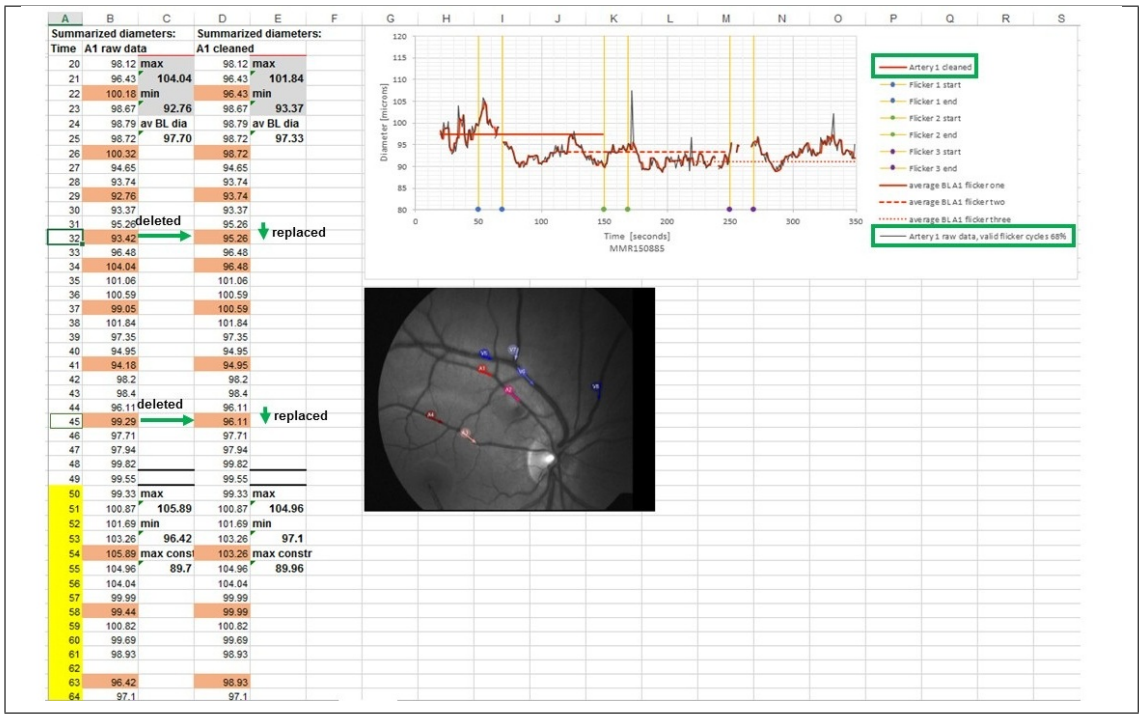

Figure 26: **Manual data cleaning process prior to SDRA. The example at data point 32 second shows that the measurement value is lower than the previous but also lower than the following value. Hence this value was replaced by the measurement value from 31 second. The time point 45 second shows the same replacement strategy but with a spike into the opposite direction.**

9.6. Ocular perfusion pressure calculation

Ocular perfusion pressure is not a direct measurement but can be computed from BP and IOP measurements. Thus, this measurement represents the blood circulation vs IOP balance in the eye. In this study mean ocular perfusion pressure (MPP), diastolic and systolic perfusion pressure (sPP) were determined using these equations:

$$MPP = \frac{2}{3} * \left(\left(sBP + \frac{1}{3} \left(sBP - sBP \right) \right) - IOP \right) \tag{11}$$

$$sPP = dBP - IOP \tag{12}$$

$$dPP = dBP - IOP \tag{13}$$

In equations 11 to 13 DBP refers to diastolic blood pressure, SBP refers to systolic blood pressure and IOP refers to intraocular pressure.

The next sections describe the measurements in detail from which MPP, sPP and sPP are derived. For statistical analysis only systolic and diastolic values were used due to the fact that MPP combines these two measures.

9.6.1. Blood pressure measurement

Ocular haemodynamic measurements are related to systemic measurements, such as BP measurements. In this study, BP was measured in accordance with the guidelines of the British Hypertension Society [http://bhsoc.org/latest-guidelines, June 2016] using the validated automated blood pressure monitor A&D, UA767 (P.M.S. instruments Ltd., Maidenhead). Three consecutive measurements were carried out after five minutes resting in a sitting position and at least one-minute break between each measurement. The

mean of the three measurements was used for statistical analysis and further calculations, such as OPP. Three consecutive sBP measurements were valid if the variation between them was less than 10 mmHg. Valid dBP measurements had less than 5 mmHg variation. If these requirements were not met, two measurements with the least difference were used to determine the average sBP or dBP. Blood pressure measurements also served to exclude uncontrolled systemic hypertension (cut-off: sBP>140 mmHG and dBP >90 mmHg, according to the British Hypertension Society [http://bhsoc.org/latest-guidelines (NICE), June 2016]. Subjects who were previously diagnosed with systemic hypertension but take regular blood pressure medication were included in this study if the BP was within the normal limits (below 140 mmHG for sBP and below 90 mmHg for dBP).

9.6.2. Intraocular pressure measurement

IOP measurement is required to calculate ocular perfusion pressure (see section 9.6) but also to exclude ocular hypertension. The IOP was determined using the I-Care ic100 rebound tonometer (Tiolat OY, Finland). The instrument measures intraocular *"pressure"* by propelling a probe of a known *"mass"* and a diameter less than 1mm (hence the surface area which will be touched by the probe is very small) with a predefined velocity (0.2 to 0.4 m/s) against the cornea and measuring the *deceleration* of the probe. The IOP is a function of the deceleration time and can be computed as follows:

- Knowing the fact that

$$Pressure = force/area \tag{14}$$

  with area tending to be very small ($\propto 0$).

- Additionally, it is known that

$$Force = mass * deceleration \tag{15}$$

  By knowing that the areas value is very small ($\propto 0$) and combining equation 14

and 15 the calculation of IOP is:

$$Pressure = mass * deceleration \tag{16}$$

This principle is proved to be comparable to the IOP measurement using Goldmann applanation tonometry [27, 235]. In contrast to applanation tonometry, it does not require the use of anaesthetics and hence, reduces the risk of adverse reactions. The measurement was carried out before the use of Tropicamide 1% and with the volunteer in a sitting position. A disposable probe was inserted in the probe base and the mean of three consecutive measurement cycles was used for analysis. Each cycle had to be of best quality indicated by the result presented in a green frame (dependent on the SD of 6 measurements). The mean of three measurement cycles was used for statistical analysis.

10. Statistical analyses

A sample size calculation based on data of nine randomly chosen subjects for each of the three study cohorts (pilot study principle) was carried out using GPower 3.1.9.2. The sample size calculation for comparisons of structural and of haemodynamic measurements in three cohorts (assuming ANOVA test statistic) revealed sample sizes between 22 and 46 subjects per group to achieve a statistical power of 80 %, with an alpha error of 5 %. The study aimed for at least forty subjects for each study cohort based on the fact that seven out of nine independent variables required a sample size below forty. In detail the sample sizes were as follows:

- N=22 for RNFL and GCL thickness measurement.
- N=32 for arterial SO2 measurement as well as N=18 for venous SO2 measurement.
- N=22 for Df measurement.
- N=15 and N=14 for CRAE and CRVE measurements, respectively.

- N=46 for DA_V measurement. Unfortunately, no sample size for DA_A measurement was computable due to the fact that means (M) and standard deviations (SD) were the same for all groups in the pilot sample.
- A sample size of 22 + n(variables) for multiple correlation analysis when a large effect size (> 0.5) was assumed.

10.1. Statistically, the study approached the research question as follows

Firstly, distribution testing (descriptive statistic) using the Shapiro-Wilk test was carried out. To explore differences in function, structure and blood circulation aspects between three study cohorts (Emmetropes, Myopes, Glaucoma) in cases of parametric (normally distributed data) distributions the one-way ANOVA (parametric) test was used. The Tukey HSD (honest significant difference) test using a harmonic mean sample size (post-hoc) was used to identify if emmetropes differ from high myopes for a particular independent variable. This test strategy is conservative when sample sizes of the compared study cohorts are unequal [299]. It also corrects for multiple comparisons. The Kruskal-Wallis one-way ANOVA (k-samples) test was used when the data distribution was non-parametric or the variances were not homogenous. A pairwise comparison (Kruskal-Wallis for k-samples) with Bonferroni correction for multiple tests was carried out to specify differences between the healthy groups. The decision for parametric or non-parametric testing strategy was made according to the distribution characteristics of at least two groups. An alpha level of .05 was used for all statistical tests.
Previous research reported an "age-related" change for some variables (see table 16). Hence, the comparison analyses were also carried out applying an age specific weighting factor (WFage). The WFage was only determined in cases when previous findings clearly showed a statistically significant dependency on age. Nagel and colleagues [218] suggested an age related reduction in baseline- corrected flicker response although non-significant. Thus, weighting was not employed for SDRA. The weighting factor for each affected variable was determined as follows: The youngest study subject (age 18 years)

was weighted with the factor one. If previous research found an increase of the investigated variable with age the WFage was smaller than one and vice versa.

The main objective in this study was to investigate if haemodynamic measures and measurement patterns differ between highly myopic eyes and emmetropic eyes and, if highly myopic eyes show similarities with glaucoma subjects. Haemodynamic patterns were determined in carrying out correlation analysis for each group separately. In addition to showing patterns in haemodynamic parameters, these group specific intra-relationships also determine multicollinearity. In case of normally distributed data Pearson correlation was applied and Spearman's rho correlation when data were not normally distributed. Correlation coefficients and significance levels are presented in correlation matrices. In order to determine haemodynamic variables (predictor variables) and/or patterns that are able to predict neuroretinal tissue thicknesses in the three study cohorts, correlation analyses were employed for each group individually. In doing so, the study might be able to identify haemodynamic parameters which are different for highly myopic eyes when compared with emmetropic eyes and hence, may suggest why highly myopic eyes are more susceptible to develop glaucoma (loss of neuroretinal tissue). The issue of multiplicity in testing multiple comparisons was controlled using the false discovery rate approach (FDR) with q= .05 [16]. FDR-controlling procedures are designed to control the expected proportion of "discoveries" (rejected null hypotheses) that are false (incorrect rejections). This approach to control the probability of committing any type I error in families of comparisons under simultaneous consideration has proved to be less stringent than previously introduced methods such as the familywise error rate (FWER) or the initially applied Bonferroni correction [16]. Only variables showing a significant correlation after controlling according to the FDR approach were further investigated employing hierarchical multivariate linear regression to predict the change in structural variables from haemodynamic measures (predictor variables/ independent variables). IBM SPSS Statistics 25 was used for statistical analyses.

independent variable	publication(s)	finding	WF/ adjustment
GCL	Zhang et al. (2016), cross-sectional design, N=192 eyes	0.17% thinning per year of age	WF $1 + (age - 18) * 0.0017$
RNFL	Zhang et al. (2016), cross-sectional design, N=192 eyes	0.21% thinning per year of age (inferior / superior)	WF $1 + (age - 18) * 0.0021$
arterial SO2	(1) Man et al. (2014), N=50 Caucasians, RVA used; (2) Mohan et al. (2015), N=89 Asians, OxymapT1 used, for both: cross-sectional design	(1) β=0.3 % increase per year of age (2) β=0.26 % increase per year of age	WF $1 - (age - 18) * 0.0028$ (mean of both study results)
venous SO2	(1) Man et al. (2014), N=50 Caucasians, RVA used; (2) Mohan et al. (2015), N=89 Asians, OxymapT1 used, for both: cross-sectional design	(1) β=0.26 % increase per year of age (2) β=0.196 % increase per year of age	WF $1 - (age - 18) * 0.0023$ (mean of both study results)
CRAE	Wong et al. (2004) Beaver Dam,[317], N=4926, cross-sectional design	0.22 µm decrease per year of age	WF $1 + (age - 18) * 0.0022$
Df	(1) Liew et al. (2008), BMES, N=100, cross-sectional design (2) Cheung et al. (2008), SiMES, N=2913, cross-sectional design	(1) age relationship β=-0.42, p<.001 (2) age relationship: $\beta_{standardised}$=-0.311, p<.001	WF $1 + (age - 18) * 0.0035$

Table 16: **Weighting (age dependency and asphericity retina) of independent variables based on previous research.**

Part V

Results of this study

The subsequent sections will present the results of this exploratory, cross-sectional study as follows: Firstly, section 11 and 12 present demographic data of the three study cohorts (emmetropic=E, highly myopic=hM and glaucoma patients=G) and the clinical findings of their retinal images. In doing so, it allows to depict possible cofounding variables such as e.g. age. Secondly, section 13 shows findings of the comparison of functional, structural and haemodynamic measurements in order to determine parameters that differ in between the study groups. Retinal haemodynamic variables that show differences between healthy emmetropes and healthy myopes, but exhibited similar results for the highly myopic cohort and the sample of glaucoma subjects may suggest a potential higher risk in physiological myopia to develop glaucoma and thus, be worth of further investigation. Finally, section 14 presents links between haemodynamic measurements and relationships of structural and haemodynamic measurements. This approach allows for identifying group-specific haemodynamic patterns (subsection 14.1) as well as haemodynamic variables capable of predicting changes in neuroretinal tissue thickness in each cohort (subsection 14.2). The correlation analyses were carried out for the group of emmetropes (referred to as control group), the highly myopic group as well as for the glaucoma group separately with the purpose to depict distinct patterns and relationships which vary in the healthy cohorts of different eye length (emmetropic vs highly myopic), but may resemble in healthy myopes and glaucoma subjects. In doing so, the study highlights specific haemodynamic parameters/patterns in healthy myopic eyes that suggest an increased risk of developing glaucoma.

The study aimed for a sample size of 40 for each group. Although intensive advertisement (posters, oral invitation, leaflets and 100 letters sent to patients of the Optometry eye clinic), the response from glaucoma subjects in particular, to the study invitation was poor. Although the recruited sample for glaucoma subjects was small, the findings may be illustrative of the condition and therefore of clinical value. Moreover, the correlation

analyses for the glaucoma sample showed large ($r > 0.5$) and very large ($r > 0.7$) effect sizes and, thus were not discarded.

11. Demographic data - Sample statistics

For this study, data of 41 healthy emmetropic (E), 32 healthy highly myopic (hM) and 11 glaucomatous (G) subjects (one eye) were collected. One emmetropic subject and one highly myopic subject had to be excluded because of glaucoma suspicion. Two more highly myopic subjects did not complete all tests and thus, were excluded. One subject of the glaucoma cohort was excluded due to nystagmus and another subject due to secondary primary open angle glaucoma. Furthermore, for various variables some data were excluded due to previously (see part IV) described image and measurement quality criteria. Table 17 lists the sample size for the individual measurements/ variables. Of the remaining 40 emmetropes, 22 were females and 18 males. In the highly myopic group, 25 subjects were females and six subjects were males. In the glaucoma group, four subjects were female and five were male.

Of nine glaucoma subjects, one subject was diabetic and therefore treated . Furthermore, six glaucoma subjects were treated with blood pressure lowering medication at the point of the measurements. One participant of the glaucoma cohort presented with a history of pituitary gland lesion and thus, the visual field results were excluded from analysis. Finally, eight out of nine glaucoma subjects were treated with combinations of anti-hypertensive medications while one glaucoma subject was treated with a prostaglandin analogue (Bimatoprost) only.

Variable	Sample size n		
	Emmetrope	Myope	Glaucoma
Visual Field variables	38	28	7
RNFL and GCL thickness	39	27	9
PP (systolic and diastolic)	40	29	9
SO2	34	27	8
Vessel architecture (Df, CRAE, CRVE)	40	29	9
Vessel reactivity (DVA according to SDRA)	33	27	7

Table 17: **Included number of data (n) for statistical analysis. Exclusion criteria were bad image quality and incomplete data.**

Age, spherical equivalent, intraocular pressure of the highly myopic group and diastolic blood pressure of the emmetropic group were not normally distributed (Shapiro-Wilk: $p<.05$), while intraocular pressure of the emmetropic cohort and glaucoma patients, diastolic blood pressure of the highly myopic and glaucoma cohort as well as axial length (for all cohorts), systolic blood pressure (for all cohorts) showed normally distributed data. Table 18 shows the p-value of the Shapiro-Wilk test statistic and group means and the standard deviation as well as median and range of these variables. Furthermore, the table shows the results of the analysis of variance (for parametric data) and the results of the Kruskal-Wallis test for k independent samples (for not normally distributed data).

The group means for IOP were E: M= 14 mmHg, SD= 3mmHg, hM: M= 14 mmHg, SD= 3mmHg and G: M= 13 mmHg, SD= 3mmHg. However, the differences in IOP between the groups were not significant ($F(2, 75) = 0.941$, p=.395).

The groups were significantly different regarding age ($H(2)$= 28.936, p=.000) with a mean rank of 29.62 for emmetropes, 42.47 for high myopes and 73.83 for glaucoma patients. Glaucomatous participants (*median*= 71 years, *range*= 52 to 86 years) were five decades older than the emmetropic and highly myopic cohort (E: *median*= 20 years, *range*= 18 to 55 years and hM: *median*= 23 years, *range*= 19 to 55 years). Despite a difference in group medians of 3 years, the age of the emmetropic and the highly myopic group was significantly different from each other (hM vs E*:* $H(1)$= -2.331, p=.059).

Refractive error was significantly different between the groups ($H(2) = 50.853$, p=.000)

with highly myopic eyes showing the largest myopic refractive error (*median*= -7.50 DS, *range*= -12.75 to -6.25 DS) and glaucomatous eyes exhibiting the largest variation (G*: range*= -14.00 to +0.25 DS, hM: *range*= -12.75 to -6.25 DS and E: *range*= -0.75 to +0.75 DS) although exhibiting a similar SE than emmetropic eyes (G: *median*= -0.25 DS and E: *median*= 0.00 DS).

For AL, all group means were different from each other. Post-hoc analysis using Tukey HSD test (harmonic mean sample sizes N= 17.586) showed that the all three groups were different from each other (three subsets). Emmetropes had the shortest eye length (*M*= 23.36 mm, *SD*= 0.68 mm). The longest eyes were found in the highly myopic group (*M*= 26.42 mm, *SD*= 0.81mm). As expected from inclusion criteria, the mean AL of the glaucoma group (*M*= 25.40 mm, *SD*=1.36mm) showed the largest variation (G: *range*= 23.53 to 27.52 mm versus hM: *range*= 24.46 to 28.26 mm and E: *range*= 22.00 to 24.60 mm).

Systolic as well as diastolic blood pressure were significantly different in between the study groups (1-way ANOVA: $F(2, 75)= 5.454$, $p=.006$ and $F(2, 75)= 3.872$, $p=.025$ for sBP and dBP, respectively). Moreover, subsequent post-hoc test using the Tukey HSD test (harmonic mean sample sizes N= 17.586) revealed that the highly myopic cohort shared the subset with both, the emmetropes and glaucoma subjects (see figure 27). The BP difference within the subsets were 4 mmHg (subset 1: E vs hM) vs 8 mmHg (subset 2: hM vs G) for sBP and 4 mmHg (subset 1: E vs hM) vs 2 mmHg (subset 2: hM vs G) for dBP. Emmetropes showed 12 mmHg (sBP) and 6mmHg (dBP) smaller BP results than the mean of the glaucoma sample. Nevertheless, all BP means were within a "normal" BP range according to the British Heart Foundation.

		p-value Shapiro-Wilk	mean (±SD)	median [IQR]	one-way ANOVA or Kruskal-Wallis (k-samples)	Post-hoc test: Tukey HSD (parametric data) or pairwise comparison KW with Bonferroni correction
Age [years]	Emmetrope n=40	.000	24 (±9)	**20 [8]**	H(2)= 28.936, p= .000	E vs hM: H(1)= -2.331, p= .059
	Myope n=29	.000	27 (±9)	**23 [11]**		
	Glaucoma n=9	.660★	68 (±11)	**71 [17]**		
SE [DS]	Emmetrope n=40	.009	0.03 (±.40)	**0.00 [0.75]**	H(2) = 50.853, p= .000	
	Myope n=29	.000	-8.00 (±1.73)	**-7.50 [1.75]**		
	Glaucoma n=9	.005	-3.14 (±4.94)	**-0.25 [6.00]**		
AL [mm]	Emmetrope n=40	.620★	**23.36 (±.68)**	23.31 [1.05]	F(2, 75)= 118.083, p= .000	3 subgroups
	Myope n=29	.989★	**26.42 (±.81)**	26.35 [1.05]		
	Glaucoma n=9	.460★	**25.40 (±1.36)**	26.01 [2.25]		
IOP [mmHg]	Emmetrope n=40	.147★	**14 (±3)**	15 [5]	F(2, 75) = .941, p= .395	NA
	Myope n=29	.003	**14 (±3)**	14 [4]		NA
	Glaucoma n=9	.535★	**13 (±3)**	13 [7]		NA
sBP [mmHg]	Emmetrope n=40	.524★	**108 (±9)**	107 [12]	F(2, 5)= 5.454, p= .006	E vs hM: p= .464
	Myope n=29	.062★	**112 (±11)**	111 [14]		
	Glaucoma n=9	.396★	**120 (±12)**	117 [20]		
dBP [mmHg]	Emmetrope n=40	.016	**70 (±7)**	70 [8]	F(2, 75)= 3.872, p= .025	E vs hM: p= .246
	Myope n=29	.926★	**74 (±9)**	74 [11]		
	Glaucoma n=9	.762★	**76 (±7)**	76 [13]		

★ *parametric distribution*

Table 18: **Summary of demographic data of the study cohorts. Bold text represents the type of average value (mean or median) used for subsequent statistical analysis.**

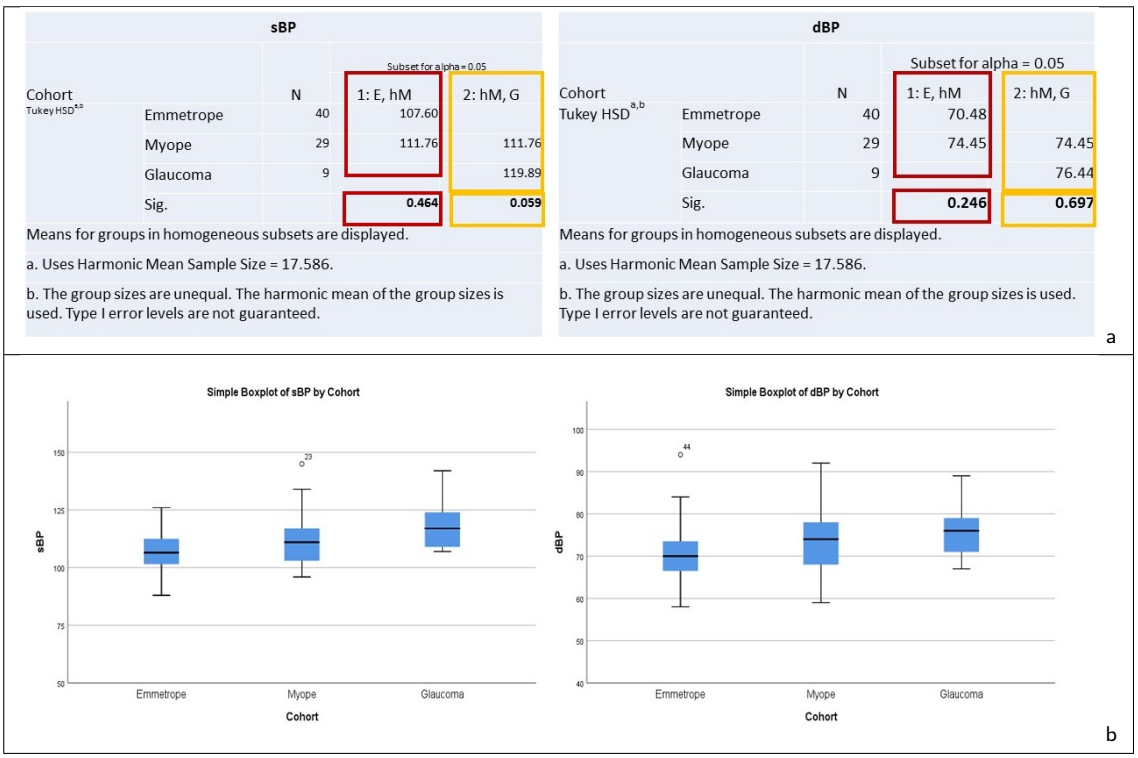

sBP

Cohort (Tukey HSD[a,b])		N	Subset for alpha = 0.05 1: E, hM	2: hM, G
	Emmetrope	40	107.60	
	Myope	29	111.76	111.76
	Glaucoma	9		119.89
	Sig.		0.464	0.059

Means for groups in homogeneous subsets are displayed.

a. Uses Harmonic Mean Sample Size = 17.586.

b. The group sizes are unequal. The harmonic mean of the group sizes is used. Type I error levels are not guaranteed.

dBP

Cohort (Tukey HSD[a,b])		N	Subset for alpha = 0.05 1: E, hM	2: hM, G
	Emmetrope	40	70.48	
	Myope	29	74.45	74.45
	Glaucoma	9		76.44
	Sig.		0.246	0.697

Means for groups in homogeneous subsets are displayed.

a. Uses Harmonic Mean Sample Size = 17.586.

b. The group sizes are unequal. The harmonic mean of the group sizes is used. Type I error levels are not guaranteed.

a

b

Figure 27: **a) Tukey HSD using harmonic mean sample size (N=17.586) revealed very similar means for the same subset for dBP (hM vs G: difference 2 mmHg). b) Box plots for sBP and dBP showing group means and 95%CI.**

12. Observational features of the retinae

The observation of retinal images and OCT images revealed that the RNFL thickness proportion according to the ISNT- rule (subsequently referred to as ISNT$_{RNFL}$-rule) was violated in 23 of the 40 emmetropic eyes (60 %), in 25 out of 29 high myopes (86 %). Unsurprisingly, the ISNT$_{RNFL}$-rule applied only in one of the nine glaucoma patient's eyes (violation percentage: 89 %). Additionally, the optic disc was found to be tilted in 12 emmetropic eyes (30 %), in 18 highly myopic eyes (62 %) and in two glaucoma eyes (22%). Fundus tessellation (either complete or partially) was found in 23 (five eyes with complete tessellation and 17 eyes with partial tessellation) emmetropic eyes (13 % complete and 43 % partial tessellation), in 25 (eighteen eyes with complete tessellation and seven eyes with partial tessellation) high myopes (62 % complete and 24 % partial tessellation) and in eight (five eyes with complete tessellation and three eyes with partial tessellation) glaucomatous eyes (56 % complete and 33 % partial tessellation). The discs exhibited crescent in three emmetropic eyes (8 %), in eleven highly myopic eyes (38 %) and in four eyes with glaucoma (44 %). Furthermore, one emmetropic eye (3

%), two highly myopic eyes (7 %) and two glaucomatous eyes (22 %) exhibited choroidal pallor. Finally, retinal vessels were found to be tortuous in eight emmetropic eyes (20 %), in four highly myopic eyes (14 %) and in three glaucomatous eyes (33 %). Figure 28 shows these results graphically.

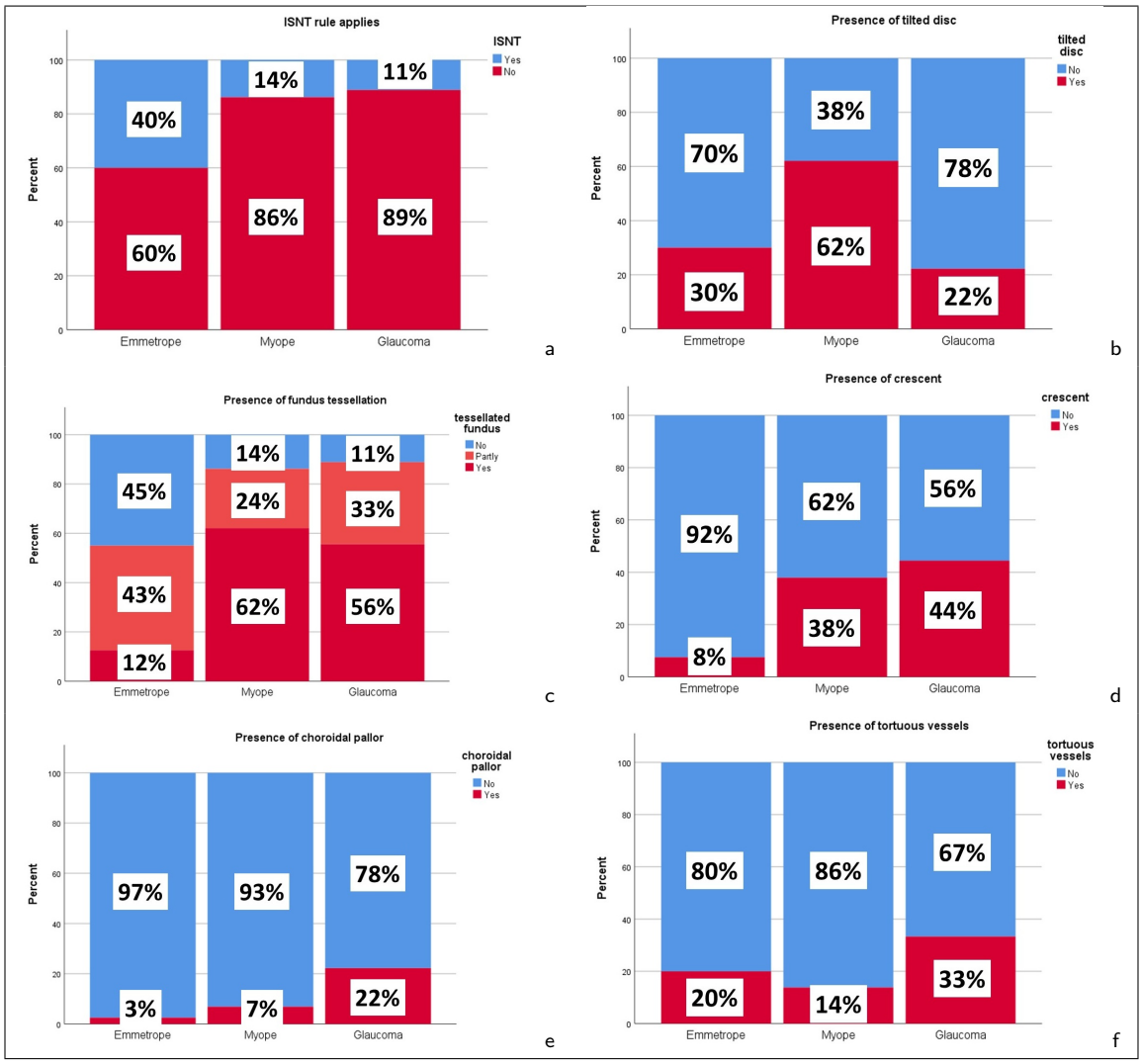

Figure 28: **Graphical representation of the observational findings shows a) proportions of subjects with RNFL thickness according to ISNT-rule (blue bars) and when ISNT-rule did not apply (red bars); b) proportions of tilted discs (red bars) versus normal disc appearance (blue bars); c) proportions of no fundus tessellation (blue bars) versus partly tessellation of the fundus (orange bars) and complete fundus tessellation (red bars); d) proportions of presence (red bars) vs absence (blue bars) of choroidal crescent; e) proportions of presence (red bars) versus absence (blue bars) of choroidal pallor and f) proportions of tortuous (red bars) versus normal retinal vessel appearance (blue bars).**

13. Group comparisons

One-way ANOVA analyses (parametric variables) with consecutive Tukey HSD post-hoc testing or Kruskal-Wallis testing for k-samples with pairwise comparisons with Bonferroni correction (non-parametric variables) were used in order to detect functional, structural and haemodynamic parameters which distinctly differ between healthy emmetropic and healthy highly myopic eyes, but show similarities between the group of healthy high myopes and glaucoma subjects. This part of the study aimed to depict parameters which are capable of indicating glaucoma suspicion in eyes with physiological myopia.

13.1. Function - Visual field testing

This study investigated the results of 30-2 SITA standard visual field assessments for 38 emmetropic eyes (E), 28 highly myopic eyes (hM) and for eight glaucomatous eyes (G) that fulfilled the inclusion criteria for reliable measurements (see section 3). Furthermore, data of two emmetropic subjects and two highly myopic subjects was excluded due to results "outside normal limits". Of the eight glaucoma subjects, data of one subject was excluded due to the history of a pituitary gland lesion. For the visual field test results of the glaucoma group, five (62.5 %) tests indicated a GHT "outside normal limits", two (25 %) test results exhibited a borderline-result for the GHT and one (12.5 %) test result exhibited a "normal" GHT analysis. Only the data for MD_H as well as data from the high myopes for C1 and P5 was normally distributed (Shapiro-Wilk test/ MD_H: p=.679 (E), p= .066 (hM), p= .958 (G) and Shapiro-Wilk test of hM for C1: p=.058 and hM for P5: p=.236). All other variables showed non-parametric distributions (see AppendixD).

13.1.1. Mean deviation and pattern standard deviation

Table 19 presents medians and interquartile ranges (IQR) for the study cohorts. For MD_H the presented data are mean and SD due to the parametric distribution of the

group data. Mean deviation (MD_H) as well as pattern standard deviation (PSD) exhibited similar results for emmetropic and highly myopic eyes: MD_H (E*): M*= -0.42 dB, *SD*= 1.28 dB and PSD (E): *median*= +1.70 dB,*IQR*= 0.38 dB and MD_H (hM): *M*= -0.60 dB, *SD*= 1.13 dB and PSD (hM): *median*= +1.74 dB, *IQR*= 0.41 dB. The post-hoc test using a pairwise comparison Kruskal-Wallis test with Bonferroni adjustment for multiple comparisons for PSD analysis and Tukey HSD with harmonic sample sizes for MD_H analysis revealed no significant difference between emmetropes and high myopes for PSD and MD_H *(H*(1)= 2.223, p= 1.0 and subset 1 (MD_H analysis): E and hM, p= .970; see table 20). The group averages for both, MD_H and PSD (absolute values) were largest for glaucomatous eyes (*G: M*= -4.56 dB, *SD*= 5.13 dB and *median*=+3.21 dB, *IQR*= 12.36 dB for MD_H and PSD, respectively). Moreover, the intra-group variation for all visual field indices was larger in the glaucoma cohort when compared with the variation in the other groups (see table 19). The largest IQR was found for N3 in the glaucoma cohort and, in the same cohort the smallest value was found for P5.

13.1.2. Glaucoma hemifield test analysis

For the differences in total deviation results between superior and inferior hemifield according to the GHT- patterns (referred to as pattern-differences; see figure 6) the emmetropic group exhibited pattern- differences of 0.33 dB (*median* C1; *IQR*= 0.70 dB) up to 1.00 dB (*median* P5, *IQR*= 1.70 dB). For the highly myopic group these pattern-differences were similar to those of the emmetropic group (lowest *median* N3= 0.50 dB, *IQR*= 0.80 dB up to *median* P4= 1.00 dB, *IQR*= 1.50 dB). For the glaucoma cohort the pattern- differences ranged from 2.67 dB (*median* C1, *IQR*= 10.70 dB) up to 4.83 dB (*median* P4, *IQR*= 20.70 dB). Figure 29 shows the results for individual variables graphically.

As for MD_H and PSD, the means of the GHT- pattern difference results were not significantly different from each other (p=1.0 for all zones) for both, emmetropes and myopes. The GHT- pattern difference results were lower than the results of the glaucoma cohort for both, emmetropic and highly myopic cohorts (see table 19).

Group	Emmetrope n=36	Myope n=26	Glaucoma n=7
MD_H in dB, Mean [SD]	-0.42 [1.28]	-0.60 [1.13]	-4.56 [5.13]
PSD in dB, Median [IQRx]	+1.70 [0.38]	+1.74 [0.41]	+3.21 [12.36]
C1-GHT in dB, Median [IQR]	0.33 [0.70]	0.67 [0.80]	2.67 [10.70]
C2-GHT in dB, Median [IQR]	0.50 [1.40]	0.63 [0.80]	3.00 [9.50]
N3-GHT in dB, Median [IQR]	0.60 [0.90]	0.50 [0.80]	3.80 [21.20]
P4-GHT in dB, Median [IQR]	0.75 [0.80]	1.00 [1.50]	4.83 [20.70]
P5-GHT in dB, Median [IQR]	1.00 [1.70]	1.00 [1.20]	3.75 [3.80]

Table 19: **Visual field test analysis: group averages.**

	Kruskal-Wallis (k-samples), n=69	pairwise comparison: Emmetrope vs Myope, n=62	
PSD	**H(2)= 8.900** p= .012	H(1)= 3.104 p= 1.00	
C1-GHT	**H(2)= 9.689** p= .008	H(1)= -3.571 p= 1.00	
C2-GHT	**H(2)= 11.197** p= .004	H(1)= 2.306 p= 1.00	
N3-GHT	**H(2)= 16.850** p= .000	H(1)= 2.097 p= 1.00	
P4-GHT	**H(2)= 12.839** p= .002	H(1)= -3.948 p= 1.00	
P5-GHT	**H(2)= 8.454** p= .015	H(1)= -0.233 p= 1.00	
MD_H one-way ANOVA	**F(2,66)= 13.939** p= .000	**P subset- comparison** harmonic n=14.347 E = hM > G	subset 1: E, hM, p= .970 subset 2: G, p= 1.00

Table 20: **Visual field test analysis group comparisons. The Kruskal-Wallis test (k-samples) revealed a significant difference in between the three study groups. Further pairwise comparison with Bonferroni correction revealed that emmetropic and highly myopic groups are not different from each other (p=1.0 for all variables).**

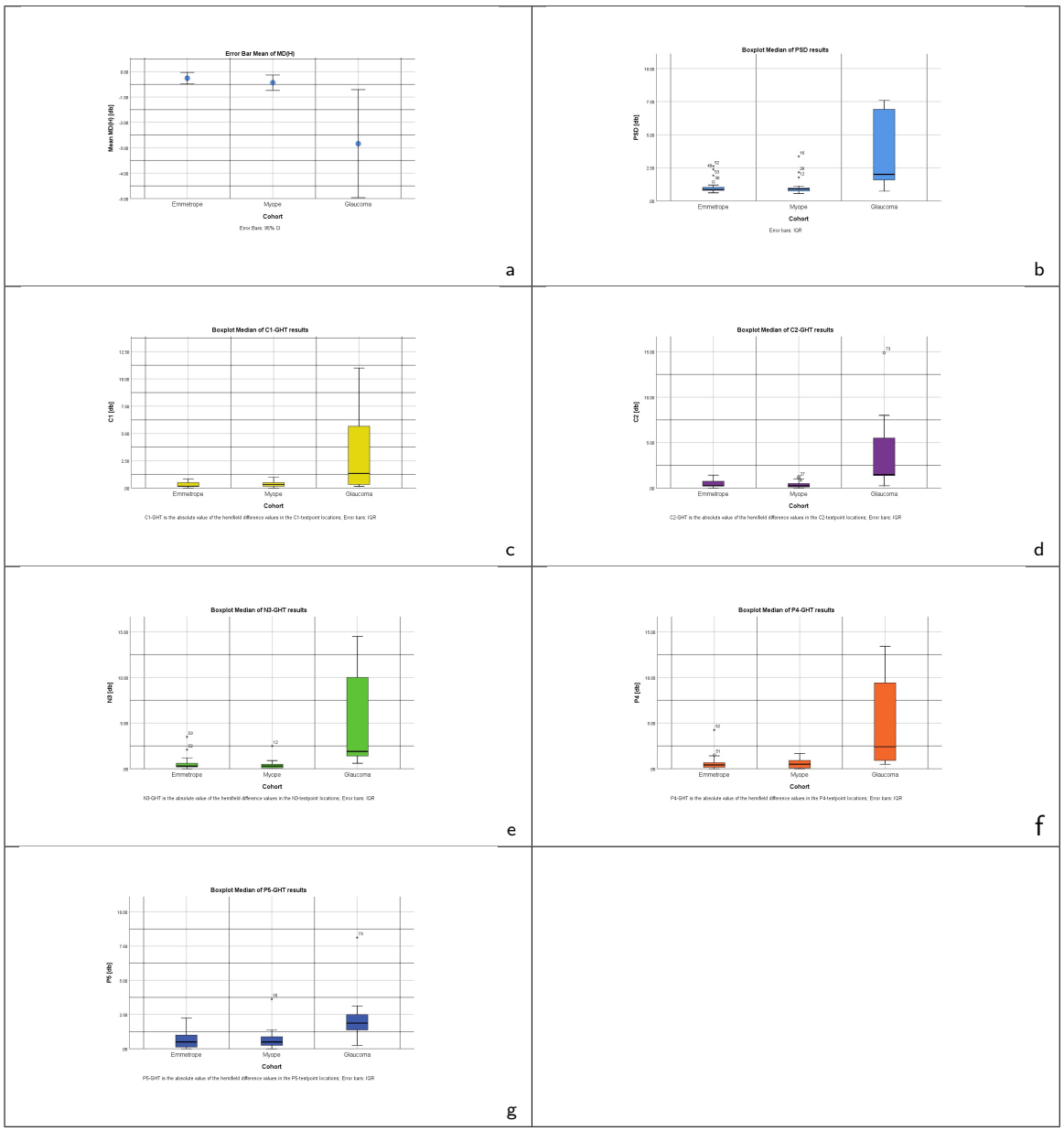

Figure 29: **Group comparisons of MD_H (a; Mean and 95% CI) , of PSD (b; Median and IQR) and of Glaucoma Hemifield Test pattern differences C1, C2, N3, P4 and P5 (images c to g; Median and IQR).**

13.2. Structural measurements

13.2.1. Retinal nerve fibre layer thickness

For RNFL thickness, data of 39 emmetropes (E), 27 high myopes (hM) and nine glaucoma patients (G) was included for analysis. The RNFL thickness data was normally distributed (see AppendixD). However, nasal and temporal thicknesses exhibited heterogeneous variances (Levene test of homogeneity of variances: $F_{Means}(2, 72) = 3.604$, $p = .032$ and $F_{Means}(2, 72) = 8.327$, $p = .001$ for nasal RNFL and temporal RNFL, respectively). Table 21 shows the group means of the raw data and the data after correction for ocular magnification (referred to as adjusted thickness). Adjusted thicknesses were used for statistical comparisons.

The group means of the 360^o average RNFL thickness as well as of the four sectors are significantly different for all groups. Table 22 represents the results of the group-comparisons. However, no significant difference in 360^o average RNFL thickness was found for emmetropic and highly myopic eyes (E: $M = 92.28$ µm, $SD = 9.91$ µm and hM: $M = 92.30$ µm, $SD = 9.98$ µm). Glaucomatous eyes exhibited a thinner 360^oaverage RNFL thickness than both healthy cohorts ($M = 72.39$ µm, $SD = 9.64$ µm). Furthermore, the median of the temporal quadrant was significantly thicker in highly myopic eyes (*median* = 76.92 µm, IQR = 29.37 µm) when compared with emmetropic (*median* = 61.90 µm, IQR = 11.73 µm) and glaucomatous (*median* = 58.49 µm, IQR = 39.81 µm) eyes. The glaucoma group exhibited a 3.5 µm thinner temporal quadrant thickness than the emmetropic group, but a 18.5 µm thinner quadrant thickness than high myopes. The group means for the inferior, superior and nasal quadrants, emmetropic eyes exhibited the thickest RNFL thickness and, glaucomatous eyes showed the thinnest RNFL thickness (see Table 21). Nevertheless, post-hoc testing showed no statistically significant differences between highly myopic and emmetropic eyes for these quadrants. For the nasal quadrant the highly myopic and the glaucoma group exhibited similar thicknesses (hM: *median* = 62.29 µm, *IQR* = 19.25 µm and G: *median* = 62.06 µm, *IQR* = 8.45 µm). In highly myopic eyes, the thickness in the inferior, superior and nasal RNFL quadrants was thinner than in emmetropic eyes and thicker than in glaucomatous eyes. The significance levels did not change after weighting for age according to section 10 (0.2 %

reduction per year of increasing age).

	Emmetrope, n=39		**Myope, n=27**		**Glaucoma, n=9**	
RNFL thickness	Raw data **[µm]**	**adjusted data [µm]**	Raw data **[µm]**	**adjusted data [µm]**	Raw data **[µm]**	**adjusted data [µm]**
360^o**average**	97.05	**92.28**	85.06	**92.30**	69.58	**72.39**
M (±SD)	(±10.17)	**(±9.91)**	(±8.49)	**(±9.98)**	(±8.60)	**(±9.64)**
inferior	125.50	**119.27**	102.96	**111.63**	74.98	**77.93**
M (±SD)	(±15.58)	**(±14.70)**	(±16.09)	**(±17.53)**	(±12.90)	**(±13.18)**
superior	123.61	**117.48**	101.99	**110.62**	82.02	**84.97**
M (±SD)	(±16.11)	**(±15.20)**	(±17.43)	**(±19.17)**	(±13.16)	**(±11.36)**
nasal	74.62	**70.95**	60.26	**65.34**	60.15	**62.59**
M (±SD)	(±11.09)	**(±10.68)**	(±12.84)	**(±13.93)**	(±5.02)	**(±6.03)**
median [IQR]	74.00 [15.67]	**69.59 [16.56]**	58.67 [17.17]	**62.29 [19.25]**	58.00 [7.83]	**62.06 [8.45]**
temporal	64.15	**61.80**	74.98	**81.58**	60.81	**63.71**
M (±SD)	(±9.94)	**(±10.02)**	(±16.30)	**(±19.04)**	(±17.50)	**(±20.14)**
median[IQR]	64.67 [11.33]	**61.90 [11.73]**	69.33 [25.33]	**76.92 [29.37]**	54.67 [34.50]	**58.49 [39.81]**

Table 21: **RNFL thickness group means**

	360^o**average RNFL thickness**	**inferior RNFL thickness**	**superior RNFL thickness**	**nasal RNFL thickness**	**temporal RNFL thickness**
1-way ANOVA	F(2, 72)= 15.973 p= .000	F(2, 72)= 25.573 p= .000	F(2, 72)= 14.353 p= .000	NA	NA
Kruskal-Wallis (k-samples) n=75	NA	NA	NA	H(2)= 7.240 p= .027	H(2)= 20.996 p= .000
comparison weighted for age	F(2, 72)= 17.029 p= .000	F(2, 72)= 27.319 p= .000	F(2, 72)= 15.332 p= .000		
Summary Post-hoc	E = hM > G Tukey HSD (harmonic sample size)	E ≥ hM >G Tukey HSD (harmonic sample size)	E ≥ hM > G Tukey HSD (harmonic sample size)	E ≥ hM =G pairwise comparison KW with Bonferroni correction for multiple testing	hM >E ≥ G
Subsets for Tukey HSD harmonic n=17.263	subset 1:E, hM p=1.00 subset 2: G	subset 1: E, hM p=.328 subset 2: G	subset 1: E, hM p=.440 subset 2: G	NA	NA
P subset-comparison pairwise comparison KW with Bonferroni correction for multiple testing				E ≥ hM, p=.063	hM > E, p=.000
P subset-comparison weighted for age harmonic n=18.443	subset 1: p=1.00	subset 1: p=.303	subset 1: p=.416	NA	NA

"<" significantly smaller; "≤" smaller but not statistically significant;

">" significantly larger; "≥" larger but not statistically significant,

Table 22: **Group comparisons of RNFL thicknesses. Emmetropes = E, high myopes = hM and glaucoma = G.**

13.2.2. Ganglion cell layer thickness

For GCL thickness, data of 39 emmetropes (E), 27 high myopes (hM) and nine glaucoma patients (G) was included for analysis. The GCL thickness data was normally distributed (see AppendixD) and showed homogenous variances (Levene test statistic was $p>.05$ for all six sectors and the 360^oaverage thickness). Table 23 represents the group means of the raw data and the data after correction for ocular magnification (referred to as adjusted thickness). Adjusted thicknesses were used for statistical comparisons.

The group means of all sectors as well as of the 360^o average GCL exhibited larger thicknesses for highly myopic eyes, while glaucomatous eyes exhibited the thinnest GCL thickness (see tables 23 and 24). Interestingly, GCL thickness was least different in between the three study cohorts in the inferior-nasal sector (E: M= 80.48 µm, SD= 7.14 µm and hM: M= 85.49 µm, SD= 7.03 µm and G: M= 75.27 µm, SD= 4.81 µm). Nevertheless, the similarity of the group means for the E vs hM subgroup in the same sector was statistically weak (after weighting for age: $p=.080$ for subset 2 (E and hM).

	Emmetrope, n=39		**Myope, n=27**		**Glaucoma, n=9**	
GCL thickness	Raw data **[µm]**	**adjusted data [µm]**	Raw data **[µm]**	**adjusted data [µm]**	Raw data **[µm]**	**adjusted data [µm]**
360^o**average M (±SD)**	84.55 (±5.38)	**80.42 (±5.84)**	77.19 (±5.41)	**83.70 (±6.00)**	67.82 (±6.20)	**70.41 (±5.09)**
inferior M (±SD)	83.51 (±5.18)	**79.43 (±5.61)**	75.01 (±6.13)	**81.33 (±6.55)**	62.63 (±8.39)	**64.94 (±7.03)**
superior M (±SD)	85.60 (±6.09)	**81.40 (±6.25)**	77.46 (±6.25)	**84.01 (±7.02)**	69.96 (±6.25)	**72.62 (±4.88)**
superior-temporal M (±SD)	84.28 (±5.72)	**80.17 (±6.24)**	76.81 (±5.47)	**83.31 (±6.23)**	70.78 (±8.41)	**73.49 (±5.09)**
inferior-temporal M (±SD)	84.82 (±5.37)	**80.68 (±5.91)**	77.61 (±5.70)	**84.19 (±6.50)**	64.00 (±9.79)	**66.42 (±9.30)**
inferior-nasal M (±SD)	84.60 (±6.87)	**80.48 (±7.24)**	78.83 (±6.40)	**85.49 (±7.03)**	72.41 (±4.94)	**75.27 (±4.81)**
superior-nasal M (±SD)	84.56 (±5.50)	**80.42 (±5.82)**	77.59 (±6.18)	**84.12 (±6.65)**	67.56 (±5.79)	**70.17 (±4.93)**

Table 23: **GCL thickness group means**

thickness	360^{o}average GCL	inferior GCL	superior GCL	superior-temporal GCL	inferior-temporal GCL	inferior-nasal GCL	superior-nasal GCL
1-way ANOVA	F(2, 72)= 17.606 p= .000	F(2, 72)= 25.316 p= .000	F(2, 72)= 10.665 p= .000	F(2, 72)= 7.908 p= .001	F(2, 72)= 24.790 p= .000	F(2, 72)= 8.489 p= .000	F(2, 72)= 17.992 p= .000
1-way ANOVA after weighting for age	F(2, 72)= 18.183 p= .000	F(2, 72)= 26.929 p= .000	F(2, 72)= 11.370 p= .000	F(2, 72)= 8.186 p= .001	F(2, 72)= 25.905 p= .000	F(2, 72)= 8.917 p= .000	F(2, 72)= 19.237 p= .000
Summary Post-hoc	G< E ≤ hM Tukey HSD (harmonic sample size)	G< E ≤ hM Tukey HSD (harmonic sample size)	G< E ≤ hM Tukey HSD (harmonic sample size)	G< E ≤ hM Tukey HSD (harmonic sample size)	G< E ≤ hM Tukey HSD (harmonic sample size)	G≤ E ≤ hM Tukey HSD (harmonic sample size)	G< E ≤ hM Tukey HSD (harmonic sample size)
Subsets for Tukey HSD, harmonic n=17.262	subset 1:E, hM, p=.228 subset 2: G	subset 1:E, hM, p=.635 subset 2: G	subset 1:E, hM, p=.461 subset 2: G	subset 1: E,hM, p=.332 subset 2: G	subset 1:E, hM, p=.268 subset 2: G	subset 2:E, hM, p=.093 subset 1: E, G	subset 1:E,hM, p=.177 subset 2: G
P subset-comparison weighted for age harmonic n=18.443	subset 1: p=.206	subset 1: p=.610	subset 1: p=.438	subset 1: p=.312	subset 1: p=.249	subset 2: p=.080	subset 1: p=.154

"<" significantly smaller; "≤" smaller but not statistically significant;

">" significantly larger; "≥" larger but not statistically significant;

✖ *non-significant;* ✹ *p<.05;* ✹✹ *p<.01;* ✹✹✹ *p<.001*

Table 24: **Group comparisons of GCL thicknesses.**

13.2.3. Summary structural measurements

The comparison analysis of neuroretinal thickness measurements showed no statistically significant difference in GCL thicknesses (all sectors as well as the 360^o average thickness) between emmetropic and highly myopic eyes. Glaucomatous eyes exhibited the thinnest GCL, although very similar to the group mean of emmetropes for the inferior-nasal sector.

Regarding the RNFL thickness, no statistically significant difference was found between the means of emmetropic and highly myopic eyes for the 360^o average thickness, the inferior, the superior and the nasal quadrants. However, for the nasal quadrant the mean RNFL thickness for highly myopic cohort was 7 µm thicker than in the glaucoma cohort. Emmetropic eyes exhibited a thicker RNFL than both, high myopes and glaucoma sample. Weighting for age had no effect on the significance levels of the analyses but improved the effect sizes.

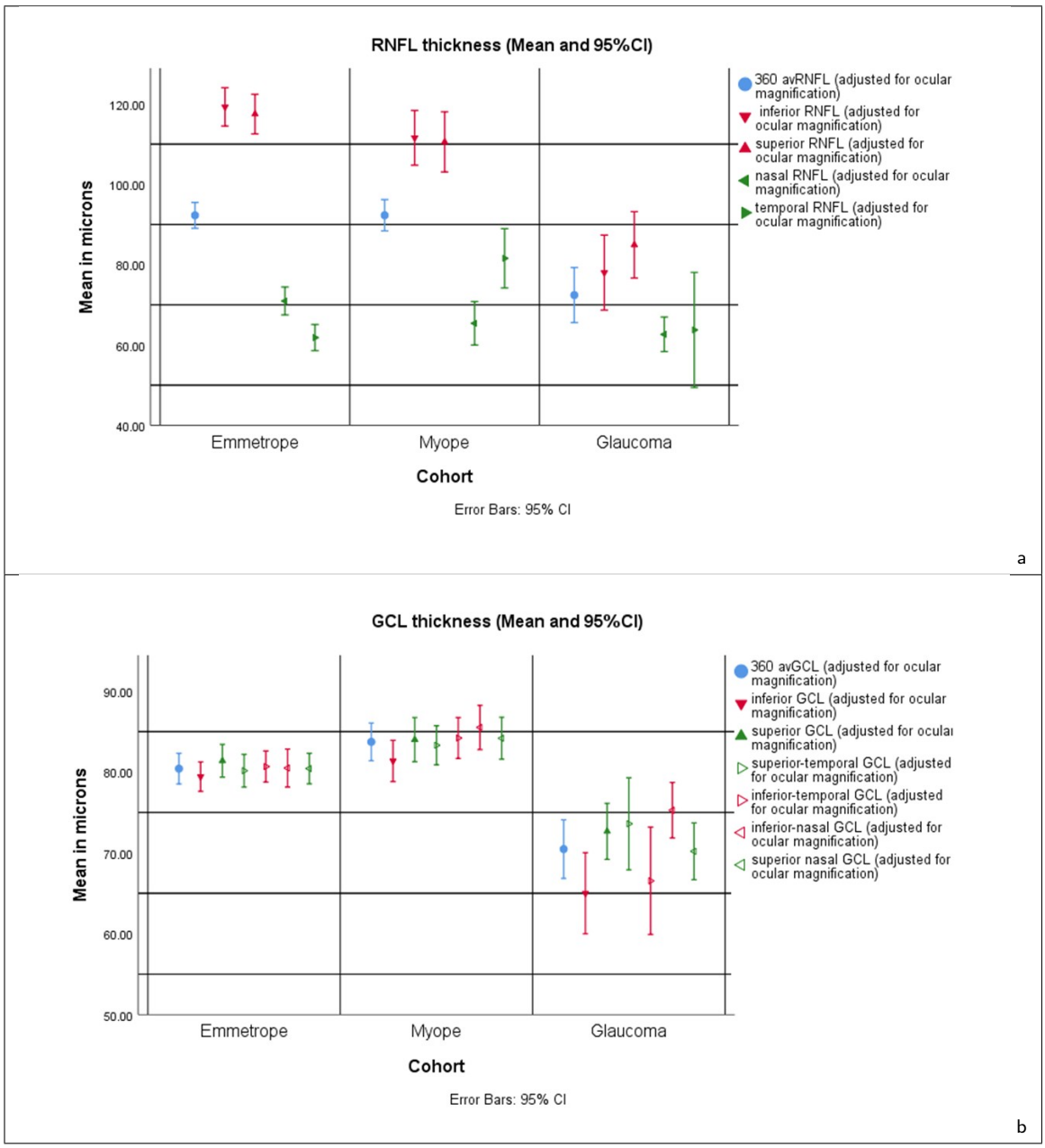

Figure 30: **Graphical representation of a) RNFL and b) GCL thickness for the study cohorts. a) A downwards trend from E to hM to G in RNFL thickness was found for the inferior, superior and nasal quadrants. Thus, these quadrants were of particular interest in further correlation and regression analysis. b) GCL was thickest in hM and thinnest in G in all six sectors. Larger neurons and their axons might be more susceptible to oxygen metabolism changes and were hence, of interest in further correlation and regression analysis.**

13.3. Retinal haemodynamic measurements and calculations

13.3.1. Retinal vessel oximetry - oxygen saturation measurement

For the comparison of SO2 group results, 34 emmetropes (E), 27 high myopes (hM) and eight glaucoma patients (G) were included for analyses based on quality criteria described in section 9.2.1. A data- transformation (see section 9.2.2) was carried out to adjust for the influence of retinal pigmentation before comparing group means. With respect to aSO2 and A-V SO2 difference the data of all groups were normally distributed (see AppendixD). Furthermore, variances were found to be homogenous for all groups (Levene test statistic p>.05). The same accounts for the vSO2 of the glaucoma cohort. In contrast, the data of vSO2 in the emmetropic and highly myopic group were not normally distributed (see AppendixD).

The group means of SO2 measurements (raw data and transformed data) can be found in table 25.

Regarding aSO2 the highly myopic cohort exhibited the lowest value (M= 83.47 %, SD= 7.50 %) and emmetropic as well as glaucoma groups had similar results (E: M= 86.39 %, SD= 6.24 % and G: M= 87.65 %, SD= 4.52 %). However, these differences were not statistically significant ($F(2, 66)$= 2.051, p= .134). After weighting for age the results of the ANOVA- analysis remained non-significant ($F(2, 66)$= 1.895, p= .159).

For vSO2 the lowest group median was found for the myopic cohort, while the glaucoma group showed the largest oxygen content (hM: *median*= 36.80 %, IQR= 12.10 %, E: *median*= 41.85 %, IQR= 6.77 % and G: *median*= 50.95 %, IQR= 8.48 %). These differences were significantly different (Kruskal-Wallis test (k-samples): $H(2)$= 13.734, p= .001) and remained different after weighting for age (no change in Kruskal-Wallis result: $H(2)$= 13.734, p= .001). Subsequent post-hoc testing using pairwise comparisons with Bonferroni correction for multiple correction revealed no statistically significant difference between emmetropes and high myopes (E vs hM, p= 1.0), although the absolute group median was 5 % smaller in high myopes.

With respect to A-V SO2 difference, glaucoma subjects exhibited the lowest group mean (M= 36.69 %, SD= 5.77 %) and the largest group mean was found for the emmetropic group (M= 45.06 %, SD= 7.00 %). The mean of A-V SO2 difference in highly myopic

eyes was M= 43.57 %, SD= 8.23 %. However, these differences were not statistically significant ($F(2, 66)$= 1.468, p= .238).

Group		arterial SO2 M (±SD)	venous SO2 M (±SD) or Median [IQR]	arterio-venous SO2 difference M (±SD)
Emmetrope n=34	Raw data **[%]**	86.20 (±13.03) ★	41.14 (±9.06) 41.35 [10.98] ✚	45.06 (±9.57) ★
	transformed data [%]	**86.39 (±6.24)** ★	41.34 (±7.07) **41.85 [6.77]** ✚	**45.06 (±7.00)** ★
Myope n=27	Raw data **[%]**	86.79 (±15.02) ★	41.56 (±9.76) 37.70 [13.50] ✚	45.24 (±12.13) ★
	transformed data [%]	**83.47 (±7.50)** ★	39.89 (±8.43) **36.80 [12.10]** ✚	**43.57 (±8.23)** ★
Glaucoma n=8	Raw data **[%]**	112.91 (±2.5) ★	62.49 (±5.47) ★ *61.75 [10.63]*	50.44 (±5.35) ★
	transformed data [%]	**87.65 (±4.52)** ★	**50.94 (±4.47)** ★ ***50.95 [8.48]***	**36.69 (±5.77)** ★

★ *parametric distribution ;* ✚ *non-parametric distribution*

Table 25: **SO2 group means**

	arterial SO2	venous SO2	A-V SO2 difference
1-way ANOVA	F(2, 66)= 2.051 *p= .137*		F(2, 66)= 1.468 *p= .238*
Kruskal-Wallis (k-samples) n=69	NA	H(2)= 13.734 p= .001	NA
after weighting for age (arteries 2.8% increase and veins 2.3% increase)	F(2, 66)= 1.895 *p= .159*	H(2)= 13.734 p= .001	NA
Summary Post-hoc harmonic n=15.670	hM≤E≤G subset 1: E, hM, G Tukey HSD (harmonic sample size)	hM≤E<G pairwise comparison KW with Bonferroni correction for multiple testing	G≤hM≤E subset 1: E, hM, G Tukey HSD (harmonic sample size)
P subset- comparison	p=.180	E ≥ hM, p=1.0	subset 1: p=.198
P subset- comparison weighted for age	p=.222 harmonic n=14.004	no change in results	NA

"<" significantly smaller; "≤" smaller but not statistically significant;

">" significantly larger; "≥" larger but not statistically significant,

Table 26: **Group comparisons of SO2 measurements.**

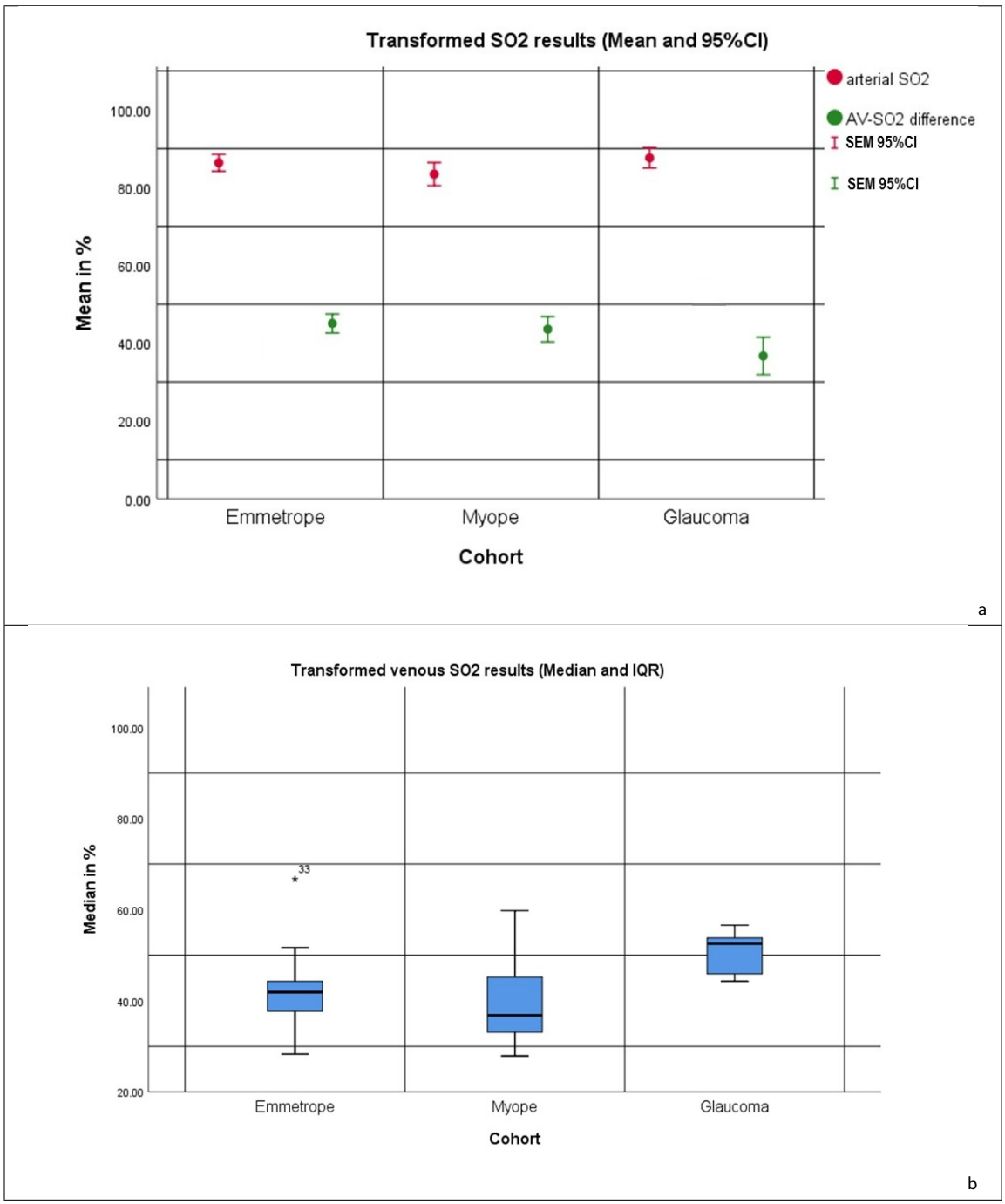

Figure 31: **Graphical representation of SO2 results (transformed data) for the three study cohorts. Arterial and A-V SO2 difference data was normally distributed for all groups and hence, results were presented as mean and 95% CI (a). Venous SO2 data was non-parametric for E and hM and hence, results are shown for all three groups as Median and IQR (b).**

13.3.2. Static vessel analysis

For CRAE, CRVE and AVR, data of 40 emmetropes (E), 29 high myopes (hM) and nine glaucoma patients (G) was included according to quality criteria described in section 9.3.1. All static vessel analysis data was normally distributed (see AppendixD) and showed homogenous variances (Levene test statistic $p>.05$).

For arteries (referred to as CRAE) glaucoma subjects exhibited the smallest group mean (G: M=119.84 µm, SD= 8.61 µm) and emmetropic subjects showed the largest CRAE (E: M= 162.58 µm, SD= 13.08 µm). Highly myopic eyes exhibited a larger mean CRAE than glaucomatous eyes, but a smaller CRAE than emmetropic eyes (hM: M= 148.59 µm, SD= 17.29 µm). This finding was significant ($F(2, 75)$= 33.811, p =.000). Post-hoc analysis applying Tukey HSD (harmonic mean sample size N= 17.586) showed three individual subgroups (see figure 32). Age-weighted analysis for CRAE did not alter this finding (see table 28).

A similar trend was found for veins (CRVE): The one-way ANOVA analysis indicated a significant difference between the groups ($F(2, 75)$= 20.593, p= .000). Other than for the CRAE, there was no significant difference between mean CRVE of the highly myopic and the emmetropic cohort (Tukey HSD (harmonic N= 17.589): p=.067 for subgroup 2: E, hM). The group means for the AVR of emmetropic (M= 0.68, SD= 0.05), highly myopic (M= 0.67, SD= 0.06) and glaucomatous eyes (M= 0.65, SD= 0.06) did not significantly differ (one-way ANOVA: F(2, 75)=1.430, p= .246).

CRAE (not weighted for age)

Cohort		N	Subset for alpha = 0.05		
			1: G	2: hM	3: E
Tukey HSD[a,b]	Glaucoma	9	119.8400		
	Myope	29		148.5934	
	Emmetrope	40			162.5773
	Sig.		1.000	1.000	1.000

Means for groups in homogeneous subsets are displayed.

a. Uses Harmonic Mean Sample Size = 17.586.

b. The group sizes are unequal. The harmonic mean of the group sizes is used. Type I error levels are not guaranteed.

a

CRAE (weighted for age)

Cohort		N	Subset for alpha = 0.05		
			1: G	2: hM	3: E
Tukey HSD[a,b]	Glaucoma	9	119.8710		
	Myope	29		148.6208	
	Emmetrope	40			162.5939
	Sig.		1.000	1.000	1.000

Means for groups in homogeneous subsets are displayed.

a. Uses Harmonic Mean Sample Size = 18.922.

b. The group sizes are unequal. The harmonic mean of the group sizes is used. Type I error levels are not guaranteed.

b

CRVE

Cohort		N	Subset for alpha = 0.05	
			1: G	2: hM, E
Tukey HSD[a,b]	Glaucoma	9	186.1400	
	Myope	29		221.9393
	Emmetrope	40		239.6718
	Sig.		1.000	**0.067**

Means for groups in homogeneous subsets are displayed.

a. Uses Harmonic Mean Sample Size = 17.586.

b. The group sizes are unequal. The harmonic mean of the group sizes is used. Type I error levels are not guaranteed.

c

Figure 32: **Post-hoc analysis using Tukey HSD with harmonic sample sizes for a+b) CRAE and c) CRVE. It is clear from figure a and b that weighting for age does not change the result of the analysis of variance (ANOVA) to compare group means. No weighting applied to the ANOVA analysis for CRVE based on the findings of the Beaver Dam Eye Study (see section 5.2).**

13.3.3. Retinal vessel complexity - fractal analysis

Regarding the spatial distribution of the retinal vessel network, data of 40 emmetropes (E), 29 high myopes (hM) and nine glaucoma patients (G) was included according to quality criteria described in section 9.4.2. The data were adjusted for the asphericity of the retina prior to statistical analysis. The adjusted data for fractal dimension measurements (Df) were normally distributed (see AppendixD) and showed homogenous variances (Levene test statistic p>.05). Despite normally distributed data for the glaucoma cohort, lac measurement results of the emmetropic and of the highly myopic group were not normally distributed (Shapiro-Wilk: p= .003 and p= .021 for the emmetropic and the highly myopic cohort, respectively).

The lowest group mean for Df showed the glaucoma cohort (M= 1.35, SD= 0.02) and the largest Df was found for the emmetropic cohort (M= 1.41, SD= 0.03). Although the mean Df in the emmetropic cohort was 0.01 larger than the mean of the highly myopic group (M= 1.39, SD= 0.03), the difference between both was not statistically significant (Post-hoc analysis using Tukey HSD: subset E and hM p=.421). The lac medians of the three groups (E: *median*= 1.10, IQR= 0.04 and hM; *median*= 1.10, IQR= 0.06 vs G: *median*= 1.10, IQR= 0.03) was not statistically significant different (see table 28), $H(2)$= 0.786, p= .675). The results of the group comparison of Df and lac did not change when the measurement results were adjusted for the eccentricity of the retina (see table 28). Weighting for age (Df) increased the effect size of the ANOVA statistic (F= 18.74 befor and F= 21.405 after weighting). Table 28 shows the one-way ANOVA results of both, retinal vessel calibre measurements and retinal vessel complexity measurements.

		Emmetrope, n=40	Myope, n=29	Glaucoma, n=9
Static vessel analysis (SVA)	**CRAE [µm] M (±SD)**	162.58 (±13.08)	148.59 (±17.29)	119.84 (± 8.61)
	CRVE [µm] M (±SD)	239.67 (±22.65)	221.94 (±24.33)	186.14 (±21.89)
	AVR [no unit] M (±SD)	0.68 (±0.05)	0.67 (±0.06)	0.65 (±0.06)
Retinal vessel complexity	**Df [AU] M (±SD**	1.41 (±0.03)	1.40 (±0.03)	1.35 (±0.02)
	Df adjusted M (±SD)	1.41 (±0.03)	1.39 (±0.03)	1.35 (±0.02)
	Lac [AU] Median [IQR]	1.10 [0.04]	1.10 [0.06]	1.10 [0.03]
	Lac [AU] adjusted Median [IQR]	1.10 [0.04]	1.10 [0.06]	1.09 [0.03]

Table 27: **Group means of architectural vessel measurements.**

	Static vessel analysis (SVA)			***Retinal vessel complexity***	
	CRAE	**CRVE**	**AVR**	**Df**	**Lac**
1-way ANOVA	F(2,75)=33.811 *p= .000*	F(2,75)=20.596 *p= .000*	F(2,75)=1.430 *p= .246*	F(2,75)=16.073 *p= .000*	NA
Kruskal-Wallis (k-samples)	NA	NA	NA	NA	H(2)= 1.264 *p= .532*
1-way ANOVA				adjusted for retinal eccentricity: F(2,75)=18.749 *p= .000*	NA
Kruskal-Wallis (k-samples)				NA	adjusted for retinal eccentricity: H(2)= 0.786 *p= .675*
after weighting for age	F(2,75)=36.696 *p= .000* **(CRAE decrease 0.22% per year)**	NA	F(2,75)=1.555 *p= .218*	eccentricity adjusted Df: F(2,78)=21.405 *p= .000*	
Summary Post-hoc	G<hM<E	G<hM≤E	G≤hM≤E	G<hM≤E	G=hM=E
Subsets for Tukey HSD	three different subsets	subset2: E, hM	subset1: E, hM, G	subset2: E, hM	NA
P subset-comparison harmonic n=17.586**,** age weighted harmonic n=18.922	subset1, 2 and 3: p=1.0 no change due to weighting factor age	subset2: p=.067	subset1: p=.168 subset1: p=.145 (after age weight)	subset2: p=.421 eccentricity adjusted measurements: subset2: p=.162	NA

"<" significantly smaller; "≤" smaller but not statistically significant;

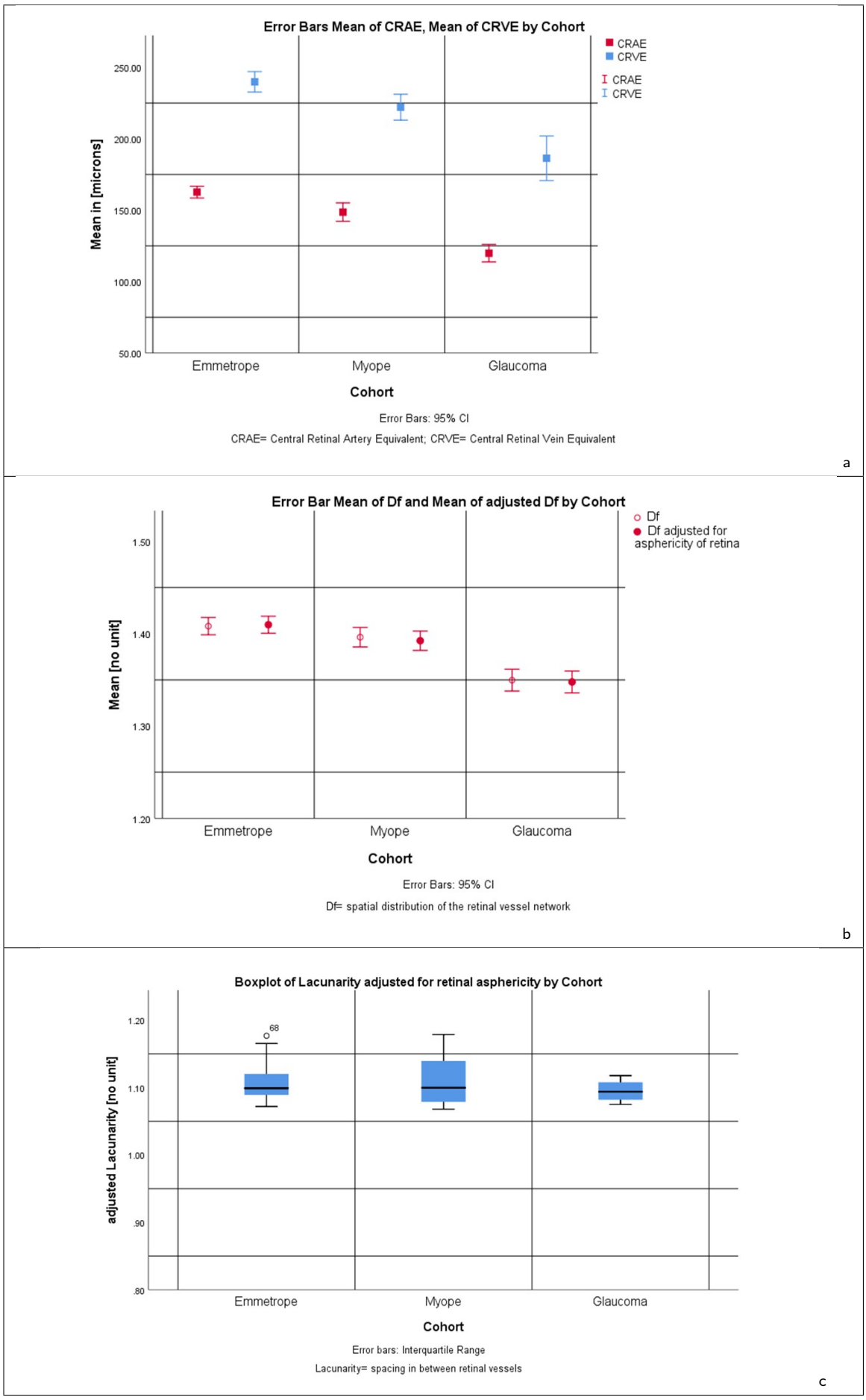

Figure 33: **Graphical representation of a) vessel diameters represented as CRAE and CRVE b) retinal vessel complexity (spatial distribution of the retinal vessel network) and c) lacunarity results for the three study cohorts.**

13.3.4. Dynamic vessel analysis - sequential and diameter response analysis (SDRA)

For statistical analysis according to SDRA principle, data of 33 emmetropes (E), 27 high myopes (hM) and seven glaucoma patients (G) was included according to quality criteria described in section 9.5. The distribution of deltaD, MD, MC and DA measurements for arteries and veins were parametric for all three cohorts (see AppendixD) and variances showed homogeneity (Levene test statistic $p>.05$).

In between the three study cohorts no statistically significant difference was found for the group means of these variables (one- way ANOVA: $p>.05$ for all variables, see table 30).

	Emmetrope n=33	**Myope n=27**	**Glaucoma n=7**
delta D_A in % M (±SD)	3.87 (±1.49)	3.66 (±1.86)	3.90 (±1.41)
MD_A in % M (±SD)	3.90 (±1.78)	3.76 (±2.06)	4.19 (±1.28)
MC_A in % M (±SD)	-3.61 (±1.64)	-3.43 (±1.47)	-2.14 (±0.90)
DA_A in % Mean (±SD)	7.51 (±2.78)	7.15 (±3.12)	6.34 (±1.90)
delta D_V in % M (±SD)	4.20 (±1.63)	4.91 (±2.47)	4.40 (±2.22)
MD_V in % M (±SD)	4.03 (±1.61)	4.93 (±2.50)	4.61 (±1.96)
MC_V in % M (±SD)	-2.11 (±1.09)	-2.14 (±0.95)	-1.59 (±0.75)
DA_V in % M (±SD)	6.15 (±2.13)	7.09 (±2.93)	6.16 (±2.31)

Table 29: **Sequential and diameter response analysis (SDRA) group means of the main variables**

	1-way ANOVA	Summary Post-hoc
delta D_A	F(2, 64)=0.291, p= .749	hM≤E≤G
MD_A	F(2, 64)=0.157, p= .855	hM≤E≤G
MC_A	F(2, 64)=2.734, p= .073	G≤hM≤E
DA_A	F(2, 64)=0.508, p= .604	G≤hM≤E
delta D_V	F(2, 64)=0.896, p= .413	E≤G≤hM
MD_V	F(2, 64)=1.476, p= .236	E≤G≤hM
MC_V	F(2, 64)=0.903, p= .410	G≤E≤hM
DA_V	F(2, 64)=1.140, p= .326	E=G≤hM

"<" significantly smaller; "≤" smaller but not statistically significant;

">" significantly larger; "≥" larger but not statistically significant,

Table 30: **Sequential and diameter response analysis (SDRA) - comparison group means of the main variables: deltaD, MD, MC and DA**

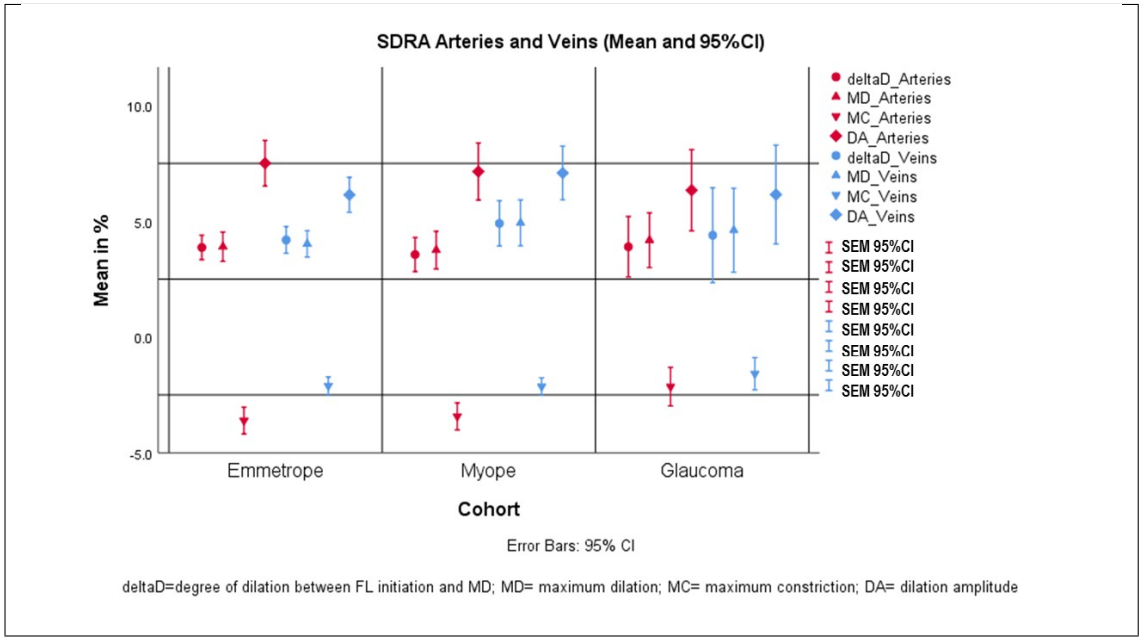

Figure 34: **Graphical representation of SDRA results for the three study cohorts.**

13.3.5. Ocular perfusion pressure analysis

For analyses of perfusion pressure calculations (described in section 9.6), data of 40 emmetropes (E), 29 high myopes (hM) and nine glaucoma patients (G) was included

according to quality criteria described in section 9.6. Data of all three groups were normally distributed (see AppendixD) and showed homogeneous variances (Levene test statistic p>.05).

The means of both, systolic and diastolic perfusion pressure were lowest in the emmetropic cohort (sPP: M= 93 mmHg, SD= 10 mmHg and dPP: M=56 mmHg, SD= 7 mmHg), while the glaucoma cohort exhibited the highest PP values (sPP: M= 107 mmHg, SD= 11 mmHg and dPP: M= 64 mmHg, SD= 8 mmHg). The mean values and standard deviation for the highly myopic cohort were M= 97 mmHg, SD= 12 mmHg and M= 60 mmHg, SD= 8 mmHg for sPP and dPP results. Systolic as well as diastolic PP means were significantly different between the three study cohorts (sPP: $F(2, 75)$= 5.995, p=.004 and dPP: $F(2, 75)$= 4.449, p=.015). Post-hoc testing revealed that neither sPP nor dPP were significantly different in between healthy emmetropes and high myopes (sPP: Tukey HSD (harmonic N=17.586): subgroup E vs hM: p=.508 and dPP: subgroup E vs hM: p=.301). Interestingly, the dPP in the highly myopic and in the glaucoma cohort were very similar (see figure 35). For dPP, the difference between high myopes and glaucoma subjects was 3.5 mmHg while this difference was 4 mmHg between both healthy cohorts.

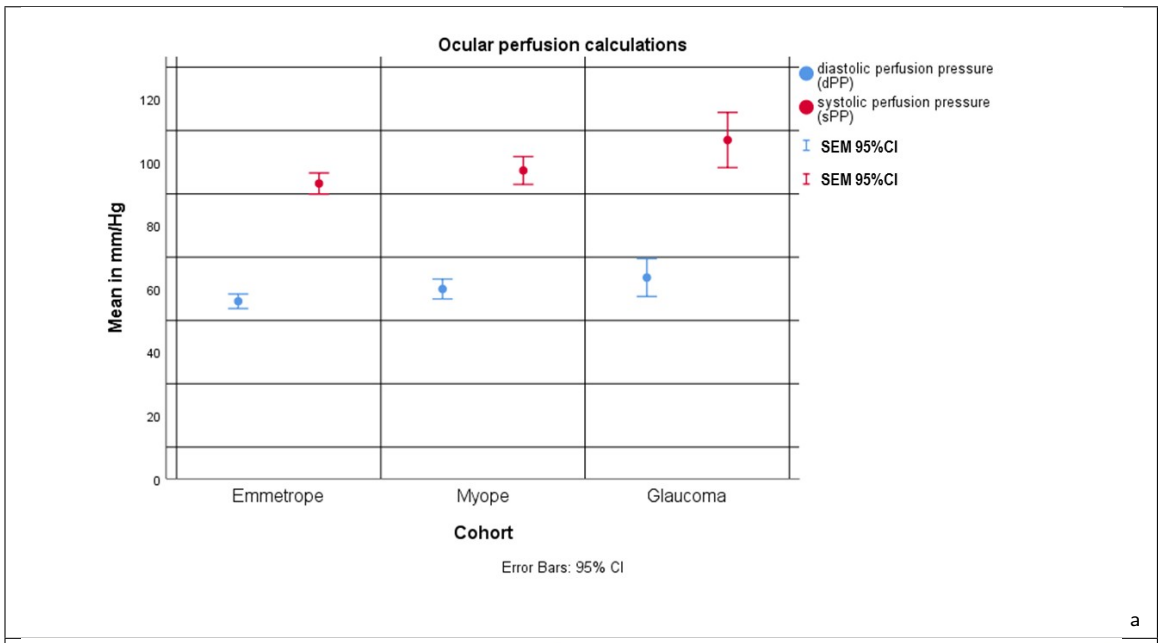

a

sPP

Cohort		N	Subset for alpha = 0.05	
			1: E, hM	**2**
Tukey HSD[a,b]	Emmetrope	40	93.28	
	Myope	29	97.38	
	Glaucoma	9		107.00
	Sig.		**0.508**	**1.000**

Means for groups in homogeneous subsets are displayed.

a. Uses Harmonic Mean Sample Size = 17.586.

b. The group sizes are unequal. The harmonic mean of the group sizes is used. Type I error levels are not guaranteed.

dPP

Cohort		N	Subset for alpha = 0.05	
			1: E, hM	**2: hM, G**
Tukey HSD[a,b]	Emmetrope	40	56.08	
	Myope	29	59.93	59.93
	Glaucoma	9		63.56
	Sig.		**0.301**	**0.345**

Means for groups in homogeneous subsets are displayed.

a. Uses Harmonic Mean Sample Size = 17.586.

b. The group sizes are unequal. The harmonic mean of the group sizes is used. Type I error levels are not guaranteed.

b

Figure 35: **Graphical representation of group means sPP and dPP (a) and Tukey HSD (harmonic N) for systolic and diastolic PP group means to specify differences between groups (b).**

13.3.6. Summary comparison of haemodynamic measurements

The comparison analyses for retinal haemodynamic measurements revealed similar parameters for emmetropic and highly myopic eyes for most of its parameters. Emmetropic eyes differ significantly from highly myopic eyes with respect to CRAE only. The smallest difference in group means between healthy high myopes and glaucoma subjects was found for dPP (3.5 mmHg).

13.4. Summary of all group comparisons

In summary, the comparison of the functional, structural and retinal haemodynamic variables in between the three study cohorts revealed that healthy emmetropes differ significantly from healthy high myopes with respect to temporal RNFL quadrant thickness and CRAE. The highly myopic cohort exhibited a significantly thicker temporal RNFL. Regarding retinal haemodynamic measurements the highly myopic cohort exhibited a significantly decreased CRAE. Similarities for the groups of healthy high myopes and glaucoma subjects were found for the nasal RNFL quadrant thickness as well as for dPP. The group means for all structural parameters were lowest in the glaucoma subjects. Despite a higher oxygen contend in veins (vSO2), the glaucoma group exhibited the lowest values for CRAE and CRVE as well as for Df.

Table **31** synthesizes all findings of the comparison of group means with respect to functional, structural and haemodynamic measurements individually.

Measurement		Emmetropic cohort vs highly Myopic cohort vs Glaucoma sample
Functional measurements	MD_H	No statistically significant difference between E and hM, but results for G cohort larger than in both healthy cohorts.
	PSD	No statistically significant difference between E and hM, but results for G cohort larger than in both healthy cohorts.
	GHT- test pattern differences	No statistically significant difference between E and hM, but results for G cohort larger than in both healthy cohorts For the N3-pattern difference G deviated the most from the healthy (E, hM) groups.
Structural measurements	RNFL thickness	360^o**average RNFL, inferior, super and nasal quadrant** thickness no statistically significant difference between E and hM, but the group mean in G thinner in all quadrants. For **nasal** RNFL thickness differences between groups are smallest. **Temporal** RNFL significantly thicker in hM than both, E and G.
	GCL thickness	No statistically significant difference between E and hM, but statistically significant thinner in G. No statistically significant difference between **inferior-nasal** GCL thickness in E and G.
Retinal Haemodynamic measurements	SO2	**Arterial SO2, vSO2 and A-V SO2** not significantly different in E and hM, whilst **vSO2** larger in G than in healthy cohorts.
	SVA (architectural haemodynamic measurement)	Statistically significant difference **in CRAE** between E, hM and G. No significant difference in **CRVE** between E and hM. **CRAE** and **CRVE** smallest in G.
	Df (architectural haemodynamic measurement)	**lower vessel complexity in G**, although E not statistically significant from hM.
	DVA (functional haemodynamic measurement)	No statistically significant differences between E and hM and G for SDRA for arteries and veins.
	OPP (systemic haemodynamic marker)	No statistically significant difference in **sPP** and **dPP** between E and hM. Smallest difference in dPP for hM and G.

Table 31: **Synthesis of findings for functional, structural and haemodynamic group comparisons. E refers to the emmetropic cohort, hM refers to the highly myopic cohort and G refers to the glaucoma cohort**

14. Relationships in emmetropic, highly myopic and eyes with glaucoma

The next step in this study was the identification of possible retinal haemodynamic variables (predictor variables) that might explain changes in neuroretinal thicknesses (predicted variables). Correlation matrices were employed to identify statistically significant relationships between haemodynamic measurements and structural measurements, which qualify as predictor variables for regression analysis. Prior to these structural vs haemodynamic correlation analysis, intra-relationships for retinal haemodynamic variables explored multicollinearity within the measurement parameters. More importantly, these haemodynamic intra-relationships also identify the interplay in between individual haemodynamic parameters (referred to as retinal haemodynamic patterns) and thus, provide insight into blood flow mechanisms in healthy eyes and in disease.
Correlation and regression analysis were carried out for the emmetropic cohort (referred to as control group), for the highly myopic cohort and for the glaucoma group separately with the aim to detect distinct associations that are specific for each cohort. A resemblance of retinal haemodynamic patterns and structural vs haemodynamic relationships in a group of healthy high myopes and in a sample of glaucoma subjects may provide an indication of retinal haemodynamic parameters that might explain the increased glaucoma susceptibility in highly myopic eyes. The issue of an increased false positive discovery rate due to multiple significance testing was controlled applying the FDR approach. In the case of testing for haemodynamic intra-relationships one general hypothesis was assumed. The number of single correlations (i) within each group was therefore 86. For structural vs haemodynamic relationships however, the hypothesis was related to single locations at the retina and thus, the number of single correlations for each location was i=13.

14.1. Haemodynamic intra-relationships - haemodynamic patterns

This analysis aims to explore differences in the mechanism of autoregulation in emmetropic, highly myopic and glaucomatous eyes, but may also provide insight into the draining mechanisms of the retinal tissue. Only direct measurements as well as systolic

and diastolic results of perfusion pressure calculations were included in the Pearson correlation analysis for haemodynamic measurements. Consequently, MOPP, AVR and A-V SO2 difference were not further explored.

Figures 36 and 37 and 38 present haemodynamic intra-relationships for the emmetropic group, for the highly myopic cohort and for the glaucoma sample. After controlling the FDR, the cohort of healthy emmetropes exhibited statistically significant correlations for sPP vs dPP (r_P= 0.695, p= .000), for CRAE vs CRVE (r_P= 0.673, p= .000) and for arterial as well venous constriction and dilation measurements vs dilation amplitude (MD_A vs DA_A: r_P= 0.835, p= .000, MC_A vs DA_A: r_P= 0.797, p= .000, MD_V vs DA_V: r_P= 0.870, p= .000, MC_V vs DA_V: r_P= 0.683, p= .000). In healthy high myopes the vessel function parameter relationships as well as the relationship between artery and vein calibres showed similar associations as for the emmetropic cohort (CRAE vs CRVE*:* r_P= 0.700, p= .000, MD_A vs DA_A: r_P= 0.916, p= .000, MC_A vs DA_A: r_P= 0.831, p= .000, MD_V vs DA_V: r_P= 0.963, p= .000, MC_V vs DA_V: r_P= 0.585, p< .001). Additionally, MD_A and MC_A exhibited a significant correlation in the highly myopic cohort (r_P= 0.541, p= .004, q= .006). Other than in the emmetropic cohort, perfusion pressure calculations were not statistically significant after controlling for multiple comparisons in the highly myopic cohort (sPP vs dPP: r_P= 0.412, p= .026, q= .011). In the glaucoma cohort only the relationship between MD_V and DA_V were significant in the controlled correlation analysis (r_P= 0.952, p= .001, q= .001). However, the effect size of the correlation analysis of sPP vs dPP correlations in the glaucoma sample was similar to the effect size in the emmetropic cohort, despite not being statistically significant (r_P= .741, p= .022, q= .004). In the highly myopic cohort, the effect size was r_p= .412. Meaningful correlations after controlling the FDR (number of correlations i=86, q=.05) are listed in table 32.

Relationships	Emmetrope	Highly Myope	Glaucoma
Perfusion	**sPP - dPP: r_P= 0.695, *p*= .000, *q*< .006** ✹	sPP - dPP: r_P= 0.412,*p*= *.026, q= .011*	sPP - dPP: r_P= 0.741, *p*= *.022, q= .004*
Arterie-Vein architectural balance	**CRAE - CRVE: r_P= 0.673, *p*= .000, q< .006** ✹	**CRAE - CRVE: r_P= 0.700, *p*= .000, q< .005**✹	CRAE - CRVE: r_P= 0.648, p=.059✖
Retinal vessel function arteries	**DA_A - MD_A: r_P= 0.835, *p*= .000, q< .006** ✹	**DA_A - MD_A: r_P= 0.916, *p*= .000, q< .005**✹	DA_A - MD_A: r_P= 0.916, *p*= .004, q= .002
	DA_A - MC_A: r_P= 0.797,*p*= .000, q< .006 ✹	**DA_A - MC_A: r_P= 0.831, *p*= .000, q< .005**✹	DA_A- MC_A: r_P= 0.804, *p*= *.029, q= .006*
	MD_A - MC_A: r_P= 0.*334*, *p= .057* ✖	**MD_A - MC_A: r_P= 0.541, *p*= .004, q= 0.006**✹	MD_A- MC_A: r_P= 0.499, *p*= *.254* ✖
Retinal vessel function veins	**DA_V - MD_V: r_P= 0.870, *p*= .000, q< .006** ✹	**DA_V - MD_V: r_P= 0.953, *p*= .000, q< .005**✹	**DA_V - MD_V: r_P= 0.952, *p*= .001, q= .001**✹
	DA_V - MC_V: r_P= 0.683, *p*= .000, q< .006 ✹	**DA_V - MC_V: r_P= 0.585, *p*= .001, q= 0.005**✹	DA_V- MC_V: r_P= 0.597, p= .157 ✖

✖ *non-significant;* ✹ *significant after controlling FDR (i=86, q=.05)*

Table 32: **Summary of haemodynamic intra-relationships analysed using Pearson correlation for three study groups. A refers to arteries and V refers to veins. If a significant relationship was found for one study cohort, the equivalent correlation for the other groups is presented too irrespective of the significance level. Bold text style represents correlations that are significant after controlling the false discovery rate (FDR, number of correlations i=86, q=.05).**

FDR		sPP	dPP	arterial_SO2	venous_SO2	CRAE	CRVE	DF	deltaD_Arteries	MD_Arteries	MC_Arteries	DA_Arteries	deltaD_Veins	MD_Veins	MC_Veins	DA_Veins
sPP	Pearson	1	.695**	0.236	0.255	-0.227	0.069	-.356*	0.054	0.028	-0.058	-0.016	0.062	0.071	0.048	0.076
	Sig. (2-tailed)		0.000	0.179	0.146	0.160	0.671	0.024	0.765	0.879	0.747	0.930	0.731	0.696	0.793	0.675
	N	40	40	34	34	40	40	40	33	33	33	33	33	33	33	33
dPP	Pearson	.695**	1	0.243	0.243	-0.111	0.149	-0.292	0.283	0.307	-0.048	0.171	0.117	0.195	-0.105	0.098
	Sig. (2-tailed)	0.000		0.166	0.165	0.496	0.358	0.067	0.111	0.082	0.789	0.343	0.518	0.277	0.561	0.588
	N	40	40	34	34	40	40	40	33	33	33	33	33	33	33	33
arterial_SO2	Pearson	0.236	0.243	1	.453**	-0.053	-0.002	0.068	0.021	-0.167	0.005	-0.121	-0.114	-0.101	-0.097	-0.130
	Sig. (2-tailed)	0.179	0.166		0.007	0.767	0.990	0.704	0.914	0.395	0.979	0.538	0.564	0.609	0.622	0.509
	N	34	34	34	34	34	34	34	28	28	28	28	28	28	28	28
venous_SO2	Pearson	0.255	0.243	.453**	1	-.401*	-.383*	-.371*	-0.278	-0.291	-0.226	-0.337	-.404*	-0.352	-0.034	-0.300
	Sig. (2-tailed)	0.146	0.165	0.007		0.019	0.026	0.031	0.151	0.133	0.247	0.079	0.033	0.066	0.862	0.121
	N	34	34	34	34	34	34	34	28	28	28	28	28	28	28	28
CRAE	Pearson	-0.227	-0.111	-0.053	-.401*	1	.673**	0.311	0.052	-0.091	-0.213	-0.180	-0.189	-0.254	-0.231	-0.309
	Sig. (2-tailed)	0.160	0.496	0.767	0.019		0.000	0.050	0.772	0.613	0.235	0.315	0.292	0.154	0.195	0.080
	N	40	40	34	34	40	40	40	33	33	33	33	33	33	33	33
CRVE	Pearson	0.069	0.149	-0.002	-.383*	.673**	1	0.152	0.207	0.141	-0.114	0.024	0.209	0.154	-0.120	0.053
	Sig. (2-tailed)	0.671	0.358	0.990	0.026	0.000		0.350	0.248	0.435	0.528	0.894	0.242	0.392	0.506	0.771
	N	40	40	34	34	40	40	40	33	33	33	33	33	33	33	33
DF	Pearson	-.356*	-0.292	0.068	-.371*	0.311	0.152	1	-0.064	-0.234	0.148	-0.060	0.312	0.202	0.098	0.197
	Sig. (2-tailed)	0.024	0.067	0.704	0.031	0.050	0.350		0.722	0.190	0.412	0.741	0.077	0.259	0.588	0.272
	N	40	40	34	34	40	40	40	33	33	33	33	33	33	33	33
deltaD_Arteries	Pearson	0.054	0.283	0.021	-0.278	0.052	0.207	-0.064	1	.817**	0.331	.716**	0.166	0.142	0.186	0.207
	Sig. (2-tailed)	0.765	0.111	0.914	0.151	0.772	0.248	0.722		0.000	0.060	0.000	0.355	0.430	0.299	0.247
	N	33	33	28	28	33	33	33	33	33	33	33	33	33	33	33
MD_Arteries	Pearson	0.028	0.307	-0.167	-0.291	-0.091	0.141	-0.234	.817**	1	0.334	.835**	0.205	0.252	0.071	0.231
	Sig. (2-tailed)	0.879	0.082	0.395	0.133	0.613	0.435	0.190	0.000		0.057	0.000	0.253	0.158	0.693	0.196
	N	33	33	28	28	33	33	33	33	33	33	33	33	33	33	33
MC_Arteries	Pearson	-0.058	-0.048	0.005	-0.226	-0.213	-0.114	0.148	0.331	0.334	1	.797**	0.261	.387*	0.134	.358*
	Sig. (2-tailed)	0.747	0.789	0.979	0.247	0.235	0.528	0.412	0.060	0.057		0.000	0.143	0.026	0.458	0.041
	N	33	33	28	28	33	33	33	33	33	33	33	33	33	33	33
DA_Arteries	Pearson	-0.016	0.171	-0.121	-0.337	-0.180	0.024	-0.060	.716**	.835**	.797**	1	0.285	.390*	0.123	.359*
	Sig. (2-tailed)	0.930	0.343	0.538	0.079	0.315	0.894	0.741	0.000	0.000	0.000		0.108	0.025	0.495	0.040
	N	33	33	28	28	33	33	33	33	33	33	33	33	33	33	33
deltaD_Veins	Pearson	0.062	0.117	-0.114	-.404*	-0.189	0.209	0.312	0.166	0.205	0.261	0.285	1	.906**	0.223	.792**
	Sig. (2-tailed)	0.731	0.518	0.564	0.033	0.292	0.242	0.077	0.355	0.253	0.143	0.108		0.000	0.212	0.000
	N	33	33	28	28	33	33	33	33	33	33	33	33	33	33	33
MD_Veins	Pearson	0.071	0.195	-0.101	-0.352	-0.254	0.154	0.202	0.142	0.252	.387*	.390*	.906**	1	0.234	.870**
	Sig. (2-tailed)	0.696	0.277	0.609	0.066	0.154	0.392	0.259	0.430	0.158	0.026	0.025	0.000		0.189	0.000
	N	33	33	28	28	33	33	33	33	33	33	33	33	33	33	33
MC_Veins	Pearson	0.048	-0.105	-0.097	-0.034	-0.231	-0.120	0.098	0.186	0.071	0.134	0.123	0.223	0.234	1	.683**
	Sig. (2-tailed)	0.793	0.561	0.622	0.862	0.195	0.506	0.588	0.299	0.693	0.458	0.495	0.212	0.189		0.000
	N	33	33	28	28	33	33	33	33	33	33	33	33	33	33	33
DA_Veins	Pearson	0.076	0.098	-0.130	-0.300	-0.309	0.053	0.197	0.207	0.231	.358*	.359*	.792**	.870**	.683**	1
	Sig. (2-tailed)	0.675	0.588	0.509	0.121	0.080	0.771	0.272	0.247	0.196	0.041	0.040	0.000	0.000	0.000	
	N	33	33	28	28	33	33	33	33	33	33	33	33	33	33	33

Figure 36: **Haemodynamic intra-relationships analysed using Pearson correlation for the emmetropic cohort. Correlations wit p< .05 are colour coded and the cell marking the significance level had the same colour code if the correlations remained statistically significant after controlling the false discovery rate (FDR, i=86, q= .05).**

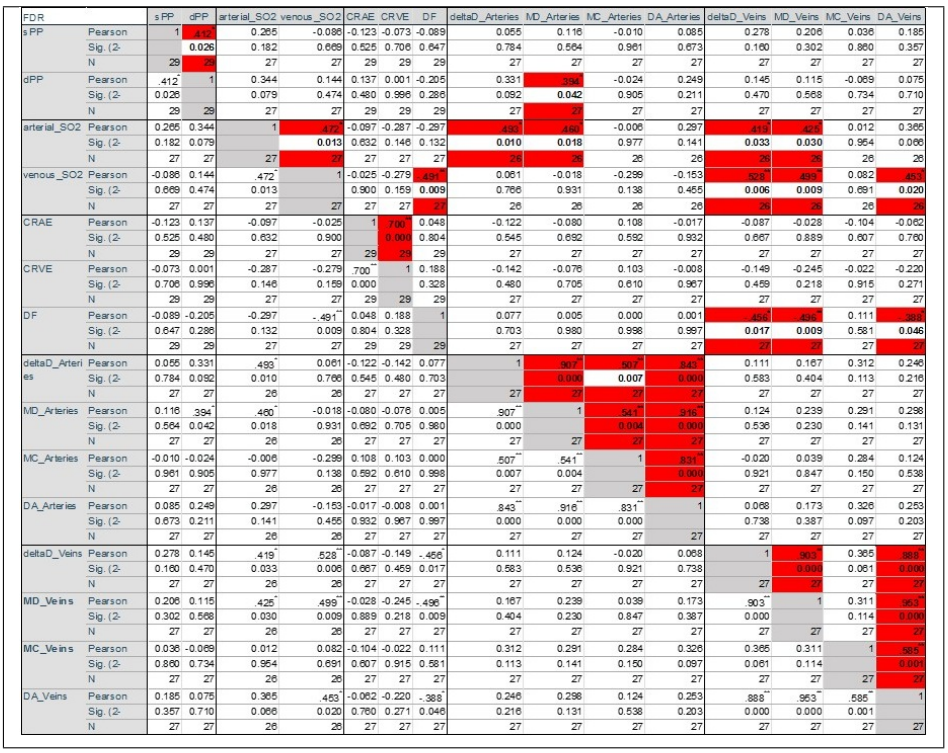

FDR		sPP	dPP	arterial_SO2	venous_SO2	CRAE	CRVE	DF	deltaD_Arteries	MD_Arteries	MC_Arteries	DA_Arteries	deltaD_Veins	MD_Veins	MC_Veins	DA_Veins
sPP	Pearson	1	.412*	0.265	-0.086	-0.123	-0.073	-0.089	0.055	0.116	-0.010	0.085	0.278	0.206	0.036	0.185
	Sig. (2-		0.026	0.182	0.669	0.525	0.706	0.647	0.784	0.564	0.961	0.673	0.160	0.302	0.860	0.357
	N	29	29	27	27	29	29	29	27	27	27	27	27	27	27	27
dPP	Pearson	.412*	1	0.344	0.144	0.137	0.001	-0.205	0.331	.396*	-0.024	0.249	0.145	0.115	-0.069	0.075
	Sig. (2-	0.026		0.079	0.474	0.480	0.996	0.286	0.092	0.042	0.905	0.211	0.470	0.568	0.734	0.710
	N	29	29	27	27	29	29	29	27	27	27	27	27	27	27	27
arterial_SO2	Pearson	0.265	0.344	1	.472*	-0.097	-0.287	-0.297	.430*	.460*	-0.006	0.297	.419*	.425*	0.012	0.365
	Sig. (2-	0.182	0.079		0.013	0.632	0.146	0.132	0.010	0.018	0.977	0.141	0.033	0.030	0.954	0.066
	N	27	27	27	27	27	27	27	26	26	26	26	26	26	26	26
venous_SO2	Pearson	-0.086	0.144	.472*	1	-0.025	-0.279	.491*	0.061	-0.018	-0.299	-0.153	.529**	.493*	0.082	.453*
	Sig. (2-	0.669	0.474	0.013		0.900	0.159	0.009	0.766	0.931	0.138	0.455	0.006	0.009	0.691	0.020
	N	27	27	27	27	27	27	27	26	26	26	26	26	26	26	26
CRAE	Pearson	-0.123	0.137	-0.097	-0.025	1	.700**	0.048	-0.122	-0.080	0.108	-0.017	-0.087	-0.028	-0.104	-0.062
	Sig. (2-	0.525	0.480	0.632	0.900		0.000	0.804	0.545	0.692	0.592	0.932	0.667	0.889	0.607	0.760
	N	29	29	27	27	29	29	29	27	27	27	27	27	27	27	27
CRVE	Pearson	-0.073	0.001	-0.287	-0.279	.700**	1	0.188	-0.142	-0.076	0.103	-0.008	-0.149	-0.245	-0.022	-0.220
	Sig. (2-	0.706	0.996	0.146	0.159	0.000		0.328	0.480	0.705	0.610	0.967	0.459	0.218	0.915	0.271
	N	29	29	27	27	29	29	29	27	27	27	27	27	27	27	27
DF	Pearson	-0.089	-0.205	-0.297	-.491*	0.048	0.188	1	0.077	0.005	0.000	0.001	.456*	.496**	0.111	.393*
	Sig. (2-	0.647	0.286	0.132	0.009	0.804	0.328		0.703	0.980	0.998	0.997	0.017	0.009	0.581	0.046
	N	29	29	27	27	29	29	29	27	27	27	27	27	27	27	27
deltaD_Arteries	Pearson	0.055	0.331	.493*	0.061	-0.122	-0.142	0.077	1	.907**	.507*	.843**	0.111	0.167	0.312	0.246
	Sig. (2-	0.784	0.092	0.010	0.766	0.545	0.480	0.703		0.000	0.007	0.000	0.583	0.404	0.113	0.216
	N	27	27	26	26	27	27	27	27	27	27	27	27	27	27	27
MD_Arteries	Pearson	0.116	.394*	.460*	-0.018	-0.080	-0.076	0.005	.907**	1	.541**	.916**	0.124	0.239	0.291	0.298
	Sig. (2-	0.564	0.042	0.018	0.931	0.692	0.705	0.980	0.000		0.004	0.000	0.536	0.230	0.141	0.131
	N	27	27	26	26	27	27	27	27	27	27	27	27	27	27	27
MC_Arteries	Pearson	-0.010	-0.024	-0.006	-0.299	0.108	0.103	0.000	.507**	.541**	1	.831**	-0.020	0.039	0.284	0.124
	Sig. (2-	0.961	0.905	0.977	0.138	0.592	0.610	0.998	0.007	0.004		0.000	0.921	0.847	0.150	0.538
	N	27	27	26	26	27	27	27	27	27	27	27	27	27	27	27
DA_Arteries	Pearson	0.085	0.249	0.297	-0.153	-0.017	-0.008	0.001	.843**	.916**	.831**	1	0.068	0.173	0.326	0.253
	Sig. (2-	0.673	0.211	0.141	0.455	0.932	0.967	0.997	0.000	0.000	0.000		0.738	0.387	0.097	0.203
	N	27	27	26	26	27	27	27	27	27	27	27	27	27	27	27
deltaD_Veins	Pearson	0.278	0.145	.419*	.528**	-0.087	-0.149	-.456*	0.111	0.124	-0.020	0.068	1	.963**	0.366	.585**
	Sig. (2-	0.160	0.470	0.033	0.006	0.667	0.459	0.017	0.583	0.536	0.921	0.738		0.000	0.061	0.000
	N	27	27	26	26	27	27	27	27	27	27	27	27	27	27	27
MD_Veins	Pearson	0.206	0.115	.425*	.499**	-0.028	-0.245	-.496**	0.167	0.239	0.039	0.173	.903**	1	0.311	.953**
	Sig. (2-	0.302	0.568	0.030	0.009	0.889	0.218	0.009	0.404	0.230	0.847	0.387	0.000		0.114	0.000
	N	27	27	26	26	27	27	27	27	27	27	27	27	27	27	27
MC_Veins	Pearson	0.036	-0.069	0.012	0.082	-0.104	-0.022	0.111	0.312	0.291	0.284	0.326	0.365	0.311	1	.585**
	Sig. (2-	0.860	0.734	0.954	0.691	0.607	0.915	0.581	0.113	0.141	0.150	0.097	0.061	0.114		0.001
	N	27	27	26	26	27	27	27	27	27	27	27	27	27	27	27
DA_Veins	Pearson	0.185	0.075	0.365	.453*	-0.062	-0.220	-.388*	0.246	0.298	0.124	0.253	.888**	.953**	.585**	1
	Sig. (2-	0.357	0.710	0.066	0.020	0.760	0.271	0.046	0.216	0.131	0.538	0.203	0.000	0.000	0.001	
	N	27	27	26	26	27	27	27	27	27	27	27	27	27	27	27

Figure 37: **Haemodynamic intra-relationships analysed using Pearson correlation for highly myopic cohort. Correlations wit p< .05 are colour coded and the cell marking the significance level had the same colour code if the correlations remained statistically significant after controlling the false discovery rate (FDR, i=86, q= .05).**

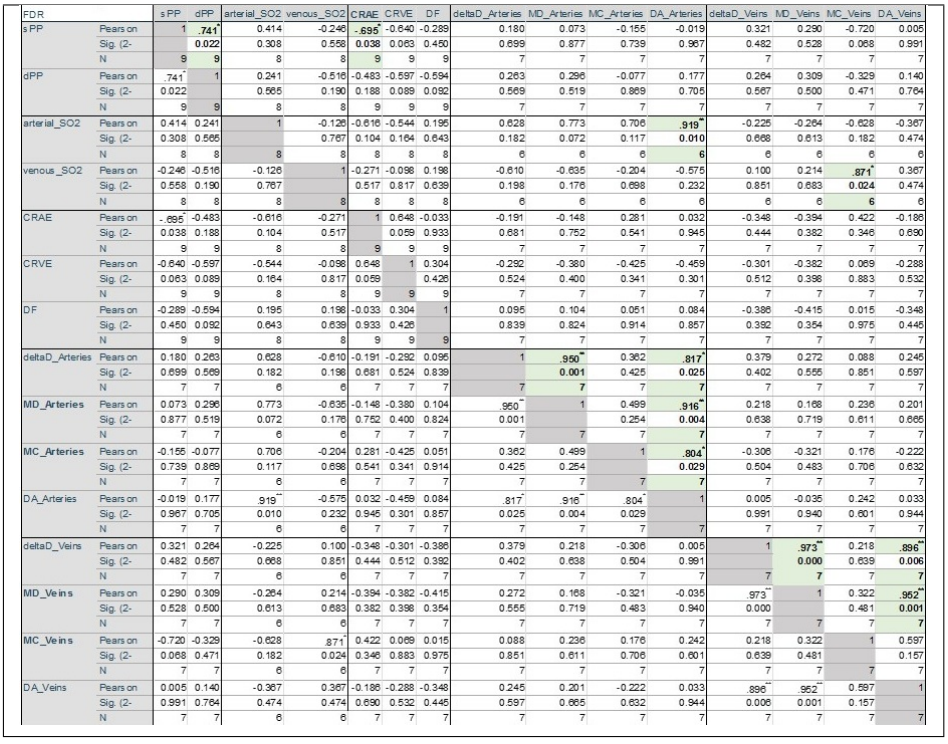

FDR		sPP	dPP	arterial_SO2	venous_SO2	CRAE	CRVE	DF	deltaD_Arteries	MD_Arteries	MC_Arteries	DA_Arteries	deltaD_Veins	MD_Veins	MC_Veins	DA_Veins
sPP	Pearson	1	.741*	0.414	-0.246	-.695*	-0.640	-0.289	0.180	0.073	-0.155	-0.019	0.321	0.290	-0.720	0.005
	Sig. (2-		0.022	0.308	0.558	0.038	0.063	0.450	0.699	0.877	0.739	0.967	0.482	0.528	0.068	0.991
	N	9	9	8	8	9	9	9	7	7	7	7	7	7	7	7
dPP	Pearson	.741*	1	0.241	-0.516	-0.483	-0.597	-0.594	0.263	0.296	-0.077	0.177	0.264	0.309	-0.329	0.140
	Sig. (2-	0.022		0.565	0.190	0.188	0.089	0.092	0.569	0.519	0.869	0.705	0.567	0.500	0.471	0.764
	N	9	9	8	8	9	9	9	7	7	7	7	7	7	7	7
arterial_SO2	Pearson	0.414	0.241	1	-0.126	-0.616	-0.544	0.195	0.628	0.773	0.706	.919**	-0.225	-0.264	-0.628	-0.367
	Sig. (2-	0.308	0.565		0.767	0.104	0.164	0.643	0.182	0.072	0.117	0.010	0.668	0.613	0.182	0.474
	N	8	8	8	8	8	8	8	6	6	6	6	6	6	6	6
venous_SO2	Pearson	-0.246	-0.516	-0.126	1	-0.271	-0.098	0.198	-0.610	-0.635	-0.204	-0.575	0.100	0.214	.871*	0.367
	Sig. (2-	0.558	0.190	0.767		0.517	0.817	0.639	0.198	0.176	0.698	0.232	0.851	0.683	0.024	0.474
	N	8	8	8	8	8	8	8	6	6	6	6	6	6	6	6
CRAE	Pearson	-.695*	-0.483	-0.616	-0.271	1	0.648	-0.033	-0.191	-0.148	0.281	0.032	-0.348	-0.394	0.422	-0.186
	Sig. (2-	0.038	0.188	0.104	0.517		0.059	0.933	0.681	0.752	0.541	0.945	0.444	0.382	0.346	0.690
	N	9	9	8	8	9	9	9	7	7	7	7	7	7	7	7
CRVE	Pearson	-0.640	-0.597	-0.544	-0.098	0.648	1	0.304	-0.292	-0.380	-0.425	-0.459	-0.301	-0.382	0.069	-0.288
	Sig. (2-	0.063	0.089	0.164	0.817	0.059		0.426	0.524	0.400	0.341	0.301	0.512	0.398	0.883	0.532
	N	9	9	8	8	9	9	9	7	7	7	7	7	7	7	7
DF	Pearson	-0.289	-0.594	0.195	0.198	-0.033	0.304	1	0.095	0.104	0.051	0.084	-0.386	-0.415	0.015	-0.348
	Sig. (2-	0.450	0.092	0.643	0.639	0.933	0.426		0.839	0.824	0.914	0.857	0.392	0.354	0.975	0.445
	N	9	9	8	8	9	9	9	7	7	7	7	7	7	7	7
deltaD_Arteries	Pearson	0.180	0.263	0.628	-0.610	-0.191	-0.292	0.095	1	.950**	0.362	.817*	0.379	0.272	0.088	0.245
	Sig. (2-	0.699	0.569	0.182	0.198	0.681	0.524	0.839		0.001	0.425	0.025	0.402	0.555	0.851	0.597
	N	7	7	6	6	7	7	7	7	7	7	7	7	7	7	7
MD_Arteries	Pearson	0.073	0.296	0.773	-0.635	-0.148	-0.380	0.104	.950**	1	0.499	.916**	0.218	0.168	0.236	0.201
	Sig. (2-	0.877	0.519	0.072	0.176	0.752	0.400	0.824	0.001		0.254	0.004	0.638	0.719	0.611	0.665
	N	7	7	6	6	7	7	7	7	7	7	7	7	7	7	7
MC_Arteries	Pearson	-0.155	-0.077	0.706	-0.204	0.281	-0.425	0.051	0.362	0.499	1	.804*	-0.306	-0.321	0.176	-0.222
	Sig. (2-	0.739	0.869	0.117	0.698	0.541	0.341	0.914	0.425	0.254		0.029	0.504	0.483	0.706	0.632
	N	7	7	6	6	7	7	7	7	7	7	7	7	7	7	7
DA_Arteries	Pearson	-0.019	0.177	.919**	-0.575	0.032	-0.459	0.084	.817*	.916**	.804*	1	0.005	-0.035	0.242	0.033
	Sig. (2-	0.967	0.705	0.010	0.232	0.945	0.301	0.857	0.025	0.004	0.029		0.991	0.940	0.601	0.944
	N	7	7	6	6	7	7	7	7	7	7	7	7	7	7	7
deltaD_Veins	Pearson	0.321	0.264	-0.225	0.100	-0.348	-0.301	-0.386	0.379	0.218	-0.306	0.005	1	.973**	0.218	.896**
	Sig. (2-	0.482	0.567	0.668	0.851	0.444	0.512	0.392	0.402	0.638	0.504	0.991		0.000	0.639	0.006
	N	7	7	6	6	7	7	7	7	7	7	7	7	7	7	7
MD_Veins	Pearson	0.290	0.309	-0.264	0.214	-0.394	-0.382	-0.415	0.272	0.168	-0.321	-0.035	.973**	1	0.322	.952**
	Sig. (2-	0.528	0.500	0.613	0.683	0.382	0.398	0.354	0.555	0.719	0.483	0.940	0.000		0.481	0.001
	N	7	7	6	6	7	7	7	7	7	7	7	7	7	7	7
MC_Veins	Pearson	-0.720	-0.329	-0.628	.871*	0.422	0.069	0.015	0.088	0.236	0.176	0.242	0.218	0.322	1	0.597
	Sig. (2-	0.068	0.471	0.182	0.024	0.346	0.883	0.975	0.851	0.611	0.706	0.601	0.639	0.481		0.157
	N	7	7	6	6	7	7	7	7	7	7	7	7	7	7	7
DA_Veins	Pearson	0.005	0.140	-0.367	0.367	-0.186	-0.288	-0.348	0.245	0.201	-0.222	0.033	.896**	.952**	0.597	1
	Sig. (2-	0.991	0.764	0.474	0.474	0.690	0.532	0.445	0.597	0.665	0.632	0.944	0.006	0.001	0.157	
	N	7	7	6	6	7	7	7	7	7	7	7	7	7	7	7

Figure 38: **Haemodynamic intra-relationships analysed using Pearson correlation for the glaucoma cohort. Correlations wit p< .05 are colour coded and the cell marking the significance level had the same colour code if the correlations remained statistically significant after controlling the false discovery rate (FDR, i=86, q= .05).**

14.2. Haemodynamic variables to predict neuroretinal thicknesses changes

This section describes the selection process of potential haemodynamic predictor variables to explain neuroretinal tissue thickness changes for the three study cohorts separately. Pearson correlation was employed to determine significantly correlating haemodynamic variables. The tables in figures 39 and 40 represent correlation results (Pearson correlation). Furthermore, appendices E.53, E.54 and E.55 show the data-distribution plots of these correlations. Summaries of the significant findings represent table 33. Due to multicollinearity of MD, MC and DA within an individual vessel type (was expected), DA was the first choice for any subsequent regression analysis, unless only one of the measurements within a vessel type showed a significant correlation. The DA combines MD and MC for a particular vessel type (artery or vein).

14.2.1. Haemodynamic vs RNFL thickness relationships

Multiple Pearson correlation analyses controlling the FDR (i=13) revealed that only the nasal quadrant RNFL thickness exhibits a significantly positive correlation with Df (architectural haemodynamic measurement) in the healthy emmetropic study cohort. No statistically significant associations were detected for highly myopes and the glaucoma subjects after controlling the FDR in the Pearson correlation analyses. Detailed correlation tables for the emmetropic (a), the highly myopic (b) and the glaucoma group (c) can be found in figure 39. Table 33 provides a summary of the results from the Pearson correlation analysis.

Correlations emmetropic group

FDR (i=13)		sPP	dPP	arterial SO2 (transformed)	venous SO2 (transformed)	CRAE	CRVE	DF	MD_Arteries	MC_Arteries	DA_Arteries	MD_Veins	MC_Veins	DA_Veins
inferior RNFL (adjusted thickness)	Pearson Correlation	0.183	-0.044	0.226	-0.035	0.137	0.286	0.190	-0.090	0.104	0.001	0.222	0.020	0.170
	Sig. (2-tailed)	0.263	0.790	0.197	0.842	0.406	0.078	0.246	0.625	0.571	0.995	0.221	0.916	0.352
	N	39	39	34	34	39	39	39	32	32	32	32	32	32
superior RNFL (adjusted thickness)	Pearson Correlation	0.180	0.125	0.244	0.162	0.049	0.127	0.014	0.143	0.245	0.239	0.255	0.123	0.251
	Sig. (2-tailed)	0.274	0.448	0.164	0.358	0.768	0.442	0.934	0.435	0.176	0.187	0.158	0.503	0.166
	N	39	39	34	34	39	39	39	32	32	32	32	32	32
nasal RNFL (adjusted thickness)	Pearson Correlation	-0.112	-0.163	.410*	-0.012	0.291	0.254	.522**	-0.172	-0.163	-0.205	0.117	-0.184	-0.007
	Sig. (2-tailed)	0.496	0.322	**0.016**	0.946	0.072	0.119	**0.001**	0.345	0.372	0.259	0.525	0.313	0.970
	N /q (critical p)	39	39	**q=0.008**	34	39	39	**q=0.004**	32	32	32	32	32	32
temporal RNFL (adjusted thickness)	Pearson Correlation	0.233	0.094	0.118	-0.138	-0.004	0.109	0.030	-0.087	-0.168	-0.154	.356*	-0.03554	0.253
	Sig. (2-tailed)	0.153	0.569	0.507	0.438	0.979	0.508	0.857	0.636	0.358	0.399	**0.046**	0.847	0.162
	N /q (critical p)	39	39	34	34	39	39	39	32	32	32	**q=0.004**	32	32

**. Correlation is significant at the 0.01 level (2-tailed).

*. Correlation is significant at the 0.05 level (2-tailed).

a

Correlations highly myopic group

FDR (i=13)		sPP	dPP	arterial SO2 (transformed)	venous SO2 (transformed)	CRAE	CRVE	DF	MD_Arteries	MC_Arteries	DA_Arteries	MD_Veins	MC_Veins	DA_Veins
inferior RNFL (adjusted thickness)	Pearson Correlation	-0.186	-0.275	-0.255	-0.094	0.229	.426	0.192	0.247	.512*	.405*	-0.143	0.178	-0.033
	Sig. (2-tailed)	0.354	0.166	0.220	0.656	0.251	**0.027**	0.339	0.234	**0.009**	**0.044**	0.496	0.395	0.875
	N /q (critical p)	27	27	25	25	27	q= 0.008	27	25	q=0.004	q=0.012	25	25	25
superior RNFL (adjusted thickness)	Pearson Correlation	-.382*	-0.041	-0.256	-0.010	0.026	0.140	0.239	0.295	0.368	0.366	-0.214	0.041	-0.141
	Sig. (2-tailed)	**0.050**	0.837	0.218	0.962	0.898	0.488	0.230	0.153	0.070	0.073	0.305	0.846	0.501
	N /q (critical p)	q=0.004	27	25	25	27	27	27	25	25	25	25	25	25
nasal RNFL (adjusted thickness)	Pearson Correlation	0.215	0.124	0.380	0.365	0.153	0.283	-0.271	.451*	0.311	.446*	0.381	0.351	.443*
	Sig. (2-tailed)	0.283	0.537	0.062	0.073	0.446	0.153	0.172	**0.024**	0.130	**0.026**	0.060	0.085	**0.027**
	N /q (critical p)	27	27	25	25	27	27	27	q=0.004	25	q=0.008	25	25	q=0.012
temporal RNFL (adjusted thickness)	Pearson Correlation	-0.183	-0.241	-0.066	0.147	-0.212	-0.342	-0.235	-0.244	-0.261	-0.287	-0.230	-0.322	-0.317
	Sig. (2-tailed)	0.362	0.226	0.754	0.483	0.289	0.081	0.239	0.241	0.208	0.165	0.269	0.118	0.123
	N	27	27	25	25	27	27	27	25	25	25	25	25	25

**. Correlation is significant at the 0.01 level (2-tailed).

*. Correlation is significant at the 0.05 level (2-tailed).

b

Correlations glaucoma group

FDR (i=13)		sPP	dPP	arterial SO2 (transformed)	venous SO2 (transformed)	CRAE	CRVE	DF	MD_Arteries	MC_Arteries	DA_Arteries	MD_Veins	MC_Veins	DA_Veins
inferior RNFL (adjusted thickness)	Pearson Correlation	-0.429	-0.181	-0.219	0.317	0.201	0.182	-0.073	0.342	-0.038	0.223	0.038	0.691	0.254
	Sig. (2-tailed)	0.250	0.641	0.602	0.445	0.605	0.640	0.853	0.453	0.936	0.632	0.936	0.086	0.583
	N	9	9	8	8	9	9	9	7	7	7	7	7	7
superior RNFL (adjusted thickness)	Pearson Correlation	0.333	-0.066	-0.158	0.416	-0.350	0.216	-0.112	-0.548	-.763*	-0.731	0.229	-0.556	0.027
	Sig. (2-tailed)	0.382	0.867	0.709	0.306	0.356	0.577	0.775	0.203	**0.046**	0.062	0.622	0.195	0.954
	N /q (critical p)	9	9	8	8	9	9	9	7	q=0.004	7	7	7	7
nasal RNFL (adjusted thickness)	Pearson Correlation	0.010	0.481	0.235	-0.379	-0.188	-0.048	-0.262	0.561	-0.155	0.323	0.067	0.149	0.090
	Sig. (2-tailed)	0.979	0.190	0.576	0.355	0.629	0.902	0.497	0.190	0.741	0.480	0.886	0.750	0.849
	N	9	9	8	8	9	9	9	7	7	7	7	7	7
temporal RNFL (adjusted thickness)	Pearson Correlation	0.259	0.405	0.216	0.064	-0.462	-0.157	-0.151	0.237	-0.460	-0.040	-0.005	-0.110	-0.053
	Sig. (2-tailed)	0.502	0.280	0.608	0.880	0.211	0.686	0.699	0.609	0.300	0.932	0.991	0.814	0.910
	N	9	9	8	8	9	9	9	7	7	7	7	7	7

*. Correlation is significant at the 0.05 level (2-tailed).

**. Correlation is significant at the 0.01 level (2-tailed).

c

Figure 39: **RNFL thickness - Haemodynamic relationships analysed using Pearson correlation. Statistically significant relationships are marked with blue for emmetropes (a), with red for high myopes (b) and green for glaucoma subjects (c). Correlations at the significance level of 0.05 before controlling the FDR are colour coded. The cell indicating the significance level remained colour coded if the correlations were statistically significant after controlling the false discovery rate (FDR, i=13, q= .05).**

RNFL thickness	Emmetrope	Highly myope	Glaucoma
Inferior quadrant	no significant correlations	CRVE: *r*= 0.426, *p*= *.027*, *q*= *.008* (n=27) DA_A: *r*= 0.*406*, *p*= *.044*, *q*= *.012* (n=25)	no significant correlations
Superior quadrant	no significant correlations	sPP: *r*= -0.*382*, *p*= *.05*, *q*= *.004* (n=27)	MC_A: *r*= -0.*763*, *p*= *.046*, *q*= *.004* (n=7)
Nasal quadrant	arterial SO2: *r*= 0.4*10*, *p*= *.016*, *q*= *.008* (n=34) Df: *r*= 0.52*2*, *p*= *.001*, *q*= *.004* ✹ *(n=39)*	DA_A: *r*= 0.4*46*, *p*= *.026*, *q*= *.008* (n=25) DA_V: *r*= 0.4*43*, *p*= .027, q= .012 (n=25)	no significant correlations
Temporal quadrant	MD_V: *r*= 0.*356*, *p*= *.046*, *q*= *.004* (n=32)	no significant correlations	no significant correlations

✖ *non-significant;* ✹ *significant after controlling FDR (i=13, q= .05)*

Table 33: **Summary of statistically significant correlations between RNFL thickness and haemodynamic measurements before and after controlling FDR. Relationships that remained significant after controlling the FDR (i=13) are marked with asterisk (✹).**

14.2.2. Haemodynamic vs GCL thickness relationships

Pearson correlation analyses controlled for multiple significance testing aiming to determine potential retinal haemodynamic predictor variables for GCL thickness changes did not reveal significant associations when the FDR controlling analysis was carried out. Detailed correlation tables for the emmetropic (a), the highly myopic (b) and the glaucoma group (c) can be found in figure 40.

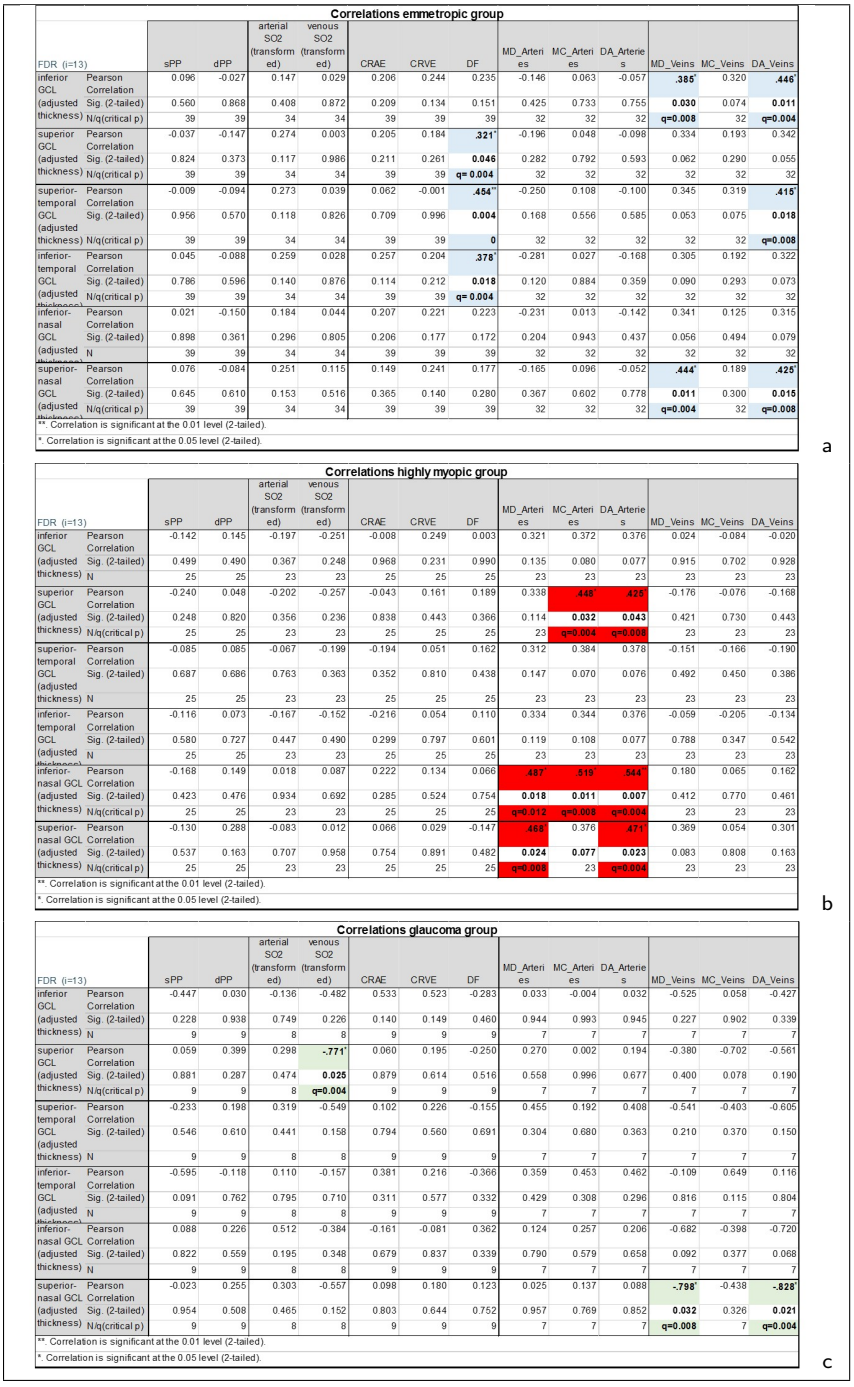

Correlations emmetropic group

FDR (i=13)		sPP	dPP	arterial SO2 (transformed)	venous SO2 (transformed)	CRAE	CRVE	DF	MD_Arteries	MC_Arteries	DA_Arteries	MD_Veins	MC_Veins	DA_Veins
inferior GCL (adjusted thickness)	Pearson Correlation	0.096	-0.027	0.147	0.029	0.206	0.244	0.235	-0.146	0.063	-0.057	.385*	0.320	.446*
	Sig. (2-tailed)	0.560	0.868	0.408	0.872	0.209	0.134	0.151	0.425	0.733	0.755	**0.030**	0.074	**0.011**
	N/q(critical p)	39	39	34	34	39	39	39	32	32	32	**q=0.008**	32	**q=0.004**
superior GCL (adjusted thickness)	Pearson Correlation	-0.037	-0.147	0.274	0.003	0.205	0.184	.321*	-0.196	0.048	-0.098	0.334	0.193	0.342
	Sig. (2-tailed)	0.824	0.373	0.117	0.986	0.211	0.261	**0.046**	0.282	0.792	0.593	0.062	0.290	0.055
	N/q(critical p)	39	39	34	34	39	39	**q= 0.004**	32	32	32	32	32	32
superior-temporal GCL (adjusted thickness)	Pearson Correlation	-0.009	-0.094	0.273	0.039	0.062	-0.001	.454**	-0.250	0.108	-0.100	0.345	0.319	.415*
	Sig. (2-tailed)	0.956	0.570	0.118	0.826	0.709	0.996	**0.004**	0.168	0.556	0.585	0.053	0.075	**0.018**
	N/q(critical p)	39	39	34	34	39	39	**0**	32	32	32	32	32	**q=0.008**
inferior-temporal GCL (adjusted thickness)	Pearson Correlation	0.045	-0.088	0.259	0.028	0.257	0.204	.378*	-0.281	0.027	-0.168	0.305	0.192	0.322
	Sig. (2-tailed)	0.786	0.596	0.140	0.876	0.114	0.212	**0.018**	0.120	0.884	0.359	0.090	0.293	0.073
	N/q(critical p)	39	39	34	34	39	39	**q= 0.004**	32	32	32	32	32	32
inferior-nasal GCL (adjusted thickness)	Pearson Correlation	0.021	-0.150	0.184	0.044	0.207	0.221	0.223	-0.231	0.013	-0.142	0.341	0.125	0.315
	Sig. (2-tailed)	0.898	0.361	0.296	0.805	0.206	0.177	0.172	0.204	0.943	0.437	0.056	0.494	0.079
	N	39	39	34	34	39	39	39	32	32	32	32	32	32
superior-nasal GCL (adjusted thickness)	Pearson Correlation	0.076	-0.084	0.251	0.115	0.149	0.241	0.177	-0.165	0.096	-0.052	.444*	0.189	.425*
	Sig. (2-tailed)	0.645	0.610	0.153	0.516	0.365	0.140	0.280	0.367	0.602	0.778	**0.011**	0.300	**0.015**
	N/q(critical p)	39	39	34	34	39	39	39	32	32	32	**q=0.004**	32	**q=0.008**

** Correlation is significant at the 0.01 level (2-tailed).

* Correlation is significant at the 0.05 level (2-tailed).

a

Correlations highly myopic group

FDR (i=13)		sPP	dPP	arterial SO2 (transformed)	venous SO2 (transformed)	CRAE	CRVE	DF	MD_Arteries	MC_Arteries	DA_Arteries	MD_Veins	MC_Veins	DA_Veins
inferior GCL (adjusted thickness)	Pearson Correlation	-0.142	0.145	-0.197	-0.251	-0.008	0.249	0.003	0.321	0.372	0.376	0.024	-0.084	-0.020
	Sig. (2-tailed)	0.499	0.490	0.367	0.248	0.968	0.231	0.990	0.135	0.080	0.077	0.915	0.702	0.928
	N	25	25	23	23	25	25	25	23	23	23	23	23	23
superior GCL (adjusted thickness)	Pearson Correlation	-0.240	0.048	-0.202	-0.257	-0.043	0.161	0.189	0.338	.448*	.425*	-0.176	-0.076	-0.168
	Sig. (2-tailed)	0.248	0.820	0.356	0.236	0.838	0.443	0.366	0.114	**0.032**	**0.043**	0.421	0.730	0.443
	N/q(critical p)	25	25	23	23	25	25	25	23	**q=0.004**	**q=0.008**	23	23	23
superior-temporal GCL (adjusted thickness)	Pearson Correlation	-0.085	0.085	-0.067	-0.199	-0.194	0.051	0.162	0.312	0.384	0.378	-0.151	-0.166	-0.190
	Sig. (2-tailed)	0.687	0.686	0.763	0.363	0.352	0.810	0.438	0.147	0.070	0.076	0.492	0.450	0.386
	N	25	25	23	23	25	25	25	23	23	23	23	23	23
inferior-temporal GCL (adjusted thickness)	Pearson Correlation	-0.116	0.073	-0.167	-0.152	-0.216	0.054	0.110	0.334	0.344	0.376	-0.059	-0.205	-0.134
	Sig. (2-tailed)	0.580	0.727	0.447	0.490	0.299	0.797	0.601	0.119	0.108	0.077	0.788	0.347	0.542
	N	25	25	23	23	25	25	25	23	23	23	23	23	23
inferior-nasal GCL (adjusted thickness)	Pearson Correlation	-0.168	0.149	0.018	0.087	0.222	0.134	0.066	.487*	.519*	.544*	0.180	0.065	0.162
	Sig. (2-tailed)	0.423	0.476	0.934	0.692	0.285	0.524	0.754	**0.018**	**0.011**	**0.007**	0.412	0.770	0.461
	N/q(critical p)	25	25	23	23	25	25	25	**q=0.012**	**q=0.008**	**q=0.004**	23	23	23
superior-nasal GCL (adjusted thickness)	Pearson Correlation	-0.130	0.288	-0.083	0.012	0.066	0.029	-0.147	.468*	0.376	.471*	0.369	0.054	0.301
	Sig. (2-tailed)	0.537	0.163	0.707	0.958	0.754	0.891	0.482	**0.024**	**0.077**	**0.023**	0.083	0.808	0.163
	N/q(critical p)	25	25	23	23	25	25	25	**q=0.008**	23	**q=0.004**	23	23	23

** Correlation is significant at the 0.01 level (2-tailed).

* Correlation is significant at the 0.05 level (2-tailed).

b

Correlations glaucoma group

FDR (i=13)		sPP	dPP	arterial SO2 (transformed)	venous SO2 (transformed)	CRAE	CRVE	DF	MD_Arteries	MC_Arteries	DA_Arteries	MD_Veins	MC_Veins	DA_Veins
inferior GCL (adjusted thickness)	Pearson Correlation	-0.447	0.030	-0.136	-0.482	0.533	0.523	-0.283	0.033	-0.004	0.032	-0.525	0.058	-0.427
	Sig. (2-tailed)	0.228	0.938	0.749	0.226	0.140	0.149	0.460	0.944	0.993	0.945	0.227	0.902	0.339
	N	9	9	8	8	9	9	9	7	7	7	7	7	7
superior GCL (adjusted thickness)	Pearson Correlation	0.059	0.399	0.298	-.771*	0.060	0.195	-0.250	0.270	0.002	0.194	-0.380	-0.702	-0.561
	Sig. (2-tailed)	0.881	0.287	0.474	**0.025**	0.879	0.614	0.516	0.558	0.996	0.677	0.400	0.078	0.190
	N/q(critical p)	9	9	8	**q=0.004**	9	9	9	7	7	7	7	7	7
superior-temporal GCL (adjusted thickness)	Pearson Correlation	-0.233	0.198	0.319	-0.549	0.102	0.226	-0.155	0.455	0.192	0.408	-0.541	-0.403	-0.605
	Sig. (2-tailed)	0.546	0.610	0.441	0.158	0.794	0.560	0.691	0.304	0.680	0.363	0.210	0.370	0.150
	N	9	9	8	8	9	9	9	7	7	7	7	7	7
inferior-temporal GCL (adjusted thickness)	Pearson Correlation	-0.595	-0.118	0.110	-0.157	0.381	0.216	-0.366	0.359	0.453	0.462	-0.109	0.649	0.116
	Sig. (2-tailed)	0.091	0.762	0.795	0.710	0.311	0.577	0.332	0.429	0.308	0.296	0.816	0.115	0.804
	N	9	9	8	8	9	9	9	7	7	7	7	7	7
inferior-nasal GCL (adjusted thickness)	Pearson Correlation	0.088	0.226	0.512	-0.384	-0.161	-0.081	0.362	0.124	0.257	0.206	-0.682	-0.398	-0.720
	Sig. (2-tailed)	0.822	0.559	0.195	0.348	0.679	0.837	0.339	0.790	0.579	0.658	0.092	0.377	0.068
	N	9	9	8	8	9	9	9	7	7	7	7	7	7
superior-nasal GCL (adjusted thickness)	Pearson Correlation	-0.023	0.255	0.303	-0.557	0.098	0.180	0.123	0.025	0.137	0.088	-.798*	-0.438	-.828*
	Sig. (2-tailed)	0.954	0.508	0.465	0.152	0.803	0.644	0.752	0.957	0.769	0.852	**0.032**	0.326	**0.021**
	N/q(critical p)	9	9	8	8	9	9	9	7	7	7	**q=0.008**	7	**q=0.004**

** Correlation is significant at the 0.01 level (2-tailed).

* Correlation is significant at the 0.05 level (2-tailed).

c

Figure 40: **GCL thickness - Haemodynamic relationships analysed using Pearson correlation. Statistically significant relationships are marked with blue for emmetropes (a), with red for high myopes (b) and green for glaucoma subjects (c). Correlations at the significance level of 0.05 before controlling the FDR are colour coded. The cell indicating the significance level remained colour coded if the correlations were statistically significant after controlling the false discovery rate (FDR, i=13, q= .05).**

14.2.3. Summary structural - haemodynamic relationships and hierarchical linear regression analysis

The results in the previous two sections show that nasal RNFL quadrant thickness can be predicted from the architectural haemodynamic measurement Df only in the healthy

emmetropic group (correlation analysis for nasal RNFL thickness vs Df: r_P= +0.522, p= .001, q= 0.004).

Consequently, a two-step hierarchical regression analysis was performed to predict nasal RNFL thickness from the spatial distribution of the retinal vessel network complexity (Df) in the group of healthy emmetropic study subjects. Previous research has identified age to be influential for the physiological loss of neuroretinal tissue [171]. Thus, the first variable entered for the hierarchical regression analysis was age. The haemodynamic predictor was entered in stage two. Distribution testing of the residuals (P-P plot) revealed normally distributed residuals (see figure 41).

The hierarchical regression model showed that a a more complex retinal vessel network (Df: β= 0.545, t= 3.789, p< .01) can significantly predict a thicker RNFL in the nasal quadrant in emmetropic eyes. The haemodynamic predictor variable explained significantly 25 % of the variation in nasal RNFL thickness (F(3,36)= 7.180, p<.01, adjusted R^2= 0.245). Age alone did not significantly predict changes in nasal RNFL thickness in this young study cohort (model 1, age: β= 0.011, t= 0.069, p= .945).

Variables to predict nasal RNFL thickness ✹✹	**β**	**t**	**sign. of r^2**	**R**	**R^2**	**ΔR^2**
model 1				0.011	0.000	0.000
age ✖	0.011	0.069	.945			
model 2				0.534	0.285	0.285 (✹)
age ✖	+0.123	0.856	.398			
Df ✹	0.545	3.789	.001			
F(2,36) = 7.180, p=.002, adjusted R^2=0.245						

✖ *non-significant;* ✹ *p<.05;* ✹✹ *p<.01;* ✹✹✹ *p<.001*

Table 34: **Summary of hierarchical regression analysis for predicting the nasal quadrant RNFL thickness from the architectural haemodynamic measurement Df in emmetropes.**

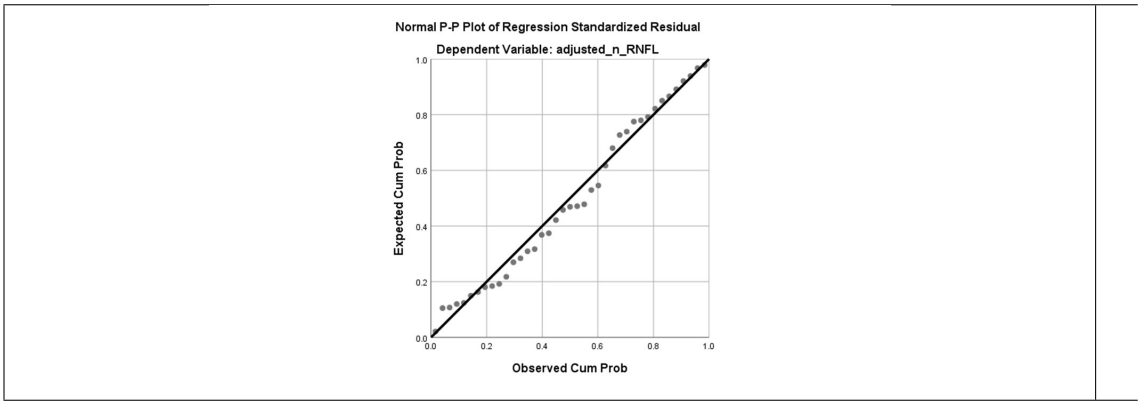

Figure 41: **Statistical distribution testing of the residuals of the linear regression model in the group of healthy emmetropic eyes. The residuals in the regression model are normally distributed.**

Part VI

Discussion of the findings

The objective of this exploratory, cross-sectional study was to investigate the following questions:

- How do otherwise healthy, highly myopic individuals differ from emmetropes with respect to structural and functional and haemodynamic parameters?
- How are retinal structure and haemodynamics related in emmetropes vs high myopes?
- How are retinal haemodynamic parameters inter-related in emmetropes vs high myopes?
- Do any of the parameters and/or relationships of highly myopic eyes resemble in an sample of patients with POAG?

To answer the aforementioned study questions, this study collected data from a cohort of healthy subjects with refractive error of ± 0.50 DS (referred to as emmetropes) and a group of healthy participants with myopic refractive error of more than -5.75 DS (referred to as high myopes). Additionally, data of a sample of POAG patients who

had a confirmed diagnosis by glaucoma specialists/ophthalmologists were collected in order to look into parameters that may be already seen in the group of highly myopes. Glaucoma in the study eye was confirmed by neuroretinal tissue loss shown in the OCT result.

Sections 15 to 19 discuss the findings of this study.

15. Sample statistics

With respect to the study objective, three study cohorts were chosen: a group of healthy emmetropic, a group of highly myopic and a group of glaucoma subjects. The two healthy study cohorts (emmetropic and highly myopic group) were of similar age (E: *median*= 20 years and hM: *median*= 23 years) whilst the glaucoma group was more than four decades older than the healthy groups (G: *median*= 71 years). Previous research has shown that neuroretinal tissue thickness decreases with increasing age [171]. Any reduction in thickness in older study subjects might be partly due to age but could also be a sign of glaucomatous neuroretinal tissue loss. Thus, it would be beneficial to have a similar age-range for the three groups to perform statistical analyses. However, impairment of systemic blood circulation as well as the onset of glaucoma are also associated with older age (blood circulation: [130] and glaucoma: [149, 42]). For the comparison of the two cohorts differing in refractive error, the study aimed for subjects showing no systemic blood circulation alterations to avoid for the retinal haemodynamic measurements to be biased by impaired systemic blood circulation. As expected, the glaucoma subjects recruited for this study were of older age [42]. As a consequence of these facts this study had to compromise on the inclusion criterion regarding age. Statistical analyses were thus, weighted for age due to the age difference between the two healthy groups and the glaucoma group. Care must be taken interpreting any comparison between a group of healthy eyes and the glaucoma subjects due to the fact that weighting for age does not reflect the true ageing process in the eye.

Refractive correction (SE) as well as axial length (AL) were used to differentiate highly myopic from emmetropic eyes. Moreover, AL defines the elongation of the eye. As expected, SE and AL of the emmetropic group were significantly different from the

highly myopic study cohort (see table 18). SE in the glaucoma cohort was similar to the emmetropic cohort although AL was significantly larger than in emmetropes and significantly smaller than in the highly myopic group. In order to compare eyes of similar AL, but differ in the absence and presence of glaucoma, this study would have improved if the glaucoma sample could have been stratified into a non-myopic and high myopic glaucoma subjects.

IOP and BP are determinants of ocular perfusion pressure (detailed description in section 5.5) calculations. Ocular perfusion determines the penetration of oxygen through the vessel walls (superficial retinal vessels) in order to nourish the retinal tissue. No significant difference in IOP was found for the three study cohorts ($p>.05$) although both systolic and diastolic blood pressure were highest in the glaucoma cohort and lowest in the emmetropic group. Similar findings for IOP in the glaucoma group might be explained by the IOP controlling medication which all glaucoma subjects received at the point of data collection. Despite exhibiting the largest sPP and dPP values, the BP results of the glaucoma cohort were still considered clinically normal (G: $M=$ 120 mmHg and $M=$ 76 mmHg for sPP and dPP, respectively). One reason for the higher values of BP in the glaucoma cohort might be the age of the subjects, although six out of nine glaucoma subjects were taking blood pressure reducing medications. Previous research has shown that BP increases with increasing age [68, 245]. The Framingham Heart Study investigated BP in a longitudinal study design from 1948 up to 1980 [68]. The authors reported a linear increase of systolic BP in 2036 subjects (age 30 up to 84 years) without BP treatment. For diastolic BP the same study reported a decrease after the age of 60 years.

16. Visual function measurements

In exploring visual fields this study aimed to identify functional markers that show generalized (MD_H) and more importantly, focal sensitivity losses in highly myopic eyes that are similar to those found in glaucoma. The visual field indices (global indices: MD_H and PSD as well as GHT related indices: the differences of the GHT patterns) showed no significant differences between the emmetropic cohort and the highly myopic cohort

(see table 20). As expected, the glaucoma cohort differed from both, the emmetropic cohort as well as the highly myopic cohort with respect to all explored visual field indices (see sections 13.1.1 and 13.1.2).

It has been suggested that global indices alter due to longer axial lengths (decrease in MD_H while increase in PSD) [259, 7]. This does not appear to be the case in this study. The highly myopic and emmetropic cohorts exhibited similar results. Rudnicka reported that MD_H decreased significantly when AL exceeded 26 mm and for SE above -5.00DS in a group of 122 young and healthy subjects. Moreover, when the AL exceeded 28 mm and the SE exceeded -10.00 DS even the local reduction in sensitivity (PSD) exhibited a significant decline. However, only one highly myopic subject exceeded the AL of 28 mm (AL=28.26 mm) in the present study, although the SE of this particular subject was -8.50 DS (ID subject: MQM220797). Unsurprisingly, for this data a difference in PSD was not observed. Moreover, the mean AL of the highly myopic study cohort was only 0.42 mm above the cut-off value of an change in MD_H that is expected to be significant according to the aforementioned study (highly myopic AL: M= 26.42 $\pm$ 0.81 mm and the median SE: *median*= -7.50 DS [-12.75 DS, -6.25 DS]).

A different approach to determine the influence of AL and SE on visual field global indices was employed by Aung et al. in 2001 [7]. The authors applied a linear regression model from which they reported a 0.33$\pm$ 0.12 dB decrease in MD_H per one millimetre increase in AL as well as a 0.20$\pm$ 0.05 dB decrease in MD_H per one dioptre increase in myopic refractive error (R^2= 0.15, p<.001). Considering the small R^2 in the study by Aung et al. (2001) , the findings of the present study might well reflect these findings: This study found a $\pm$ 0.81 mm standard deviation (*SD)* for AL and a standard error of means (SEM) of 0.22 dB for MD_H in the highly myopic cohort. Multiplying these two findings of the present study (SD of AL with SEM of MD_H) results in a value of 0.27 dB. This value is well within the reported range of change in MD_H due to AL (0.33$\pm$ 0.12 dB) [7]. Thus, the SEM in the present study might well reflect the variation of axial length in the highly myopic study cohort. Nevertheless, in accordance with these results, the aforementioned study showed that focal visual field defects represented as PSD are rare in highly myopic eyes. Aung et. al. (2001) also reported a reproducible focal visual

field defect in only one out of 150 male subjects (0.7 %). Besides PSD reflecting local visual field losses, the present study employed hemifield differences according to the GHT patterns (C1, C2, N3, P4 and P5, see figure 6) to determine local sensitivity differences between superior and inferior hemifield. As for PSD, the results of the GHT marker yielded no difference between the emmetropic and the highly myopic cohorts implying that no focal defects were present in the study population.

More importantly, the glaucoma group exhibited a large error value (IQR $>$ 3.80 dB) for all indices when compared with the other study cohorts ($IQR < 1.70$ dB for both, the emmetropic and the highly myopic cohorts) indicating a wide variability in global indices in glaucoma subjects. This finding might be explained by different progression rates between individual glaucoma subjects in this study. An additional explanation for the large errors values in the glaucoma sample (reflecting the variety of visual field defects) might be the duration of glaucoma in this group. Duration times ranged from four up to 18 years. Of the eight subjects included for visual field analysis, three glaucoma subjects had a glaucoma history of less than ten years, two subjects of ten years and three subjects were diagnosed 18 years prior to participating in this study. However, visual field results in glaucoma patients demonstrate wide variability mainly due to the different stage of progression in glaucoma, but also due to patient reliability [116, 76]. Gardiner et al. (2014) reported that the reliability of visual field results might be questionable below a sensitivity threshold of 15 dB because ganglion cells saturate with high-contrast stimuli [76]. These reports might explain the high error rates found in this study. Consistent with previous findings, these results suggest that focal defects in particular, manifest when the pathology (glaucoma) is already present [277]. Sommer et al. (1991) reported that a MD_H of -5 dB represents a GC loss of 20 % and hypothesized that neuroretinal tissue loss precedes visual field defects.

Nevertheless, the findings of this study indicate that visual field indices, either generalized (MD_H) or focal (PSD, GHT patterns), are not suitable as a marker to indicate glaucoma susceptibility in highly myopic eyes due to the fact that visual field indices were not significantly different between highly myopic and emmetropic eyes. Thus, in this study visual field parameters were not investigated further.

17. Locations prone to the loss of neuroretinal tissue in healthy eyes

As known from the literature, glaucoma is defined by loss of neuroretinal tissue which is reflected in thinning of the ganglion cell layer and its axons (referring to as RNFL) [34]. Thus, comparing the group means (emmetropes, high myopes and glaucoma patients) of these structural thickness measures could provide vital information about the tissue (and its location) at risk of developing thickness loss in the highly myopic group when compared to the emmetropic (control group) counterpart. A potential location with increased risk of tissue loss may be one in which the thickness might be smaller than found in emmetropes but might still be thicker than in the glaucoma sample. Previous research has identified the inferior quadrant as well as the 360^o average RNFL thickness as valuable marker for visual field loss as seen in glaucoma [25, 145, 238, 92].

The one-way ANOVA revealed a similar GCL in the highly myopic study cohort for the 360^o average GCL thickness as well as for the six sectors when compared to emmetropes (see table 24 and figure 30 b). GCL thickness was thinnest in the glaucoma cohort for all locations which remained after weighting for age in the statistical analysis. However, the glaucoma cohort exhibited the least difference in GCL thickness in between the study cohorts after correction for OM for the inferior-nasal GCL sector (see post-hoc test for this sector in table 24). The finding that the GCL thicknesses in emmetropes did not differ from thicknesses in high myopes may be due to the adjustment for OM. Adjusting measurement data for OM does not alter the measurement area, but is an estimation of the change in thickness due to minification caused by varying AL. Although, it might be more precise to employ software that selects the measurement area according to the individual axial length, this option was not available in this study and hence, a correction for OM determined by the individual's axial length was the best way to normalize for different image sizes due to longer (or shorter) eyes. In agreement with previous studies, this finding indicates that the GCL is not thinner in highly myopic eyes when compared to emmetropic eyes [144]. Kim et al. (2010) reported a similar GCL thickness in highly myopic and non-myopic eyes. Moreover, previous research suggests that GCL thickness

measurements have a similar diagnostic value as RNFL thickness measurements in diagnosing glaucoma [156, 190, 229, 90].

The theory of the sequence of neuroretinal tissue loss in glaucoma suggests that it originates with the loss of axons and ends with loss of the ganglion cells themselves due to apoptosis [232, 310, 92]. Supporting this theory, a more recent study of Hammel et al. (2017) found that the reduction in RNFL thickness happened more rapidly than the reduction of the GCL thickness, suggesting that the RNFL will be affected prior to the GCL [92].

In addition to the findings for GCL thickness measures, the results of the corrected RNFL thickness yielded no significant difference for 360^o average RNFL thickness as well as for the nasal, inferior and superior quadrant thickness between emmetropic and highly myopic cohorts. The temporal RNFL quadrant thickness was significantly larger in the highly myopic cohort when compared with the emmetropic cohort. The glaucoma group however, exhibited a thinner mean RNFL thickness than the healthy counterparts across all quadrants as well as for the 360^o average. The result for thickness comparison in the two healthy cohorts is consistent with previous findings by Kang et al. (2010) and Hoh et al. (2006) regarding average RNFL thickness [124, 140]. Kang et al. (2010) investigated the effect of myopia on RNFL thickness measurements and found no statistically significant dependence of average RNFL thickness on the axial length, but a thicker temporal quadrant and thinner inferior and thinner superior RNFL thicknesses were associated with increasing AL after correction for ocular magnification [140]. The study by Hoh et al. (2006) did explore the relationship between AL and SE and average RNFL thickness in various scan areas and found no significant relationship between the investigated variables. Previous findings however were not consistent. Another study by Rauscher et al. (2009) reported a thinner 360^o average RNFL thickness with increasing AL [257]. This study did not observe a reduced 360^o average RNFL thickness in high myopes. Nevertheless, this study found a significantly thicker temporal quadrant thickness in high myopes, whilst a trend of a thinner RNFL was observed for the nasal, inferior and superior quadrants when compared with an emmetropic cohort. The finding of this study indicates the previously suggested redistribution of the RNFL in highly myopic

eyes [140]. Regarding glaucoma, previous studies have demonstrated that the inferior, superior and nasal RNFL thicknesses have the greatest diagnostic value in glaucoma and for determining glaucoma progression [25, 222, 238]. Bowd et al. (2000) reported that the inferior and nasal quadrants were capable of significantly distinguishing ocular hypertensive from normal eyes, whilst glaucoma patients showed a significantly thinner RNFL in all quadrants [25]. The highest power in discriminating normal from glaucoma suspect eyes was found for the inferior and superior quadrants in a study published by Nouri-Mahdavi et al. in 2004 [222]. Finally, a study published by Parikh et al. in 2007 showed that the inferior quadrant as well as the average RNFL thickness had the best combination of sensitivity and specificity to discriminate normal from early glaucomatous eyes [238].

However, the two findings that (1) longer axial length is related with a decrease in inferior and superior RNFL thickness and, that (2) these quadrants are the most sensitive for diagnosing glaucoma might explain the likelihood of misdiagnoses in highly myopic eyes. The same knowledge may partly explain the increased risk in myopic eyes for development of glaucoma. Bowd et al. (2000) reported a significantly thinner nasal quadrant of the RNFL in glaucomatous eyes than in the glaucoma suspects or in an ocular hypertensive group, suggesting a diagnostic value in examination of RNFL thickness in this quadrant [25]. Thus, the nasal quadrant might be particularly sensitive to changes as seen in glaucoma. The RNFL thickness of the nasal quadrant exhibited the smallest differences in between the study cohorts (represented by a small effect size, see table 22) as well as a similar thicknesses in the highly myopic and glaucoma groups (hM: *median*= 62.29 µm vs G: *median*= 62.02 µm, p= 1.00, see table 21).The current results further suggest that the 360^{o}average RNFL thickness might be capable of distinguishing pathology related losses from physiologically altered thickness distributions of nerve fibres.

Consistent with the literature, this study found that the temporal RNFL sector was thickest in the highly myopic cohort suggesting the influence of mechanical stretch on the myopic retina [140, 257]. The glaucoma cohort again, exhibited the smallest RNFL thickness in this sector (see table 22).

This study explored in consecutive steps the relationships between these RNFL thick-

nesses and haemodynamic measurements in an attempt to explore if the RNFL thickness changes may be predicted from retinal haemodynamic parameters. Significant findings would support the hypothesis of a vascular contribution to neuroretinal tissue loss and the vascular theory in glaucoma. This aspect is described in detail in section 19.

18. Retinal haemodynamic measurements

18.1. Similarities and differences in between study cohorts

The vascular theory of glaucoma states that glaucoma occurs and progresses due to an imbalance between blood circulation (haemodynamic measurements) and intraocular pressure in the eye [62, 193, 168, 65, 19]. Thus, comparing haemodynamic measurements in an emmetropic, a highly myopic group and a group of glaucoma subjects may provide crucial information about haemodynamic aspects and patterns potentially indicating risk factors for the onset and progression of glaucoma in both, emmetropic and highly myopic eyes. It might also show differences between emmetropes and high myopes that might account for the increased glaucoma risk in myopes. Retinal haemodynamic measurements investigated in this study were the (1) oxygen content in retinal vessels (oximetry, SO2), the (2) retinal vessel architecture such as vessel calibres (CRAE, CRVE) and the complexity of the retinal vessel network (Df and Lac), (3) the functional ability of the retinal vessels to adapt to changes in oxygen demand in the retinal tissue (referred to as vessel reactivity) and (4) the ocular perfusion calculations determining the vascular regulation. Combined, these measurements might be capable of describing the quality of the retinal tissue metabolism, specifically for the neuroretinal tissue.

18.1.1. Oximetry

The results of this study revealed no significant difference between the three study cohorts for arterial SO2 and A-V SO2 difference (transformed data), although venous SO2 (transformed data) was higher in the glaucoma cohort when compared to both, the emmetropes and high myopes.

Similar findings for aSO2 were reported by Zheng et al. (2015). The aforementioned

study compared SO2 results as well as vessel diameters in highly myopic eyes (n= 54) and emmetropic eyes (n= 54). The authors reported a significantly lower aSO2, but also a significantly lower A-V SO2 difference in the group of high myopes. The same study further divided the myopic group into subjects showing grade one or zero (group A; comparable to the highly myopic study cohort in the present study) in the myopia grading scheme as well as grade two or more (group B) in the same grading scheme (AVILA grading [8]). The comparison of SO2 measurements between group A and the emmetropic control group resulted in significant lower findings for A-V SO2 difference only, while aSO2 was not significantly different. The authors suggested an altered oxygen metabolism in highly myopic eyes, particularly in eyes with signs of myopic retinopathies. However, the lower value for aSO2 in aforementioned study could be a result of a measurement artefact i.e., due to narrower vessels in highly myopic eyes. The stretch of the retina in eyes with longer AL may also result in a stretch to retinal blood vessels and consequently, narrowing of arteries and veins (see also findings for vessel calibres discussed in section 18.1.2). A study by Hammer et al. (2008) found increasing SO2 results with decreasing vessel diameters [97]. They also introduced a compensation algorithm which was subsequently incorporated into the Vesselmap software. This algorithm compensates well for vessel diameters between 100 and 150 µm (see Hammer et al. (2008), figure 2b). Nevertheless, in vessels narrower than 100 µm the compensation algorithm leads to lower SO2 results. In this study, it seems to be likely that similar aSO2 for all three study cohorts might be explained by either the absence of systemic diseases (i.e. healthy cohorts) or well controlled systemic hypertension in the older subjects (glaucoma group). It is known that patients with systemic blood circulatory diseases show a reduced aSO2 [296]. Only subjects with sBP$<$ 140 mmHg and dBP$<$ 90 mmHg independently of any blood pressure medication were included for the present study and hence, no alteration in aSO2 was expected.

The observed significant increase in vSO2 in the glaucoma cohort might be explained by a reduced oxygen consumption in retinas with a loss of neuroretinal tissue. This finding is in agreement with previous research, reporting an 3 % increased vSO2 (see results of meta-analysis, 11). A 10 % (E) up to 14 % (hM) higher vSO2 was found for the

glaucoma cohort when compared to the healthy groups. Conversely, an approximately 10 to 14 percent higher value for vSO2 in the present study could also be the consequence of the age effect in glaucoma group. Mohan et al. and Man et al. reported a 1.9 % and 2.6 % increase in venous SO2 per decade of increasing age (five decades age difference means an estimated increase of venous SO2 of 9.5%). Thus, in this study the increase in vSO2 result (10 % an 14 %) for the glaucoma cohort when compared to the healthy (emmetropic and highly myopic) groups could also be the result of an five decades older study group (vSO2 E: M= 41.34 % vs hM: M= 39.89 % vs G: M= 50.94 %). However, previous research findings regarding age-related SO2 changes are not conclusive (see Meta-analysis in section 5.1). Other authors have reported a decrease in venous SO2 and an increase in A-V SO2 difference with increasing age while aSO2 remained stable [80, 131]. The impact of age on SO2 findings must be interpreted with caution due to the cross-sectional study design of all studies conducted so far. Moreover, it must be highlighted that retinal vessel oximetry is a relative measurement, calculated from vessel reflection and its relation to reflection of the surrounding tissue. Hence, many factors could influence SO2 results such as i.e., vessel wall reflection [271], the pigmentation of the retinal tissue [97] and media opacity [111]. In this study, a investigation of the raw data showed a relationship between SO2 and the pigmentation value of the neighbouring retinal tissue (arteries: r_P= 0.857, p< .001 and veins: r_P= 0.633, p< .001). The data used for statistical analysis were pigmentation-corrected and thus, are less likely to be biased by the effect of retinal pigmentation. However, the results in the glaucoma cohort regarding vSO2 are likely to be a combination of both, the effect of age as well as the effect of glaucoma.

For the calculated A-V SO2 difference, a decreased value is expected based on the findings for arterial and venous SO2. No statistically significant difference in the A-V SO2 difference was found for the three study cohorts, despite a lower group mean in the glaucoma cohort (Mean/SD: 36.69/$\pm$5.70 %) when compared to both other groups (E: 45.06/$\pm$7.00 % and hM: 43.57/$\pm$8.23 %) (one-way ANOVA p=.238, see tables 25 and 26).

Nevertheless, these results confirm previous findings regarding higher vSO2 findings in

glaucoma [301, 253, 228, 302, 194]. Olafsdottir et al. (2014) reported significantly higher venous SO2 and significantly lower A-V SO2 difference results in an advanced glaucoma group (MD_H>10 dB) in a study investigating the effect of the stage of glaucoma (defined by MD_H from visual field assessments) on oximetry measurements. In mild stages of glaucoma only the venous SO2 was found to be significantly higher [228]. In the research presented in this thesis only one subject exceeded 10 dB (MD_H) and thus, the non-significant finding for A-VSO2 difference may reflect the stage of glaucoma in the glaucoma group in the present study (mild or moderate).

With respect to SO2 in healthy myopic eyes, this study found no statistically significant differences from results in emmetropic eyes, suggesting a similar oxygen metabolism in highly myopic and emmetropic eyes. A possible explanation of this might be the similar amount of neuroretinal tissue (average 360^o RNFL thickness) present in both groups (E: M= 92.28 μm vs hM: M= 92.30 μm) and therefor, similar oxygen metabolism. However, the findings of this research do not support the previous research which reported that A-V SO2 difference decreased significantly with increasing AL resulting in a decreased oxygen metabolism [183].

18.1.2. Retinal vessel architecture - Static vessel analysis and vessel complexity

For CRAE the means of all groups were significantly different from each other (the post-hoc test revealed three subsets), while the group means of the emmetropic and highly myopic group were not significantly different from each other (p=.067) for CRVE. The glaucoma cohort presented smallest mean values in vessel calibres for both arteries and veins. These findings confirm previous research suggesting an association between arterial narrowing and the incidence of glaucoma [196, 142, 4, 35]. The cross-sectional [196] as well as the longitudinal findings [142] of the BMES reported that arterial narrowing is two times more likely in eyes with glaucoma than eyes without glaucoma. Moreover, arterial narrowing was associated with the glaucomatous eye, but not with the individual who has glaucoma in the same study [196]. The authors concluded that haemodynamic processes in glaucoma might rather be of local than of systemic origin. Findings regarding the association of glaucoma and narrowing of retinal veins are conflicting. Whilst the

BMES reported an association only for arterial narrowing and glaucoma, an investigation by Amerasinghe et al. (2008) showed that the likelihood of having glaucoma increased by 1.29-fold (OR) if the CRAE was decreased and by 1.49-fold (OR) if the CRVE was decreased [4]. Additionally, Chang et al. (2011) reported a positive relationship between RNFL and CRAE [35]. However, it is still uncertain as to whether the change in vessel calibres is causative to glaucoma or a consequence of it.

This research has revealed that high myopes exhibit significantly smaller artery calibres (CRAE) than emmetropes. It can be assumed that smaller vessel diameters in longer eyes (highly myopic group) could be a result of image minification (OM) due to the elongation of myopic eyes. This study used a telecentric camera system which overcomes the problem of OM in retinal image acquisition. Smaller arteries (CRAE) in highly myopic eyes and in glaucomatous eyes may therefore identify a common feature and thus, could signal a potential glaucoma risk factor in high myopes. This finding for myopes and emmetropes is consistent with findings reported by Zheng et al. in 2015 [330], Patton et al. in 2005 [240] and Wong et al. in 2004 (BMES, [318]. The authors reported reduced vessel calibres for both, arteries and veins in longer eyes, independent of the method used to determine the relationship. While Zheng et al. analysed diameters only, Patton et al. and Wong et al. (BMES) applied the revised Parr-Hubbard formula to determine vessel calibres.

Regarding retinal vessel complexity, the results of Df were similar for emmetropes and high myopes (Tukey HSD post-hoc analysis corrected for eccentricity retina: p= .162), while the glaucoma cohort displayed a less dense retinal vessel network (M= 1.35, SD= 0.02). This finding was significant (F(2,75)= 16.073, p= .000) and resulted in an even stronger effect when the analysis was adjusted for the effect of eccentricity (see table 28) of the retina (F(2,75)= 18.749, p= .000). The results of this study suggest that despite a more prolonged retina, the vessel network pattern is not sparser in highly myopic eyes when compared with emmetropic eyes. Additionally, the spacing between the retinal vessels (referred to as lac) in the three study groups did not differ significantly from each other (see table 27 and 28). The findings for Df and Lac imply that emmetropes and high myopes exhibit similar vessel patterns, despite arterial narrowing in highly myopic

eyes. This result for the retinal vessel network complexity in myopic eyes has not been previously documented. The SiMES (Singapore Malay Eye Study; sample size=2913) reported a positive relationship between Df and refractive error ($\beta = 0.152$, $p < .001$). The authors concluded that a sparser vessel network in myopic eyes combined with narrower vessel calibres might be associated with a reduced blood flow in myopia [38]. However, the present study compared the results of two groups of distinct refractive errors (+0.00 DS and - 7.50 DS) rather than conducting a regression analysis for continuous data for SE (SiMES data: $M = -0.03$ DS $SD = 1.94$ DS). The present study compared findings from two healthy groups of similar age (age: E: $M = 24 \pm 9$ years and hM: $M = 27 \pm 9$ years), whereas the SiMES used data from an older population which was adjusted for age ($M = 58 \pm 11$ years). Thus, the present results may be considered more suitable for the comparison of emmetropic versus highly myopic eyes.

A recently published study by Li et. al. (2016) used a different technique to investigate the complexity of the retinal microvasculature [174]. Li et al. also reported a less denser vessel network in myopic eyes using optical coherence tomography angiography (OCTA) to determine Df in the superficial and deeper retinal microvasculature. In contrast to their approach, the present study determined the complexity of the superficial retinal vessels rather than the complexity of the superficial capillary plexus and, thus cannot be compared with the results published by Li and co-workers.

Interestingly, the SiMES did not find an association between age- related eye diseases (i.e., AMD or glaucoma) and the complexity of the vessel network in a group of 2913 Malayans between 40 and 80 years of age [38]. This study however, showed a significantly weaker vessel network in the glaucoma group when compared with the healthy groups, which remained statistically significant after adjustment for age was made. The result of the present study is in agreement with previous findings conducted with OCTA principles that glaucomatous eyes exhibit a weaker retinal vessel network to supply and drainage the retinal tissue [201, 255, 324]. Moghimi et al. (2018) carried out OCTA at the ONH and the macula area to determine the complexity of the retinal micro-vasculature in glaucoma subjects and reported a reduced complexity of the micro-vasculature at the ONH and within the macula-annulus.

18.1.3. Retinal vessel function - Retinal vessel reactivity

The one-way ANOVA showed no significant difference in group means for the SDRA markers, suggesting that the retinal vessel function in highly myopes and emmetropes is similar. Additionally, the glaucoma cohort did not exhibit differences in vessel responses from healthy cohorts, indicating that the retinal vessel response to adapt to alterations in oxygen demand of the retinal tissue is not impaired in glaucoma. The findings of this study regarding the healthy cohorts are in agreement with previous investigations regarding emmetropia and high myopia [158]. La Spina et al. (2016) used the traditional vessel analysis method (provided by the RVA software) and the same flicker protocol to determine vessel response marker in highly myopic eyes and found no difference when compared to emmetropic eyes.

With respect to glaucoma however, this research was not able to demonstrate the previously reported reduced venous vessel response [77, 88, 253]. There are two possible explanations for the conflicting finding: Firstly, this study used a different analysis concept to determine MC and MD (SDRA according to a publication of Heitmar et al. in 2010, [112]). Secondly, the sample size of the glaucoma cohort was small, with only seven subjects eligible for analysis. Thus, the statistical power of the one-way ANOVA for DA was low (veins: statistical power= 0.23, effect size= 0.19).

18.1.4. Perfusion pressure calculations

The perfusion pressure calculations showed no significant difference in sPP and dPP between the two healthy study cohorts. For dPP however, the means of highly myopic eyes and glaucoma eyes were similar (hM and G difference only 3.5 mmHg). In the present study dPP was similar in both, the glaucoma and highly myopic group. This finding might indicate a potential glaucoma risk in highly myopic eyes. To date, there is still controversy about the influence of ocular perfusion on development and progression of glaucoma. While some authors reported a negative relationship between OPP and dPP in particular, with a higher risk for glaucoma onset and progression [332, 175], other studies did not find significant relationships between ocular perfusion and glaucoma [261, 136]. A significantly higher risk of OAG prevalence for subjects with dBP, MOPP

and dPP in the lowest quartile was reported in the SiMES [332]. In particular, nocturnal MAP and OPP fluctuations were found to be responsible for the progression of NTG in a longitudinal study published by Sung et al. (2009) [283]. Opposing results were published from a population-based cross-sectional Central India Eye and Medical Study including data from 4711 Indian subjects between 30 years and 100 years of age [136]. This study published by Jonas et al. (2015) found a significant relationship between translamina pressure difference (TLPD) as well as IOP and the prevalence of POAG, but no significant relationship with OPP and the prevalence of POAG. Similar to the findings of Jonas, a study by Samsudin et al. (2016) did not find a significant difference in OPP between glaucoma and control group. The latter study investigated blood flow in the ophthalmic artery (OAF) and MOPP in thirty-one NTG subjects and compared the results with a group of fifteen healthy subjects. However, both studies did not distinguish between systolic and diastolic perfusion pressure which has been carried out in studies that reported a significant relationship. Hence, in OPP investigations it might be crucial to differentiate between systolic and diastolic PP. Moreover, IOP is a surrogate for the venous pressure and, it may not always be appropriate to replace IOP for venous pressure. An interesting aspect might be the impact of OPP challenges on vessel reactivity. This effect of OPP was studied previously by Nagel and Vilser in 2004 [215]. The authors reported an increase of arteries by $+1.9 \pm 4.5$ % and a decrease of veins by -2.6 $\pm$ 3.5 % when IOP was increased from 13.7 $\pm$ 2.9 mmHg to 21.2 $\pm$ 3.5 mmHg (OPP reduced), suggesting OPP changes alter the autoregulatory behaviour of retinal vessels.

The present findings regarding OPP have to be interpreted carefully due to two aspects: Firstly, BP and IOP are determinants of the OPP calculation. It is well reported that BP increases with increasing age and thus, influencing PP results [68, 245]. The Framingham Heart Study explored longitudinally (4 up to 16 biennial measurements) changes in BP in a group of normotensive subjects and three groups of untreated hypertensives aiming to determine the effect of age on BP. The authors reported a linear increase in sPP with increasing age. and a decrease of dBP after the age of 60 years. This study included only glaucoma subjects receiving anti-hypertensive drug therapy and thus, statistical age-adjustment was not appropriate for group comparison. Secondly, this study did not

investigate short-term (24 hours) or long-term OPP fluctuations, which were reported influential in glaucoma progression and might thus, be a crucial parameter in glaucoma risk investigation [43, 181].

In summary, the group comparisons for retinal haemodynamic measurements highlighted CRAE and dPP as possible links between physiological high myopia and glaucoma.

18.2. Haemodynamic intra-relationships in emmetropic vs in highly myopic and in a sample of glaucomatous eyes

The result of haemodynamic intra-relationships (i.e. heamodynamic pattern) represents the interplay of the infrastructure (size and complexity) and the function (SDRA) of the retinal vessel network that supplies the neuroretinal tissue with oxygen and drains it from waste products and exceeding oxygen. While arterial measurements represent autoregulative mechanisms, venous measurements represent the drainage mechanisms. A balance between supply and drainage of the tissue may determine the state of health in the retinal tissue. A difference in haemodynamic pattern between the healthy emmetropic and the healthy highly myopic group may indicate differences in autoregulation patterns and/or vascular dysregulation as was suggested by previous research [72].

Arterial vessel calibres and venous vessel calibres were significantly positive correlated in both healthy study cohorts, suggesting a similar ratio between arterial and venous vessel calibres independent of eye-length. This finding may be explained due to the retinal stretch effecting also the embedded vessels. This finding was confirmed by the non-significant finding for AVR in the group comparison of emmetropic and high myopic cohorts. The correlation result (CRAE vs CRVE) in the glaucoma cohort exhibited a similarly large effect size (r_P= 0.648) as in the healthy cohorts, although this finding was not statistically significant. A possible explanation for the non-significant finding might be the small sample size in the glaucoma sample. The large effect size in this cohort signals an effect, which may become significant in a larger sample (Cohen criteria revised by Elliot: small $>$ 0.1, medium $>$ 0.3 and large $>$ 0.5, very large $>$ 0.7 [55]).

The results regarding vessel function showed no difference in both healthy study cohorts. For arteries, MD contributed 51 % towards DA in emmetropic eyes and 52 % in highly

myopic eyes. For veins, MD contributed 56 % towards DA in emmetropes and, in high myopes this value was 61 %. In the glaucoma sample, the contribution of MD_V towards DA_V was also 61 %. A subsequent Z-test analysis investigating differences in MD vs DA and MC vs DA patterns for arteries and veins separately, revealed no statistically significant differences between both healthy cohorts (the critical Z for the 0.05 significance level is 1.96 ; Z_{MDA}= - 0.022 and Z_{MCA}= 0.022 and Z_{MDV}= - 0.100 and Z_{MCV}= 0.100). These results suggest that the elongation of the eye in high myopia does not influence the ability of the retinal vessels to dilate and constrict and thus, suggests that the autoregulation mechanism is not impaired in highly myopic eyes. The findings for vessel reactivity in highly myopic eyes are in agreement with previous research. La Spina et al. (2016) explored dynamic and static vessel parameters in a group of 20 highly myopic eyes with pathological myopia, 20 highly myopic eyes without pathological myopia and a control group of 20 age- and sex-matched subjects [158]. The authors reported that highly myopic eyes are functionally comparable to control subjects, despite showing a reduced vessel diameter. Similar effect sizes as for the healthy cohorts was found in the glaucoma group (CRAE vs CRVE: r_P= 0.648, MD vs DA: r_PA= 0.916 and r_PV= 0.952 and MC vs DA: r_PA= 0.804 and r_PV= 0.597 in arteries=A and veins=V). However, the Pearson correlation results were only statistically significant for MD_V vs DA_V (p= .001, q= .001) in the glaucoma sample with small sample size (n=7). A possible explanation for the non-significant findings may be the small sample size in this cohort. The large effect size in the group of glaucomatous eyes suggest an effect, worthy of further exploration. Moreover, the non-significant finding for the correlation of MC_V vs DA_V prior to controlling for multiple comparison testing in the glaucoma group may support the hypothesis of a venous stasis suggested by Josef Flammer and co-workers [67].

The sPP vs dPP correlation was found to be statistically significant only in the healthy emmetropic study cohort (r_P= 695, p= .000, q=< .0005). Neither the highly myopic nor the glaucoma subjects exhibited significant associations after controlling the FDR (hM: p= .026, q= .01 and G: p= .022, q= .004). Moreover, the in the highly myopic cohort the effect size was only medium (r_P= 0.412) suggesting that systemic blood flow alterations may at least partly explain glaucoma susceptibility in highly myopes. A pos-

sible explanation for the difference in effect size between the healthy cohorts may be the fact that OPP calculations are based on the assumption, that venous pressure (RVP) is roughly the same value as IOP. Nevertheless, RVP and IOP are not identical values and thus, the OPP calculation is rather an estimation [57, 279].

The glaucoma cohort and the emmetropic cohort showed a similar effect sizes for the relationship between sPP and dPP. This result must be interpreted with caution because OPP results are altered in the glaucoma group due to the IOP lowering as well as anti-hypertensive medication taken in this cohort. The effect size (r_P= 0.741) in this sample may rather represent the controlling mechanisms in this cohort than being suitable for comparisons with healthy subjects.

In summary, the haemodynamic patterns in healthy emmetropes and healthy high myopes did exhibit a difference only for the relationship between sPP and dPP. Previous research has identified systemic blood circulation alterations as a potential risk factor for the incidence of glaucoma. Ocular perfusion pressure calculations are derived from systemic pressure (BP) values and IOP and thus, represent systemic circulatory aspects. The Los Angeles Latino Eye Study reported that both, low dBP and high sBP are associated with increased prevalence of POAG [192]. Thus, an imbalance between systolic and diastolic PP might partly explain the increased glaucoma risk in high myopes.

18.3. Implications of all haemodynamic findings

This study identified a significantly decreased CRAE in the group of healthy high myopes when compared to the emmetropic counterpart. Furthermore, the results of the haemodynamic intra-relationships suggest that the decreased CRAE is accompanied by decreased CRVE. Regarding the adaption of retinal vessel to changes in tissue need (i.e. retinal vessel reactivity), highly myopic eyes were not different from emmetropic eyes. It is worth stressing, that highly myopic eyes might already show a reduced blood flow rate due to narrower arterial calibres. The blood flow rate might be further diminished in the glaucoma cohort due to even smaller arterial vessel calibres (CRAE). The glaucoma cohort exhibited the smallest CRAE (M=119.84 $\pm$8.61 µm). Blood flow (defined as flow

rate) determines the supply of the retinal tissue with vital nutrients and oxygen. Hence, a reduction in the flow rate might indicate a malnutrition of the retinal tissue (RNFL and GCL in particular). According to the Poiseuille's law (see equation 1) the relationship between flow rate (Q) and radius (r) is $Q \approx r^4$. In this study, highly myopic eyes showed a thirty percent (30 %) reduced flow rate when compared to the emmetropic group when the flow rate was calculated (Poiseuille's law) from the given CRAE group means and a constant pressure difference in each group was assumed. These results confirm previous findings of a reduced blood flow in myopic eyes [13]. For the glaucoma cohort the same calculation exhibited a seventy percent (70 %) reduction in flow rate when compared with the emmetropic cohort. The system would need to increase the blood pressure in order to adapt the flow rate to a reduced vessel radius (autoregulation). Although the glaucoma group exhibited a higher systolic BP (M= 120 $\pm$12 mmHg) than the emmetropic (M= 108 $\pm$9 mmHg) and highly myopic groups (M= 112 $\pm$11 mmHg), the detected sBP difference between the glaucoma cohort and the emmetropic cohort (12 mmHg between emmetropic and glaucoma cohort) is not sufficient to explain a similar flow rate in the glaucoma cohort as for the emmetropic cohort (relationship: $Q \approx \Delta$P). Likewise, for the highly myopic cohort, the 4 mmHg higher sBP than in emmetropes cannot counterbalance the difference in CRAE to maintain a similar flow rate as for the emmetropic group. Moreover, a theoretical study on the pressure distribution on hemispherical surfaces (i.e. high myopia) suggested that highly myopic eyes require more pressure in retinal vessels to sufficiently distribute oxygen to the retinal tissue [52].

A reduced flow rate in the glaucoma sample could also be a consequence of a reduced oxygen demand due to neuroretinal tissue loss. Previous research investigating OA blood flow characteristics in a group of highly myopic glaucoma subjects vs non-myopic glaucoma subjects found pronounced OA blood flow abnormalities in the group of high myopic glaucoma subjects [72]. Based on the findings of Galassi et al. (1999), the above conducted calculations may support the hypothesis of haemodynamic impairment due to reduced vessel calibres in highly myopic eyes. This in turn may lead to a reduced blood flow and consequently, to the loss of neuroretinal tissue as seen in glaucoma due to hypoxia.

19. Structural vs haemodynamic relationships and regression analyses

19.1. Predicting RNFL thickness from haemodynamic measurements

The results of structural vs haemodynamic correlation analysis aiming to identify haemodynamic predictor variables capable of explaining changes in RNFL quadrant thicknesses as well as changes in GCL sectors thicknesses did not find significant correlations in the group of healthy myopic eyes and in the glaucoma cohort. In the healthy emmetropic cohort however, a thicker nasal RNFL quadrant can be predicted from a denser retinal vessel network ($\beta = 0.545$, $t = 3.789$, $p < .01$). Retinal vessel network complexity explained 25% of the variation in nasal RNFL quadrant thickness. This finding indicates that besides retinal vessel architectural properties such as Df in healthy emmetropes, there may be other cofounding parameters determining the loss of neuroretinal tissue in the nasal RNFL quadrant.

The sample size (N) may partly explain non-significant findings in the multiple correlation analyses of this study. According to Maxwell et al. (2000) a N of 392 + p is needed to detect a small effect ($r > 0.1$) with statistical power of 80 % [188]. In order to detect medium effect ($r > 0.3$) a N of 52 + p is required and 22 + p to detect a large effect ($r > 0.5$). In this equation "p" defines the number of predictor variables. In this part of the study, nine predictor variables were considered due to the fact that only one variable (either MD or MC or DA) was selected for retinal vessel reactivity parameters. Thus, a sample size of 31 participants within each group was needed to detect a large effect size, while 61 subjects per group were required for detecting a medium size effect with statistical power of 0.8. In this study, the sample size in the glaucoma cohort was only nine participants. However, the correlation coefficients in the glaucoma group indicate a very large (>0.7) negative effect. Thus, there might be an effect of haemodynamic parameters on neuroretinal thickness changes despite non-significant correlations. Further investigations including a larger glaucoma sample are needed to confirm the current results.

20. Summary of findings of this study

The main objective of this study was to identify parameters of visual function (visual field indices), structural (RNFL and GCL thicknesses) and retinal haemodynamic (architectural and functional vessel measurements) nature, that are distinctly different in healthy highly myopic eyes when compared with healthy emmetropic eyes. This study also aimed to compare retinal haemodynamic patterns in healthy highly myopic eyes and in healthy emmetropic eyes. Distinct patterns in high myopes that resemble those of a group of eyes with glaucoma may indicate a similarity in autoregulation mechanisms. This study furthermore explored relationships between neuroretinal tissue thickness and retinal haemodynamic variables in order to determine retinal haemodynamic parameters that predict changes in neuroretinal tissue thickness. If so, the difference in predictive parameters between high myopes and emmetropes may account for the difference in glaucoma risk between healthy emmetropic and healthy myopic eyes [185]. Moreover, any similarity in predictor variables in the group of healthy highly myopic eyes and the glaucoma sample may indicate haemodynamic mechanisms responsible for neuroretinal tissue loss in healthy high myopic eyes and as seen in disease. This broad approach specifies parameters that qualify for further, more specific investigations.

20.1. Visual function parameters

In this study, visual function measurements (i.e. visual field indices and GHT-pattern analysis) did not significantly differ between emmetropic and highly myopic eyes and thus, was not further explored in correlation and regression analysis. As expected, the glaucoma sample exhibited the largest variation in between the subjects despite a small sample size (n=7). While IQR in the healthy cohorts did not exceed 1.70 dB, the glaucoma group exhibited IQR from 3.8db up to 21.20dB. The largest variation within the glaucoma group was found for the N3 and P4 GHT- pattern analyses (IQR= 21.20dB and IQR= 20.70 for N3 and P4 analysis, respectively), which are the regions of glaucoma specific functional losses.

20.2. Structural parameters

The comparison of neuroretinal tissue thicknesses revealed no statistically significant differences of RNFL thickness as well as GCL thickness in the healthy cohorts differing in refractive error, whilst the neuroretinal thickness (RNFL and GCL) in the glaucoma sample was smaller in all locations. Moreover, the highly myopic cohort exhibited the same 360^oaverage RNFL thickness as the emmetropic cohort (E: 92.28 (SD$\pm$9.91) µm vs hM: 92.30 (SD$\pm$9.98) µm) indicating a similar amount of neuroretinal tissue in eyes of varying eye length. As observed in previous research [140], the quadrant specific thickness analysis revealed a significantly thicker temporal RNFL thickness in highly myopic eyes when compared to the group of emmetropic eyes (E: 61.90 (IQR 11.73) µm vs hM: 76.92 (IQR 29.37) µm; pairwise Kruskal-Wallis analysis with Bonferroni correction for multiple comparisons: p= .000). Regarding GCL thickness the inferior-nasal sector exhibited the least difference (lowest effect size) in between the study cohorts suggesting similar thicknesses in healthy eyes as well as in a glaucoma (weighted F(2, 72)= 8.917, p= .000).

20.3. Heamodynamic parameters and patterns

With respect to single retinal haemodynamic parameters, the highly myopic group showed significantly different results from the emmetropic group only for CRAE (two separate subsets for the Tukey HSD post-hoc analysis). High myopes exhibited a significantly smaller CRAE than the emmetropes (E: 162.58 (SD$\pm$13.08) µm vs hM: 148.59 (SD$\pm$17.29) µm).

Subsequently, the study investigated the interplay (intra-relationships) of haemodynamic variables as well as the relationship between haemodynamic and structural measurements using correlation analysis for the three study cohorts separately. Haemodynamic intra-relationships identified multicollinearity and provided crucial information about the interplay of retinal vessel architectural (CRAE, CRVE, Df) and functional (MD, MC, DA, SO2 and PP) variables in emmetropic, highly myopic and in glaucoma conditions. Retinal vessel functional measurements are MD, MC and DA (magnitude of vessel diameter change) and were determined for arteries and veins separately. The physiological function

of dilation and constriction in arteries is the adaptation of blood flow to the tissue need (i.e. autoregulation), while the same measures in veins represent the drainage quality of the tissue. The relationship between any of these two markers (i.e. MD, MC) with the dilation amplitude (DA) represent the impact of this marker onto the process of autoregulation or tissue drainage. The percentage of which MD and MC contribute towards DA was similar for emmetropic and highly myopic eyes. This was true for retinal arteries and for retinal veins. For CRAE and CRVE (retinal vessel architectural measurement) a similar relationship was observed for both healthy cohorts (E: r_P= .673, p= .000 vs hM: r_P= .700, p= .000). Despite a similar effect size (large), no significant relationship was observed in the glaucoma sample (r_P= 0.648). The relationship between systolic and diastolic ocular perfusion pressure calculations representing the influence of the systemic blood-circulation on the eye, was statistically significant in the group of healthy emmetropes (r_P= .695, p= .000). For the same association in highly myopic eyes, the effect size was only medium and not significant when the analysis was controlled for the FDR (r_P= .412, p= .026, q= .011) suggesting systemic circulatory imbalances in highly myopic eyes.

20.4. Predictability of neuroretinal tissue changes from haemodynamic parameters

After controlling the FDR in testing multiple correlations, no statistically significant haemodynamic vs structural relationships were found in the highly myopic and the glaucoma groups. In the emmetropic cohort an increased Df was able to significantly explain a thicker RNFL quadrant thickness. Twenty-five percent of the variation in nasal RNFL thickness could be explained by Df, suggesting other aspects (e.g. of cell-biologic nature) impacting neuroretinal tissue reduction. Nevertheless, correlation analyses in the glaucoma sample exhibited very large effect sizes (> 0.7) suggesting the presence of an effect despite non-significance due to a small sample size.

Part VII

A proposed hypothesis from findings of this research

In summary, the aforementioned relationships and regression analysis propose the hypothesis that an impairment of retinal vessel architecture (smaller vessel diameter) may lead to impaired autoregulation in high myopes. The neuroretinal tissue in myopic eyes may be at risk to be damaged due to hypoxia as a consequence of vascular dysregulation (reperfusion impairment).

The regression model in the healthy emmetropic cohort was not able to predict more than 25 % of the variation in neuroretinal tissue thickness. It is likely that besides retinal haemodynamic parameters assessed in this study, there are other factors which contribute to the loss of neuroretinal tissue leading to the development of optic neuropathies such as glaucoma.

In recent years, an increasing evidence from research has shown an involvement of oxidative stress, defined as an imbalance between free radical production and antioxidant defences, in the development of myopia-associated complications as well as in glaucoma. Bosch-Morell et al. (2015) reviewed previous investigations on the molecular aspect of pathological myopia [23]. Oxidative stress was also associated with vascular dysregulation in glaucoma [287]. Oxidative stress causes alterations in endothelial functions, especially the production of ET 1 and NO [2, 85]. Whereas the effect of ET-1 directly effects IOP due to vasoconstriction of ocular vessels resulting in aqueous humour outflow alterations, NO induces the release of glutamate in endothelial cells leading to neuronal toxicity [179, 32, 219]. Elevated NO levels were found in the aqueous humour of glaucoma patients [297, 81]. However, it is still unclear if the elevation of NO is causative or an effect of the pathology [287].

The findings of animal studies suggest that NO modulates choroidal thickening [221]. Nickla et al. in 2004 reported a reduced choroidal thickening (as seen in myopisation)

when NO inhibitors were injected into the vitreous of chicks with induced myopia. This research did not explore NO levels and thus, its conclusions are somewhat speculative. Nevertheless, the mechanism identified from retinal haemodynamic parameters in this study suggest that molecular aspects (e.g. NO levels or ET-1) play at least a part in the development of glaucoma in highly myopic eyes. Despite similar vessel complexity as in the emmetropic cohort, smaller vessel calibres and an imbalance in ocular perfusion were found in the highly myopic cohort. These findings suggest that a diminished vessel architecture may trigger a continuous vessel reactivity in order to maintain a stable blood flow. A possible consequence of this are higher NO and ET-1 levels in the retina of a highly myopic eye. The constant exposure of the retina to NO (neurotoxic effect) might play a part in the increased glaucoma susceptibility in highly myopic eyes. Future studies are needed to explore NO and ET-1 levels in myopic eyes. An elevation of these molecules could explain glaucoma susceptibility in myopic eyes due to causing oxidative stress. Figure 42 shows graphically the proposed processes that may lead to glaucomatous optic neuropathy.

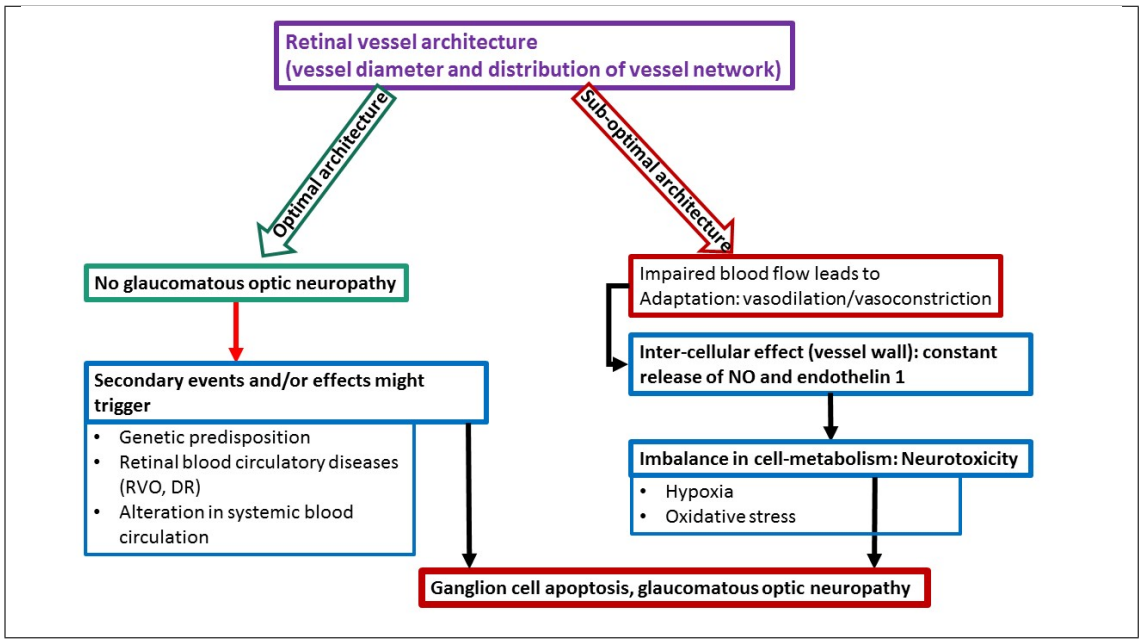

Figure 42: **Proposed linkage between retinal haemodynamic parameters and the developement of glaucomatous optic neuropathies.**

Part VIII

Limitations of this research and future studies

This study investigated a variety of structural and haemodynamic variables in groups of emmetropic, highly myopic and glaucoma subjects separately, with the aim of detecting parameters that are similar for myopic and glaucoma subjects but are different from those in emmetropic subjects. In exploring these aspects for each group separately, the study intended to detect features and mechanisms that are limited to a particular group. Undoubtedly, these results add to the understanding of retinal haemodynamic parameters in healthy eyes of different axial lengths as well as in glaucoma. The findings for retinal haemodynamic intra-relationships indicate that retinal blood circulation is a complex process determined by its architecture and function. A lack of architectural features of the vessels might be compensated by vessel function (reactivity). This in turn may trigger cellular reactions leading to neurodegenerative effects (ganglion cell loss) as found in glaucoma. Numerous research laboratories have extensively explored individual retinal haemodynamic as well as structural aspects in glaucoma and in myopia with similar results as in this study. However, none of the previous investigations explored the topic to the extent of this thesis.

Despite the vast range of investigated parameters, this study was not without limitations which must be addressed in future research. Firstly, this cross-sectional, exploratory study aimed to find retinal haemodynamic aspects able to explain neuroretinal tissue loss as found in glaucoma. There is evidence that, although not to the same extent, both aspects are influenced by the effect of age. Previous research has suggested that age influences neuroretinal tissue loss [135, 151, 28, 329, 171]. Age is also considered to have an effect on vessel diameter narrowing [317, 244, 282] and oximetry measurements. This study recruited young subjects for the healthy study cohorts to avoid effects of systemic blood circulation alterations with increasing age [68, 245]. As expected, the glaucoma

cohort was considerably older than both healthy cohorts (mean age was five decades older). Consequently, this exploratory, cross-sectional study controlled for age in statistical analyses, which does not fully reflect the effect of ageing in the eye. Despite the limitations of an older study cohort such as a higher likelihood of systemic hypertension and optical media opacity biasing image analysis [111], a subsequent study might include emmetropes and highly myopic subjects of a similar age as the glaucoma cohort to avoid age compensations in statistical analysis. Additionally, the effect of glaucoma and high myopia can be determined more specifically, if the glaucoma cohort consists of a subgroup of emmetropic glaucoma subjects and a subgroup of highly myopic glaucoma subjects. In doing so the effect of physiological high myopia may be distinguished from the effect of glaucoma. The stratification of the glaucoma cohort into emmetropic and highly myopic patients was not feasible due to recruitment difficulties in this study. Additionally, a longitudinal study design, exploring retinal haemodynamic changes in healthy eyes of different eye length would enable to investigate haemodynamic changes leading to the onset of glaucoma. Unfortunately, such a study design was outside the practicalities of a PhD research (time frame three years).

The effect of AL on retinal heamodynamic parameters could not be investigated in this study due to the fact that data of an emmetropic and a highly myopic cohort were collected. On retrospect, the study would have improved if all types of myopia would have been included. In doing so, the study will be able to determine the effect of ocular elongation on retinal haemodynamic parameters.

A further limitation of this study is the small sample size, especially of the glaucoma cohort. The study aimed for samples of forty to sixty subjects for each study cohort to reach sufficient statistical power (80 %) for the one-way ANOVA as well as for multiple correlation analysis Although extensive efforts in patient recruitment, only eleven glaucoma subjects signed up for participation. Of these eleven, two subjects had to be excluded (see section 11). Despite the small sample size of the glaucoma group, the results of this exploratory study agreed with previous investigations regarding thinner neuroretinal tissue [25, 145, 238], narrower vessel calibres [196] and sparser vessel network [201, 255, 324]. Moreover, the large effect sizes in the correlation analyses ($r>0.7$)

indicate an effect despite non-significant findings due to the small sample size. Thus, the findings of this study may add to the knowledge in the area of retinal haemodynamic mechanisms and how it relates to neuroretinal thickness in healthy eyes and in glaucoma. This study was not able to identify significant differences in between the cohorts for retinal vessel reactivity. Caution has to be applied when comparing with previous research findings due to the fact that the present study used a new method to analyse retinal vessel reactivity to flicker light (referred to as SDRA). Heitmar et al. (2010) proposed this method because it provides more sensitive information about retinal vessel reactivity (MD in particular) due to addressing for variation in vessel response times [112]. However, it is not widely used to date. Further studies are needed to validate the SDRA analysis method in retinal vessel reactivity analysis (i.e. dynamic vessel analysis). In summary, an extended time frame for data collection as well as collaborations with glaucoma units in regional hospitals might improve the sample sizes for healthy participants and for glaucoma patients as well as allowing for a longitudinal investigation in future studies.

This study collected structural and haemodynamic data using the current state-of-the-art measurement techniques. Still, some limitations became apparent when applying these techniques: First of all, the investigation of RNFL and GCL thickness was somewhat limited by a fixed measurement area (implemented in the device software) resulting in difficulties when comparing the three groups means (for a more detailed description see section 8.2.5). Ocular magnification due to different axial lengths leads to different sizes of the measurement area in which RNFL and GCL thickness is measured and thus, made the comparison difficult [71]. The software does not allow adjustment of the measurement area. Consequently, the study compensated for OM as described in section 8.2.5 to best overcome the effect of comparing locations of different size before statistical analyses. In future studies a customized software adjusting the measurement area based on AL data might help to compare neuroretinal thicknesses in eyes with different axial lengths.

Secondly, blood circulation aspects and its meaning may well be different for arteries than it is for veins. Thus, arterial and venous results were investigated separately for

retinal vessel calibres, vessel reactivity and oxygen content in retinal vessels. For the retinal vessel network complexity (Df and Lac), the commercially available software does not distinguish arteries from veins. Knowing architectural properties of the supplying (arteries) and draining (veins) system separately would provide additional information about the balance between both. Hence, further software development is needed to allow for analysis of retinal vessel network complexity of arteries and veins, separately. Additionally, oxygen is distributed to the tissue via the capillaries. These were not explored in this study due to the technology used in this research. New OCT angiography techniques would facilitate the investigation of retinal capillary haemodynamic parameters. The option of OCT angiography became available at the end of data collection. Nevertheless, a future study might explore the retinal capillary architecture in more detail with the ONH area being of particular interest [40, 201].

Finally, in this study the estimation of the oxygen content in retinal vessels referred to as SO2 measurement or oximetry was influenced by retinal pigmentation. Previous research has demonstrated an effect of retinal pigmentation on venous results, but not for arterial results in a group of Caucasian subjects [97]. This finding lead to a compensation algorithm in the RVA software. The study population of this study consisted of mixed-race cohorts exhibiting a much broader range of retinal pigmentation states. Hence, a greater impact of pigmentation on oximetry results was expected. Figure 19/a shows the results of arterial and venous SO2 measurements related to the pigmentation value (given by the RVA system). The graphs support the hypothesis of an association between the amount of retinal pigment and arterial as well as venous SO2 results, despite the software algorithm compensating for it already. It suggests a linear relationship. In this study raw data of the healthy study subjects were used to determine values for a data rotation matrix. Subsequently, these transformation values were applied to transform arterial and venous SO2 results for all cohorts before statistical analysis. A future study may investigate the relationship of the retinal pigmentation value with SO2 measurements applying a software without compensation terms in a mixed cohort. In doing so the exact relationship and a better compensation term for retinal pigmentation can be determined. This would enable the comparison of individual oximetry results

independent of subject ethnicity.

In summary, future investigations might explore the following questions:

- How do retinal heamodynamic, functional and structural parameters in emmetropic glaucoma subjects differ from those of highly myopic glaucoma subjects?
- How is AL related to retinal heamodynamic measurements in healthy myopic eyes?
- How do retinal capillary haemodynamic parameters (Df) differ in healthy emmetropic, healthy highly myopic, emmetropic glaucoma and highly myopic glaucoma subjects?

In spite of its limitations, the study certainly adds to our understanding of haemodynamic patterns as well as single haemodynamic measures in healthy eyes of different axial lengths as well as in glaucoma. Haemodynamic intra-relationships indicate that retinal blood circulation is a complex process determined by its architecture and function. A lack of architectural features might be compensated functionally. This however triggers cellular reactions which potentially lead to neurodegenerative effects (ganglion cell loss) as found in glaucoma.

Part IX

Bibliography

[1] A. Agar, S. S. Yip, M. A. Hill, and M. T. Coroneo. Pressure related apoptosis in neuronal cell lines. *Journal of Neuroscience Research*, 60(4):495–503, 2000.

[2] R. Agarwal, S. K. Gupta, P. Agarwal, R. Saxena, and Sh. S. Agrawal. Current concepts in the pathophysiology of glaucoma. *Indian J Ophthalmol.*, 57(4):257, 2009.

[3] J. Alvarado, C. Murphy, and R. Juster. Trabecular meshwork cellularity in primary open-angle glaucoma and nonglaucomatous normals. *Ophthalmology*, 91(6):564 – 579, 1984.

[4] N. Amerasinghe, T. Aung, N. Cheung, Ch. W. Fong, J. J. Wang, P. Mitchell, S.-M. Saw, and T. Y. Wong. Evidence of retinal vascular narrowing in glaucomatous eyes in an asian population. *Invest Ophthalmol Vis Sci*, 49(12):5397–5402, 2008.

[5] P. Asman and A. Heijl. Glaucoma hemifield test: Automated visual field evaluation. *Arch Ophthalmol*, 110(6):812–819, 1992.

[6] D. A. Atchison, N. Pritchard, K. L. Schmid, D. H. Scott, C. E. Jones, and J. M. Pope. Shape of the retinal surface in emmetropia and myopia. *Invest Ophthalmol Vis Sci*, 46(8):2698–2707, 2005.

[7] T. Aung, P. J. Foster, S. K. Seah, S.-P. Chan, W.-K. Lim, Hui-Min Wu, A. T. H. Lim, L. Lee, and S.-J. Chew. Automated static perimetry: the influence of myopia and its method of correction. *Ophthalmology*, 108(2):290–295, 2001.

[8] M. P. Avila, J. J. Weiter, A. E. Jalkh, C. L. Trempe, R. C. Pruett, and Ch. L. Schepens. Natural history of choroidal neovascularization in degenerative myopia. *Ophthalmology*, 91(12):1573–1581, 1984.

[9] R. Battu, A. Mohan, A. Khanna, A. Kumar, and R. Shetty. Retinal oxygen saturation in retinitis pigmentosa and macular dystrophies in asian-indian eyes. *Invest Ophthalmol Vis Sci*, 56(5):2798–2802, 2015.

[10] J. M. Beach. Pathway to retinal oximetry. *TVST*, 3(5):9, 2014.

[11] J. M. Beach, K. J. Schwenzer, S. Srinivas, D. Kim, and J. S. Tiedeman. Oximetry of retinal vessels by dual-wavelength imaging: calibration and influence of pigmentation. *J Appl Physiol*, 86(2):748–758, 1999.

[12] J. M. Beach, J. S. Tiedeman, M. F. Hopkins, and Y. S. Sabharwal. Multispectral fundus imaging for early detection of diabetic retinopathy. *Proc. SPIE*, 3603:114–121, 1999.

[13] A. Benavente-Perez, S. L. Hosking, N. S. Logan, and D. C. Broadway. Ocular blood flow measurements in healthy human myopic eyes. *Graefes Arch Clin Exp Ophthalmol*, 248(11):1587–1594, 2010.

[14] B. Bengtsson and A. Heijl. Sita fast, a new rapid perimetric threshold test. description of methods and evaluation in patients with manifest and suspect glaucoma. *Acta Ophthalmol Scand*, 76(4):431–437, 1998.

[15] M. C. Bengtsson, B.and Leske, L. Hyman, and A. Heijl. Fluctuation of intraocular pressure and glaucoma progression in the early manifest glaucoma trial. *Ophthalmology*, 114(2):205 – 209, 2007.

[16] Y. Benjamini and Y. Hochberg. Controlling the false discovery rate: a practical and powerful approach to multiple testing. *Journal of the Royal statistical society: series B (Methodological)*, 57(1):289–300, 1995.

[17] A. G. Bennett, A. R. Rudnicka, and D. F. Edgar. Improvements on littmann's method of determining the size of retinal features by fundus photography. *Graefes Arch Clin Exp Ophthalmol*, 232(6):361–367, 1994.

[18] N. L. Benowitz, H. Porchet, L. Sheiner, and P. Jacob. Nicotine absorption and cardiovascular effects with smokeless tobacco use: comparison with cigarettes and nicotine gum. *Clin Pharmacol Ther*, 44(1):23–28, 1988.

[19] J. Boeckaert, E. Vandewalle, and I. Stalmans. Oximetry: Recent insights into retinal vasopathies and glaucoma. *Bull Soc Belge Ophtalmol*, (319):75–83, 2012.

[20] L. Bonomi, G. Marchini, M. Marraffa, P. Bernardi, R. Morbio, and A. Varotto. Vascular risk factors for primary open angle glaucoma: The egna neumarkt study. *Ophthalmology*, 107(7):1287–1293, 2000.

[21] M. Borenstein, L. V. Hedges, and J. P. T. Higgins. *Introduction to Meta Analysis (2)*. Wiley, 2009.

[22] M. Borenstein, J. P. T. Higgins, L. V. Hedges, and H. R. Rothstein. Basics of meta-analysis: I2 is not an absolute measure of heterogeneity. *Research Synthesis Methods*, 8:5–18, 2017.

[23] F. Bosch-Morell, S. Merida, and A. Navea. Oxidative stress in myopia. *Oxidative medicine and cellular longevity*, 2015:12, 2015.

[24] R. R. A. Bourne, G. A. Stevens, R. A. White, J. L. Smith, S. R. Flaxman, H. Price, J. B. Jonas, J. Keeffe, J. Leasher, K. Naidoo, K. Pesudovs, S. Resnikoff, and H. R. Taylor. Causes of vision loss worldwide 1990 - 2010: a systematic analysis. *The Lancet Global Health*, 1(6):339–349, 2013.

[25] C. Bowd, R. N. Weinreb, J. M. Williams, and L. M. Zangwill. The retinal nerve fiber layer thickness in ocular hypertensive, normal, and glaucomatous eyes with optical coherence tomography. *Arch Ophthalmol*, 118(1):22–26, 2000.

[26] D. S. Bredt and S. H. Snyder. Nitric oxide: a physiologic messenger molecule. *Annu. Rev. Biochem.*, 63(1):175–195, 1994.

[27] P. Brusini, M. L. Salvetat, M. Zeppieri, C. Tosoni, and L. Parisi. Comparison of icare tonometer with goldmann applanation tonometer in glaucoma patients. *J Glaucoma*, 15(3):213–217, 2006.

[28] D. L. Budenz, D. R. Anderson, R. Varma, J. Schuman, L. Cantor, J. Savell, D. S. Greenfield, V. M. Patella, H. A. Quigley, and J. M. Tielsch. Determinants of normal retinal nerve fiber layer thickness measured by stratus oct. *Ophthalmology*, 114(6):1046–1052, 2007.

[29] D. L. Budenz, K. Barton, J. Whiteside-de Vos, and et al. Prevalence of glaucoma in an urban west african population: The tema eye survey. *JAMA Ophthalmology*, 131(5):651–658, 2013.

[30] D. L. Budenz, P. Rhee, W. J. Feuer, J. McSoley, A. Ch. Johnson, and D. R. Anderson. Sensitivity and specificity of the swedish interactive threshold algorithm for glaucomatous visual field defects. *Ophthalmology*, 109(6):1052–1058, 2002.

[31] D. L. Budenz, P. Rhee, W. J. Feuer, J. McSoley, C. A. Johnson, and D. R. Anderson. Comparison of glaucomatous visual field defects using standard full threshold and swedish interactive threshold algorithms. *Arch Ophthalmol*, 120(9):1136–1141, 2002.

[32] A. L. Burnett, C. J. Lowenstein, D. S. Bredt, T. S. Chang, and S. H. Snyder. Nitric oxide: a physiologic mediator of penile erection. *Science*, 257(5068):401–403, 1992.

[33] J. Caprioli and A. L. Coleman. Intraocular pressure fluctuation: A risk factor for visual field progression at low intraocular pressures in the advanced glaucoma intervention study. *Ophthalmology*, 115(7):1123 – 1129.e3, 2008.

[34] R. J. Casson, G. Chidlow, J. P. M. Wood, J. G. Crowston, and I. Goldberg. Definition of glaucoma: clinical and experimental concepts. *Clin Experiment Ophthalmol*, 40(4):341–349, 2012.

[35] M. Chang, Ch. Yoo, S.-W. Kim, and Y. Y. Kim. Retinal vessel diameter, retinal nerve fiber layer thickness, and intraocular pressure in korean patients with normal-tension glaucoma. *Am J Ophthalmol*, 151(1):100–105, 2011.

[36] B. C. Chauhan, J. Pan, M. L. Archibald, T. L. LeVatte, M. E. M. Kelly, and F. Tremblay. Effect of intraocular pressure on optic disc topography, electroretinography, and axonal loss in a chronic pressure-induced rat model of optic nerve damage. *Investigative Ophthalmology & Visual Science*, 43(9):2969–2976, 09 2002.

[37] C. Y. Cheung, S. Y. Ong, M. K. Ikram, Y. T. Ong, ChP Chen, N. Venketasubramanian, and T. Y. Wong. Retinal vascular fractal dimension is associated with cognitive dysfunction. *Journal of Stroke and Cerebrovascular Diseases*, 23(1):43–50, 2014.

[38] C. Y. Cheung, G. N. Thomas, W. Tay, M. K. Ikram, W. Hsu, M. L. Lee, Q. P. Lau, and T. Y. Wong. Retinal vascular fractal dimension and its relationship with cardiovascular and ocular risk factors. *Am J Ophthalmol*, 154(4):663–674, 2012.

[39] Jr Chylack, L. T., M. C. Leske, D. McCarthy, P. Khu, T. Kashiwagi, and R. Sperduto. Lens opacities classification system ii (locs ii). *Arch Ophthalmol*, 107(7):991–997, 07 1989.

[40] M. Ciancaglini, G. Guerra, L. Agnifili, R. Mastropasqua, V. Fasanella, M. Cinelli, C. Costagliola, and L. Ambrosone. Fractal dimension as a new tool to analyze optic nerve head vasculature in primary open angle glaucoma. *In Vivo*, 29(2):273–279, 2015.

[41] A.F. Clark, S.T. Miggans, K. Wilson, S. Browder, and M.D. McCartney. Cytoskeletal changes in cultured human glaucoma trabecular meshwork cells. *Journal of glaucoma*, 4(3):183–188, June 1995.

[42] A. L. Coleman and St. Miglior. Risk factors for glaucoma onset and progression. *Surv Ophthalmol*, 53(6, Supplement):3–10, 2008.

[43] N. Collignon, W. Dewe, S. Guillaume, and J. Collignon-Brach. Ambulatory blood pressure monitoring in glaucoma patients. the nocturnal systolic dip and its relationship with disease progression. *Int Ophthalmol*, 22(1):19–25, Jan 1998.

[44] R. Connors, P. Boseman, and R. J. Olson. Accuracy and reproducibility of biometry using partial coherence interferometry. *Journal of Cataract & Refractive Surgery*, 28(2):235–238, 2002.

[45] Ch. A. Curcio and K. A. Allen. Topography of ganglion cells in human retina. *The Journal of Comparative Neurology*, 300(1):5–25, 1990.

[46] B. J. Curtin and D. B. Karlin. Axial length measurements and fundus changes of the myopic eye. i. the posterior fundus. *Trans Am Ophthalmol Soc*, 68:312–334, 1970.

[47] F. C. Delori. Noninvasive technique for oximetry of blood in retinal vessels. *Appl Opt*, 27(6):1113–1125, 3 1988.

[48] I. Dielemans, J. R. Vingerling, R. C. W. Wolfs, A. Hofman, D. E. Grobbee, and P. T. V. M. de Jong. The prevalence of primary open-angle glaucoma in a population-based study in the netherlands. *Ophthalmology*, 101(11):1851–1855, 1994.

[49] G. T. Dorner, G. Garhoefer, B. Kiss, E. Polska, K. Polak, Ch. E. Riva, and L. Schmetterer. Nitric oxide regulates retinal vascular tone in humans. *Am J Physiol*, 285(2):631–636, 2003.

[50] W. Drexler, O. Findl, R. Menapace, G. Rainer, C. Vass, Ch. K. Hitzenberger, and A. F. Fercher. Partial coherence interferometry: a novel approach to biometry in cataract surgery. *Am J Ophthalmol*, 126(4):524–534, 1998.

[51] St. Duke-Elder and K. C. Wybar. *System of Ophthalmology: The Anatomy of the Visual System*. Kimpton, 1958.

[52] A. Dziubek, G. Guidoboni, A. Hirani, and A. Harris. Effect of ocular curvature and myopia on retinal blood flow: a theoretical study. *Invest Ophthalmol Vis Sc*, 54(15):1901–1901, 2013.

[53] M. Egger, G. D. Smith, M. Schneider, and C. Minder. Bias in meta-analysis detected by a simple, graphical test. *BMJ*, 315(7109):629–634, sep 1997.

[54] T. S. Eliasdottir, D. Bragason, S. H. Hardarson, G. Kristjansdottir, and E. Stefansson. Venous oxygen saturation is reduced and variable in central retinal vein occlusion. *Graefes Arch Clin Exp Ophthalmol*, Volume 253(Issue 10):1653–1661, First online: 18 November 2014 2015.

[55] P. D. Ellis. Thresholds for interpreting effect sizes, 2009.

[56] T. Eysteinsson, S. H. Hardarson, D. Bragason, and E. Stefansson. Retinal vessel oxygen saturation and vessel diameter in retinitis pigmentosa. *Acta Ophthalmol (Copenh)*, 92(5):449–453, 2014.

[57] L. Fang, M. Baertschi, and M. Mozaffarieh. The effect of flammer-syndrome on retinal venous pressure. *BMC ophthalmology*, 14:121, 10 2014.

[58] R. H. Farkas and C. L. Grosskreutz. Apoptosis, neuroprotection, and retinal ganglion cell death: an overview. *International ophthalmology clinics*, 41(1):111–130, 2001. 00004397-200101000-00011.

[59] A. F. Fercher, W. Drexler, C. K. Hitzenberger, and T. Lasser. Optical coherence tomography - principles and applications. *Rep Prog Phys*, 66(2):239–303, 2003.

[60] A. F. Fercher, Ch. K. Hitzenberger, W. Drexler, G. Kamp, and H. Sattmann. In vivo optical coherence tomography. *Am J Ophthalmol*, 116(1):113–114, 1993.

[61] J. H. Fingert. Primary open-angle glaucoma genes. *Eye*, 25(5):587–595, 2011.

[62] J. Flammer. The vascular concept of glaucoma. *Surv Ophthalmol*, 38, Supplement:3–6, 1994. Ocular Blood Flow in the Progression and Therapy of Glaucoma.

[63] J. Flammer. *Glaucoma, 3rd revised edition*. Hogrefe and Huber, third revised edition, 2006.

[64] J. Flammer. *Glaucoma, 3rd revised edition*. Hogrefe and Huber, third revised edition, 2006.

[65] J. Flammer and M. Mozaffarieh. What is the present pathogenetic concept of glaucomatous optic neuropathy? *Surv Ophthalmol*, 52(6, Supplement):162–173, 2007.

[66] J. Flammer and S. Orguel. Optic nerve blood-flow abnormalities in glaucoma. *Prog Retin Eye Res*, 17(2):267–289, 1998.

[67] J. Flammer, S. Orguel, V. P. Costa, N. Orzalesi, G. K. Krieglstein, L. Metzner Serra, J. P. Renard, and E. Stefansson. The impact of ocular blood flow in glaucoma. *Prog Retin Eye Res*, 21(4):359–393, 2002.

[68] St. S. Franklin, W. Gustin IV, N. D. Wong, M. G. Larson, M. A. Weber, W. B. Kannel, and D. Levy. Hemodynamic patterns of age-related changes in blood pressure: the framingham heart study. *Circulation*, 96(1):308–315, 1997.

[69] L. Franssen, J. E. Coppens, and T. J. T. P. van den Berg. Grading of iris color with an extended photographic reference set. *Journal of Optometry*, 1(1):36–40, 2008.

[70] R. Fuchshofer, U. Welge-Lussen, and E. Luetjen-Drecoll. The effect of tgf-î²2 on human trabecular mesh work extracellular proteolytic system. $ExpEyeRes, 77(6) : 757 - -765, 2003.$

[71] M. L. Gabriele, H. Ishikawa, G. Wollstein, R. A. Bilonick, K. A. Townsend, L. Kagemann, M. Wojtkowski, V. J. Srinivasan, J. G. Fujimoto, J. S. Duker, and J. S. Schuman. Optical coherence tomography scan circle location and mean retinal nerve fiber layer measurement variability. *Invest Ophthalmol Vis Sci*, 49(6):2315–2321, 07 2008.

[72] F. Galassi, A. Sodi, F. Ucci, A. Harris, and H. S. Chung. Ocular haemodynamics in glaucoma associated with high myopia. *Int Ophthalmol*, 22(5):299–305, 1999.

[73] Y. Gao, B. Wan, P. Li, Y. Zhang, and X. Tang. Short-term reproducibility of intraocular pressure and ocular perfusion pressure measurements in chinese volunteers and glaucoma patients. *BMC Ophthalmol*, 16(1):145, Aug 2016.

[74] E. Garcia-Martin, M. Satue, I. Fuertes, S. Otin, R. Alarcia, R. Herrero, M. P. Bambo, J. Fernandez, and L. E. Pablo. Ability and reproducibility of fourierdomain optical coherence tomography to detect retinal nerve fiber layer atrophy in parkinsons disease. *Ophthalmology*, 119(10):2161–2167, 2012.

[75] E. Garcia-Valenzuela, N. G. Anderson, M. Pons, and R. Iezzi. Retinal thickness by oct in subjects with emmetropia, hyperopia and myopia. *Invest Ophthalmol Vis Sci*, 43(13):2574–2574, 2002.

[76] St. K. Gardiner, W. H. Swanson, D. Goren, St. L. Mansberger, and Sh. Demirel. Assessment of the reliability of standard automated perimetry in regions of glaucomatous damage. *Ophthalmology*, 121(7):1359–1369, 2014.

[77] G. Garhoefer, C. Zawinka, H. Resch, K. H. Huemer, L. Schmetterer, and G. T. Dorner. Response of retinal vessel diameters to flicker stimulation in patients with early open angle glaucoma. *J Glaucoma*, 13(4):340–344, 2004.

[78] S. Gehlert, J. Dawczynski, M. Hammer, and J. Strobel. Haemoglobin oxygenation of retinal vessels in branch retinal artery occlusions over time and correlation with clinical outcome. *Klin Monatsbl Augenheilkd*, 227(12):976–980, December 2010.

[79] A. Geirsdottir, S. H. Hardarson, O. B. Olafsdottir, and E. Stefansson. Retinal oxygen metabolism in exudative age-related macular degeneration. *Acta Ophthalmol (Copenh)*, 92(1):27–33, 2014.

[80] A. Geirsdottir, O. Palsson, S. H. Hardarson, O. B. Olafsdottir, J. V. Kristjansdottir, and E. Stefansson. Retinal vessel oxygen saturation in healthy individuals. *Invest Ophthalmol Vis Sci*, 53(9):5433–5442, 2012.

[81] A. A. Ghanem, A. M. Elewa, and L. F. Arafa. Endothelin-1 and nitric oxide levels in patients with glaucoma. *Ophthalmic Res*, 46(2):98–102, 2011.

[82] I. Goharian, S. M. Iverson, R. C. Ruiz, K. Kishor, D. S. Greenfield, and M. Sehi. Reproducibility of retinal oxygen saturation in normal and treated glaucomatous eyes. 99(3):318–322, 2015.

[83] O. Golubnitschaja-Labudova, R. Liu, C. Decker, P. Zhu, I. O. Haefliger, and J. Flammer. Altered gene expression in lymphocytes of patients with normal-tension glaucoma. *Curr Eye Res*, 21(5):867–876, 2000.

[84] M. O. Gordon, J. A. Beiser, J. D. Brandt, and et al. The ocular hypertension treatment study: Baseline factors that predict the onset of primary open-angle glaucoma. *Arch Ophthalmol*, 120(6):714–720, 2002.

[85] M. C. Grieshaber, M. Mozaffarieh, and J. Flammer. What is the link between vascular dysregulation and glaucoma? *Surv Ophthalmol*, 52(6):144–154, 2007.

[86] Collaborative Normal-Tension Glaucoma Study Group et al. Natural history of normal-tension glaucoma. *Ophthalmology*, 108(2):247–253, 2001.

[87] K. Gugleta, A. Kochkorov, N. Waldmann, A. Polunina, R. Katamay, J. Flammer, and S. Orguel. Dynamics of retinal vessel response to flicker light in glaucoma patients and ocular hypertensives. *Graefes Arch Clin Exp Ophthalmol*, 250(4):589–594, 2012.

[88] K. Gugleta, N. Waldmann, A. Polunina, A. Kochkorov, R. Katamay, J. Flammer, and S. Orguel. Retinal neurovascular coupling in patients with glaucoma and ocular hypertension and its association with the level of glaucomatous damage. *Graefes Arch Clin Exp Ophthalmol*, 251(6):1577–1585, 2013.

[89] L. Guo, S. E. Moss, R. A. Alexander, R. R. Ali, F. W. Fitzke, and M. F. Cordeiro. Retinal ganglion cell apoptosis in glaucoma is related to intraocular pressure and iop induced effects on extracellular matrix. *Invest Ophthalmol Vis Sci*, 46(1):175–182, 2005.

[90] D. Gupta and S. Asrani. Macular thickness analysis for glaucoma diagnosis and management. *Taiwan Journal of Ophthalmology*, 6(1):3–7, 2016.

[91] N. Gupta and R. N. Weinreb. New definitions of glaucoma. *Curr Opin Ophthalmol*, 8(2):38–41, 1997.

[92] N. Hammel, A. Belghith, R. N. Weinreb, F. A. Medeiros, N. Mendoza, and L. M. Zangwill. Comparing the rates of retinal nerve fiber layer and ganglion cell inner plexiform layer loss in healthy eyes and in glaucoma eyes. *Am J Ophthalmol*, 178:38–50, 2017.

[93] M. Hammer, T. Heller, S. Jentsch, J. Dawczynski, D. Schweitzer, S. Peters, K.-U. Schmidtke, and U.-A. Mueller. Retinal vessel oxygen saturation under flicker light stimulation in patients with nonproliferative diabetic retinopathy. *Invest Ophthalmol Vis Sci*, 53(7):4063–4068, 2012.

[94] M. Hammer, D. Schweitzer, L. Leistritz, M. Scibor, K.-H. Donnerhacke, and J. Strobel. Imaging spectroscopy of the human ocular fundus in vivo. *J Biomed Opt*, 2(4):418–425, 1997.

[95] M. Hammer, W. Vilser, T. Riemer, F. Liemt, S. Jentsch, J. Dawczynski, and D. Schweitzer. Retinal venous oxygen saturation increases by flicker light stimulation. *Invest Ophthalmol Vis Sci*, 52(1):274–277, 2011.

[96] M. Hammer, W. Vilser, T. Riemer, A. Mandecka, D. Schweitzer, U. Kuehn, J. Dawczynski, F. Liemt, and J. Strobel. Diabetic patients with retinopathy show increased retinal venous oxygen saturation. *Graefes Arch Clin Exp Ophthalmol*, 247(8):1025–1030, 2009.

[97] M. Hammer, W. Vilser, T. Riemer, and D. Schweitzer. Retinal vessel oximetry-calibration, compensation for vessel diameter and fundus pigmentation, and reproducibility. *J Biomed Opt*, 13(5):054015, 2008.

[98] S. H. Hardarson, A. Harris, R. A. Karlsson, G. H. Halldorsson, L. Kagemann, E. Rechtman, G. M. Zoega, T. Eysteinsson, J. A. Benediktsson, A. Thorsteinsson, P. Jensen, J. Beach, and E. E. Stefansson. Automatic retinal oximetry. *Invest Ophthalmol Vis Sci*, 47(11):5011–5016, 2006.

[99] S. H. Hardarson and E. Stefansson. Oxygen saturation in central retinal vein occlusion. *Am J Ophthalmol*, 150(6):871–875, 2010.

[100] S. H. Hardarson and E. Stefansson. Oxygen saturation in branch retinal vein occlusion. *Acta Ophthalmol (Copenh)*, 90(5):466–470, 2012.

[101] S. H. Hardarson and E. Stefansson. Retinal oxygen saturation is altered in diabetic retinopathy. 96(4):560–563, 2012.

[102] N. Harizman, C. Oliveira, A. Chiang, and et al. The isnt rule and differentiation of normal from glaucomatous eyes. *Arch Ophthalmol*, 124(11):1579–1583, 2006.

[103] T. R. Hartley, B. H. Sung, G. A. Pincomb, Th. L. Whitsett, M. F. Wilson, and W. R. Lovallo. Hypertension risk status and effect of caffeine on blood pressure. *Hypertension*, 36 1:137–41, 2000.

[104] R. S. Harwerth and H. A. Quigley. Visual field defects and retinal ganglion cell losses in patients with glaucoma. *Arch Ophthalmol*, 124(6):853–859, 2006.

[105] H. Hashemi, M. Khabazkhoob, M. Miraftab, M. H. Emamian, M. Shariati, T. Abdolahinia, and A. Fotouhi. The distribution of axial length, anterior chamber depth, lens thickness, and vitreous chamber depth in an adult population of shahroud, iran. *BMC Ophthalmol*, 12(1):1–8, 2012.

[106] S. S. Hayreh. The blood supply of the optic nerve head and the evaluation of it - myth and reality. *Prog Retin Eye Res*, 20(5):563–593, 2001.

[107] S. S. Hayreh. Pathophysiology of glaucomatous optic neuropathy: role of optic nerve head vascular insufficiency. *Journal of Current Glaucoma Practice*, 2(1):6–17, 2008.

[108] S. S. Hayreh. *Structure of the optic nerve*, pages 7–34. Springer Berlin Heidelberg, Berlin, Heidelberg, 2011.

[109] A. Heijl and V. M. Patell. *Essential Perimetry (Third edition)*. Carl Zeiss Meditec, Inc., third edition, 2002.

[110] A. Heijl, V. M. Patella, and B. Bengtsson. *Effective Perimetry*, volume P/N 2660021148492. Carl Zeiss Meditec, Inc., fourth edition edition, 2012.

[111] R. Heitmar and A. Attardo. The influence of simulated cataract on retinal vessel oximetry measurements. *Acta Ophthalmol (Copenh)*, 94(1):48–55, 2016.

[112] R. Heitmar, A. D. Blann, R. P. Cubbidge, G. Y. H. Lip, and D. Gherghel. Continuous retinal vessel diameter measurements: the future in retinal vessel assessment? *Invest Ophthalmol Vis Sci*, 51(11):5833–5839, 2010.

[113] R. Heitmar and R. P. Cubbidge. The impact of flash intensity on retinal vessel oxygen saturation measurements using dual wavelength oximetry. *Invest Ophthalmol Vis Sci*, 54(4):2807–2811, 2013.

[114] R. Heitmar, R. P. Cubbidge, G. Y. H. Lip, D. Gherghel, and A. D. Blann. Altered blood vessel responses in the eye and finger in coronary artery disease. *Invest Ophthalmol Vis Sci*, 52(9):6199–6205, 2011.

[115] R. Heitmar and S. Safeen. Regional differences in oxygen saturation in retinal arterioles and venules. *Graefes Arch Clin Exp Ophthalmol*, 250(10):1429–1434, 2012.

[116] D. B. Henson, Sh. Chaudry, P. H. Artes, E. B. Faragher, and A. Ansons. Response variability in the visual field: comparison of optic neuritis, glaucoma, ocular hypertension, and normal eyes. *Invest Ophthalmol Vis Sci*, 41(2):417–421, 2000.

[117] J. B. Hickam and R. Frayser. Studies of the retinal circulation in man observations on vessel diameter, arteriovenous oxygen difference, and mean circulation time. *Circulation*, 33(2):302–316, 1966.

[118] J. B. Hickam, H. O. Sieker, and R. Frayser. Studies of retinal circulation and av oxygen difference in man. *Trans Am Clin Climatol Assoc*, 71:34–44, 1960.

[119] J. P. T. Higgins and S. G. Thompson. Quantifying heterogeneity in a meta analysis. *Stat Med*, 21(11):1539–1558, 2002.

[120] J. P. T. Higgins, S. G. Thompson, J. J. Deeks, and D. G. Altman. Measuring inconsistency in meta-analyses. *BMJ*, 327(7414):557–560, 2003.

[121] C. K. Hitzenberger. Optical measurement of the axial eye length by laser doppler interferometry. *Invest Ophthalmol Vis Sci*, 32(3):616–624, 1991.

[122] C. K. Hitzenberger, W. Drexler, C. Dolezal, F. Skorpik, M. Juchem, A. F. Fercher, and H. D. Gnad. Measurement of the axial length of cataract eyes by laser doppler interferometry. *Invest Ophthalmol Vis Sci*, 34(6):1886–1893, 1993.

[123] E. M. Hoffmann, F. A. Medeiros, P. A. Sample, C. Boden, Ch. Bowd, R. R. Bourne, L. M. Zangwill, and R. N. Weinreb. Relationship between patterns of visual field loss and retinal nerve fiber layer thickness measurements. *Am J Ophthalmol*, 141(3):463–471, 2006.

[124] S.-T. Hoh, M. C. C. Lim, St. K. L. Seah, A. T. H. Lim, S.-J. Chew, P. J. Foster, and T. Aung. Peripapillary retinal nerve fiber layer thickness variations with myopia. *Ophthalmology*, 113(5):773–777, 2006.

[125] B. A. Holden, T. R. Fricke, D. A. Wilson, M. Jong, K. S. Naidoo, P. Sankaridurg, T. Y. Wong, T. J. Naduvilath, and S. Resnikoff. Global prevalence of myopia and high myopia and temporal trends from 2000 through 2050. *Ophthalmology*, 123(5):1036–1042, 2016.

[126] W. F. Hoyt and O. Luis. Visual fiber anatomy in the infrageniculate pathway of the primate: Uncrossed and crossed retinal quadrant fiber projections studied with nauta silver stain. *Arch Ophthalmol*, 68(1):94–106, 1962.

[127] D. Huang, E. A. Swanson, C. P. Lin, J. S. Schuman, W. G. Stinson, W. Chang, M. R. Hee, T. Flotte, K. Gregory, C. A. Puliafito, and al. et. Optical coherence tomography. *Science*, 254(5035):1178–1181, 1991.

[128] L. D. Hubbard, R. J. Brothers, W. N. King, L. X. Clegg, R. Klein, L. S. Cooper, A. R. Sharrett, M. D. Davis, and J. Cai. Methods for evaluation of retinal microvascular abnormalities associated with hypertension , sclerosis in the atherosclerosis risk in communities study. *Ophthalmology*, 106(12):2269–2280, 1999.

[129] Eduard Jaeger. *Ueber glaucom und seine Heilung durch Iridectomie*. Druck von C. Gerold's Sohn, 1858.

[130] B. Jani and C. Rajkumar. Ageing and vascular ageing. *Postgrad Med J*, 82(968):357–362, 2006.

[131] P. D. Jani, J.-C. Mwanza, K. B. Billow, A. M. Waters, S. Moyer, and S. Garg. Normative values and predictors of retinal oxygen saturation. *Retina*, 34(2):394–401, 2014.

[132] S. W. Jin and S. Y. Noh. Long-term clinical course of normal-tension glaucoma: 20 years of experience. *Journal of Ophthalmology*, 2017:6, 2017.

[133] J. B. Jonas, T. Aung, R. R. Bourne, A. M. Bron, R. Ritch, and S. Panda-Jonas. Glaucoma. *The Lancet*, 390(10108):2183–2193, 2017.

[134] J. B. Jonas, G. C. Gusek, and G. O. Naumann. Optic disc, cup and neuroretinal rim size, configuration and correlations in normal eyes. *Invest Ophthalmol Vis Sci*, 29(7):1151–1158, 07 1988.

[135] J. B. Jonas, A. M. Schmidt, J. A. Mueller-Bergh, U. M. Schloetzer-Schrehardt, and G. O. Naumann. Human optic nerve fiber count and optic disc size. *Invest Ophthalmol Vis Sci*, 33(6):2012–2018, 1992.

[136] J. B. Jonas, N. Wang, and V. Nangia. Ocular perfusion pressure vs estimated translamina cribrosa pressure difference in glaucoma: The central india eye and medical study (an american ophthalmological society thesis). *Trans Am Ophthalmol Soc*, 113:1–13, 2015.

[137] J. B. Jonas, N. Wang, and D. Yang. Translamina cribrosa pressure difference as potential element in the pathogenesis of glaucomatous optic neuropathy. *Asia Pac J Ophthalmol*, 5(1):5–10, 2016.

[138] Ch. M. Jorgensen and T. Bek. Increasing oxygen saturation in larger retinal vessels after photocoagulation for diabetic retinopathyoxygen saturation in diabetic retinopathy. *Invest Ophthalmol Vis Sci*, 55(8):5365–5369, 2014.

[139] Ch. M. Jorgensen, S. H. Hardarson, and T. Bek. The oxygen saturation in retinal vessels from diabetic patients depends on the severity and type of vision-threatening retinopathy. *Acta Ophthalmol (Copenh)*, 92(1):34–39, 2014.

[140] Sh. H. Kang, S. W. Hong, S. K. Im, S. H. Lee, and M. D. Ahn. Effect of myopia on the thickness of the retinal nerve fiber layer measured by cirrus hd optical coherence tomography. *Invest Ophthalmol Vis Sci*, 51(8):4075–4083, 2010.

[141] J. Katz, A. Sommer, D. E. Gaasterland, and D. R. Anderson. Comparison of analytic algorithms for detecting glaucomatous visual field loss. *Arch Ophthalmol*, 109(12):1684–1689, 1991.

[142] R. Kawasaki, J. J. Wang, E. Rochtchina, A. J. Lee, T. Y. Wong, and P. Mitchell. Retinal vessel caliber is associated with the 10-year incidence of glaucoma: the blue mountains eye study. *Ophthalmology*, 120(1):84–90, 2013.

[143] B. Khoobehi, K. Firn, H. Thompson, M. Reinoso, and J. Beach. Retinal arterial and venous oxygen saturation is altered in diabetic patients. *Invest Ophthalmol Vis Sci*, 54(10):7103–7106, 2013.

[144] N. R. Kim, E. S. Lee, G. J. Seong, S. Y. Kang, J. H. Kim, S. Hong, and Ch. Y. Kim. Comparing the ganglion cell complex and retinal nerve fibre layer measurements by fourier domain oct to detect glaucoma in high myopia. *Br J Ophthalmol*, 2010:7, 2010.

[145] N. R. Kim, E. S. Lee, G. J. Seong, J. H. Kim, H. G. An, and Ch. Y. Kim. Structure function relationship and diagnostic value of macular ganglion cell complex measurement using fourier-domain oct in glaucoma. *Invest Ophthalmol Vis Sci*, 51(9):4646–4651, 2010.

[146] S. M. Kim, J. S. Lee, J. Lee, J. K. Na, J. H. Han, D. K. Yoon, S. H. Baik, D. S. Choi, and K. M. Choi. Prevalence of diabetes and impaired fasting glucose in korea. *Diabetes Care*, 29(2):226–231, 2006.

[147] O. N. Klefter, A. O. Lauritsen, and M. Larsen. Retinal hemodynamic oxygen reactivity assessed by perfusion velocity, blood oximetry and vessel diameter measurements. *Acta Ophthalmol (Copenh)*, 93(3):232–241, 2015.

[148] O. N. Klefter, T. Vilsboll, F. K. Knop, and M. Larsen. Retinal vascular and structural dynamics during acute hyperglycaemia. *Acta Ophthalmol (Copenh)*, 93(8):697–705, 2015.

[149] B. E. K. Klein, R. Klein, W. E. Sponsel, T. Franke, L. B. Cantor, J. Martone, and M. J. Menage. Prevalence of glaucoma. *Ophthalmology*, 99(10):1499–1504, 1992.

[150] M. Kneser, Th.s Kohlmann, J. Pokorny, and F. Tost. Age related decline of microvascular regulation measured in healthy individuals by retinal dynamic vessel analysis. *Med Sci Monit*, 15(8):436–441, 2009. PMI: 19644422.

[151] O. J. Knight, C. A. Girkin, D. L. Budenz, M. K. Durbin, W. J. Feuer, and for the Cirrus O. C. T. Normative Database Study Group. Effect of race, age, and axial length on optic nerve head parameters and retinal nerve fiber layer thickness measured by cirrus hd-oct. *Arch Ophthalmol*, 130(3):312–318, 2012.

[152] M. D. Knudtson, K. E. Lee, L. D. Hubbard, T. Y. Wong, R. Klein, and B. E. K. Klein. Revised formulas for summarizing retinal vessel diameters. *Curr Eye Res*, 27(3):143–149, 2003.

[153] P. Kolar. Definition and classification of retinal vein occlusion. *International Journal of Ophthalmic Research*, 2(2):124–129, 2016.

[154] H. Kolb. Morphology and circuitry of ganglion cells by helga kolb, 1994.

[155] G. Koller, A. Haas, M. Zulauf, F. Koerner, and D. Mojon. Influence of refractive correction on peripheral visual field in static perimetry. *Graefes Arch Clin Exp Ophthalmol*, 239(10):759–762, 2001.

[156] J. Kotowski, L. S. Folio, G. Wollstein, H. Ishikawa, Y. Ling, R. A. Bilonick, L. Kagemann, and J. S. Schuman. Glaucoma discrimination of segmented cirrus spectral domain optical coherence tomography (sd-oct) macular scans. *Br J Ophthalmol*, 96(11):1420–1425, 2012.

[157] A. A. Kuzin, R. Varma, H. S. Reddy, M. Torres, and S. P. Azen. Ocular biometry and open angle glaucoma: The los angeles latino eye study. *Ophthalmology*, 117(9):1713–1719, 2010.

[158] C. La Spina, F. Corvi, F. Bandello, and G. Querques. Static characteristics and dynamic functionality of retinal vessels in longer eyes with or without pathologic myopia. *Graefes Arch Clin Exp Ophthalmol*, 254(5):827–834, 2016.

[159] G. Landini, P. I. Murray, and G. P. Misson. Local connected fractal dimensions and lacunarity analyses of 60 degrees fluorescein angiograms. *Invest Ophthalmol Vis Sci*, 36(13):2749–2755, 1995.

[160] M. Lasta, St. Palkovits, A. Boltz, D. Schmidl, S. Kaya, A. P. Cherecheanu, G. Garhoefer, and L. Schmetterer. Reproducibility of retinal vessel oxygen saturation measurements in healthy young subjects. *Acta Ophthalmol (Copenh)*, 90(8):616–620, 2012.

[161] S. E. LeBlanc, M. Atanya, K. Burns, and R. Munger. Quantitative impact of small angle forward scatter on whole blood oximetry using a beer–lambert absorbance model. *Analyst*, 136(8):1637–1643, 2011.

[162] J. Lee, N. R. Kim, H. Kim, J. Han, E. S. Lee, G. J. Seong, and C. Y. Kim. Negative refraction power causes underestimation of peripapillary retinal nerve fibre layer thickness in spectral-domain optical coherence tomography. *Br J Ophthalmol*, 95(9):1284–1289, 2011.

[163] M. T. Leite, H. L. Rao, R. N. Weinreb, L. M. Zangwill, Ch. Bowd, P. A. Sample, A. Tafreshi, and F. A. Medeiros. Agreement among spectral domain optical coherence tomography instruments for assessing retinal nerve fiber layer thickness. *Am J Ophthalmol*, 151(1):85–92, 2011.

[164] M. T. Leite, H. L. Rao, L. M. Zangwill, R. N. Weinreb, and F. A. Medeiros. Comparison of the diagnostic accuracies of the spectralis, cirrus, and rtvue optical coherence tomography devices in glaucoma. *Ophthalmology*, 118(7):1334–1339, 2011.

[165] A. Leske, M. C.and Heijl, L. Hyman, B. Bengtsson, L. Dong, and Z. Yang. Predictors of long-term progression in the early manifest glaucoma trial. *Ophthalmology*, 114(11):1965 – 1972, 2007.

[166] M. C. Leske, A. S. Connell, A. P. Schachat, and L. Hyman. The barbados eye study: Prevalence of open angle glaucoma. *Arch Ophthalmol*, 112(6):821–829, 1994.

[167] M. C. Leske, S.-Y. Wu, A. Hennis, R. Honkanen, and B. Nemesure. Risk factors for incident open angle glaucoma: The barbados eye studies. *Ophthalmology*, 115(1):85 – 93, 2008.

[168] M. C. Leske, S.-Y. Wu, B. Nemesure, A. Hennis, and Barbados Eye Studies Group. Incident open-angle glaucoma and blood pressure. *Arch Ophthalmol*, 120(7):954–959, 2002.

[169] Ch. K.-S. Leung, C. Y.-l. Cheung, R. N. Weinreb, Q. Qiu, S. Liu, H. Li, G. Xu, N. Fan, L. Huang, Chi-Pui Pang, D. Shun, and C. Lam. Retinal nerve fiber layer imaging with spectral domain optical coherence tomography: a variability and diagnostic performance study. *Ophthalmology*, 116(7):1257–1263, 2009.

[170] Ch. K.-S. Leung, Sh. Mohamed, K. S. Leung, C. Y.-L. Cheung, S. L. Chan, D. K. Cheng, A. K. Lee, G. Y. Leung, S. K. Rao, and D. Sh. Ch. Lam. Retinal nerve fiber layer measurements in myopia: an optical coherence tomography study. *Invest Ophthalmol Vis Sci*, 47(12):5171–5176, 2006.

[171] Ch. K.-S. Leung, M. Yu, R. N. Weinreb, C. Ye, Sh. Liu, G. Lai, and D. S. C. Lam. Retinal nerve fiber layer imaging with spectral domain optical coherence tomography: a prospective analysis of age-related loss. *Ophthalmology*, 119(4):731–737, 2012.

[172] Christopher K. S. Leung, Cong Ye, Robert N. Weinreb, Marco Yu, Gilda Lai, and Dennis S. Lam. Impact of age-related change of retinal nerve fiber layer and macular thicknesses on evaluation of glaucoma progression. *Ophthalmology*, 120(12):2485–2492, 2013.

[173] H. Levkovitch-Verbin, H. A. Quigley, K. R. G. Martin, D. Valenta, L. A. Baumrind, and M. E. Pease. Translimbal laser photocoagulation to the trabecular meshwork as a model of glaucoma in rats. *Investigative Ophthalmology & Visual Science*, 43(2):402–410, 02 2002.

[174] M. Li, Y. Yang, H. Jiang, G. Gregori, L. Roisman, F. Zheng, B. Ke, D. Qu, and J. Wang. Retinal microvascular network and microcirculation assessments in high myopia. *Am J Ophthalmol*, 174:56–67, 2017.

[175] Y. B. Liang, Q. Zhou, D. S. Friedman, L.X. Guo, L. P. Sun, Q.F. Zong, X. D. Yang, and N. L. Wang. A population-based assessment of 24-hour ocular perfusion pressure among patients with primary open angle glaucoma: The handan eye study. *Asia Pac J Ophthalmol*, 5(2):127–132, 2016.

[176] G. Liew, J. J. Wang, N. Cheung, Y. P. Zhang, W. Hsu, M. L. Lee, P. Mitchell, G. Tikellis, B. Taylor, and T. Y. Wong. The retinal vasculature as a fractal: methodology, reliability, and relationship to blood pressure. *Ophthalmology*, 115(11):1951–1956, 2008.

[177] L.-L. Lin, Y.-M. Dong, Y. Zong, Q.-Sh. Zheng, Y. Fu, Y.-G. Yuan, X. Huang, G. Qian, and Q.-Y. Gao. Study of retinal vessel oxygen saturation in ischemic and non-ischemic branch retinal vein occlusion. *Int J Ophthalmol*, 9(1):99–107, 2016.

[178] R. A. Linsenmeier and H. F. Zhang. Retinal oxygen: From animals to humans. *Prog Retin Eye Res*, page 105, 2017.

[179] St. A. Lipton. Neuronal protection and destruction by no. *Cell death and differentiation*, 6(10):943, 1999.

[180] J. H. K. Liu, A. J. Sit, and R. N. Weinreb. Variation of 24-hour intraocular pressure in healthy individuals: Right eye versus left eye. *Ophthalmology*, 112(10):1670 – 1675, 2005.

[181] J. H. K. Liu, X. Zhang, D. F. Kripke, and R. N. Weinreb. Twenty-four-hour intraocular pressure pattern associated with early glaucomatous changes. *Invest Ophthalmol Vis Sci*, 44(4):1586–1590, 04 2003.

[182] R. E. K. Man, R. Kawasaki, Zh. Wu, Ch. D. Luu, J. J. Wang, T. Y. Wong, and E. L. Lamoureux. Reliability and reproducibility of retinal oxygen saturation measurements using a predefined peri-papillary annulus. *Acta Ophthalmol (Copenh)*, 91(8):590–594, 2013.

[183] R. E. K. Man, E. L. Lamoureux, Y. Taouk, J. Xie, M. B. Sasongko, W. J. Best, J. E. Noonan, R. Kawasaki, J. J. Wang, and C. D. Luu. Axial length, retinal function, and oxygen consumption: A potential mechanism for a lower risk of diabetic retinopathy in longer eyesaxial length and oxygen consumption. *Invest Ophthalmol Vis Sci*, 54(12):7691–7698, 2013.

[184] R. E. K. Man, M. B. Sasongko, R. Kawasaki, J. E. Noonan, T. Ch. Sh. Lo, Ch. D. Luu, and J. J. Lamoureux, E. L.and Wang. Associations of retinal oximetry in healthy young adultsoxygen saturation of retinal vasculature. *Invest Ophthalmol Vis Sci*, 55(3):1763–1769, 2014.

[185] Michael W. Marcus, Margriet M. de Vries, Francisco G. Junoy Montolio, and Nomdo M. Jansonius. Myopia as a risk factor for open-angle glaucoma: a systematic review and meta-analysis. *Ophthalmology*, 118(10):1989–1994, 2011.

[186] P. Massin, E. Vicaut, B. Haouchine, A. Erginay, M. Paques, and A. Gaudric. Reproducibility of retinal mapping using optical coherence tomography. *Arch Ophthalmol*, 119(8):1135–1142, 2001.

[187] B. R. Masters. Fractal analysis of the vascular tree in the human retina. *Annu Rev Biomed Eng*, 6(1):427–452, 2004. PMID: 15255776.

[188] S. E. Maxwell. Sample size and multiple regression analysis. *Psychol Methods*, 5(4):434–458, 2000.

[189] K. McGeechan, G. Liew, P. Macaskill, L. Irwig, R. Klein, B. E. K. Klein, J. J. Wang, P. Mitchell, J. R. Vingerling, T. V. M. Paulus, et al. Meta-analysis: retinal vessel caliber and risk for coronary heart disease. *Ann Intern Med*, 151(6):404–413, 2009.

[190] F. A. Medeiros, R. Lisboa, R. N. Weinreb, J. M. Liebmann, Ch. Girkin, and L. M. Zangwill. Retinal ganglion cell count estimates associated with early development of visual field defects in glaucoma. *Ophthalmology*, 120(4):736–744, 2013.

[191] Carl Zeiss Meditec. *Cirrus HD-OCT Model 4000*, b2016.

[192] F. Memarzadeh, M. Ying-Lai, J. Chung, St. P. Azen, and R. Varma. Blood pressure, perfusion pressure, and open-angle glaucoma: The los angeles latino eye study. *Invest Ophthalmol Vis Sci*, 51(6):2872–2877, 2010.

[193] G. Michelson, M. J. Langhans, and M. J. M. Groh. Perfusion of the juxtapapillary retina and the neuroretinal rim area in primary open angle glaucoma. *J Glaucoma*, 5(2):91–98, 1996.

[194] G. Michelson and M. Scibor. Intravascular oxygen saturation in retinal vessels in normal subjects and open-angle glaucoma subjects. *Acta Ophthalmol Scand*, 84(3):289–295, 2006.

[195] M. Mikuni, K. Ishii, and R. Makabe. On the diameter of the optic nerve papilla in the japanese. *Klin Monatsbl Augenheilkd*, 136:544–557, 1960.

[196] H. Mitchell, P.and Leung, J. J. Wang, E. Rochtchina, A. J. Lee, T. Y. Wong, and R. Klein. Retinal vessel diameter and open-angle glaucoma the blue mountains eye study. *Ophthalmology*, 112(2):245–250, 2005.

[197] P. Mitchell, F. Hourihan, J. Sandbach, and J. J. Wang. The relationship between glaucoma and myopia: The blue mountains eye study. *Ophthalmology*, 106(10):2010–2015, 1999.

[198] P. Mitchell, A. J. Lee, E. Rochtchina, and J. J. Wang. Open-angle glaucoma and systemic hypertension: The blue mountains eye study. *J Glaucoma*, 13(4):319–326, 2004.

[199] P. Mitchell, W. Smith, K. Attebo, and P. R. Healey. Prevalence of open angle glaucoma in australia. *Ophthalmology*, 103(10):1661–1669, 1996.

[200] S. Moghimi, H. Hosseini, J. Riddle, G. Y. Lee, E. Bitrian, J. A. Giaconi, J. Caprioli, and K. Nouri-Mahdavi. Measurement of optic disc size and rim area with spectral-domain oct and scanning laser ophthalmoscopy. *Invest Ophthalmol Vis Sci*, 53(8):4519–4530, 2012.

[201] S. Moghimi, L. M. Zangwill, R. C. Penteado, K. Hasenstab, E. Ghahari, H. Hou, M. Christopher, A. Yarmohammadi, P. I. C. Manalastas, T. Shoji, Ch. Bowd, and R. N. Weinreb. Macular and optic nerve head vessel density and progressive retinal nerve fiber layer loss in glaucoma. *Ophthalmology*, 125(11):1720–1728, 2018.

[202] A. Mohan, S. Dabir, N. K. Yadav, M. Kummelil, R. S. Kumar, and R. Shetty. Normative database of retinal oximetry in asian indian eyes. *PLoS ONE*, 10(4):1–8, 2015.

[203] F. G. J. Montolio, Ch. Wesselink, M. Gordijn, and N. M. Jansonius. Factors that influence standard automated perimetry test results in glaucoma: test reliability, technician experience, time of day, and seasonfactors that influence perimetry test results. *Invest Ophthalmol Vis Sci*, 53(11):7010–7017, 2012.

[204] D. J. Mordant, I. Al-Abboud, G. Muyo, A. Gorman, A. R. Harvey, and A. I. McNaught. Oxygen saturation measurements of the retinal vasculature in treated asymmetrical primary open-angle glaucoma using hyperspectral imaging. *Eye*, 28(10):1190–1200, 2014.

[205] I. Morgan and K. Rose. How genetic is school myopia? *Prog Retin Eye Res*, 24(1):1–38, 2005.

[206] I. G. Morgan, K. Ohno-Matsui, and S.-M. Saw. Myopia. *The Lancet*, 379(9827):1739–1748, 2012.

[207] J. C. Morrison, C. G. Moore, L. M. H. Deppmeier, B. G. Gold, Ch. K. Meshul, and E. C. Johnson. A rat model of chronic pressure-induced optic nerve damage. *Experimental eye research*, 64(1):85–96, 1997.

[208] M. Motallebipour, A. Rada-Iglesias, M. Jansson, and C. Wadelius. The promoter of inducible nitric oxide synthase implicated in glaucoma based on genetic analysis and nuclear factor binding. *Mol Vis*, 11:950–957, 2005.

[209] S. Mroczkowska, A. Benavente-Perez, A. Negi, V. Sung, S. R. Patel, and D. Gherghel. Primary open-angle glaucoma vs normal-tension glaucoma: The vascular perspective. *JAMA Ophthalmology*, 131(1):36–43, 2013.

[210] C. D. Murray. The physiological principle of minimum work. *Proceedings of the National Academy of Sciences*, 12(3):207–214, 1926.

[211] J.-C. Mwanza, . K. Durbin, D. L. Budenz, Ch. A. Girkin, Ch. K. Leung, J. M. Liebmann, J. H. Peace, J. S. Werner, and G. Wollstein. Profile and predictors of normal ganglion cell inner plexiform layer thickness measured with frequency-domain optical coherence tomography. *Invest Ophthalmol Vis Sci*, 52(11):7872–7879, 2011.

[212] J.-C. Mwanza, M. K. Durbin, D. L. Budenz, F. E. Sayyad, R. T. Chang, D. G. Neelakantan, A.and Godfrey, R. Carter, and A. S. Crandall. Glaucoma diagnostic accuracy of ganglion cell inner plexiform layer thickness: comparison with nerve fiber layer and optic nerve head. *Ophthalmology*, 119(6):1151–1158, 2012.

[213] J.-C. Mwanza, J. D. Oakley, D. L. Budenz, and D. R. Anderson. Ability of cirrus hd oct optic nerve head parameters to discriminate normal from glaucomatous eyes. *Ophthalmology*, 118(2):241–248, 2011.

[214] J.-C. Mwanza, J. D. Oakley, D. L. Budenz, R. T. Chang, O. J. Knight, and W. J. Feuer. Macular ganglion cell inner plexiform layer: automated detection and thickness reproducibility with spectral domainâoptical coherence tomography in glaucoma. *Invest Ophthalmol Vis Sci*, 52(11):8323–8329, 2011.

[215] E. Nagel and W. Vilser. Autoregulative behavior of retinal arteries and veins during changes of perfusion pressure: a clinical study. *Graefes Arch Clin Exp Ophthalmol*, 242(1):13–17, 2004.

[216] E. Nagel and W. Vilser. Flicker observation light induces diameter response in retinal arterioles: a clinical methodological study. *Br J Ophthalmol*, 88(1):54–56, 2004.

[217] E. Nagel, W. Vilser, A. Fink, and T. Riemer. Variance of retinal vessel diameter response to flicker light. *Der Ophthalmologe*, 103(2):114–119, 2006.

[218] W. Nagel, E.and Vilser and I. Lanzl. Age, blood pressure, and vessel diameter as factors influencing the arterial retinal flicker response. *Invest Ophthalmol Vis Sci*, 45(5):1486–1492, 2004.

[219] A. H. Neufeld. Nitric oxide: a potential mediator of retinal ganglion cell damage in glaucoma. *Surv Ophthalmol*, 43:129–135, 1999.

[220] Th. T. Nguyen, A. J. Kreis, R. Kawasaki, J. J. Wang, B.-U. Seifert, W. Vilser, E. Nagel, and T. Y. Wong. Reproducibility of the retinal vascular response to flicker light in asians. *Curr Eye Res*, 34(12):1082–1088, 2009.

[221] D. L. Nickla and C. F. Wildsoet. The effect of the nonspecific nitric oxide synthase inhibitor ng-nitro-l-arginine methyl ester on the choroidal compensatory response to myopic defocus in chickens. *Optom Vis Sci*, 81(2):111–118, 2004. 1040-5488/04/8102-0111/0.

[222] K. Nouri-Mahdavi, D. Hoffman, D. P. Tannenbaum, S. K. Law, and J. Caprioli. Identifying early glaucoma with optical coherence tomography. *Am J Ophthalmol*, 137(2):228–235, 2004.

[223] K. Nouri-Mahdavi, S. Nowroozizadeh, N. Nassiri, N. Cirineo, Sh. Knipping, J. Giaconi, and J. Caprioli. Macular ganglion cell/inner plexiform layer measurements by spectral domain optical coherence tomography for detection of early glaucoma and comparison to retinal nerve fiber layer measurements. *Am J Ophthalmol*, 156(6):1297–1307, 2013.

[224] S. Nowroozizadeh, N. Cirineo, N. Amini, S. Knipping, T. Chang, T. Chou, J. Caprioli, and K. Nouri-Mahdavi. Influence of correction of ocular magnification on spectral-domain oct- retinal nerve fiber layer measurement variability and performance-influence. *Invest Ophthalmol Vis Sci*, 55(6):3439–3446, 2014.

[225] R. A. O Connell, A. J. Anderson, S. L. Hosking, A. H. Batcha, and B. V. Bui. Test-retest reliability of retinal oxygen saturation measurement. *Optom Vis Sci*, 91(6):608–614, 2014.

[226] Y. Oku, H. Oku, M. Park, K. Hayashi, H. Takahashi, T. Shouji, and E. Chihara. Long axial length as risk factor for normal tension glaucoma. *Graefes Arch Clin Exp Ophthalmol*, 247(6):781–787, 2009.

[227] O. B. Olafsdottir, S. H. Hardarson, M. S. Gottfredsdottir, A. Harris, and E. Stefansson. Retinal oximetry in primary open angle glaucoma. *Invest Ophthalmol Vis Sci*, 52(9):6409–6413, 2011.

[228] O. B. Olafsdottir, E. Vandewalle, L. Abegao Pinto, A. Geirsdottir, E. De Clerck, P. Stalmans, M. S. Gottfredsdottir, J. V. Kristjansdottir, J. Van Calster, Th. Zeyen, et al. Retinal oxygen metabolism in healthy subjects and glaucoma patients. *Br J Ophthalmol*, 98(3):329–333, 2014.

[229] A. Oli and D. Joshi. Can ganglion cell complex assessment on cirrus hd oct aid in detection of early glaucoma? *Saudi Journal of Ophthalmology*, 29(3):201–204, 2015.

[230] S. Orguel, K. Gugleta, and J. Flammer. Physiology of perfusion as it relates to the optic nerve head. *Survey of ophthalmology*, 43:S17–S26, 1999.

[231] N. N. Osborne, J. Melena, G. Childow, and J. P. Wood. A hypothesis to explain ganglion cell death caused by vascular insults at the optic nerve head: possible implication for the treatment of glaucoma. *Br J Ophthalmol*, 2001(85):1252â1259, 2001.

[232] N. N. Osborne, J. P. M. Wood, G. Chidlow, J.-H. Bae, J. Melena, and M. S. Nash. Ganglion cell death in glaucoma: what do we really know? *Br J Ophthalmol*, 83(8):980–986, 1999.

[233] M. Pache and J. Flammer. A sick eye in a sick body? systemic findings in patients with primary open-angle glaucoma. *Survey of Ophthalmology*, 51(3):179 – 212, 2006.

[234] M. Pache, E. Nagel, and J. Flammer. Reproducibility of measurements with the retinal vessel analyzer under optimal conditions. *Klin Monatsbl Augenheilkd*, 219(7):523–527, July 2002.

[235] N. Pakrou, T. Gray, R. Mills, J. Landers, and J. Craig. Clinical comparison of the icare tonometer and goldmann applanation tonometry. *J Glaucoma*, 17(1):43–47, 2008.

[236] S. Palkovits, M. Lasta, R. Told, D. Schmidl, A. Boltz, K. J. Napora, R. M. Werkmeister, A. Popa-Cherecheanu, G. Garhoefer, and L. Schmetterer. Retinal oxygen metabolism during normoxia and hyperoxia in healthy subjectsretinal oxygen metabolism in humans. *Invest Ophthalmol Vis Sci*, 55(8):4707–4713, 2014.

[237] O. Palsson, A. Geirsdottir, S. H. Hardarson, O. B. Olafsdottir, J. V. Kristjansdottir, and E. Stefansson. Retinal oximetry images must be standardized: a methodological analysis. *Invest Ophthalmol Vis Sci*, 53(4):1729–1733, 2012.

[238] R. S. Parikh, Sh. Parikh, G. Ch. Sekhar, R. S. Kumar, S. Prabakaran, J. G. Babu, and R. Thomas. Diagnostic capability of optical coherence tomography (stratus oct 3) in early glaucoma. *Ophthalmology*, 114(12):2238–2243, 2007.

[239] M. Parthasarathy and M. Bhende. Effect of ocular magnification on macular measurements made using spectral domain optical coherence tomography. *Indian J Ophthalmol*, 63(5):427–431, 2015.

[240] N. Patton, R. Maini, T. MacGillivary, Ta. M. Aslam, I. J. Deary, and B. Dhillon. Effect of axial length on retinal vascular network geometry. *Am J Ophthalmol*, 140(4):648–648, 2005.

[241] Sh. A. Perera, T. Y. Wong, W.-T. Tay, P. J. Foster, S.-M. Saw, and T. Aung. Refractive error, axial dimensions, and primary open-angle glaucoma: The singapore malay eye study. *Arch Ophthalmol*, 128(7):900–905, 2010.

[242] L. E. Pillunat, D. R. Anderson, R. W. Knighton, K. M. Joos, and W. J. Feuer. Autoregulation of human optic nerve head circulation in response to increased intraocular pressure. *Exp Eye Research*, 64(5):737 – 744, 1997.

[243] A. Popa Cherecheanu, G. Garhofer, D. Schmidl, R. Werkmeister, and L. Schmetterer. Ocular perfusion pressure and ocular blood flow in glaucoma. *Curr Opin Pharmacol*, 13(1):36–42, 2013. Neurosciences.

[244] A. Pose-Reino, F. Gomez-Ulla, B. Hayik, M. Rodriguez-Fernandez, M. J. Carreira-Nouche, A. Mosquera-Gonzalez, M. Gonzalez-Penedo, and F. Gude. Computerized measurement of retinal blood vessel calibre: description, validation and use to determine the influence of ageing and hypertension. *J Hypertens*, 23(4):843–850, 2005.

[245] D. Prabhakaran, P. Jeemon, Sh. Ghosh, R. Shivashankar, V. S. Ajay, D. Kondal, R. Gupta, M. K. Ali, D. Mohan, V. Mohan, M. M. Kadir, N. Tandon, K. S. Reddy, and K. M. V. Narayan. Prevalence and incidence of hypertension: Results from a representative cohort of over 16,000 adults in three cities of south asia. *Indian Heart Journal*, 69(4):434–441, 2017.

[246] H. Quigley and D. R. Anderson. The dynamics and location of axonal transport blockade by acute intraocular pressure elevation in primate optic nerve. *Invest Ophthalmol Vis Sci*, 15(8):606–616, 08 1976.

[247] H. A. Quigley, E. M. Addicks, W. R. Green, and A. E. Maumenee. Optic nerve damage in human glaucoma: The site of injury and susceptibility to damage. *Arch Ophthalmol*, 99(4):635–649, 1981.

[248] H. A. Quigley and A. T. Broman. The number of people with glaucoma worldwide in 2010 and 2020. *Br J Ophthalmol*, 90(3):262–267, 2006.

[249] H. A. Quigley, G. R. Dunkelberger, and W. R. Green. Retinal ganglion cell atrophy correlated with automated perimetry in human eyes with glaucoma. *Am J Ophthalmol*, 107(5):453–464, 1989.

[250] H. A. Quigley, R. M. Sanchez, G. R. Dunkelberger, N. L. L'Hernault, and T. A. Baginski. Chronic glaucoma selectively damages large optic nerve fibers. *Invest Ophthalmol Vis Sci*, 28(6):913–920, 1987.

[251] H. A. Quigley, S. K. West, J. Rodriguez, B. Munoz, R. Klein, and R. Snyder. The prevalence of glaucoma in a population-based study of hispanic subjects: Proyecto ver. *Arch Ophthalmol.*, 119(12):1819–1826, 2001.

[252] M. Quigley and S. Cohen. A new pressure attenuation index to evaluate retinal circulation: A link to protective factors in diabetic retinopathy. *Arch Ophthalmol*, 117(1):84–89, 1999.

[253] L. Ramm, S. Jentsch, S. Peters, R. Augsten, and M. Hammer. Investigation of blood flow regulation and oxygen saturation of the retinal vessels in primary open-angle glaucoma. *Graefes Arch Clin Exp Ophthalmol*, 252(11):1803–1810, 2014.

[254] L. Ramm, S. Jentsch, S. Peters, L. Sauer, R. Augsten, and M. Hammer. Dependence of diameters and oxygen saturation of retinal vessels on visual field damage and age in primary open-angle glaucoma. *Acta Ophthalmol (Copenh)*, 94(3):276–281, 2016.

[255] H. L. Rao, Z. S. Pradhan, R. N. Weinreb, H. B. Reddy, M. Riyazuddin, S. Dasari, M. Palakurthy, N. K. Puttaiah, D. A. S. Rao, and C. A. B. Webers. Regional comparisons of optical coherence tomography angiography vessel density in primary open-angle glaucoma. *Am J Ophthalmol*, 171:75–83, 2016.

[256] H. L. Rao, Z. S. Pradhan, R. N. Weinreb, M. Riyazuddin, S. Dasari, J. P. Venugopal, N. K. Puttaiah, D. A. S. Rao, S.i Devi, K. Mansouri, and C. A. B. Webers. Vessel density and structural measurements of optical coherence tomography in primary angle closure and primary angle closure glaucoma. *Am. J. Ophthalmol.*, 177:106–115, 2017.

[257] F. M. Rauscher, N. Sekhon, W. J. Feuer, and D. L. Budenz. Myopia affects retinal nerve fiber layer measurements as determined by optical coherence tomography. *J Glaucoma*, 18(7):501–505, 2009.

[258] S. Rilven, Th. L. Torp, and J. Grauslund. Retinal oximetry in patients with ischaemic retinal diseases. *Acta Ophthalmol (Copenh)*, page 9, 2016.

[259] A. R. Rudnicka and D. F. Edgar. Automated static perimetry in myopes with peripapillary crescents, part i. *Ophthalmic Physiol Opt*, 15(5):409–412, 1995.

[260] A. R. Rudnicka and D. F. Edgar. Automated static perimetry in myopes with peripapillary crescents, part ii. *Ophthalmic Physiol Opt*, 16(5):416–429, 1996.

[261] A. Samsudin, N. Isaacs, M.-L. Sh. Tai, N. Ramli, Z. Mimiwati, and M. M. Choo. Ocular perfusion pressure and ophthalmic artery flow in patients with normal tension glaucoma. *BMC Ophthalmol*, 16(1):39, Apr 2016.

[262] J. Santodomingo-Rubido, E. A. H. Mallen, B. Gilmartin, and J. S. Wolffsohn. A new non-contact optical device for ocular biometry. *Br J Ophthalmol*, 86(4):458–462, 2002.

[263] S.-M. Saw. A synopsis of the prevalence rates and environmental risk factors for myopia (invited review). *Clin Experiment Ophthalmol*, 86(5):289–294, 2003.

[264] S.-M. Saw, G. Gazzard, E. C. Shih-Yen, and W.-H. Chua. Myopia and associated pathological complications. *Ophthalmic Physiol Opt*, 25(5):381–391, 2005.

[265] D. Schmidl, G. Garhofer, and L. Schmetterer. The complex interaction between ocular perfusion pressure and ocular blood flow and relevance for glaucoma. *Exp Eye Res*, 93(2):141–155, 2011. What Damages Ganglion Cells in Glaucoma? A Tribute to M. Rosario Hernandez.

[266] F. L. Schmidt, I.-S. Oh, and Th. L. Hayes. Fixed versus random effects models in meta-analysis: Model properties and an empirical comparison of differences in results. *Br J Math Stat Psychol*, 62(1):97–128, 2009.

[267] A. Schulze, J. Lamparter, N. Pfeiffer, F. Berisha, I. Schmidtmann, and E. M. Hoffmann. Diagnostic ability of retinal ganglion cell complex, retinal nerve fiber layer, and optic nerve head measurements by fourier-domain optical coherence tomography. *Graefes Arch Clin Exp Ophthalmol*, 249(7):1039–1045, 2011.

[268] J. S. Schuman, M. R. Hee, C. A. Puliafito, C. Wong, T. Pedut-Kloizman, Ch. P. Lin, E. Hertzmark, J. A. Izatt, E. A. Swanson, and J. G. Fujimoto. Quantification of nerve fiber layer thickness in normal and glaucomatous eyes using optical coherence tomography: a pilot study. *Archives of ophthalmology*, 113(5):586–596, 1995.

[269] D. Schweitzer, M. Hammer, J. Kraft, E. Thamm, E. Konigsdorffer, and J. Strobel. In vivo measurement of the oxygen saturation of retinal vessels in healthy volunteers. *IEEE Transactions on Biomedical Engineering*, 46(12):1454–1465, Dec 1999.

[270] D. Schweitzer, A. Lasch, S. van der Vorst, K. Wildner, M. Hammer, U. Voigt, M. Juette, and U. A. Mueller. Change of retinal oxygen saturation in healthy subjects and in early stages of diabetic retinopathy during breathing of 100 *Klin Monatsbl Augenheilkd*, 224(Issue 5):402–410, may 2007.

[271] D. Schweitzer, E. Thamm, M. Hammer, and J. Kraft. A new method for the measurement of oxygen saturation at the human ocular fundus. pages 347–353, 2001.

[272] K. D. Schweitzer, D. Ehmann, and R. Garcia. Nerve fibre layer changes in highly myopic eyes by optical coherence tomography. *Can J Ophthalmol*, 44(3):13–16, 2009.

[273] B.-U. Seifert and W. Vilser. Retinal vessel analyzer (rva), design and function. *Biomedizinische Technik/Biomedical Engineering*, 47(s1b):678–681, 2002.

[274] L. Shen, R. B. Melles, R. Metlapally, L. Barcellos, C. Schaefer, N. Risch, L. J. Herrinton, Ch. Wildsoet, and E. Jorgenson. The association of refractive error with glaucoma in a multiethnic population. *Ophthalmology*, 123(1):92–101, 2016.

[275] Y. Shiose, Y. Kitazawa, S. Tsukahara, T. Akamatsu, K. Mizokami, R. Futa, H. Katsushima, and H. Kosaki. Epidemiology of glaucoma in japan, a nationwide glaucoma survey. *Jpn J Ophthalmol*, 35(2):133–155, 1990.

[276] W. Smith, J. Assink, R. Klein, P. Mitchell, C. C. W. Klaver, B. E. K. Klein, A. Hofman, S. Jensen, J. J. Wang, and P. T. V. M. de Jong. Risk factors for age-related macular degeneration: pooled findings from three continents. *Ophthalmology*, 108(4):697–704, 2001.

[277] A. Sommer, J. Katz, H. A. Quigley, and et al. Clinically detectable nerve fiber atrophy precedes the onset of glaucomatous field loss. *Arch Ophthalmol*, 109(1):77–83, 1991.

[278] B. B. Sramek. *Systemic hemodynamics and hemodynamic management*. InstantPublisher.com, 10 2002.

[279] R. Stodtmeister, S. Heyde, M.and Georgii, E. Matthe, E. Spoerl, and L. E. Pillunat. Retinal venous pressure is higher than the airway pressure and the intraocular pressure during the valsalva manoeuvre. *Acta Ophthalmol*, 96(1):e68–e73, 2018.

[280] E. M. Stone, J. H. Fingert, W. L. M. Alward, Th. D. Nguyen, J. R. Polansky, S. L. F. Sunden, D. Nishimura, A. F. Clark, A. Nystuen, B. E. Nichols, D. A. Mackey, R. Ritch, J. W. Kalenak, E. R. Craven, and V.C. Sheffield. Identification of a gene that causes primary open angle glaucoma. *Science*, 275(5300):668–670, 1997.

[281] C. Sun, G. Liew, J. J. Wang, P. Mitchell, S. M. Saw, T. Aung, E. Sh. Tai, and T. Y. Wong. Retinal vascular caliber, blood pressure, and cardiovascular risk factors in an asian population: The singapore malay eye study. *Invest Ophthalmol Vis Sci*, 49(5):1784–1790, 05 2008.

[282] C. Sun, J. J. Wang, D. A. Mackey, and T. Y. Wong. Retinal vascular caliber: systemic, environmental, and genetic associations. *Surv Ophthalmol*, 54(1):74–95, 2009.

[283] K. R. Sung, S. Lee, S. B. Park, J. Choi, S. T. Kim, S.-Ch. Yun, S. Y. Kang, J. W. Cho, and M. S. Kook. Twenty-four hour ocular perfusion pressure fluctuation and risk of normal-tension glaucoma progression. *Invest Ophthalmol Vis Sci*, 50(11):5266–5274, 2009.

[284] S. Talu. Characterization of retinal vessel networks in human retinal imagery using quantitative descriptors. *International Journal of the Bioflux Society*, 5(Issue 2):52–57, 2013.

[285] F. Tayyari, L.-A. Khuu, J. G. Flanagan, Sh. Singer, M.l H. Brent, and Ch. Hudson. Retinal blood flow and retinal blood oxygen saturation in mild to moderate diabetic retinopathy. *Invest Ophthalmol Vis Sci*, 56(11):6796–6800, 2015.

[286] O.-Y. Tektas and E. Luetjen-Drecoll. Structural changes of the trabecular meshwork in different kinds of glaucoma. *Experimental Eye Research*, 88(4):769 – 775, 2009. Current aspects of aqueous humor dynamics and glaucoma.

[287] G. Tezel. The immune response in glaucoma: A perspective on the roles of oxidative stress. *Exp Eye Res*, 93(2):178–186, 2011. What Damages Ganglion Cells in Glaucoma? A Tribute to M. Rosario Hernandez.

[288] Y.-Ch. Tham, X. Li, T. Y. Wong, H. A. Quigley, T. Aung, and Ch.-Y. Cheng. Global prevalence of glaucoma and projections of glaucoma burden through 2040: A systematic review and meta-analysis. *Ophthalmology*, 121(11):2081–2090, 2014.

[289] E. Thamm, D. Schweitzer, and M. Hammer. A data reduction scheme for improving the accuracy of oxygen saturation calculations from spectrometric in vivo measurements. *Phys Med Biol*, 43(6):1401–1411, 1998. PII: S0031-9155(98)85276-7.

[290] J. M. Tielsch, J. Katz, A. Sommer, H. A. Quigley, and J. C. Javitt. Hypertension, perfusion pressure, and primary open-angle glaucoma: A population based assessment. *Arch Ophthalmol*, 113(2):216–221, 1995.

[291] J. M. Tielsch, A. Sommer, J. Katz, R. M. Royall, H. A. Quigley, and J. Javitt. Racial variations in the prevalence of primary open-angle glaucoma: The baltimore eye survey. *JAMA*, 266(3):369–374, 1991.

[292] James M. Tielsch, Joanne Katz, Kuldev Singh, Harry A. Quigley, John D. Gottsch, Jonathan Javitt, and Alfred Sommer. A population-based evaluation of glaucoma screening: The baltimore eye survey. *Am J Epidemiol*, 134(10):1102–1110, 11 1991.

[293] M. G. Todorova, C.z Tuerksever, A. Schoetzau, D. F. Schorderet, and Ch. Valmaggia. Metabolic and functional changes in retinitis pigmentosa: comparing retinal vessel oximetry to full-field electroretinography, electrooculogram and multifocal electroretinography. *Acta Ophthalmol (Copenh)*, page 12, 2015.

[294] R. Told, A. Boltz, L. Schmetterer, G. Garhoefer, St. Sacu, U. Schmidt-Erfurth, and A. Pollreisz. Method comparison of two non-invasive dual-wavelength spectrophotometric retinal oximeters in healthy young subjects during normoxia. *Acta Ophthalmol (Copenh)*, page 5, 2018.

[295] S. Traustason, M. la Cour, and M. Larsen. Retinal vascular oximetry during ranibizumab treatment of central retinal vein occlusion. *Br J Ophthalmol*, 98(9):1208–1211, 2014.

[296] S. Traustason, A. Schophuus Jensen, H. S. Arvidsson, I. Ch. Munch, L. Sondergaard, and M. Larsen. Retinal oxygen saturation in patients with systemic hypoxemia. *Invest Ophthalmol Vis Sci*, 52(8):5064–5067, 2011.

[297] D.-Ch. Tsai, W.-M. Hsu, Ch.-K. Chou, Sh.-J. Chen, Ch.-H. Peng, Ch.-W. Chi, L. L.-T. Ho, J.-H. Liu, and S.-H. Chiou. Significant variation of the elevated nitric oxide levels in aqueous humor from patients with different types of glaucoma. *Ophthalmologica*, 216(5):346–350, 2002.

[298] C. Tuerksever, S. Orguel, and M. G. Todorova. Reproducibility of retinal oximetry measurements in healthy and diseased retinas. *Acta Ophthalmol (Copenh)*, 93(6):439–445, 2015.

[299] J. W. Tukey. Comparing individual means in the analysis of variance. *Biometrics*, 5(2):99–114, 1949.

[300] T. Ueda-Consolvo, Ch. Fuchizawa, M. Otsuka, T. Nakagawa, and A. Hayashi. Analysis of retinal vessels in eyes with retinitis pigmentosa by retinal oximeter. *Acta Ophthalmol (Copenh)*, 93(6):446–450, 2015.

[301] K. Van Keer, L. Abegao Pinto, K. Willekens, I. Stalmans, and E. Vandewalle. Correlation between peripapillary choroidal thickness and retinal vessel oxygen saturation in young healthy individuals and glaucoma patientsctâso2 relation in young healthy and oag groups. *Invest Ophthalmol Vis Sci*, 56(6):3758–3762, 2015.

[302] E. Vandewalle, L. Abegao Pinto, O. B. Olafsdottir, E. De Clerck, P. Stalmans, J. Van Calster, Th Zeyen, E. StefÃ¡nsson, and I. Stalmans. Oximetry in glaucoma: correlation of metabolic change with structural and functional damage. *Acta Ophthalmol (Copenh)*, 92(2):105–110, 2014.

[303] A. Vogel, H. B. Dick, and F. Krummenauer. Reproducibility of optical biometry using partial coherence interferometry : intraobserver and interobserver reliability. *Journal of Cataract & Refractive Surgery*, 27(12):1961–1968, 2001.

[304] B. Vojnikovic and E. Tamajo. Gullstrands optical schematic system of the eye-modified by vojnikovic & tamajo. *Coll Antropol*, 37 Suppl 1:41–5, 2013.

[305] C. K. Vorwerk, S. A. Lipton, D. Zurakowski, B. T. Hyman, B. A. Sabel, and E. B. Dreyer. Chronic low-dose glutamate is toxic to retinal ganglion cells. toxicity blocked by memantine. *Invest Ophthalmol Vis Sci*, 37(8):1618–1624, 07 1996.

[306] J. P. Vrabec and L. A. Levin. The neurobiology of cell death in glaucoma. *Eye*, 21(S1):S11, 2007.

[307] A. Wainwright, G. Liew, G. Burlutsky, E. Rochtchina, Y. P. Zhang, W. Hsu, J. M. L. Lee, T. Y. Wong, P. Mitchell, and J. J. Wang. Effect of image quality, color, and format on the measurement of retinal vascular fractal dimension. *Invest Ophthalmol Vis Sci*, 51(11):5525–5529, 2010.

[308] G. Wang, K. L. Qiu, X. H. Lu, L. X. Sun, X. J. Liao, H. L. Chen, and M. Zh. Zhang. The effect of myopia on retinal nerve fibre layer measurement: a comparative study of spectral-domain optical coherence tomography and scanning laser polarimetry. *Br J Ophthalmol*, 95(2):255–260, 2011.

[309] N. D. Wangsa-Wirawan and R. A. Linsenmeier. Retinal oxygen: Fundamental and clinical aspects. *Arch Ophthalmol*, 121(4):547–557, 2003.

[310] A. J. Weber, P. L. Kaufman, and W. C. Hubbard. Morphology of single ganglion cells in the glaucomatous primate retina. *Invest Ophthalmol Vis Sci*, 39(12):2304–2320, 1998.

[311] R. N. Weinreb, J. M. Liebmann, G. A. Cioffi, I. Goldberg, J. D. Brandt, Ch. A. Johnson, L. M. Zangwill, S. Schneider, H. Badger, and M. Bejanian. Oral memantine for the treatment of glaucoma: Design and results of 2 randomized, placebo-controlled, phase 3 studies. *Ophthalmology*, 125(12):1874 – 1885, 2018.

[312] R. N. Weinreb and J. P. Perlman. The effect of refractive correction on automated perimetric thresholds. *Am J Ophthalmol*, 101(6):706–709, 1986.

[313] R. N. Weinreb, S. Shakiba, P. A. Sample, Sh. in Shahrokni, St. van Horn, V. S. Garden, and . Asawaphureekorn, S.and Zangwill. Association between quantitative nerve fiber layer measurement and visual field loss in glaucoma. *Am J Ophthalmol*, 120(6):732–738, 1995.

[314] G. N. Wise, C. T. Dollery, and P. Henkind. *The retinal circulation*. New York : Harper & Row, [c1971], 1971.

[315] T. Y. Wong, A. Kamineni, R. Klein, A. R. Sharrett, B. E. Klein, D. S. Siscovick, M. Cushman, and B. B. Duncan. Quantitative retinal venular caliber and risk of cardiovascular disease in older persons: The cardiovascular health study. *Arch Intern Med*, 166(21):2388–2394, 11 2006.

[316] T. Y. Wong, B. E. K. Klein, R. Klein, M. Knudtson, and K. E. Lee. Refractive errors, intraocular pressure, and glaucoma in a white population. *Ophthalmology*, 110(1):211–217, 2003.

[317] T. Y. Wong, M. D. Knudtson, R. Klein, B. E. K. Klein, S. M. Meuer, and L. D. Hubbard. Computer-assisted measurement of retinal vessel diameters in the beaver dam eye study: methodology, correlation between eyes, and effect of refractive errors. *Ophthalmology*, 111(6):1183–1190, 2004.

[318] T. Y. Wong, J. J. Wang, E. Rochtchina, R. Klein, and P. Mitchell. Does refractive error influence the association of blood pressure and retinal vessel diameters? the blue mountains eye study. *Am J Ophthalmol*, 137(6):1050–1055, 2004.

[319] R. Wu, C. Y. Cheung, S. M. Saw, P. Mitchell, T. Aung, and T. Y. Wong. Retinal vascular geometry and glaucoma: the singapore malay eye study. *Ophthalmology*, 120(1):77–83, 2013.

[320] L. Xu, Y. Wang, Sh. Wang, Y. Wang, and J. B. Jonas. High myopia and glaucoma susceptibility: The beijing eye study. *Ophthalmology*, 114(2):216–220, 2007.

[321] L. Xu, Y. X. Wang, and J. B. Jonas. Ocular perfusion pressure and glaucoma: the beijing eye study. *Eye*, 23(3):734, 2009.

[322] E. Yamada. Some structural features of the fovea centralis in the human retina. *Arch Ophthalmol*, 82(2):151–159, 1969.

[323] Z. Yaqoob, J. Wu, and Ch. Yang. Spectral domain optical coherence tomography: a better oct imaging strategy. *Biotechniques*, 39:6–13, 2005.

[324] A. Yarmohammadi, L. M. Zangwill, A. Diniz-Filho, M. H. Suh, S. Yousefi, L. J. Saunders, A. Belghith, P. I. C. Manalastas, F. A. Medeiros, and R. N. Weinreb. Relationship between optical coherence tomography angiography vessel density and severity of visual field loss in glaucoma. *Ophthalmology*, 123(12):2498–2508, 2016.

[325] W. F. Yip, R. Siantar, Sh A. Perera, N. Milastuti, K. K. Ho, B. Tan, T. Y. Wong, and C. Y. Cheung. Reliability and determinants of retinal vessel oximetry measurements in healthy eyes. *Invest Ophthalmol Vis Sci*, 55(11):7104–7110, 2014.

[326] T. L. Young. The molecular genetics of human myopia: An update. *Optom Vis Sci*, 86(1):28, 2009.

[327] S. Zahid, R. Dolz-Marco, K. B. Freund, Ch. Balaratnasingam, K. Dansingani, F. Gilani, N. Mehta, E. Young, M. R. Klifto, B. Chae, L. A. Yannuzzi, and J. A. Young. Fractal dimensional analysis of optical coherence tomography angiography in eyes with diabetic retinopathy. *Invest Ophthalmol Vis Sci*, 57(11):4940–4947, 2016.

[328] X. Zhang, M. Cheng, and Sh. K. Chintala. Kainic acidâmediated upregulation of matrix metalloproteinase-9 promotes retinal degeneration. *Invest Ophthalmol Vis Sci*, 45(7):2374–2383, 07 2004.

[329] X. Zhang, B. A. Francis, A. Dastiridou, V. Chopra, O. Tan, R. Varma, D. S. Greenfield, J. S. Schuman, D. Huang, and for the Advanced Imaging for Glaucoma Study Group. Longitudinal and cross sectional analyses of age effects on retinal nerve fiber layer and ganglion cell complex thickness by fourier-domain oct. *TVST*, 5(2):1–9, 2016.

[330] Q. Zheng, Y. Zong, L. Li, X. Huang, L. Lin, W. Yang, Y. Yuan, Y. Li, H. He, and Q. Gao. Retinal vessel oxygen saturation and vessel diameter in high myopia. *Ophthalmic Physiol Opt*, 35(5):562–569, 2015.

[331] Y. Zheng, N. Cheung, T. Aung, P. Mitchell, M. He, and T. Y. Wong. Relationship of retinal vascular caliber with retinal nerve fiber layer thickness: The singapore malay eye study. *Invest Ophthalmol Vis Sci*, 50(9):4091–4096, 2009.

[332] Y. Zheng, T. Y. Wong, P. Mitchell, D. S. Friedman, M. He, and T. Aung. Distribution of ocular perfusion pressure and its relationship with open angle glaucoma: The singapore malay eye study. *Invest Ophthalmol Vis Sci*, 51(7):3399–3404, 2010.

[333] W. G. Zijlstra, A. Buursma, and O. W. van Assendelft. *Visible and near infrared absorption spectra of human and animal haemoglobin: determination and application*. VSP, bv 2000 edition, 2000.

[334] Y. Zong, L. Lin, Ch. Yi, X. Huang, Y. Fu, Y. Dong, X. Qian, Y. Li, and Q. Gao. Retinal vessel oxygen saturation and vessel diameter in retinitis pigmentosa at various ages. *Graefes Arch Clin Exp Ophthalmol*, 254(2):243–252, 2015.

Part X

Appendices

AppendixA. Authors permission to use graphic

From: Arland, Frank
To: Hirsch, Katrin
Subject: AW: Anfrage fuer Bildrecht bezueglich meiner Dissertation
Date: 05 September 2016 11:52:49

Nehmen Sie gerne einfach meine Mail als schriftliche Bestätigung. Für dieses eine Bild und der genannten Verwendung müssen wir keinen weiteren Aufwand betreiben.

VG
Frank Arland

Von: Hirsch, Katrin [mailto:k.hirsch@aston.ac.uk]
Gesendet: Montag, 5. September 2016 12:01
An: Arland, Frank <frank.arland@zeiss.com>
Betreff: RE: Anfrage fuer Bildrecht bezueglich meiner Dissertation

Vielen Dank Herr Arland!

War das schon alles? Oder bekomme ich dafür noch eine art schriftliche form?

Danke und herzlichen Gruss

Katrin Hirsch

Clinical Demonstrator/PhD

School of Life and Health Sciences
Aston University
Birmingham, B4 7ET
Phone: 0121-204-4712

From: Arland, Frank [frank.arland@zeiss.com]
Sent: 05 September 2016 10:10
To: Hirsch, Katrin
Subject: AW: Anfrage fuer Bildrecht bezueglich meiner Dissertation

Hallo Frau Hirsch,

Sie können die Grafik gerne in Ihrer Arbeit nutzen.

Danke und VG
Frank Arland

Von: Hirsch, Katrin [mailto:k.hirsch@aston.ac.uk]
Gesendet: Montag, 5. September 2016 09:58
An: Arland, Frank <frank.arland@zeiss.com>
Betreff: RE: Anfrage fuer Bildrecht bezueglich meiner Dissertation

Sehr geehrter Herr Arland,

Es reicht also nicht, ihnen die Seite im Manual zu nennen?
Ich kann von meiner Outlook version zu Hause leider keine Dokumente anhängen. Sonst hätte ich es schon getan.
Dann sende ich ihnen den Internet link zu diesem manual: https://www.doctor-hill.com/physicians/docs/IOLMaster_Practical_Operation_Guide.pdf .
Hier ist es Chapter 4.2 (pg 27, das obere Bild)

AppendixB.

AppendixB.1. Protocol study 1

Aston University

Study Protocol

ASSESSMENT OF STRUCTURAL AND FUNCTIONAL PARAMETERS OF THE OCULAR FUNDUS IN HIGHLY MYOPIC VS EMMETROPIC YOUNG HEALTHY INDIVIDUALS: AN EXPLORATORY, CROSS-SECTIONAL STUDY

BACKGROUND

Myopia is a refractive status which is linked to a higher risk of developing several ocular abnormalities, such as myopic maculopathy, cataract or glaucoma [1]. One major aspect in myopia is an increased ocular length, which results from elongation of the eye ball and is associated with thinning of the retina. The elongation of the eye ball also affects the retinal vasculature by stretching the retinal vessels resulting in decreased vessel diameters and changes in the Retinal Nerve Fiber Layer (RNFL) thickness. A study by Yuan and coworkers [2] described an association between visual field indices, such as mean sensitivity or mean defect, and the thickness of the RNFL. Other investigators found that the ocular blood flow (OBF) is reduced in high myopia [3]. One plausible explanation of the OBF reduction can be found by the relationship of blood velocity and vessel diameter alone ($OBF = Velocity * Vesseldiameter^2$). But due to the retinal thinning there might be a reduced oxygen demand in high myopes compared to their emmetropic counterparts. This aspect has been examined [4, 5] in previous studies. However, these have revealed a reduced oxygen consumption in high myopic patients.

While most studies focused on either retinal function or structure, to date there is very limited information available on the interplay of structure and function. Decreased diameter alone can explain part of the reduction in metabolic markers measured, however it doesn't always explain why some individuals will progress to myopia related pathology and others don't. Hence a more complex investigation examining the vessel complexity (i.e. coverage), reactivity and diameters, paired with structural assessment of the retina and visual function can provide a deeper understanding of the interplay between ocular stretch and altered oxygen parameters in high myopic individuals.

OBJECTIVES

This cross-sectional study will investigate the relationship between structural (retinal thickness, axial length (AL), vessel complexity) and functional (including Visual Field Analysis) parameters of the retina in highly myopic and emmetropic individuals. This will provide a better understanding of their interplay and allow us further insight into the link between structure, metabolism and function.

The main research questions of the study are:

1. How do otherwise healthy, myopic individuals differ from emmetropes in regards to structural and functional parameters?
2. How does retinal vessel complexity relate to oxygen parameter?
3. Do thinner retinas require less oxygen?
4. How retinal structure, metabolism, visual function and vasculature are related in emmetropes vs myopes?

PROCEDURES

We will recruit 120 subjects as follows:

Group A: 60 individuals with high myopia (refractive error > -6D (spherical equivalent SE)) and

Group B: 60 individuals which are emmetropic (refractive error within +/-0.5D (spherical equivalent SE))

Inclusion criteria:

- Age : 18yrs of age and older
- Free from ocular trauma and any ocular or systemic disease (such as glaucoma, Diabetes Mellitus and hypertension)
- Clear ocular media

Exclusion:

- Refractive errors outside those detailed above and astigmatism larger than +/-2D
- History of strabismus and amblyopia
- Any previous ocular surgery
- Known adverse reactions to the used drug to dilate the pupil (Tropicamide 1%)

All study participants will be recruited from Aston University staff, students and other volunteers. Each will be provided with a patient-information sheet and a consent form to be completed (according to the guideline of the Declaration of Helsinki). The study purpose and instructions will be explained and any questions answered. The study-procedure will take approximately 60-90 minutes and includes dilation of the study eye with one drop Tropicamide 1%. To ensure patient safety and comfort we use only the minimum amount of

drops required to reach full dilation and measure IOP and anterior angle before instillation of tropicamide. If the subject reports of any previous adverse reactions to tropicamide, they will be excluded from the study.

Each participant will undergo the following measurements in one unselected eye:

Each participant will be instructed to refrain from any caffeinated products and smoking for 4 hrs prior to the study appointment. Contact lens wearers will be instructed to arrive without wearing their lenses (i.e. lenses have to be removed at least 4 hrs prior to the study).

Visual/Retinal function measurements:

1. Visual Acuity (logMAR) testing with current correction on the study eye to gain information about visual function.
2. Visual field measurement (Humphreys Visual Field Analyser, Zeiss): 30-2 including macula threshold.
3. Multifocal electroretinogram (mfERG) for retinal function measurement.

Classification of refractive error:

1. Autorefraction with the Shin Nippon open field autorefractor (Shin-Nippon, Tokyo Japan).
2. Biometry measurements with the Zeiss IOL-Master (axial length, anterior chamber depth and keratometry).

Systemic/ Intraocular Pressure measurements:

1. Intraocular pressure measurements will be obtained by rebound-tonometry (I-Care, Mainline Instruments LTD).
2. Digital sphygmomanometer to obtain systolic and diastolic blood pressure and heart rate (Blood pressure monitor UA-767Plus, A&D Medical) following room acclimatization of a minimum of 15 min resting in a sitting position.
3. Finger pulse oximetry (Pulse Oximeter, Merlin Medical) to evaluate the systemic oxygen saturation.

Vascular retinal parameters:

1. Dual wavelength retinal vessel oxygen saturation (SO2) measurements (Imedos, Germany).

2. Retinal vessel reactivity measurements: continuous retinal vessel diameter measurements including flicker light stimulation using the Retinal Vessel Analyser (RVA, Imedos, Germany) of one retinal arteriole and one venule.
3. Retinal vessel calibers (central retinal artery equivalent [CRAE] and vein equivalent [CRVE]) using monochromatic retinal photographs (Zeiss FF450+, Zeiss, Germany).
4. Ocular coherence tomography to measure retinal layer thickness and anterior structural parameters including anterior chamber dimensions.
5. Retinal vessel complexity will be analyzed using monochromatic retinal photographs. Vessel complexity will be done by box counting technique of skeletonized vessel tree information.

All data collected will be kept confidential. Data files will be named in such a way that the patient's identity is protected. Only the study-team will have access to these data (data storage will be on Aston University computers which are password protected in locked rooms).

STATISTIC ANALYSIS/ RELIABILITY OF DATA

All data will be analysed using Statistica version 12.0 (StatSoft, Germany). Distribution will be tested prior to any test being applied. Associations between the measured parameters will be assessed using multiple regression analyses. Group comparisons between myopic and emmetropic participants will be performed using students' t-test in case of normal distributed data or the appropriate non-parametric test if normal distribution is absent.

BIBLIOGRAPHY

[1] Seang-Mei Saw, Gus Gazzard, Edwin Chan Shih-Yen, Wei-Han Chua. Myopia and associated pathological complications. *Ophthalmic and Physiological Optics*, 25(5):381—391, 2005. URL http://dx.doi.org/10.1111/j.1475-1313.2005.00298.x.

[2] Y-Zandi Feng Yuan, B-Y Li, M-Q Shen, X-P Chen, Ch-H Zhang, Ch-Q andYuan Dong. The Relationship between Visual Field Global Indices and Retinal Nerve Fiber Layer Thickness in Healthy Myopes. , 2014:8, 2014.

[3] Noriaki Shimada, Kyoko Ohno-Matsui, Seiyo Harino, Takeshi Yoshida, Kenjiro Yasuzumi, Ariko Kojima, Kanako Kobayashi, Soh Futagami, Takashi Tokoro, Manabu Mochizuki. Reduction of retinal blood flow in high myopia. *Graefe's Archive for Clinical and Experimental Ophthalmology*, 242(4):284—288, 2004. URL http://dx.doi.org/10.1007/s00417-003-0836-0.

[4] Ryan Eyn Kidd Man, Ecosse L. Lamoureux, Yamna Taouk, Jing Xie, Muhammad Bayu Sasongko, William J. Best, Jonathan E. Noonan, Ryo Kawasaki, Jie Jin Wang, Chi D. Luu. Axial Length, Retinal Function, and Oxygen Consumption: A Potential Mechanism for a Lower Risk of Diabetic Retinopathy in Longer EyesAxial Length and Oxygen Consumption. *Investigative Ophthalmology & Visual Science*, 54(12):7691, 2013. URL http://dx.doi.org/10.1167/iovs.13-12412.

[5] Qishan Zheng, Yao Zong, Li Li, Xia Huang, Leilei Lin, Wei Yang, Yongguang Yuan, Yujie Li, Huining He, Qianying Gao. Retinal vessel oxygen saturation and vessel diameter in high myopia. *Ophthalmic and Physiological Optics*, 35(5):562—569, 2015. URL http://dx.doi.org/10.1111/opo.12223.

AppendixB.2. Approval Aston University Ethics Committee study 1

Aston University

Aston University
Aston Triangle
Birmingham
B4 7ET
0121 204 3000

Date: 27th September 2016

Life and Health Sciences

Dear Rebekka Heitmar

Study title:	**ASSESSMENT OF STRUCTURAL AND FUNCTIONAL PARAMETERS OF THE OCULAR FUNDUS IN HIGHLY MYOPIC VS EMMETROPIC YOUNG HEALTHY INDIVIDUALS**
REC REF:	Ethics application #986

Confirmation of Ethical Opinion

On behalf of the Committee, I am pleased to confirm a favourable opinion for the above research based on the basis described in the application form, protocol and supporting documentation listed below.

Approved documents

The final list of documents reviewed and approved by the Committee is as follows:

Document	*Version*	*Date*
Consent Form (PatientConsentMyE2016_revised consent form)	Version: C	01.04.16
Participant Information Sheet (PIS MyE2016_revised form)	1.2	2.06.2016
Response to feedback from UREC – including text to be sent out to potential participants (Response and list of changes made to application 986)		25.08.2016

With the Committee's best wishes for the success of this project.
Yours sincerely

Dr Nichola Seare
Chair of the University Research Ethics Committee

AppendixB.3. Protocol study 2

Aston University
Birmingham

Aston Triangle
Birmingham B4 7ET
United Kingdom
Tel +44 (0)121 204 3000

www.aston.ac.uk

Memo

To: Dr Nichola Seare

From: Dr Robert Cubbidge

Date: 29/1/2019

Subject: Amendment request for project Ref 986

Dear Nichola,

On behalf of myself and my PhD student Katrin Hirsch, I would like to request following additions and changes to the above project:

1. We would like to **extend the proposed end date** to the 30th December 2018. The data has taken longer than expected to acquire because of a delay in start date of the study as well as the repair of the main imaging device.
2. We would like to change the **order of the associate investigators** on the existing ethics to reflect Dr Rebekka Heitmar going on maternity leave in January 2018. Dr Robert Cubbidge has been made the primary investigator. Dr Rebekka Heitmar is the associate supervisor for the duration of her maternity leave. These changes have been recorded by the LHS research office.
3. We would like to request the addition of a **third subject group (group C); namely glaucoma patients.** The aim of the study (PhD project) is to determine retinal feature(s) that allow to predict whether a high short-sighted eye might develop glaucoma later on in life. Previous research in this area has shown that short-sighted eyes are at a higher risk of developing glaucoma (an 1.88 fold higher than in an emmetropic eye, Marcus et al. 2011). Thus, in addition to the existing healthy emmetropic and highly short-sighted subjects being recruited, we wish to recruit some subjects with glaucoma in order to compare and correlate functional, structural and hemodynamic measurements in these cohorts. These measurements will determine if there are structural and functional similarities in eyes that have glaucoma compared to myopic eyes.

At the beginning of the study it was planned that glaucoma patients would be recruited from hospitals in the local area and intended to make an NHS REC ethics application. Problems with potential collaborations have rendered this option unviable. Consequently, we wish to recruit glaucoma patients from the Aston optometry clinic, friends and family. We will perform the same assessments as with the emmetropic and short-sighted study subjects. All measurements will be carried out by Katrin Hirsch, a qualified optometrist. All data will be secured according to the existing protocols which have been approved.

To reflect the above changes, attached are amended PIS, consent form and updated Risk Assessment form with changes to the approved ethics highlighted in red.

With best wishes,

Dr Robert P Cubbidge
Senior Lecturer
ORG/LHS
r.p.cubbidge@aston.ac.uk

ASSESSMENT OF STRUCTURAL AND FUNCTIONAL PARAMETERS OF THE OCULAR FUNDUS IN HIGHLY MYOPIC VS EMMETROPIC HEALTHY INDIVIDUALS AND GLAUCOMA PATIENTS: AN EXPLORATORY, CROSS-SECTIONAL STUDY

BACKGROUND

Myopia is a refractive status which is linked to a higher risk of developing several ocular abnormalities, such as myopic maculopathy, cataract or glaucoma [1]. A good example of an increased risk to develop glaucoma in people with a myopic refractive error showed a study of Marcus et al (2011) [2]. This meta-analysis revealed a 1.88fold higher risk to develop primary open angle glaucoma (POAG) in eyes with a SE above -3.00D.

One major aspect in myopia is an increased ocular length, which results from elongation of the eye ball and is associated with thinning of the retina. The elongation of the eye ball also affects the retinal vasculature by stretching the retinal vessels resulting in decreased vessel diameters and changes in the Retinal Nerve Fiber Layer (RNFL) thickness. A study by Yuan and coworkers [3] described an association between visual field indices, such as mean sensitivity or mean defect, and the thickness of the RNFL. Moreover, a decrease in RNFL thickness which leads to visual field defects is the characteristic feature in glaucomatous eyes [2].

Other investigators found that the ocular blood flow (OBF) is reduced in high myopia and in glaucoma [4,5]. One plausible explanation of the OBF reduction in high myopia can be found by the relationship of blood velocity and vessel diameter alone ($OBF=Velocity*Vesseldiameter^2$). However, due to the retinal thinning there might be a reduced oxygen demand in high myopes compared to their emmetropic counterparts. This aspect has been examined [6, 7] in previous studies. The authors concluded that oxygen consumption is reduced in highly myopic eyes, which was also found in glaucomatous eyes [8].

While most studies focused on either retinal function or structure, to date there is very limited information available on the interplay of structure and function. Decreased diameter alone can explain part of the reduction in metabolic markers measured, however it doesn't always explain why some individuals will progress to myopia related pathology such as glaucoma and others don't. Hence a more complex investigation examining the vessel complexity (i.e. coverage), reactivity and diameters, paired with structural assessment of the retina and visual function can provide a deeper understanding of the interplay between ocular stretch and altered oxygen parameters in high myopic individuals.

OBJECTIVES

This cross-sectional study will investigate the relationship between structural (retinal thickness, axial length (AL), vessel complexity) and functional (including Visual Field Analysis) parameters of the retina in healthy highly myopic, emmetropic individuals and glaucoma patients. This will provide a better understanding of their interplay in these study cohorts and allow us further insight into the link between structure, metabolism and function.

The main research questions of the study are:

1. How do otherwise healthy, myopic individuals differ from emmetropes in regards to structural and functional parameters?
2. How does retinal vessel complexity relate to oxygen parameter?
3. Do thinner retinas require less oxygen?
4. How retinal structure, metabolism, visual function and vasculature are related in emmetropes vs myopes?
5. Do any of the parameters and/or relationships of highly myopic eyes resemble in glaucoma patients eyes?

PROCEDURES

We will recruit 120 subjects as follows:

Group A: 40 individuals with high myopia (refractive error > -6D (spherical equivalent SE)) and

Group B: 40 individuals which are emmetropic (refractive error within +/-0.5D (spherical equivalent SE))

Group C: 40 individuals with glaucoma

Inclusion criteria:

- Age : 18yrs of age and older (group A and B)
- Free from ocular trauma and any ocular or systemic disease (such as glaucoma, Diabetes Mellitus and hypertension) (group A and B)
- Clear ocular media (group A and B and C)
- Glaucoma patients (group C)

Exclusion:

- Refractive errors outside those detailed above and astigmatism larger than +/-2D
- History of strabismus and amblyopia
- Any previous ocular surgery (only for group A and B)
- Known adverse reactions to the used drug to dilate the pupil (Tropicamide 1%)

All study participants will be recruited from Aston University staff, students and other volunteers. Each will be provided with a patient-information sheet and a consent form to be completed (according to the guideline of the Declaration of Helsinki). The study purpose and instructions will be explained and any questions answered. The study-procedure will take approximately 60-90 minutes and includes dilation of the study eye with one drop Tropicamide 1%. To ensure patient safety and comfort we use only the minimum amount of drops required to reach full dilation and measure IOP and anterior angle before instillation of tropicamide. If the subject reports of any previous adverse reactions to tropicamide, they will be excluded from the study.

Each participant will undergo the following measurements in one unselected eye:

Each participant will be instructed to refrain from any caffeinated products and smoking for 4 hrs prior to the study appointment. Contact lens wearers will be instructed to arrive without wearing their lenses (i.e. lenses have to be removed at least 4 hrs prior to the study).

Visual/Retinal function measurements:

1. Visual Acuity (logMAR) testing with current correction on the study eye to gain information about visual function.
2. Visual field measurement (Humphreys Visual Field Analyser, Zeiss): 30-2 including macula threshold.
3. Multifocal electroretinogram (mfERG) for retinal function measurement.

Classification of refractive error:

1. Autorefraction with the Shin Nippon open field autorefractor (Shin-Nippon, Tokyo Japan).
2. Biometry measurements with the Zeiss IOL-Master (axial length, anterior chamber depth and keratometry).

Systemic/ Intraocular Pressure measurements:

1. Intraocular pressure measurements will be obtained by rebound-tonometry (I-Care, Mainline Instruments LTD).

2. Digital sphygmomanometer to obtain systolic and diastolic blood pressure and heart rate (Blood pressure monitor UA-767Plus, A&D Medical) following room acclimatization of a minimum of 15 min resting in a sitting position.

3. Finger pulse oximetry (Pulse Oximeter, Merlin Medical) to evaluate the systemic oxygen saturation.

Vascular retinal parameters:

1. Dual wavelength retinal vessel oxygen saturation (SO2) measurements (Imedos, Germany).

2. Retinal vessel reactivity measurements: continuous retinal vessel diameter measurements including flicker light stimulation using the Retinal Vessel Analyser (RVA, Imedos, Germany) of one retinal arteriole and one venule.

3. Retinal vessel calibers (central retinal artery equivalent [CRAE] and vein equivalent [CRVE]) using monochromatic retinal photographs (Zeiss FF450+, Zeiss, Germany).

4. Ocular coherence tomography to measure retinal layer thickness and anterior structural parameters including anterior chamber dimensions.

5. Retinal vessel complexity will be analyzed using monochromatic retinal photographs. Vessel complexity will be done by box counting technique of skeletonized vessel tree information (iFlexis software).

All data collected will be kept confidential. Data files will be named in such a way that the patient's identity is protected. Only the study-team will have access to these data (data storage will be on Aston University computers which are password protected in locked rooms).

STATISTIC ANALYSIS/ RELIABILITY OF DATA

All data will be analyzed using SPSS version 20 (IBM). Distribution will be tested prior to any test being applied. Associations between the measured parameters will be assessed using multiple regression analyses. Group comparisons between myopic and emmetropic participants will be performed using student's t-test in case of normal distributed data or the appropriate non-parametric test if normal distribution is absent. Consecutively, relationships will be explored in each group separately to identify common features.

BIBLIOGRAPHY

[1] Seang-Mei Saw, Gus Gazzard, Edwin Chan Shih-Yen, Wei-Han Chua. Myopia and associated pathological complications. *Ophthalmic and Physiological Optics*, 25(5):381—391, 2005. URL http://dx.doi.org/10.1111/j.1475-1313.2005.00298.x.

[2] Casson RJ, Chidlow G, Wood JPM, Crowston JG, Goldberg I. Definition of glaucoma: clinical and experimental concepts. Clinical & Experimental Ophthalmology. 2012; 40(4):341-9. http://dx.doi.org/10.1111/j.1442-9071.2012.02773.x

[3] Y-Zandi Feng Yuan, B-Y Li, M-Q Shen, X-P Chen, Ch-H Zhang, Ch-Q andYuan Dong. The Relationship between Visual Field Global Indices and Retinal Nerve Fiber Layer Thickness in Healthy Myopes. , 2014:8, 2014.

[4] Noriaki Shimada, Kyoko Ohno-Matsui, Seiyo Harino, Takeshi Yoshida, Kenjiro Yasuzumi, Ariko Kojima, Kanako Kobayashi, Soh Futagami, Takashi Tokoro, Manabu Mochizuki. Reduction of retinal blood flow in high myopia. *Graefe's Archive for Clinical and Experimental Ophthalmology*, 242(4):284—288, 2004. URL http://dx.doi.org/10.1007/s00417-003-0836-0.

[5] Galassi F, Sodi A, Ucci F, et al. Ocular haemodynamics in glaucoma associated with high myopia. International ophthalmology. 1998; 22(5):299-305. http://dx.doi.org/10.1023/A:1006347509491

[6] Ryan Eyn Kidd Man, Ecosse L. Lamoureux, Yamna Taouk, Jing Xie, Muhammad Bayu Sasongko, William J. Best, Jonathan E. Noonan, Ryo Kawasaki, Jie Jin Wang, Chi D. Luu. Axial Length, Retinal Function, and Oxygen Consumption: A Potential Mechanism for a Lower Risk of Diabetic Retinopathy in Longer EyesAxial Length and Oxygen Consumption. *Investigative Ophthalmology & Visual Science*, 54(12):7691, 2013. URL http://dx.doi.org/10.1167/iovs.13-12412.

[7] Qishan Zheng, Yao Zong, Li Li, Xia Huang, Leilei Lin, Wei Yang, Yongguang Yuan, Yujie Li, Huining He, Qianying Gao. Retinal vessel oxygen saturation and vessel diameter in high myopia. *Ophthalmic and Physiological Optics*, 35(5):562—569, 2015. URL http://dx.doi.org/10.1111/opo.12223.

[8] Olafsdottir, O B and Vandewalle, E and Abegao Pinto, L and Geirsdottir, A and De Clerck, E and Stalmans, P and Gottfredsdottir, M S and Kristjansdottir, J V and Van Calster, J and Zeyen, Th and others. Retinal oxygen metabolism in healthy subjects and glaucoma patients. *British Journal of Ophthalmology*, Vol.98(3):329-333,2014.

AppendixB.4. Approval Aston University Ethics Committee study 2

Aston University

Aston University
Aston Triangle
Birmingham
B4 7ET
0121 204 3000

Date: 22/03/18

Life and Health Sciences

Dear Katrin Hirsch

Study title:	**ASSESSMENT OF STRUCTURAL AND FUNCTIONAL PARAMETERS OF THE OCULAR FUNDUS IN HIGHLY MYOPIC VS EMMETROPIC YOUNG HEALTHY INDIVIDUALS**
REC REF:	Ethics application #986

Confirmation of Ethical Opinion

On behalf of the Committee, I am pleased to confirm a favourable opinion for the above research based on the basis described in the application form, protocol and supporting documentation listed below.

Approved documents

The final list of documents reviewed and approved by the Committee is as follows:

Document	*Version*	*Date*
Amendment letter Aston 19.02.2018 RC		19.02.2018
Patient Information MyE2018_GI18		21.02.2018
Protocol_MyvsEm2016_GI2018		21.02.2018
Risk Assessment and Control Form MyE2016Glauc2018		21.02.2018
PatientConsentMyE2016GI2018		21.02.2018

With the Committee's best wishes for the success of this project.
Yours sincerely

Dr Nichola Seare
Chair of the University Research Ethics Committee

AppendixC.

AppendixC.1. Patient invitation and Patient Consent Form study 1

Study participants required …

WHO is eligible?

- Emmetropic (no spectacles needed) or
- High short-sighted (spectacle correction more than -5.75D) with
- NO history of eye diseases or ocular surgery

WHAT is it about?

I explore the blood circulation (RVA), structure (OCT) and function (Humphreys HFA 750) of the retina in both eye-sight conditions.

All measurements are **NON-INVASIVE**

DURATION/Location of appointment?

90 minutes, Vision Science building – reception

HOW to book an appointment?

https://wass.aston.ac.uk/pages/login.page.php calendar name: "Hirsch, Katrin"

CONTACT for further questions?

k.hirsch@aston.ac.uk (Katrin Hirsch)

Aston University Participant Consent Form

Study ID_____

TITLE OF THE PROJECT: ASSESSMENT OF STRUCTURAL AND FUNCTIONAL PARAMETERS OF THE OCULAR FUNDUS IN HIGHLY MYOPIC VS EMMETROPIC YOUNG HEALTHY INDIVIDUALS: AN EXPLORATORY, CROSS-SECTIONAL STUDY

LAY TITLE: Structure and Function of eyes of healthy individuals with short sightedness.

Names of Investigators

Principal Investigator: Ms Katrin Hirsch

Associate Investigators: Dr Rebekka Heitmar

Dr Robert Cubbidge

	Initials
1. I confirm that I have read and understand the information sheet (version 1.2) for the above study. I have had the opportunity to consider the information, ask questions and had these answered satisfactorily.	☐
2. I understand that my participation is voluntary and that I am free to withdraw at any time without giving any reason and without my legal rights being affected.	☐
3. I agree to take part in the above study.	☐

_____	_____	_____
Name of volunteer/participant	Date	Signature
_____	_____	_____
Name of Person taking Consent	Date	Signature

1 copy for Participant / 1 copy for Investigator

02/06/2016 Version: C 01.04.16

AppendixC.2. Patient invitation and Patient Consent Form study 2

Aston University

Are you a glaucoma patient?

Dear patient of the Aston optometry clinic,

I am writing to ask if you would consider taking part in my research project. I am currently looking for people diagnosed with **GLAUCOMA**. You are eligible if one or both of your eyes has been diagnosed.

You might want to know what my study question is: My research project aims to answer the question why highly short-sighted people have a higher risk to develop glaucoma. To answer this question I measure **non-invasively** blood circulation aspects of the retina at the back of the eye, the thickness of the nerve tissue (the wires that transfer visual signals towards the brain) and the visual function (visual field test) of one eye.

How long will it take and what do you have to consider: If you are interested in the study, you should be aware that the whole measurement session will take **90 minutes** and includes enlargement of one pupil to capture images of the back of the eye. Therefore, you should **not drive** or operate machinery for at least **6 hours after** the appointment.

Furthermore, you should **refrain** from **caffeinated** products, cigarettes and alcohol for **6 hours before** you volunteer for this study. These products effect the blood circulation as they lead to a vessel constriction in your whole body (including the eye).

Where do the measurements take place: All measurements will take place in the **Vision Sciences** building and the Optegra eye hospital on the University campus. Parking spaces are available at the Vision Sciences patient carpark without charges (see plan at the back of this page).

If you are interested in taking part and would like to book an appointment or if you have questions regarding this study, please contact **Katrin Hirsch** via phone: 07910-924708 or via email: k.hirsch@aston.ac.uk . The **closing date** for this study is 30th September 2018.

I am looking forward hearing from you soon.

Kind regards

Katrin Hirsch

Study invitation

Aston University Patient Consent Form

Study ID_____

TITEL OF THE PROJECT: ASSESSMENT OF STRUCTURAL AND FUNCTIONAL DIFFERENCES OF THE OCULAR FUNDUS IN MYOPIC AND EMMETROPIC HEALTHY INDIVIDUALS AND GLAUCOMA PATIENTS: AN EXPLORATORY, CROSS-SECTIONAL STUDY

LAY TITLE: Structure and Function of eyes of healthy individuals with short sightedness and glaucoma patients

Names of Investigators

Principle investigator: Ms Katrin Hirsch

Associate Investigators: Dr. Robert P. Cubbidge

Dr. Rebekka Heitmar

Initials

1. I confirm that I have read and understand the information sheet for the above study. I have had the opportunity to consider the information, ask questions and had these answered satisfactorily. ☐
2. I understand that my participation is voluntary and that I am free to withdraw at any time without giving any reason and without my legal rights being affected. ☐
3. I agree to take part in the above study. ☐

_____	_____	_____
Name of volunteer/participant	Date	Signature
_____	_____	_____
Name of Person taking Consent	Date	Signature

1 copy for Participant / 1 copy for Investigator

12/02/2018 Version: C 12.02.18

AppendixD. Distribution analysis of data

Tests of Normality

		Kolmogorov-Smirnov*			Shapiro-Wilk		
Cohort		Statistic	df	Sig.	Statistic	df	Sig.
Age	Emmetrope	0.241	40	0.000	0.710	40	0.000
	Myope	0.241	29	0.000	0.804	29	0.000
	Glaucoma	0.204	9	.200*	0.947	9	0.660
AxialLength	Emmetrope	0.060	40	.200*	0.978	40	0.620
	Myope	0.065	29	.200*	0.989	29	0.989
	Glaucoma	0.230	9	0.187	0.928	9	0.460
SphericalEquivalent	Emmetrope	0.163	40	0.009	0.922	40	0.009
	Myope	0.170	29	0.032	0.836	29	0.000
	Glaucoma	0.276	9	0.046	0.749	9	0.005
IOP	Emmetrope	0.140	40	0.047	0.958	40	0.147
	Myope	0.156	29	0.069	0.876	29	0.003
	Glaucoma	0.150	9	.200*	0.936	9	0.535
sBP	Emmetrope	0.101	40	.200*	0.975	40	0.524
	Myope	0.115	29	.200*	0.932	29	0.062
	Glaucoma	0.153	9	.200*	0.920	9	0.396
dBP	Emmetrope	0.137	40	0.056	0.930	40	0.016
	Myope	0.096	29	.200*	0.984	29	0.926
	Glaucoma	0.142	9	.200*	0.957	9	0.762

*. This is a lower bound of the true significance.

a. Lilliefors Significance Correction

Test of Homogeneity of Variance

		Levene Statistic	df1	df2	Sig.
Age	Based on Mean	0.354	2	75	0.703
	Based on Median	0.274	2	75	0.761
	Based on Median and with adjusted df	0.274	2	74.857	0.761
	Based on trimmed mean	0.447	2	75	0.641
AxialLength	Based on Mean	7.336	2	75	0.001
	Based on Median	4.269	2	75	0.018
	Based on Median and with adjusted df	4.269	2	43.489	0.020
	Based on trimmed mean	7.394	2	75	0.001
SphericalEquivalent	Based on Mean	27.247	2	75	0.000
	Based on Median	10.423	2	75	0.000
	Based on Median and with adjusted df	10.423	2	13.215	0.002
	Based on trimmed mean	22.497	2	75	0.000
IOP	Based on Mean	0.631	2	75	0.535
	Based on Median	0.788	2	75	0.458
	Based on Median and with adjusted df	0.788	2	74.796	0.458
	Based on trimmed mean	0.696	2	75	0.502
sBP	Based on Mean	0.558	2	75	0.574
	Based on Median	0.452	2	75	0.638
	Based on Median and with adjusted df	0.452	2	70.754	0.638
dPP	Based on Mean	0.329	2	75	0.720
	Based on Median	0.108	2	75	0.898
	Based on Median and with adjusted df	0.108	2	70.353	0.898
	Based on trimmed mean	0.300	2	75	0.742

Figure D.43: **Sample statistic - distribution data: age, axial length (AL), spherical equivalent (SE), intraocular pressure (IOP), systolic blood pressure (sBP) and diastolic blood pressure (dBP). Red text marks a non parametric distribution and green text marks normal distribution.**

Tests of Normality

Cohort		Kolmogorov-Smirnov[a]			Shapiro-Wilk		
		Statistic	df	Sig.	Statistic	df	Sig.
PSD	Emmetrope	0.214	36	0.000	0.700	36	0.000
	Myope	0.246	26	0.000	0.663	26	0.000
	Glaucoma	0.358	7	0.007	0.733	7	0.008
MD	Emmetrope	0.152	36	0.034	0.978	36	0.679
	Myope	0.134	26	.200*	0.927	26	0.066
	Glaucoma	0.187	7	.200*	0.980	7	0.958
C1_GHT	Emmetrope	0.256	36	0.000	0.884	36	0.001
	Myope	0.140	26	.200*	0.925	26	0.058
	Glaucoma	0.364	7	0.006	0.748	7	0.012
C2_GHT	Emmetrope	0.237	36	0.000	0.847	36	0.000
	Myope	0.205	26	0.006	0.861	26	0.002
	Glaucoma	0.346	7	0.011	0.700	7	0.004
N3_GHT	Emmetrope	0.192	36	0.002	0.884	36	0.001
	Myope	0.209	26	0.005	0.870	26	0.004
	Glaucoma	0.369	7	0.005	0.732	7	0.008
P4_GHT	Emmetrope	0.163	36	0.017	0.874	36	0.001
	Myope	0.144	26	0.178	0.893	26	0.011
	Glaucoma	0.340	7	0.014	0.758	7	0.015
P5_GHT	Emmetrope	0.161	36	0.019	0.886	36	0.001
	Myope	0.160	26	0.084	0.950	26	0.236
	Glaucoma	0.346	7	0.011	0.748	7	0.012

*. This is a lower bound of the true significance.

a. Lilliefors Significance Correction

Figure D.44: **Distribution Visual field measurements: generalised visual field loss (or MD_H), focal visual field loss PSD, hemifield differences according to the GHT pattern locations (C1, C2, N3, P4, P5). Red text marks a non parametric distribution and green text marks normal distribution.**

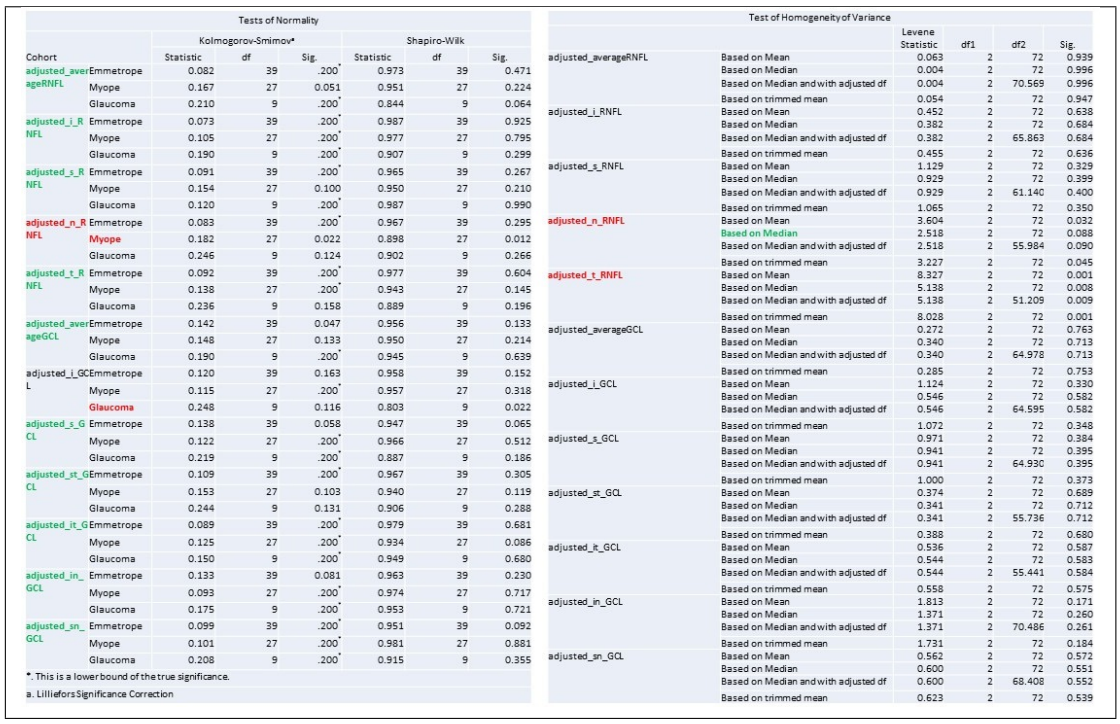

Tests of Normality

Cohort		Kolmogorov-Smirnov[a] Statistic	df	Sig.	Shapiro-Wilk Statistic	df	Sig.
adjusted_averageRNFL	Emmetrope	0.082	39	.200*	0.973	39	0.471
	Myope	0.167	27	0.051	0.951	27	0.224
	Glaucoma	0.210	9	.200*	0.844	9	0.064
adjusted_i_RNFL	Emmetrope	0.073	39	.200*	0.987	39	0.925
	Myope	0.105	27	.200*	0.977	27	0.795
	Glaucoma	0.190	9	.200*	0.907	9	0.299
adjusted_s_RNFL	Emmetrope	0.091	39	.200*	0.965	39	0.267
	Myope	0.154	27	0.100	0.950	27	0.210
	Glaucoma	0.120	9	.200*	0.987	9	0.990
adjusted_n_RNFL	Emmetrope	0.083	39	.200*	0.967	39	0.295
	Myope	0.182	27	0.022	0.898	27	0.012
	Glaucoma	0.246	9	0.124	0.902	9	0.266
adjusted_t_RNFL	Emmetrope	0.092	39	.200*	0.977	39	0.604
	Myope	0.138	27	.200*	0.943	27	0.145
	Glaucoma	0.236	9	0.158	0.889	9	0.196
adjusted_averageGCL	Emmetrope	0.142	39	0.047	0.956	39	0.133
	Myope	0.148	27	0.133	0.950	27	0.214
	Glaucoma	0.190	9	.200*	0.945	9	0.639
adjusted_i_GCL	Emmetrope	0.120	39	0.163	0.958	39	0.152
	Myope	0.115	27	.200*	0.957	27	0.318
	Glaucoma	0.248	9	0.116	0.803	9	0.022
adjusted_s_GCL	Emmetrope	0.138	39	0.058	0.947	39	0.065
	Myope	0.122	27	.200*	0.966	27	0.512
	Glaucoma	0.219	9	.200*	0.887	9	0.186
adjusted_st_GCL	Emmetrope	0.109	39	.200*	0.967	39	0.305
	Myope	0.153	27	0.103	0.940	27	0.119
	Glaucoma	0.244	9	0.131	0.906	9	0.288
adjusted_it_GCL	Emmetrope	0.089	39	.200*	0.979	39	0.681
	Myope	0.125	27	.200*	0.934	27	0.086
	Glaucoma	0.150	9	.200*	0.949	9	0.680
adjusted_in_GCL	Emmetrope	0.133	39	0.081	0.963	39	0.230
	Myope	0.093	27	.200*	0.974	27	0.717
	Glaucoma	0.175	9	.200*	0.953	9	0.721
adjusted_sn_GCL	Emmetrope	0.099	39	.200*	0.951	39	0.092
	Myope	0.101	27	.200*	0.981	27	0.881
	Glaucoma	0.208	9	.200*	0.915	9	0.355

*. This is a lower bound of the true significance.

a. Lilliefors Significance Correction

Test of Homogeneity of Variance

		Levene Statistic	df1	df2	Sig.
adjusted_averageRNFL	Based on Mean	0.063	2	72	0.939
	Based on Median	0.004	2	72	0.996
	Based on Median and with adjusted df	0.004	2	70.569	0.996
	Based on trimmed mean	0.054	2	72	0.947
adjusted_i_RNFL	Based on Mean	0.452	2	72	0.638
	Based on Median	0.382	2	72	0.684
	Based on Median and with adjusted df	0.382	2	65.863	0.684
	Based on trimmed mean	0.455	2	72	0.636
adjusted_s_RNFL	Based on Mean	1.129	2	72	0.329
	Based on Median	0.929	2	72	0.399
	Based on Median and with adjusted df	0.929	2	61.140	0.400
	Based on trimmed mean	1.065	2	72	0.350
adjusted_n_RNFL	Based on Mean	3.604	2	72	0.032
	Based on Median	2.518	2	72	0.088
	Based on Median and with adjusted df	2.518	2	55.984	0.090
	Based on trimmed mean	3.227	2	72	0.045
adjusted_t_RNFL	Based on Mean	8.327	2	72	0.001
	Based on Median	5.138	2	72	0.008
	Based on Median and with adjusted df	5.138	2	51.209	0.009
	Based on trimmed mean	8.028	2	72	0.001
adjusted_averageGCL	Based on Mean	0.272	2	72	0.763
	Based on Median	0.340	2	72	0.713
	Based on Median and with adjusted df	0.340	2	64.978	0.713
	Based on trimmed mean	0.285	2	72	0.753
adjusted_i_GCL	Based on Mean	1.124	2	72	0.330
	Based on Median	0.546	2	72	0.582
	Based on Median and with adjusted df	0.546	2	64.595	0.582
	Based on trimmed mean	1.072	2	72	0.348
adjusted_s_GCL	Based on Mean	0.971	2	72	0.384
	Based on Median	0.941	2	72	0.395
	Based on Median and with adjusted df	0.941	2	64.930	0.395
	Based on trimmed mean	1.000	2	72	0.373
adjusted_st_GCL	Based on Mean	0.374	2	72	0.689
	Based on Median	0.341	2	72	0.712
	Based on Median and with adjusted df	0.341	2	55.736	0.712
	Based on trimmed mean	0.388	2	72	0.680
adjusted_it_GCL	Based on Mean	0.536	2	72	0.587
	Based on Median	0.544	2	72	0.583
	Based on Median and with adjusted df	0.544	2	55.441	0.584
	Based on trimmed mean	0.558	2	72	0.575
adjusted_in_GCL	Based on Mean	1.813	2	72	0.171
	Based on Median	1.371	2	72	0.260
	Based on Median and with adjusted df	1.371	2	70.486	0.261
	Based on trimmed mean	1.731	2	72	0.184
adjusted_sn_GCL	Based on Mean	0.562	2	72	0.572
	Based on Median	0.600	2	72	0.551
	Based on Median and with adjusted df	0.600	2	68.408	0.552
	Based on trimmed mean	0.623	2	72	0.539

Figure D.45: **Distribution RNFL and GCL thickness measurements. Red text marks a non parametric distribution and green text marks normal distribution.**

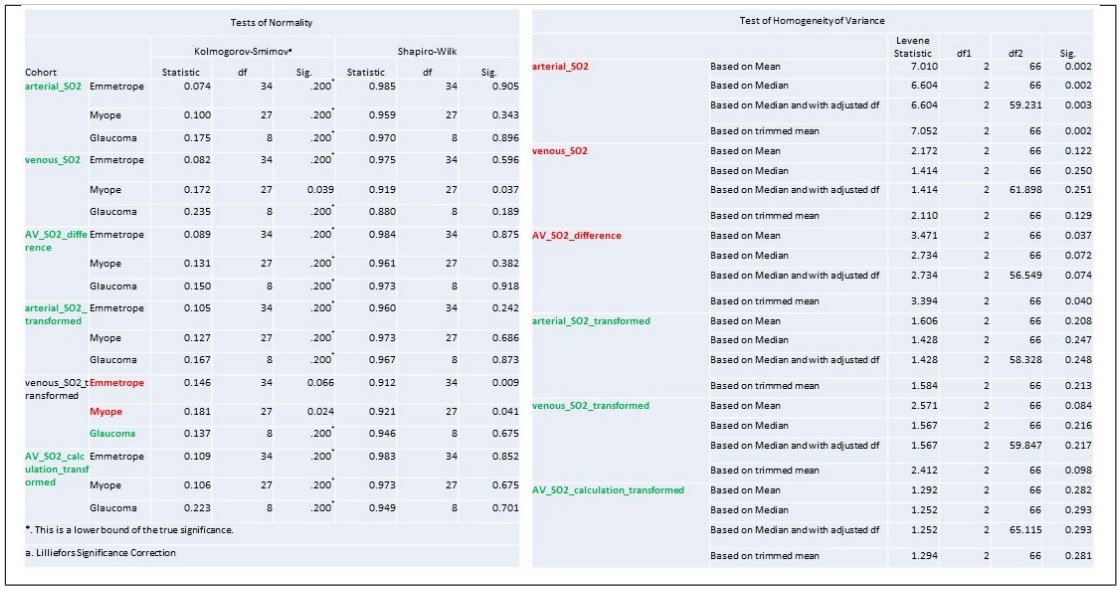

Tests of Normality

Cohort		Kolmogorov-Smirnov[a] Statistic	df	Sig.	Shapiro-Wilk Statistic	df	Sig.
arterial_SO2	Emmetrope	0.074	34	.200*	0.985	34	0.905
	Myope	0.100	27	.200*	0.959	27	0.343
	Glaucoma	0.175	8	.200*	0.970	8	0.896
venous_SO2	Emmetrope	0.082	34	.200*	0.975	34	0.596
	Myope	0.172	27	0.039	0.919	27	0.037
	Glaucoma	0.235	8	.200*	0.880	8	0.189
AV_SO2_difference	Emmetrope	0.089	34	.200*	0.984	34	0.875
	Myope	0.131	27	.200*	0.961	27	0.382
	Glaucoma	0.150	8	.200*	0.973	8	0.918
arterial_SO2_transformed	Emmetrope	0.105	34	.200*	0.960	34	0.242
	Myope	0.127	27	.200*	0.973	27	0.686
	Glaucoma	0.167	8	.200*	0.967	8	0.873
venous_SO2_transformed	Emmetrope	0.146	34	0.066	0.912	34	0.009
	Myope	0.181	27	0.024	0.921	27	0.041
	Glaucoma	0.137	8	.200*	0.946	8	0.675
AV_SO2_calculation_transformed	Emmetrope	0.109	34	.200*	0.983	34	0.852
	Myope	0.106	27	.200*	0.973	27	0.675
	Glaucoma	0.223	8	.200*	0.949	8	0.701

*. This is a lower bound of the true significance.

a. Lilliefors Significance Correction

Test of Homogeneity of Variance

		Levene Statistic	df1	df2	Sig.
arterial_SO2	Based on Mean	7.010	2	66	0.002
	Based on Median	6.604	2	66	0.002
	Based on Median and with adjusted df	6.604	2	59.231	0.003
	Based on trimmed mean	7.052	2	66	0.002
venous_SO2	Based on Mean	2.172	2	66	0.122
	Based on Median	1.414	2	66	0.250
	Based on Median and with adjusted df	1.414	2	61.898	0.251
	Based on trimmed mean	2.110	2	66	0.129
AV_SO2_difference	Based on Mean	3.471	2	66	0.037
	Based on Median	2.734	2	66	0.072
	Based on Median and with adjusted df	2.734	2	56.549	0.074
	Based on trimmed mean	3.394	2	66	0.040
arterial_SO2_transformed	Based on Mean	1.606	2	66	0.208
	Based on Median	1.428	2	66	0.247
	Based on Median and with adjusted df	1.428	2	58.328	0.248
	Based on trimmed mean	1.584	2	66	0.213
venous_SO2_transformed	Based on Mean	2.571	2	66	0.084
	Based on Median	1.567	2	66	0.216
	Based on Median and with adjusted df	1.567	2	59.847	0.217
	Based on trimmed mean	2.412	2	66	0.098
AV_SO2_calculation_transformed	Based on Mean	1.292	2	66	0.282
	Based on Median	1.252	2	66	0.293
	Based on Median and with adjusted df	1.252	2	65.115	0.293
	Based on trimmed mean	1.294	2	66	0.281

Figure D.46: **Distribution SO2 raw data and transformed (adjusted for retinal pigmentation) SO2 data. Red text marks a non parametric distribution and green text marks normal distribution.**

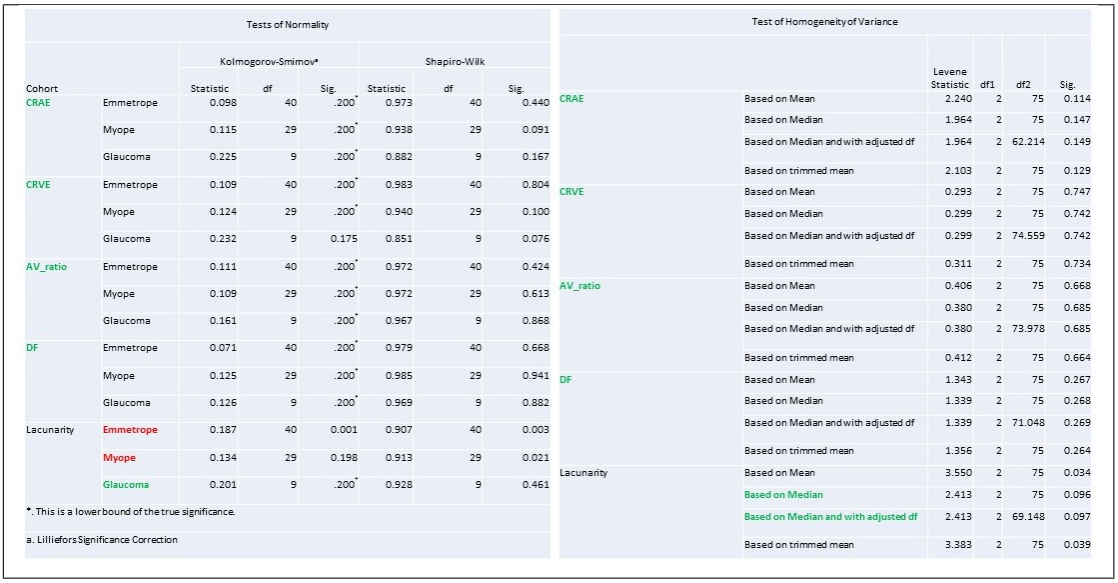

Tests of Normality

Cohort		Kolmogorov-Smirnov[a] Statistic	df	Sig.	Shapiro-Wilk Statistic	df	Sig.
CRAE	Emmetrope	0.098	40	.200*	0.973	40	0.440
	Myope	0.115	29	.200*	0.938	29	0.091
	Glaucoma	0.225	9	.200*	0.882	9	0.167
CRVE	Emmetrope	0.109	40	.200*	0.983	40	0.804
	Myope	0.124	29	.200*	0.940	29	0.100
	Glaucoma	0.232	9	0.175	0.851	9	0.076
AV_ratio	Emmetrope	0.111	40	.200*	0.972	40	0.424
	Myope	0.109	29	.200*	0.972	29	0.613
	Glaucoma	0.161	9	.200*	0.967	9	0.868
DF	Emmetrope	0.071	40	.200*	0.979	40	0.668
	Myope	0.125	29	.200*	0.985	29	0.941
	Glaucoma	0.126	9	.200*	0.969	9	0.882
Lacunarity	Emmetrope	0.187	40	0.001	0.907	40	0.003
	Myope	0.134	29	0.198	0.913	29	0.021
	Glaucoma	0.201	9	.200*	0.928	9	0.461

*. This is a lower bound of the true significance.

a. Lilliefors Significance Correction

Test of Homogeneity of Variance

		Levene Statistic	df1	df2	Sig.
CRAE	Based on Mean	2.240	2	75	0.114
	Based on Median	1.964	2	75	0.147
	Based on Median and with adjusted df	1.964	2	62.214	0.149
	Based on trimmed mean	2.103	2	75	0.129
CRVE	Based on Mean	0.293	2	75	0.747
	Based on Median	0.299	2	75	0.742
	Based on Median and with adjusted df	0.299	2	74.559	0.742
	Based on trimmed mean	0.311	2	75	0.734
AV_ratio	Based on Mean	0.406	2	75	0.668
	Based on Median	0.380	2	75	0.685
	Based on Median and with adjusted df	0.380	2	73.978	0.685
	Based on trimmed mean	0.412	2	75	0.664
DF	Based on Mean	1.343	2	75	0.267
	Based on Median	1.339	2	75	0.268
	Based on Median and with adjusted df	1.339	2	71.048	0.269
	Based on trimmed mean	1.356	2	75	0.264
Lacunarity	Based on Mean	3.550	2	75	0.034
	Based on Median	2.413	2	75	0.096
	Based on Median and with adjusted df	2.413	2	69.148	0.097
	Based on trimmed mean	3.383	2	75	0.039

Figure D.47: **Distribution vessel calibres (CRAE and CRVE and AVR) as well as retinal vessel complexity measurements (Df and lacunarity). Red text marks a non parametric distribution and green text marks normal distribution.**

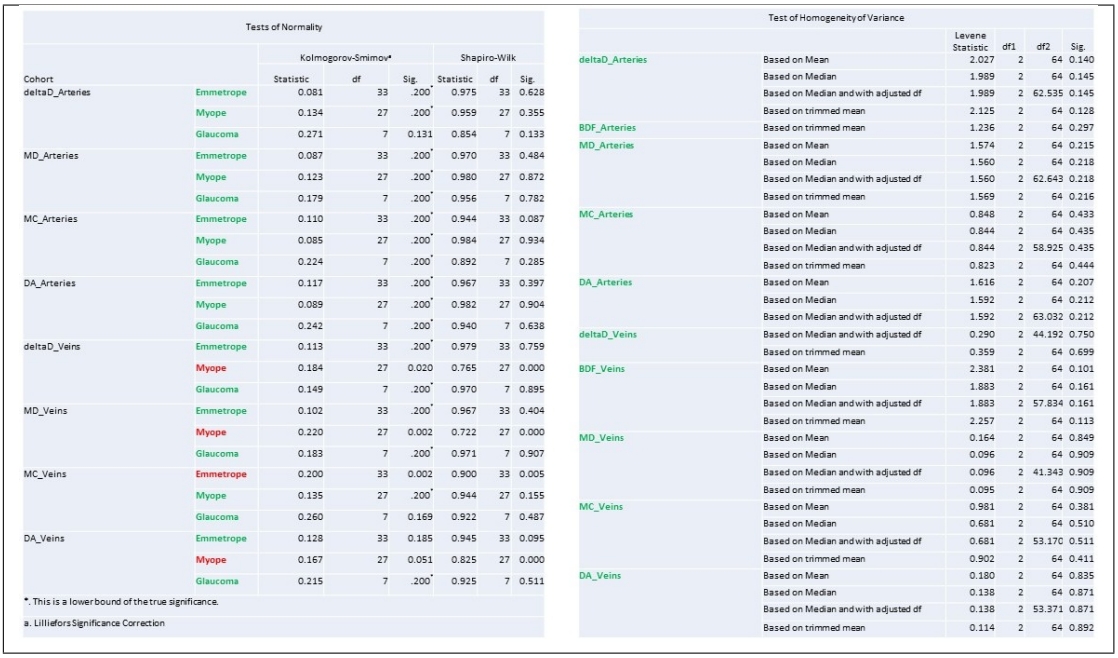

Tests of Normality

Cohort		Kolmogorov-Smirnov[a] Statistic	df	Sig.	Shapiro-Wilk Statistic	df	Sig.
deltaD_Arteries	Emmetrope	0.081	33	.200*	0.975	33	0.628
	Myope	0.134	27	.200*	0.959	27	0.355
	Glaucoma	0.271	7	0.131	0.854	7	0.133
MD_Arteries	Emmetrope	0.087	33	.200*	0.970	33	0.484
	Myope	0.123	27	.200*	0.980	27	0.872
	Glaucoma	0.179	7	.200*	0.956	7	0.782
MC_Arteries	Emmetrope	0.110	33	.200*	0.944	33	0.087
	Myope	0.085	27	.200*	0.984	27	0.934
	Glaucoma	0.224	7	.200*	0.892	7	0.285
DA_Arteries	Emmetrope	0.117	33	.200*	0.967	33	0.397
	Myope	0.089	27	.200*	0.982	27	0.904
	Glaucoma	0.242	7	.200*	0.940	7	0.638
deltaD_Veins	Emmetrope	0.113	33	.200*	0.979	33	0.759
	Myope	0.184	27	0.020	0.765	27	0.000
	Glaucoma	0.149	7	.200*	0.970	7	0.895
MD_Veins	Emmetrope	0.102	33	.200*	0.967	33	0.404
	Myope	0.220	27	0.002	0.722	27	0.000
	Glaucoma	0.183	7	.200*	0.971	7	0.907
MC_Veins	Emmetrope	0.200	33	0.002	0.900	33	0.005
	Myope	0.135	27	.200*	0.944	27	0.155
	Glaucoma	0.260	7	0.169	0.922	7	0.487
DA_Veins	Emmetrope	0.128	33	0.185	0.945	33	0.095
	Myope	0.167	27	0.051	0.825	27	0.000
	Glaucoma	0.215	7	.200*	0.925	7	0.511

*. This is a lower bound of the true significance.

a. Lilliefors Significance Correction

Test of Homogeneity of Variance

		Levene Statistic	df1	df2	Sig.
deltaD_Arteries	Based on Mean	2.027	2	64	0.140
	Based on Median	1.989	2	64	0.145
	Based on Median and with adjusted df	1.989	2	62.535	0.145
	Based on trimmed mean	2.125	2	64	0.128
BDF_Arteries	Based on trimmed mean	1.236	2	64	0.297
MD_Arteries	Based on Mean	1.574	2	64	0.215
	Based on Median	1.560	2	64	0.218
	Based on Median and with adjusted df	1.560	2	62.643	0.218
	Based on trimmed mean	1.569	2	64	0.216
MC_Arteries	Based on Mean	0.848	2	64	0.433
	Based on Median	0.844	2	64	0.435
	Based on Median and with adjusted df	0.844	2	58.925	0.435
	Based on trimmed mean	0.823	2	64	0.444
DA_Arteries	Based on Mean	1.616	2	64	0.207
	Based on Median	1.592	2	64	0.212
	Based on Median and with adjusted df	1.592	2	63.032	0.212
deltaD_Veins	Based on Median and with adjusted df	0.290	2	44.192	0.750
	Based on trimmed mean	0.359	2	64	0.699
BDF_Veins	Based on Mean	2.381	2	64	0.101
	Based on Median	1.883	2	64	0.161
	Based on Median and with adjusted df	1.883	2	57.834	0.161
	Based on trimmed mean	2.257	2	64	0.113
MD_Veins	Based on Mean	0.164	2	64	0.849
	Based on Median	0.096	2	64	0.909
	Based on Median and with adjusted df	0.096	2	41.343	0.909
	Based on trimmed mean	0.095	2	64	0.909
MC_Veins	Based on Mean	0.981	2	64	0.381
	Based on Median	0.681	2	64	0.510
	Based on Median and with adjusted df	0.681	2	53.170	0.511
	Based on trimmed mean	0.902	2	64	0.411
DA_Veins	Based on Mean	0.180	2	64	0.835
	Based on Median	0.138	2	64	0.871
	Based on Median and with adjusted df	0.138	2	53.371	0.871
	Based on trimmed mean	0.114	2	64	0.892

Figure D.48: **Distribution SDRA results (referred to as retinal vessel reactivity or retinal vessel function). Red text marks a non parametric distribution and green text marks normal distribution.**

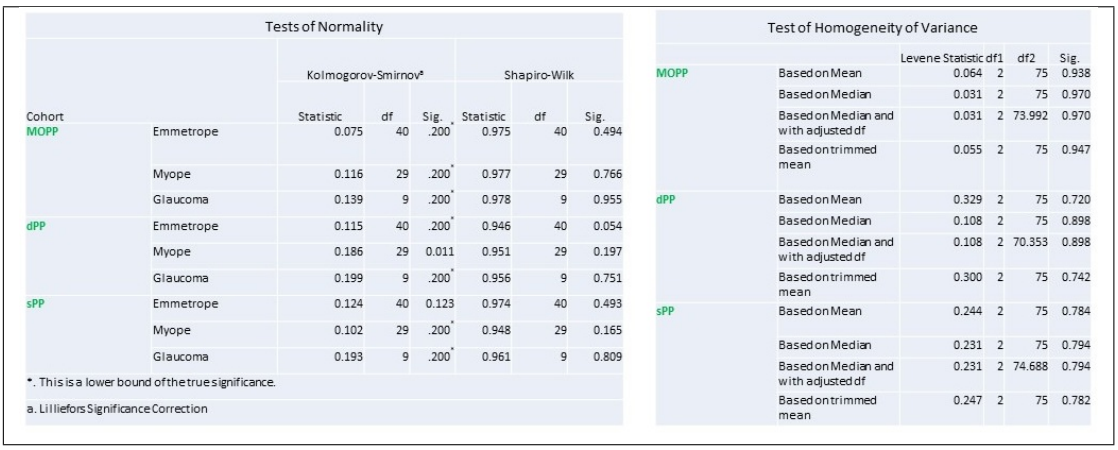

Tests of Normality

		Kolmogorov-Smirnov[a]			Shapiro-Wilk		
Cohort		Statistic	df	Sig.	Statistic	df	Sig.
MOPP	Emmetrope	0.075	40	.200*	0.975	40	0.494
	Myope	0.116	29	.200*	0.977	29	0.766
	Glaucoma	0.139	9	.200*	0.978	9	0.955
dPP	Emmetrope	0.115	40	.200*	0.946	40	0.054
	Myope	0.186	29	0.011	0.951	29	0.197
	Glaucoma	0.199	9	.200*	0.956	9	0.751
sPP	Emmetrope	0.124	40	0.123	0.974	40	0.493
	Myope	0.102	29	.200*	0.948	29	0.165
	Glaucoma	0.193	9	.200*	0.961	9	0.809

*. This is a lower bound of the true significance.

a. Lilliefors Significance Correction

Test of Homogeneity of Variance

		Levene Statistic	df1	df2	Sig.
MOPP	Based on Mean	0.064	2	75	0.938
	Based on Median	0.031	2	75	0.970
	Based on Median and with adjusted df	0.031	2	73.992	0.970
	Based on trimmed mean	0.055	2	75	0.947
dPP	Based on Mean	0.329	2	75	0.720
	Based on Median	0.108	2	75	0.898
	Based on Median and with adjusted df	0.108	2	70.353	0.898
	Based on trimmed mean	0.300	2	75	0.742
sPP	Based on Mean	0.244	2	75	0.784
	Based on Median	0.231	2	75	0.794
	Based on Median and with adjusted df	0.231	2	74.688	0.794
	Based on trimmed mean	0.247	2	75	0.782

Figure D.49: **Distribution ocular perfusion pressure calculations: mean ocular perfusion pressure (MOPP), diastolic perfusion pressure (dPP) and systolic perfusion pressure (sPP). Red text marks a non parametric distribution and green text marks normal distribution.**

AppendixE. Correlation matrices and correlation data plots

FDR		sPP	dPP	arterial_SO2	venous_SO2	CRAE	CRVE	DF	deltaD_Arteries	MD_Arteries	MC_Arteries	DA_Arteries	deltaD_Veins	MD_Veins	MC_Veins	DA_Veins
sPP	Pearson	1	.695**	0.236	0.255	-0.227	0.069	-.356*	0.054	0.028	-0.058	-0.016	0.062	0.071	0.048	0.076
	Sig. (2-tailed)		0.000	0.179	0.146	0.160	0.671	0.024	0.765	0.879	0.747	0.930	0.731	0.696	0.793	0.675
	N	40	40	34	34	40	40	40	33	33	33	33	33	33	33	33
dPP	Pearson	.695**	1	0.243	0.243	-0.111	0.149	-0.292	0.283	0.307	-0.048	0.171	0.117	0.195	-0.105	0.098
	Sig. (2-tailed)	0.000		0.166	0.165	0.496	0.358	0.067	0.111	0.082	0.789	0.343	0.518	0.277	0.561	0.588
	N	40	40	34	34	40	40	40	33	33	33	33	33	33	33	33
arterial_SO2	Pearson	0.236	0.243	1	.453**	-0.053	-0.002	0.068	0.021	-0.167	0.005	-0.121	-0.114	-0.101	-0.097	-0.130
	Sig. (2-tailed)	0.179	0.166		0.007	0.767	0.990	0.704	0.914	0.395	0.979	0.538	0.564	0.609	0.622	0.509
	N	34	34	34	34	34	34	34	28	28	28	28	28	28	28	28
venous_SO2	Pearson	0.255	0.243	.453**	1	-.401*	-.383*	-.371*	-0.278	-0.291	-0.226	-0.337	-.404*	-0.352	-0.034	-0.300
	Sig. (2-tailed)	0.146	0.165	0.007		0.019	0.026	0.031	0.151	0.133	0.247	0.079	0.033	0.066	0.862	0.121
	N	34	34	34	34	34	34	34	28	28	28	28	28	28	28	28
CRAE	Pearson	-0.227	-0.111	-0.053	-.401*	1	.673**	0.311	0.052	-0.091	-0.213	-0.180	-0.189	-0.254	-0.231	-0.309
	Sig. (2-tailed)	0.160	0.496	0.767	0.019		0.000	0.050	0.772	0.613	0.235	0.315	0.292	0.154	0.195	0.080
	N	40	40	34	34	40	40	40	33	33	33	33	33	33	33	33
CRVE	Pearson	0.069	0.149	-0.002	-.383*	.673**	1	0.152	0.207	0.141	-0.114	0.024	0.209	0.154	-0.120	0.053
	Sig. (2-tailed)	0.671	0.358	0.990	0.026	0.000		0.350	0.248	0.435	0.528	0.894	0.242	0.392	0.506	0.771
	N	40	40	34	34	40	40	40	33	33	33	33	33	33	33	33
DF	Pearson	-.356*	-0.292	0.068	-.371*	0.311	0.152	1	-0.064	-0.234	0.148	-0.060	0.312	0.202	0.098	0.197
	Sig. (2-tailed)	0.024	0.067	0.704	0.031	0.050	0.350		0.722	0.190	0.412	0.741	0.077	0.259	0.588	0.272
	N	40	40	34	34	40	40	40	33	33	33	33	33	33	33	33
deltaD_Arteries	Pearson	0.054	0.283	0.021	-0.278	0.052	0.207	-0.064	1	.817**	0.331	.716**	0.166	0.142	0.186	0.207
	Sig. (2-tailed)	0.765	0.111	0.914	0.151	0.772	0.248	0.722		0.000	0.060	0.000	0.355	0.430	0.299	0.247
	N	33	33	28	28	33	33	33	33	33	33	33	33	33	33	33
MD_Arteries	Pearson	0.028	0.307	-0.167	-0.291	-0.091	0.141	-0.234	.817**	1	0.334	.835**	0.205	0.252	0.071	0.231
	Sig. (2-tailed)	0.879	0.082	0.395	0.133	0.613	0.435	0.190	0.000		0.057	0.000	0.253	0.158	0.693	0.196
	N	33	33	28	28	33	33	33	33	33	33	33	33	33	33	33
MC_Arteries	Pearson	-0.058	-0.048	0.005	-0.226	-0.213	-0.114	0.148	0.331	0.334	1	.797**	0.261	.387*	0.134	.358*
	Sig. (2-tailed)	0.747	0.789	0.979	0.247	0.235	0.528	0.412	0.060	0.057		0.000	0.143	0.026	0.458	0.041
	N	33	33	28	28	33	33	33	33	33	33	33	33	33	33	33
DA_Arteries	Pearson	-0.016	0.171	-0.121	-0.337	-0.180	0.024	-0.060	.716**	.835**	.797**	1	0.285	.390*	0.123	.359*
	Sig. (2-tailed)	0.930	0.343	0.538	0.079	0.315	0.894	0.741	0.000	0.000	0.000		0.108	0.025	0.495	0.040
	N	33	33	28	28	33	33	33	33	33	33	33	33	33	33	33
deltaD_Veins	Pearson	0.062	0.117	-0.114	-.404*	-0.189	0.209	0.312	0.166	0.205	0.261	0.285	1	.906**	0.223	.792**
	Sig. (2-tailed)	0.731	0.518	0.564	0.033	0.292	0.242	0.077	0.355	0.253	0.143	0.108		0.000	0.212	0.000
	N	33	33	28	28	33	33	33	33	33	33	33	33	33	33	33
MD_Veins	Pearson	0.071	0.195	-0.101	-0.352	-0.254	0.154	0.202	0.142	0.252	.387*	.390*	.906**	1	0.234	.870**
	Sig. (2-tailed)	0.696	0.277	0.609	0.066	0.154	0.392	0.259	0.430	0.158	0.026	0.025	0.000		0.189	0.000
	N	33	33	28	28	33	33	33	33	33	33	33	33	33	33	33
MC_Veins	Pearson	0.048	-0.105	-0.097	-0.034	-0.231	-0.120	0.098	0.186	0.071	0.134	0.123	0.223	0.234	1	.683**
	Sig. (2-tailed)	0.793	0.561	0.622	0.862	0.195	0.506	0.588	0.299	0.693	0.458	0.495	0.212	0.189		0.000
	N	33	33	28	28	33	33	33	33	33	33	33	33	33	33	33
DA_Veins	Pearson	0.076	0.098	-0.130	-0.300	-0.309	0.053	0.197	0.207	0.231	.358*	.359*	.792**	.870**	.683**	1
	Sig. (2-tailed)	0.675	0.588	0.509	0.121	0.080	0.771	0.272	0.247	0.196	0.041	0.040	0.000	0.000	0.000	
	N	33	33	28	28	33	33	33	33	33	33	33	33	33	33	33

a

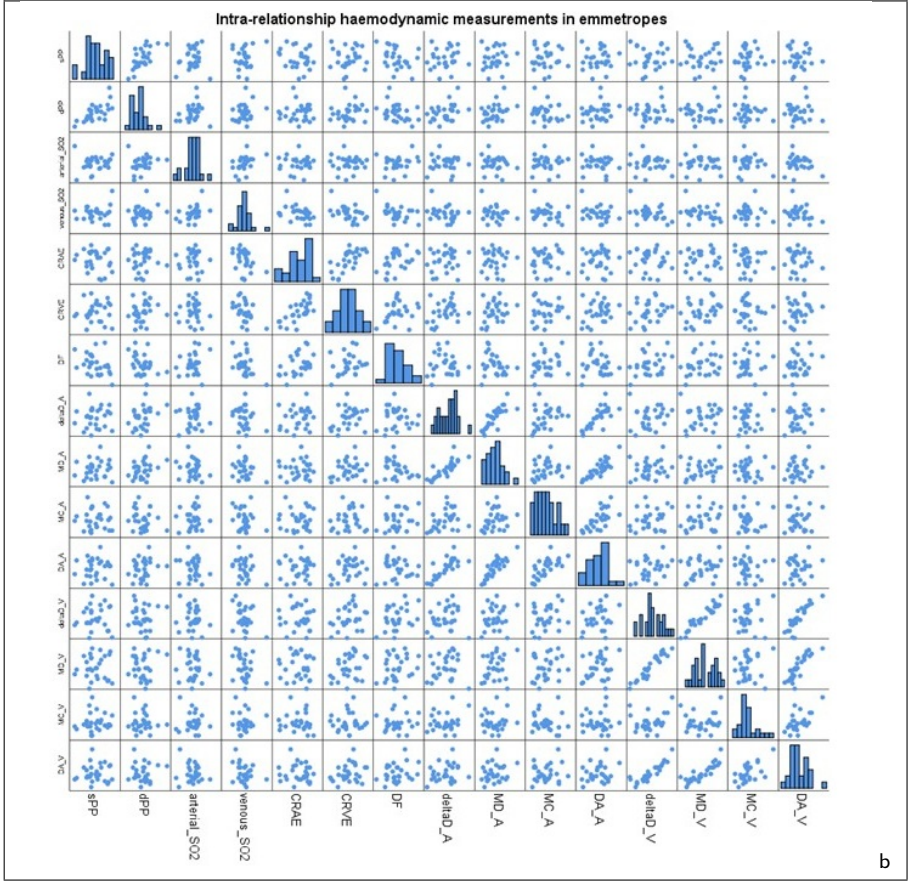

b

Figure E.50: **Haemodynamic intra-relationships analysed using Pearson correlation for the emmetropic cohort (a). Correlations wit p< .05 are marked in blue and the cell marking significance had the same colour code if the correlations remained statistically significant after controlling the false discovery rate (FDR, i=86, q= .05). A data-point representation of the same relationships shows graph b.**

FDR		sPP	dPP	arterial_SO2	venous_SO2	CRAE	CRVE	DF	deltaD_Arteries	MD_Arteries	MC_Arteries	DA_Arteries	deltaD_Veins	MD_Veins	MC_Veins	DA_Veins
sPP	Pearson	1	.412*	0.265	-0.086	-0.123	-0.073	-0.089	0.055	0.116	-0.010	0.085	0.278	0.206	0.036	0.185
	Sig. (2-		0.026	0.182	0.669	0.525	0.706	0.647	0.784	0.564	0.961	0.673	0.160	0.302	0.860	0.357
	N	29	29	27	27	29	29	29	27	27	27	27	27	27	27	27
dPP	Pearson	.412*	1	0.344	0.144	0.137	0.001	-0.205	0.331	.394*	-0.024	0.249	0.145	0.115	-0.069	0.075
	Sig. (2-	0.026		0.079	0.474	0.480	0.996	0.286	0.092	0.042	0.905	0.211	0.470	0.568	0.734	0.710
	N	29	29	27	27	29	29	29	27	27	27	27	27	27	27	27
arterial_SO2	Pearson	0.265	0.344	1	.472*	-0.097	-0.287	-0.297	.439*	.460*	-0.006	0.297	.419*	.425*	0.012	0.365
	Sig. (2-	0.182	0.079		0.013	0.632	0.146	0.132	0.010	0.018	0.977	0.141	0.033	0.030	0.954	0.066
	N	27	27	27	27	27	27	27	26	26	26	26	26	26	26	26
venous_SO2	Pearson	-0.086	0.144	.472*	1	-0.025	-0.279	.491*	0.061	-0.018	-0.299	-0.153	.528**	.499*	0.082	.453*
	Sig. (2-	0.669	0.474	0.013		0.900	0.159	0.009	0.766	0.931	0.138	0.455	0.006	0.009	0.691	0.020
	N	27	27	27	27	27	27	27	26	26	26	26	26	26	26	26
CRAE	Pearson	-0.123	0.137	-0.097	-0.025	1	.700**	0.048	-0.122	-0.080	0.108	-0.017	-0.087	-0.028	-0.104	-0.062
	Sig. (2-	0.525	0.480	0.632	0.900		0.000	0.804	0.545	0.692	0.592	0.932	0.667	0.889	0.607	0.760
	N	29	29	27	27	29	29	29	27	27	27	27	27	27	27	27
CRVE	Pearson	-0.073	0.001	-0.287	-0.279	.700**	1	0.188	-0.142	-0.076	0.103	-0.008	-0.149	-0.245	-0.022	-0.220
	Sig. (2-	0.706	0.996	0.146	0.159	0.000		0.328	0.480	0.705	0.610	0.967	0.459	0.218	0.915	0.271
	N	29	29	27	27	29	29	29	27	27	27	27	27	27	27	27
DF	Pearson	-0.089	-0.205	-0.297	-.491*	0.048	0.188	1	0.077	0.005	0.000	0.001	-.456*	-.496**	0.111	.388*
	Sig. (2-	0.647	0.286	0.132	0.009	0.804	0.328		0.703	0.980	0.998	0.997	0.017	0.009	0.581	0.046
	N	29	29	27	27	29	29	29	27	27	27	27	27	27	27	27
deltaD_Arteries	Pearson	0.055	0.331	.439*	0.061	-0.122	-0.142	0.077	1	.907**	.507**	.843**	0.111	0.167	0.312	0.246
	Sig. (2-	0.784	0.092	0.010	0.766	0.545	0.480	0.703		0.000	0.007	0.000	0.583	0.404	0.113	0.216
	N	27	27	26	26	27	27	27	27	27	27	27	27	27	27	27
MD_Arteries	Pearson	0.116	.394*	.460*	-0.018	-0.080	-0.076	0.005	.907**	1	.541**	.916**	0.124	0.239	0.291	0.298
	Sig. (2-	0.564	0.042	0.018	0.931	0.692	0.705	0.980	0.000		0.004	0.000	0.536	0.230	0.141	0.131
	N	27	27	26	26	27	27	27	27	27	27	27	27	27	27	27
MC_Arteries	Pearson	-0.010	-0.024	-0.006	-0.299	0.108	0.103	0.000	.507**	.541**	1	.831**	-0.020	0.039	0.284	0.124
	Sig. (2-	0.961	0.905	0.977	0.138	0.592	0.610	0.998	0.007	0.004		0.000	0.921	0.847	0.150	0.538
	N	27	27	26	26	27	27	27	27	27	27	27	27	27	27	27
DA_Arteries	Pearson	0.085	0.249	0.297	-0.153	-0.017	-0.008	0.001	.843**	.916**	.831**	1	0.068	0.173	0.326	0.253
	Sig. (2-	0.673	0.211	0.141	0.455	0.932	0.967	0.997	0.000	0.000	0.000		0.738	0.387	0.097	0.203
	N	27	27	26	26	27	27	27	27	27	27	27	27	27	27	27
deltaD_Veins	Pearson	0.278	0.145	.419*	.528**	-0.087	-0.149	-.456*	0.111	0.124	-0.020	0.068	1	.903**	0.365	.888**
	Sig. (2-	0.160	0.470	0.033	0.006	0.667	0.459	0.017	0.583	0.536	0.921	0.738		0.000	0.061	0.000
	N	27	27	26	26	27	27	27	27	27	27	27	27	27	27	27
MD_Veins	Pearson	0.206	0.115	.425*	.499*	-0.028	-0.245	-.496**	0.167	0.239	0.039	0.173	.903**	1	0.311	.963**
	Sig. (2-	0.302	0.568	0.030	0.009	0.889	0.218	0.009	0.404	0.230	0.847	0.387	0.000		0.114	0.000
	N	27	27	26	26	27	27	27	27	27	27	27	27	27	27	27
MC_Veins	Pearson	0.036	-0.069	0.012	0.082	-0.104	-0.022	0.111	0.312	0.291	0.284	0.326	0.365	0.311	1	.585**
	Sig. (2-	0.860	0.734	0.954	0.691	0.607	0.915	0.581	0.113	0.141	0.150	0.097	0.061	0.114		0.000
	N	27	27	26	26	27	27	27	27	27	27	27	27	27	27	27
DA_Veins	Pearson	0.185	0.075	0.365	.453*	-0.062	-0.220	-.388*	0.246	0.298	0.124	0.253	.888**	.963**	.585**	1
	Sig. (2-	0.357	0.710	0.066	0.020	0.760	0.271	0.046	0.216	0.131	0.538	0.203	0.000	0.000	0.001	
	N	27	27	26	26	27	27	27	27	27	27	27	27	27	27	27

a

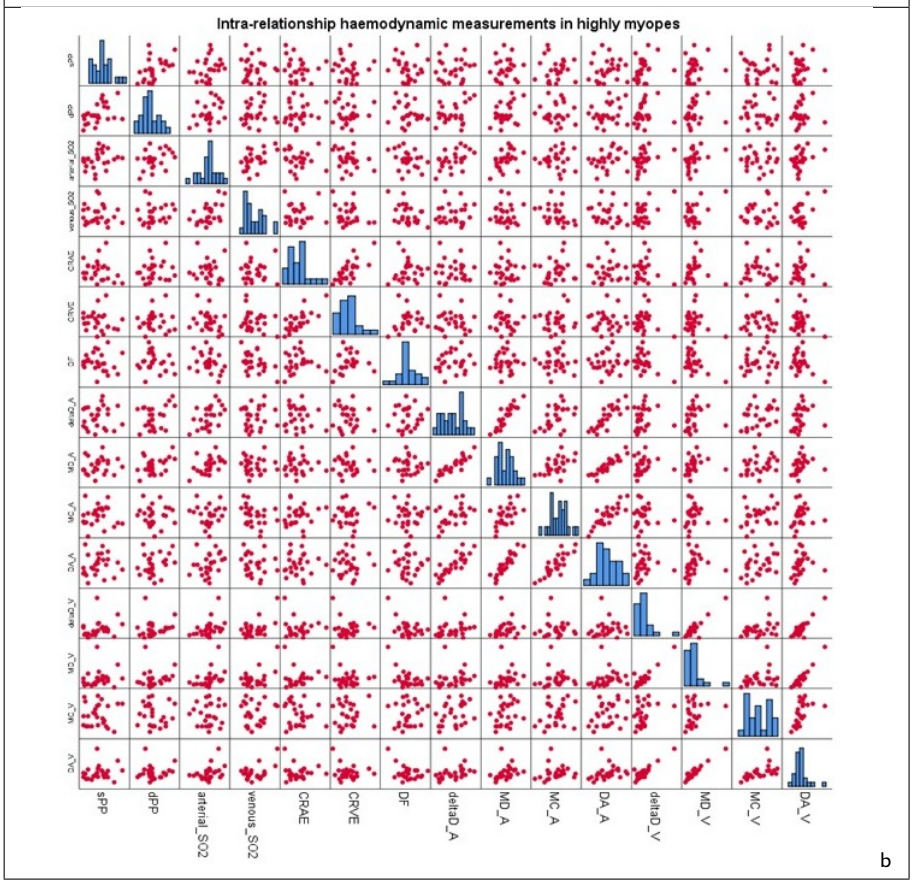

b

Figure E.51: **Haemodynamic intra-relationships analysed using Pearson correlation for the highly myopic cohort (a). Correlations wit p< .05 are marked in red and the cell marking significance had the same colour code if the correlations remained statistically significant after controlling the false discovery rate (FDR, i=86, q= .05). A data-point representation of the same relationships shows graph b.**

FDR		sPP	dPP	arterial_SO2	venous_SO2	CRAE	CRVE	DF	deltaD_Arteries	MD_Arteries	MC_Arteries	DA_Arteries	deltaD_Veins	MD_Veins	MC_Veins	DA_Veins
sPP	Pearson	1	.741*	0.414	-0.246	-.695*	-0.640	-0.289	0.180	0.073	-0.155	-0.019	0.321	0.290	-0.720	0.005
	Sig. (2-		0.022	0.308	0.558	0.038	0.063	0.450	0.699	0.877	0.739	0.967	0.482	0.528	0.068	0.991
	N	9	9	8	8	9	9	9	7	7	7	7	7	7	7	7
dPP	Pearson	.741*	1	0.241	-0.516	-0.483	-0.597	-0.594	0.263	0.296	-0.077	0.177	0.264	0.309	-0.329	0.140
	Sig. (2-	0.022		0.565	0.190	0.188	0.089	0.092	0.569	0.519	0.869	0.705	0.567	0.500	0.471	0.764
	N	9	9	8	8	9	9	9	7	7	7	7	7	7	7	7
arterial_SO2	Pearson	0.414	0.241	1	-0.126	-0.616	-0.544	0.195	0.628	0.773	0.706	.919**	-0.225	-0.264	-0.628	-0.367
	Sig. (2-	0.308	0.565		0.767	0.104	0.164	0.643	0.182	0.072	0.117	0.010	0.668	0.613	0.182	0.474
	N	8	8	8	8	8	8	8	6	6	6	6	6	6	6	6
venous_SO2	Pearson	-0.246	-0.516	-0.126	1	-0.271	-0.098	0.198	-0.610	-0.635	-0.204	-0.575	0.100	0.214	.871*	0.367
	Sig. (2-	0.558	0.190	0.767		0.517	0.817	0.639	0.198	0.176	0.698	0.232	0.851	0.683	0.024	0.474
	N	8	8	8	8	8	8	8	6	6	6	6	6	6	6	6
CRAE	Pearson	-.695*	-0.483	-0.616	-0.271	1	0.648	-0.033	-0.191	-0.148	0.281	0.032	-0.348	-0.394	0.422	-0.186
	Sig. (2-	0.038	0.188	0.104	0.517		0.059	0.933	0.681	0.752	0.541	0.945	0.444	0.382	0.346	0.690
	N	9	9	8	8	9	9	9	7	7	7	7	7	7	7	7
CRVE	Pearson	-0.640	-0.597	-0.544	-0.098	0.648	1	0.304	-0.292	-0.380	-0.425	-0.459	-0.301	-0.382	0.069	-0.288
	Sig. (2-	0.063	0.089	0.164	0.817	0.059		0.426	0.524	0.400	0.341	0.301	0.512	0.398	0.883	0.532
	N	9	9	8	8	9	9	9	7	7	7	7	7	7	7	7
DF	Pearson	-0.289	-0.594	0.195	0.198	-0.033	0.304	1	0.095	0.104	0.051	0.084	-0.386	-0.415	0.015	-0.348
	Sig. (2-	0.450	0.092	0.643	0.639	0.933	0.426		0.839	0.824	0.914	0.857	0.392	0.354	0.975	0.445
	N	9	9	8	8	9	9	9	7	7	7	7	7	7	7	7
deltaD_Arteries	Pearson	0.180	0.263	0.628	-0.610	-0.191	-0.292	0.095	1	.950**	0.362	.817*	0.379	0.272	0.088	0.245
	Sig. (2-	0.699	0.569	0.182	0.198	0.681	0.524	0.839		0.001	0.425	0.025	0.402	0.555	0.851	0.597
	N	7	7	6	6	7	7	7	7	7	7	7	7	7	7	7
MD_Arteries	Pearson	0.073	0.296	0.773	-0.635	-0.148	-0.380	0.104	.950**	1	0.499	.916**	0.218	0.168	0.236	0.201
	Sig. (2-	0.877	0.519	0.072	0.176	0.752	0.400	0.824	0.001		0.254	0.004	0.638	0.719	0.611	0.665
	N	7	7	6	6	7	7	7	7	7	7	7	7	7	7	7
MC_Arteries	Pearson	-0.155	-0.077	0.706	-0.204	0.281	-0.425	0.051	0.362	0.499	1	.804*	-0.306	-0.321	0.176	-0.222
	Sig. (2-	0.739	0.869	0.117	0.698	0.541	0.341	0.914	0.425	0.254		0.029	0.504	0.483	0.706	0.632
	N	7	7	6	6	7	7	7	7	7	7	7	7	7	7	7
DA_Arteries	Pearson	-0.019	0.177	.919**	-0.575	0.032	-0.459	0.084	.817*	.916**	.804*	1	0.005	-0.035	0.242	0.033
	Sig. (2-	0.967	0.705	0.010	0.232	0.946	0.301	0.857	0.025	0.004	0.029		0.991	0.940	0.601	0.944
	N	7	7	6	6	7	7	7	7	7	7	7	7	7	7	7
deltaD_Veins	Pearson	0.321	0.264	-0.225	0.100	-0.348	-0.301	-0.386	0.379	0.218	-0.306	0.005	1	.973**	0.218	.896**
	Sig. (2-	0.482	0.567	0.668	0.851	0.444	0.512	0.392	0.402	0.638	0.504	0.991		0.000	0.639	0.006
	N	7	7	6	6	7	7	7	7	7	7	7	7	7	7	7
MD_Veins	Pearson	0.290	0.309	-0.264	0.214	-0.394	-0.382	-0.415	0.272	0.168	-0.321	-0.035	.973**	1	0.322	.952**
	Sig. (2-	0.528	0.500	0.613	0.683	0.382	0.398	0.354	0.555	0.719	0.483	0.940	0.000		0.481	0.001
	N	7	7	6	6	7	7	7	7	7	7	7	7	7	7	7
MC_Veins	Pearson	-0.720	-0.329	-0.628	.871*	0.422	0.069	0.015	0.088	0.236	0.176	0.242	0.218	0.322	1	0.597
	Sig. (2-	0.068	0.471	0.182	0.024	0.346	0.883	0.975	0.851	0.611	0.706	0.601	0.639	0.481		0.157
	N	7	7	6	6	7	7	7	7	7	7	7	7	7	7	7
DA_Veins	Pearson	0.005	0.140	-0.367	0.367	-0.186	-0.288	-0.348	0.245	0.201	-0.222	0.033	.896**	.952**	0.597	1
	Sig. (2-	0.991	0.764	0.474	0.474	0.690	0.532	0.445	0.597	0.665	0.632	0.944	0.006	0.001	0.157	
	N	7	7	6	6	7	7	7	7	7	7	7	7	7	7	7

a

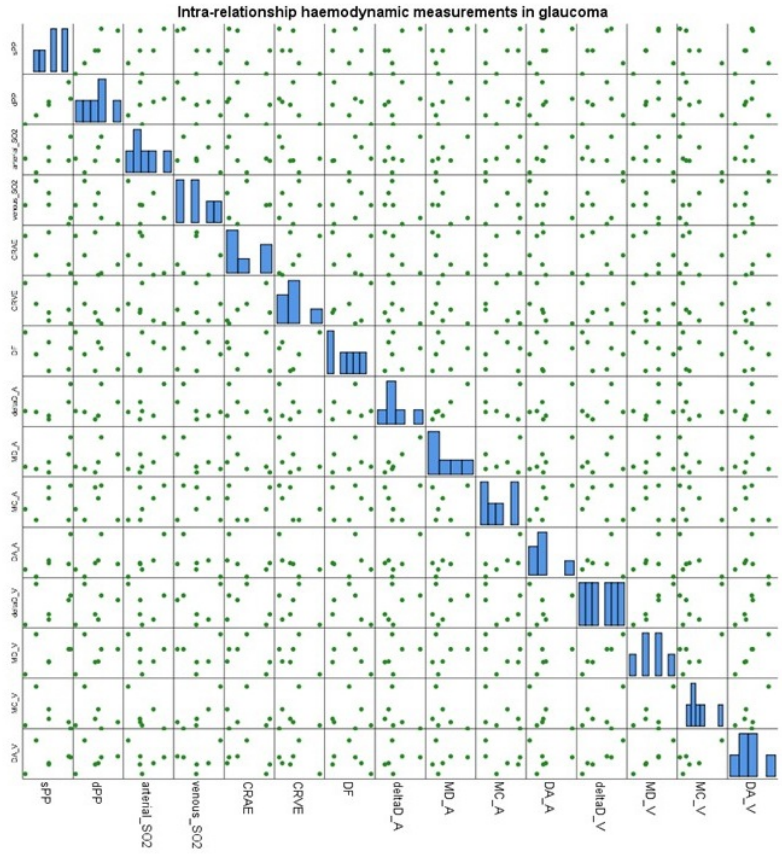

b

Figure E.52: **Haemodynamic intra-relationships analysed using Pearson correlation for the glaucoma cohort (a). Correlations wit p< .05 are marked in green and the cell marking significance had the same colour code if the correlations remained statistically significant after controlling the false discovery rate (FDR, i=86, q= .05). A data-point representation of the same relationships shows graph b.**

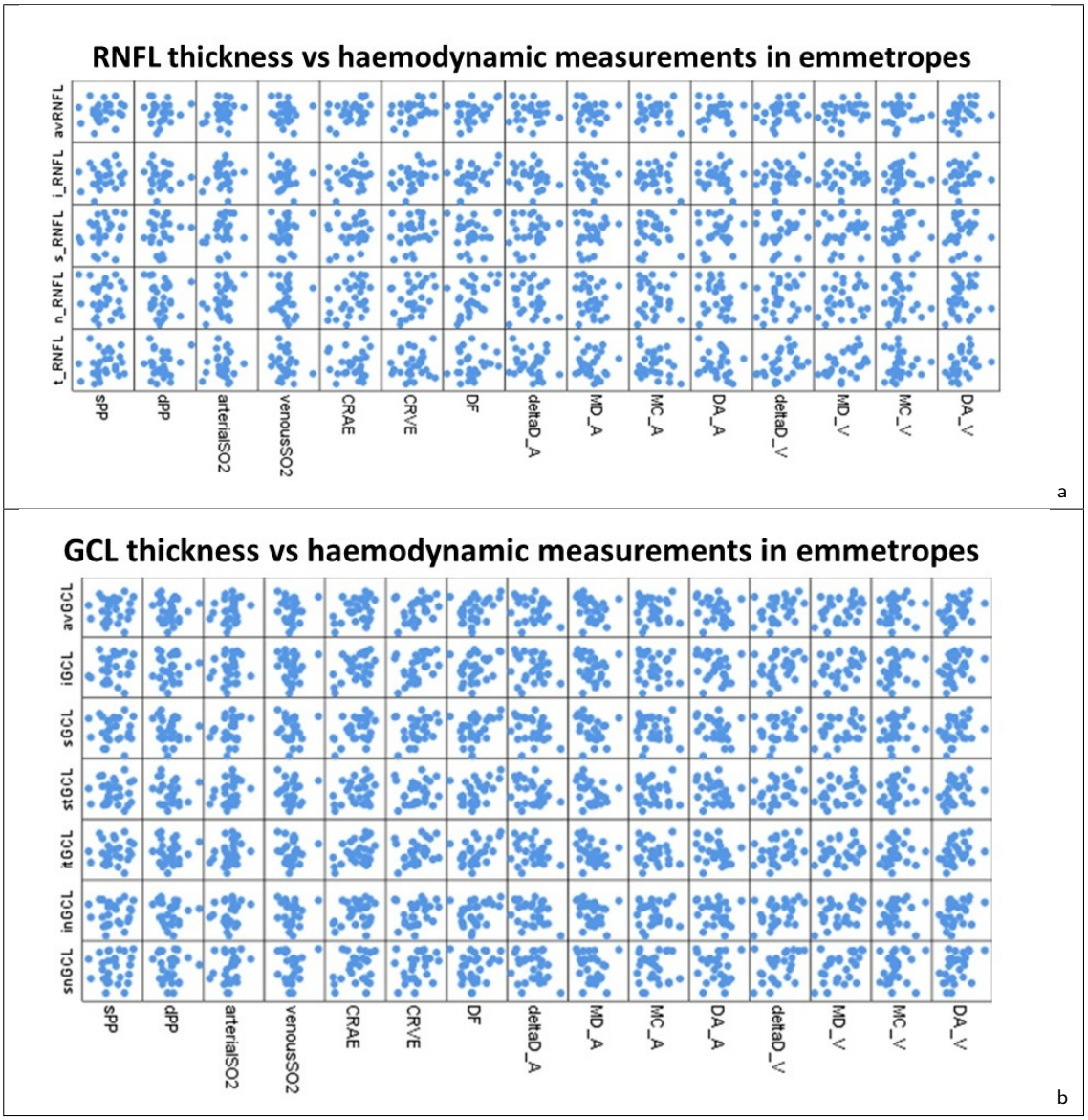

Figure E.53: **Data-point representation of the structural vs haemodynamic relationships in emmetropes shows the RNFL thickness relationships in graph a and the GCL thickness relationships in graph b.**

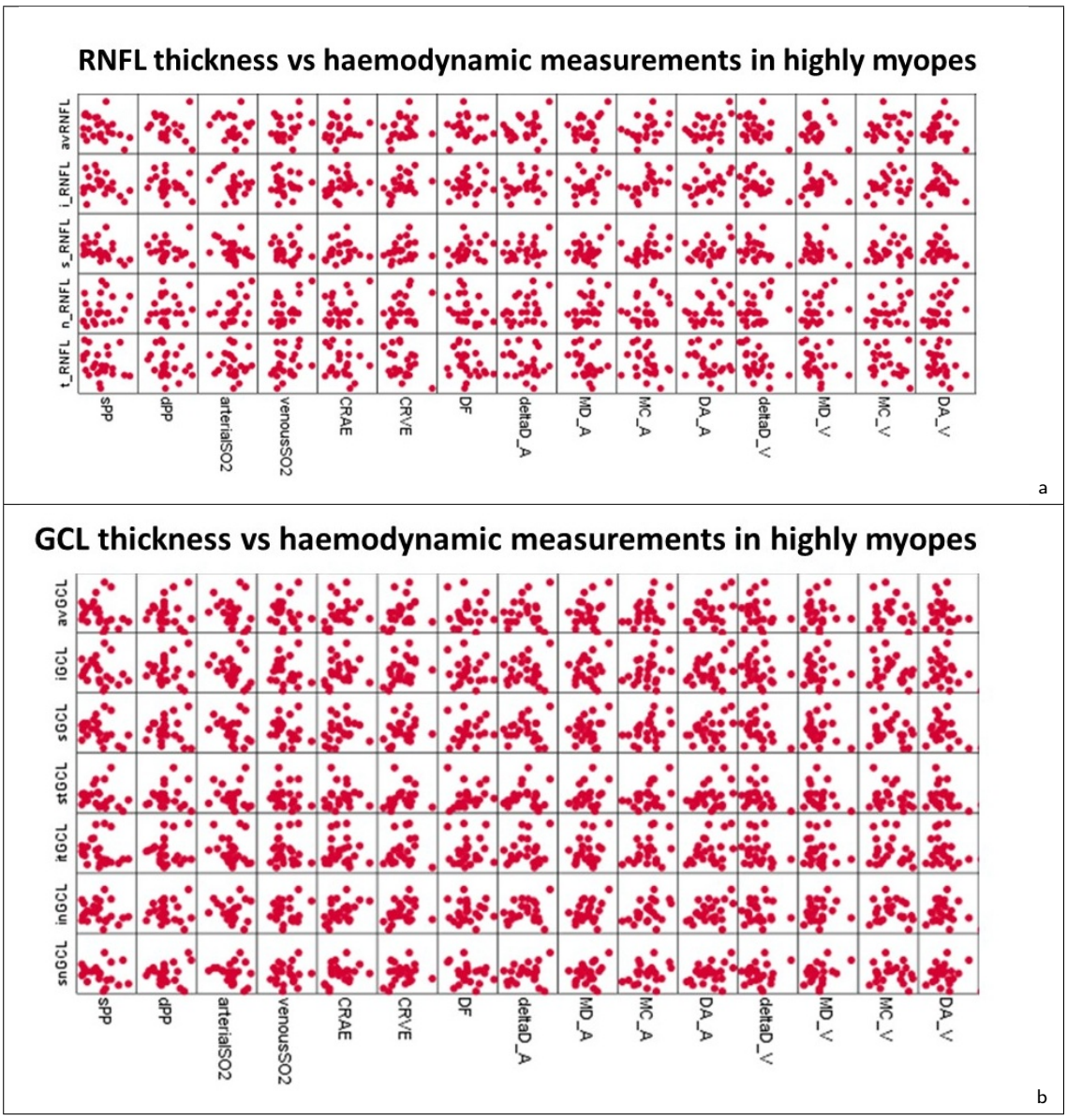

Figure E.54: **Data-point representation of the structural vs haemodynamic relationships in high myopes shows the RNFL thickness relationships in graph a and the GCL thickness relationships in graph b.**

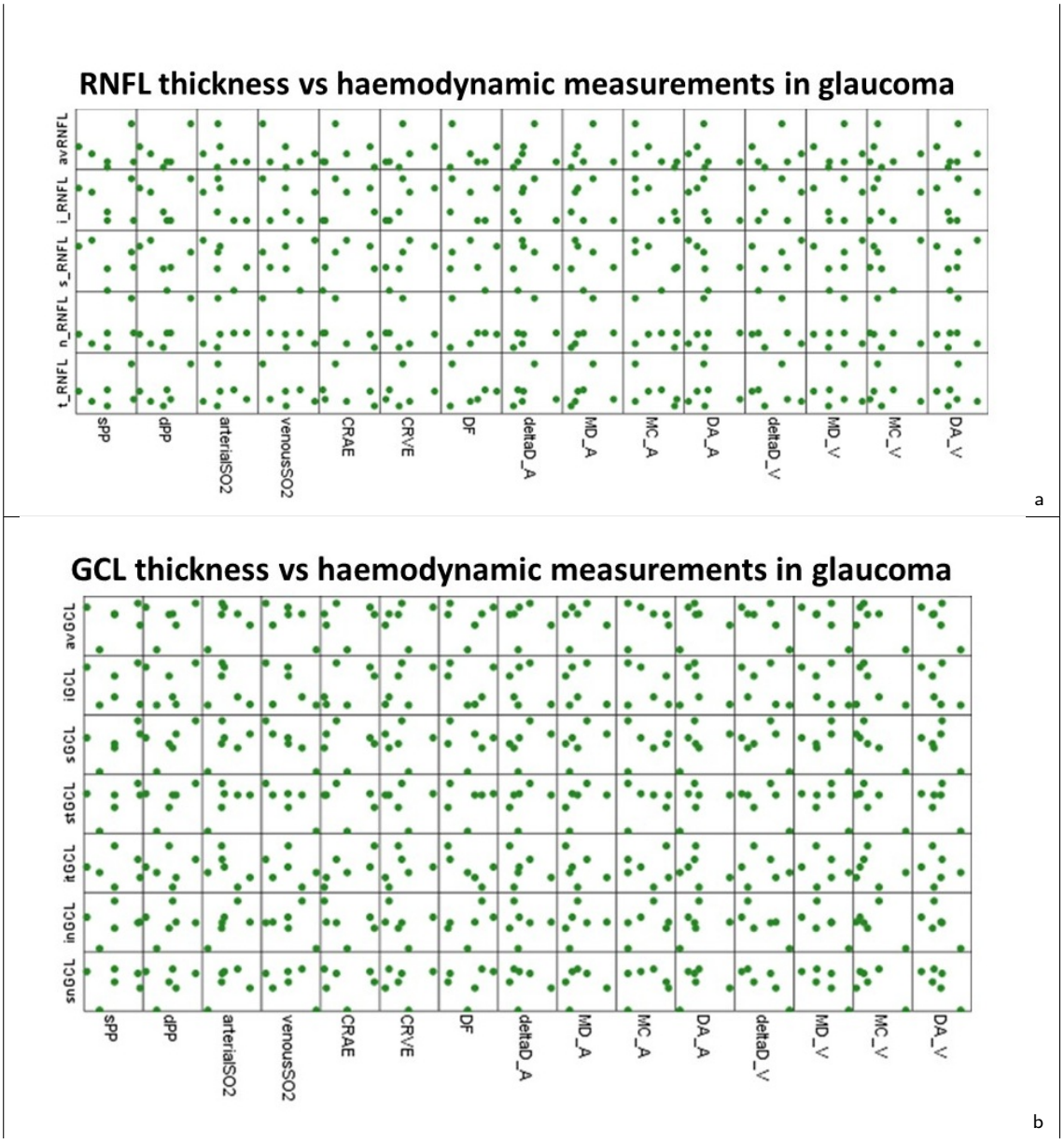

Figure E.55: **Data-point representation of the structural vs haemodynamic relationships in glaucoma subjects shows the RNFL thickness relationships in graph a and the GCL thickness relationships in graph b.**

AppendixF. Model summaries of hierarchical multiple linear regression

Model Summary[c]

Model	R	R Square	Adjusted R Square	Std. Error of the Estimate	Change Statistics					Durbin-Watson
					R Square Change	F Change	df1	df2	Sig. F Change	
1	.011[a]	.000	-.027	10.81881	.000	.005	1	37	.945	
2	.534[b]	.285	.245	9.27396	.285	14.354	1	36	.001	2.065

a. Predictors: (Constant), Age

b. Predictors: (Constant), Age, adj_Df

c. Dependent Variable: adjusted_n_RNFL

Coefficients[a]

Model		Unstandardized Coefficients		Standardized Coefficients	t	Sig.	95.0% Confidence Interval for B		Correlations			Collinearity Statistics	
		B	Std. Error	Beta			Lower Bound	Upper Bound	Zero-order	Partial	Part	Tolerance	VIF
1	(Constant)	70.623	5.088		13.881	.000	60.314	80.932					
	Age	.014	.196	.011	.069	.945	-.384	.411	.011	.011	.011	1.000	1.000
2	(Constant)	-209.432	74.049		-2.828	.008	-359.610	-59.254					
	Age	.147	.172	.123	.856	.398	-.201	.496	.011	.141	.121	.958	1.044
	adj_Df	196.324	51.820	.545	3.789	.001	91.229	301.419	.520	.534	.534	.958	1.044

a. Dependent Variable: adjusted_n_RNFL

ANOVA[a]

Model		Sum of Squares	df	Mean Square	F	Sig.
1	Regression	.556	1	.556	.005	.945[b]
	Residual	4330.727	37	117.047		
	Total	4331.283	38			
2	Regression	1235.053	2	617.526	7.180	.002[c]
	Residual	3096.230	36	86.006		
	Total	4331.283	38			

a. Dependent Variable: adjusted_n_RNFL

b. Predictors: (Constant), Age

c. Predictors: (Constant), Age, adj_Df

Figure F.56: **Hierarchical regression model summary to predict RNFL thickness from haemodynamic measurements in emmetropes.**